Westfälische
Wilhelms-Universität
Münster

ILÖK
Institut für Landschaftsökologie

# Understanding spatial growth and resilience of megacities based on the DPSIR conceptual model

## Study case: Greater Cairo Metropolis, Egypt

Ahmed Abdelhalim Mostafa Hassan

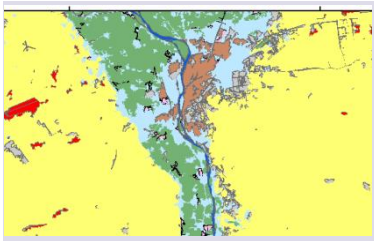

2013

Landschaftsökologie

# Understanding spatial growth and spatial resilience of megacities based on the DPSIR conceptual model

Study case: Greater Cairo Metropolis, Egypt

Inaugural-Dissertation
zur Erlangung des Doktorgrades der Naturwissenschaften
im Fachbereich Geowissenschaften
der Mathematisch-Naturwissenschaftlichen Fakultät
der Westfälischen Wilhelms-Universität Münster

vorgelegt von
*Ahmed Abdelhalim M Hassan*
geboren in *Kairo, Ägypten*
*– 2013 –*

Dekan: Prof. Dr. Hans Kerp
Erstgutachter: Prof. Dr. Tillmann Buttschardt
Zweitgutachter: Prof. Dr. Ingo Hahn
Tag der mündlichen Prüfung: 13/12/2013
Tag der Promotion: 13/12/2013

*"We do not inherit the earth from our ancestors, but we borrow it from our children"* (UN environmental program)

River Nile and the Nile Island in Greater Cairo Metropolis, Egypt

# ACKNOWLEDGEMENTS

I would like to thank the Egyptian Scholarship Program for providing me with the chance to pursue my studies at the University of Muenster, Germany. My sincere thanks are also due to the Environmental Planning Working Group, Institute of Landscape Ecology, Earth Science Department, and the University of Muenster.

I would like to express my sincere and special thanks to my supervisors Prof. Dr. Tillmann Buttschardt, and my second reviewer Prof. Dr. Ingo Hahn for their helpful and valuable comments and suggestions.

I would also like to thank Dr. Laila El-Jouani for her encouragement, feedback and moral support. My thanks and appreciations go to Jenny Schmidt for her assistance during the writing process and to Judit Hejkal for her help.

My deep gratitude also goes to all the staff of Planet Action Program, eCognition Trimble, and ILÖK (especially AG climatology) and IFGI for their support and for all their contributions during my work. I would like to thank my roommates and friends Dr. Jan Thiele, André Große-Stoltenberg, Julia Baumeister, Witold, and others during the four years.

I would like to express my special thanks and appreciation to my mother (Mahdya El-Kholy), my big brother and patron Ibrahim, my wife Shimaa El-Sayed, my other brothers (Ismail and Mohamed), my daughter Safa and my son Abdallah, and my friends in Egypt for their encouragement (Adham, Adel Tehawy, and others). It is very difficult to make a whole list of individuals who helped me to complete this study and I prefer to express my sincere thanks to all of them.

Last but not least, my deepest and heart-felt gratitude goes to my late father Abdelhalim Mostafa Hassan.

Above all, thanks to God, who gave me the ability to complete this study.

# Abstract

Planning the sustainable development of a complex socio-ecological system such as a megacity requires an understanding of the physical change of the main components of the system. From that point of view, this study introduced the analysis of spatial growth and resilience as a fundamental concept to find out the relation between social actors and activities, and their physical and environmental expressions and impacts in time and space. Therefore, the approach is focused here on the relation between the growth of Greater Cairo Metropolis (GCM) and its spatial impact in order to contribute eventually to an effective response. The thesis therefore examines how spatial indicators can be applied to monitor landscape structure, and to detect the dynamic expansion of the metropolis. The conceptualization follows a model which was first suggested by the European Environment Agency and which is now used as a framework to describe and interpret socio-environmental systems. The model distinguishes between “driving forces”, “pressures”, “states”, “impacts”, and “responses” (DPSIR). The DPSIR model was used to analyze the main spatial components which affect the growth of GCM. Thereby, the DPSIR scheme and applications of remote sensing techniques were integrated so as to work with different levels of the developed monitor framework within this study. The comparison between pixel-based and object-based classification techniques took place to detect and clarify the land use/land cover (LULC) states and the impacts of spatial changes over the last three decades. There are eleven rock types covering more than fifty percent of the GCM area which to some extent drive the growth trends. That cover is composed of carbonates and clastics with dispersed basaltic exposures.

In this study, the fine resolution TM and ETM satellite data were used to initiate a first monitoring level. And to coarse resolution, SPOT data were applied to provide the second monitor level. The first one is focused on the whole Greater Cairo Metropolis (GCM) area, while second deals with the impact of some developments in different sectors of the study area. At the first level I could show that urbanization activity increased rapidly by taking two trajectories; the first is related to the extensive construction of new cites in the hinterland (desert of GCM), while the second is represented by urban sprawl on the cultivated land. Also, the results referred to some difficulties in separating some land units at this scale of spatial resolution. At the second level, urban density is classified into low, medium and high to represent the urban patterns and to show the mechanisms of growth. High density urbanization is mainly concentrated in the core areas and partially in the periphery that spatio-temporally increased and expanded in different ways. Meanwhile, medium and low densities are dominating most new urban areas. In those new urban areas, the low density urbanization could be transformed to medium density forced by human needs, investment and

development drivers. The green cover was classified and categorized into agriculture and sparse vegetation subclasses based on the uniformity and density of its spatial form. Most spatial changes of the green cover classes referred to negative change with the exception of reclamation parks in the desert. Some artificial water bodies were recognized in the hinterland (new cities) in 2008 which had not been there before (1999).

The study could show that there are about fourteen hot spot areas which are in need of different responses by land management based on their types, properties and spatial features. Most of them can be categorized as open corridors of urban sprawl and saturated closed slums.

It can be concluded that land use / land cover change (LULCC) is a process that shapes the state of land over time, while spatial resilience is a broader concept of spatial dynamic systems. Accordingly, the spatial growth and resilience (dynamic change) of mega cities like GCM could be conceptualized at different levels based on the information and data available. Moreover, the study shows that the workflow based on the DPSIR framework coincides fairly well with the classification tree and rule set created by using remote sensing techniques. Generally, it can be claimed that the east-west zones of GCM are slightly resilient while the north-south zone is resilient. That means that the slightly resilient represents the most restricted and saturated urbanization areas, while the resilient represents the open corridors and hot zones identified in this study.

**Key words**: Spatial growth; Spatial resilience; Land use / land cover change, DPSIR socio-ecological conceptual model; Megacity; Greater Cairo Metropolis.

# Contents

# List of Figures

# List of Tables

# Acronyms and Abbreviations

**a.s.l** above sea level

**ADB** Asian Development Bank

**AG** Agriculture Fields

**ASTER** Advanced Spaceborne Thermal Emission and Reflection Radiometer

**BS** Bare Soil

**CAPMASS** Central Agency for Public Mobilization and Statistics

**CL** Cultivated Land

**CNC** Core New City Sector

**CU** Cultivated to Urban areas

**D** Desert

**DPSIR** Driving Forces, Pressures, States, Impacts, Responses

**DRTPC** Development research and Technological Planning Center

**EEA** European Environment Agency

**EEAA** Egyptian Environmental Affairs Agency

**EMA** Egyptian Meteorological Authority

**ETM**+ Enhanced Thematic Mapped

**FAO** World Food and Agriculture Organization

**GCM** Greater Cairo Metropolis

**GDEM** Global Digital Elevation Model

**GDP** Gross Domestic Product

**GIS** Geographical Information System.

**GIZ** Deutsche Gesellschaft für Internationale Zusammenarbeit GmbH

**GLCF** Global Land Cover Facility

**GNDVI** Green normalized difference vegetation index = (NIR-green)/(NIR+green)

**GOPP** General Organization for Physical Planning

**GPS** Global Positioning System

**GTZ** Deutsche Gesellschaft für Technische Zusammenarbeit (German Technical Cooperation); today **GIZ** (Gesellschaft für Internationale Zusammenarbeit)

**HUD** High Urban Density

**IDRC** International Development Research Center

**LUD** low urban density

**LULC** Land Use and Land Cover

**LULCC** Land Use and Land Cover Change

**LWM** Land water mask = ([Mean Layer 3NIR]) / ([Mean Layer 1Green])*100

**MA** Metro Autostrad Sector

**METI** Ministry of Economy, Trade, and Industry of Japan

**MSS** Multispectral Scanner

**MUD** Medium Urban Density

**NASA** United States National Aeronautics and Space Administration

**NDMI** Normalized difference moisture Index = (NIR-IR) / (NIR+IR)

**NDVI** Normalized Difference Vegetation Index

**NDVI** Normalized difference vegetation index = ([Mean Layer 3NIR]-[Mean Layer 2red])/ ([Mean Layer 3NIR] + [Mean Layer 2red])

**NGO** Non-Governmental Organization

**OB** Object Based

**OBIA** Object Based Image Analysis

**OECD** Organization for Economic Co-operation and Development

**PB** Pixel Based

**PCSU** Privatization Coordination Support Unit

**PDP** Participatory Development Programme in Urban Areas

**PDP** Participatory Urban Development Program in Urban Areas

**RST** Remote Sensing Techniques

**RVI** Ratio vegetation index (RVI) = NIR / Red

**SES** Social Ecological System

**SINs** social internet networks

**SPOT** Satellite Pour l'Observation de la Terre

**SV** Sparse Vegetation

**TM** Enhanced Thematic Mapper

**U** Urban areas

**UN HABITAT** United Nations Human Settlements Program

**UN** United Nations

**UNDP** United Nations Development Program

**UNESCO** United Nations Educational, Scientific and Cultural Organization

**USAID** United States Agency for International Development

**USGS** United States Soil and Geological Survey

**VHR** Very High Resolution

**WB** Water Bodies

**WGC** West Greater Cairo Sector

**YMs** Youth Movements

# 1 Introduction

## 1.1 General Introduction and background

The rapid development of newly established quarters has played a dominant role in growing cities, increasing the population concentration and affecting the demographic structure. This has led to distinct large urban areas and cities with a socio-ecological system that is more complex (Darbkin et al. 1978; Aguilar 1987; Olpadwala and Goldsmith 1992; and Steo 2011). Such a large urban area with a population of more than ten million is defined as a Megacity by the United Nations (UN-Habitat 2006). Currently, three out of six human beings live in cities, two of whom live in developing cities, and megacities are home to fewer than ten per cent of the global urban population (UN-Hbitat 2006/7). In addition, a recent publication by the United Nations (UN 2009) stated that until 1975 there were just three megacities in the world: New York, Tokyo and Mexico City. By 2005, their number had increased to twenty and it is projected that there will be 29 megacities in 2025. Countries of the global south will have 17 of these 29 megacities and, the megacities may then account for 10.3 per cent of the world urban population (Fig. 1).

This thesis examines how pressures exerted on the city`s resources, land use and ecological system influence these megacities. The increase in human needs and the resulting shortage in resources often cause environmental degradation and social problems, which impact on all levels of urban development. Generally, significant problems and challenges such as food security, water supply and quality, increased energy consumption, dense urban infrastructure, waste management, air quality, increasing poverty, human health hazards, etc., all of which affect the quality of life of urban inhabitants, the natural urban environment and the climate in megacities, are reported by UN publications (2006 and 2009) and many other authors and scientists (Darbkin et al. 1978; Hardoy and Satterthwaite 1984; Olbadwala and Goldsmith 1992; Planet Earth 2005; Hunga et al. 2006; Duha et al. 2008; and Megacities Meeting 2010).

Therefore, while megacities sustain their growth, it has become of paramount importance to establish an innovative response for reducing vulnerability to rapid development and associated environmental change impacts that will place further strain on the availability of resources and the quality of life for all those who live in the city, or are affected by it.

A megacity of fewer than twenty million people can be a single metropolitan area or two or more metropolitan areas which have grown to such an extent that they now form one urban area (Blumentfeld 1967).

However, the terms hyper-city, agglomerate-city and global-city are sometimes used to describe cities with more than twenty million people (UN 2009; Metropolis report 2009; and Duha et al. 2008).

This case study focuses on Greater Cairo (GC), capital of Egypt (Fig. 2), which is the largest and one of the most densely populated cities in the MENA region (Middle East and North Africa) (UN 2009). Furthermore, GC is more than just a large city. Its scale creates new dynamics, a new complexity and a new simultaneity of events and processes in physical, social and economic ways. It hosts intense and complex interactions between different demographic, social, political, economic and ecological processes (Aguilar 1987; Fahmi and Sutton 2008; and Metropolis 2009).

During the last three decades, development, population rate and urbanization have been growing rapidly in GCM. Because of such rapid growth, the living conditions in Greater Cairo Metropolis (GCM) have deteriorated. This study sets out how GC is creating an increased demand for land combined with environmental degradation.

However, this present thesis deals with the monitoring and analysis of the dynamic change and spatial resilience of GCM based on a socio-ecological conceptual framework. As a result, it detected and evaluated the impact of the rapid development and growth of the metropolis on urbanization and the use of fertile land for urban sprawl.. This would contribute strongly to the vision of decision makers for GCM-2050 and support different kinds of stakeholders such as planners, researchers, investors and students.

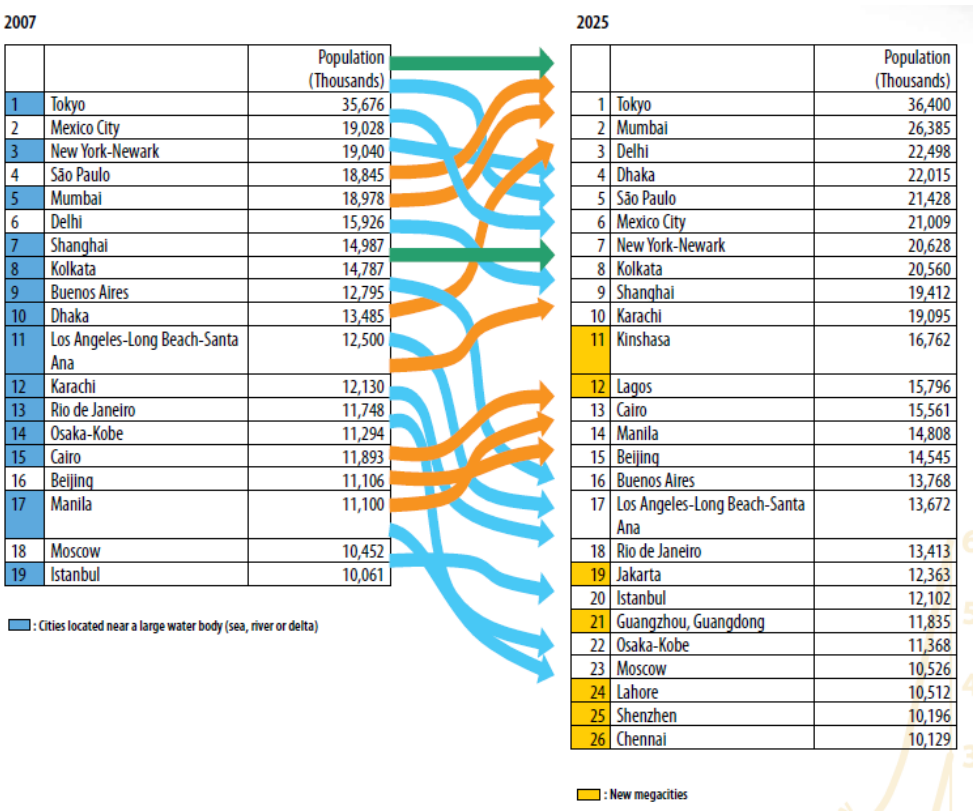

2007

| | | Population (Thousands) |
|---|---|---|
| 1 | Tokyo | 35,676 |
| 2 | Mexico City | 19,028 |
| 3 | New York-Newark | 19,040 |
| 4 | São Paulo | 18,845 |
| 5 | Mumbai | 18,978 |
| 6 | Delhi | 15,926 |
| 7 | Shanghai | 14,987 |
| 8 | Kolkata | 14,787 |
| 9 | Buenos Aires | 12,795 |
| 10 | Dhaka | 13,485 |
| 11 | Los Angeles-Long Beach-Santa Ana | 12,500 |
| 12 | Karachi | 12,130 |
| 13 | Rio de Janeiro | 11,748 |
| 14 | Osaka-Kobe | 11,294 |
| 15 | Cairo | 11,893 |
| 16 | Beijing | 11,106 |
| 17 | Manila | 11,100 |
| 18 | Moscow | 10,452 |
| 19 | Istanbul | 10,061 |

: Cities located near a large water body (sea, river or delta)

2025

| | | Population (Thousands) |
|---|---|---|
| 1 | Tokyo | 36,400 |
| 2 | Mumbai | 26,385 |
| 3 | Delhi | 22,498 |
| 4 | Dhaka | 22,015 |
| 5 | São Paulo | 21,428 |
| 6 | Mexico City | 21,009 |
| 7 | New York-Newark | 20,628 |
| 8 | Kolkata | 20,560 |
| 9 | Shanghai | 19,412 |
| 10 | Karachi | 19,095 |
| 11 | Kinshasa | 16,762 |
| 12 | Lagos | 15,796 |
| 13 | Cairo | 15,561 |
| 14 | Manila | 14,808 |
| 15 | Beijing | 14,545 |
| 16 | Buenos Aires | 13,768 |
| 17 | Los Angeles-Long Beach-Santa Ana | 13,672 |
| 18 | Rio de Janeiro | 13,413 |
| 19 | Jakarta | 12,363 |
| 20 | Istanbul | 12,102 |
| 21 | Guangzhou, Guangdong | 11,835 |
| 22 | Osaka-Kobe | 11,368 |
| 23 | Moscow | 10,526 |
| 24 | Lahore | 10,512 |
| 25 | Shenzhen | 10,196 |
| 26 | Chennai | 10,129 |

: New megacities

**Figure 1: Ranking of the world`s megacities, 2007 and 2025 (prediction), Source of table: UN-Habitat 2008. Notice; mentioned is only Cairo City not GCM**

## 1.2 Problem statement

In the last thirty years, rapid population growth and urbanization have become issues in big cities like Greater Cairo (GC). Because of explosive growth, the living conditions of Greater Cairo Metropolis have deteriorated. Development trends of the last thirty years have increased general wealth and modernization, but they have also created an increased demand for land combined with environmental degradation.

The area concerned in this thesis includes a variety of land uses associated with a complex mix of land cover, such as a central business district (CBD), urban and suburban residential areas and some rural areas (e.g. cultivated areas and soil). The urban sprawl affects in particular cultivated areas in the Greater Cairo area. This problem has caused an irretrievable loss of very fertile soils which are highly suitable for agricultural use. The fast rate of these processes makes the problem even more severe. The Government has recognized the problem and has passed several laws to control the land-use changes through urbanization. These laws prohibit any activities other than to farm the fertile lands (El Araby 2002; and Ibrahim and El Hefnawi 2005).

In Greater Cairo, the misuse of land to build slums and informal settlements, the resulting increased urban density, and the unsustainable use of the infrastructure can not only lead to social inequality but can also have dramatic environmental consequences (e.g. El Dewaka crisis, Cairo 2008; UNDP 2008). These phenomena began just after the 1952 revolution and the beginnings of extensive industrial activity (which increased in the following decade with the growth of the city), when migration from Upper Egypt and the Delta caused housing pressures to become critical (PDP 2010). Since the 1980s, some scientists have strongly recommended building new urban centers in the desert regions in order to attract people out of the old city of Cairo. It was seen as very important to promote decentralized authorities and to re-distribute the administrations all over the different governorates (Fouad 1980, and Ali 2003). Accordingly, many new cities have been built on the areas surrounding GCM (mainly desert). For example: New Cairo City, 6th October City, El-Qatamayia City, El-Mokattam Park, 15th May City, and El-Oboor City. These new cities represent a major effort to move investment and population away from Cairo and the Delta, and to use desert land (Fouad 1980, and Ali 2003). Nevertheless, the emphasis on the New Cities as counter-attractions has failed in the absence of effective controls on the growth of Greater Cairo and the Delta region (Ali, 2003; Khader et al 2010; and Mahmoud 2011). Furthermore, the increasing population, and the different zones with various urban patterns and different socio-economic characteristics leave GCM in continuous need of more roads and infrastructures for development (Neill 2000; Sims 2003; and DRTPC 2009).

Sutton and Fahmi (2001) concluded that the development of infrastructures such as a ring road is a successful element to move people out from the GC core to remote cities. Considering the latter, this study examined the effect of the ring road and related highways constructed in GCM on the increase of urbanization density and urban sprawl.

Planning sustainable development of such a metropolis as GC requires an understanding of the physical change of the main environmental indicators, drivers, and factors (Hardoy 1984; Fernandes 1998; Cumming 2008; and Lang 2012). In addition, a better understanding of the links between the acceleration of development elements and spatial environmental degradation is required (Duh et al. 2008). Thus, this work monitors and analyze s the dynamic environmental changes to capture spatial resilience in Greater Cairo Metropolis based on a conceptual framework, Remote Sensing Techniques (RST) and Geographic Information Science (GIS). Moreover, the present work attempts to find an effective, flexible and easy framework to delineate the relation between development elements such as roads, metro, and completely new cities, and the spatial structure of the GCM. In addition, the impact of these elements on the spatial structure and form of GCM, and on urban

densities, still need to be understood and analyzed. Thus, this study examines impact of the aforementioned development elements on the spatial resilience pattern and structure, the growth of GCM, and related environmental degradation.

I have adjusted the perspective of my study accordingly and formulated the main research questions in the next paragraph.

## 1.3 Research questions

There are six research questions that are examined within this thesis.

a) How can the spatial change and spatial resilience of Greater Cairo Metropolis (GCM) be understood and analyzed?

b) What are the consequences of the intensive resource use of GCM on its spatial dynamic?

c) What are the relations between the rapid development during the last three decades and the spatial growth and spatial resilience of GCM, and how can they be examined?

d) What are the key elements that drive growth, and what are the related indicators?

e) Has the development of new cities, new roads, and metros led to a reduction in building concentration in the core areas of the old city, the centers, and the other dense areas in GCM?

f) How can the spatial analysis of GCM contribute to develop responses?

## 1.4 Objective

The study has one main objective and several secondary objectives.

The main objective is:

- To understand the rapid spatial development and the dynamic growth of Greater Cairo Metropolis (GCM) over the last three decades.

The secondary objectives are:

- To apply an empirical model to monitor and analyze spatial patterns and landscape structural changes using the spatial data available.
- To extract the main indicators that show aspects of growth of GCM, and integrate them into a socio-ecological conceptual framework.
- To give baseline information that can support future research and development activities.

- To understand the physiographic setting that limits future planning.
- To cover the gap between the huge scientific spatial information existing for GCM, and the different levels of stakeholders by using an advanced dissemination tool.
- To look for the megacity challenges, not only to improve the worst state but also to understand the causes.

## 1.5 Greater Cairo Metropolis (GCM) case study area

The selected case study focuses on the metropolitan area of Greater Cairo and its surroundings, which is known as the capital of Egypt and one of the fastest growing megacities worldwide. If it reaches a population of more than 35 million by 2050, it will be described as a metacity (UN 2009).

The whole area covers about 3543.7 km$^2$. The following coordinates delimit it approximately (Fig. 2). Nevertheless, the effective urban area with which this study is concerned is about 1271.6 km$^2$.

- Latitudes: 29$^o$ 46′ 300″ to 30$^o$ 10′ 30″ N
- Longitudes: 30° 51′ 30″ to 31° 38′ 20″ E

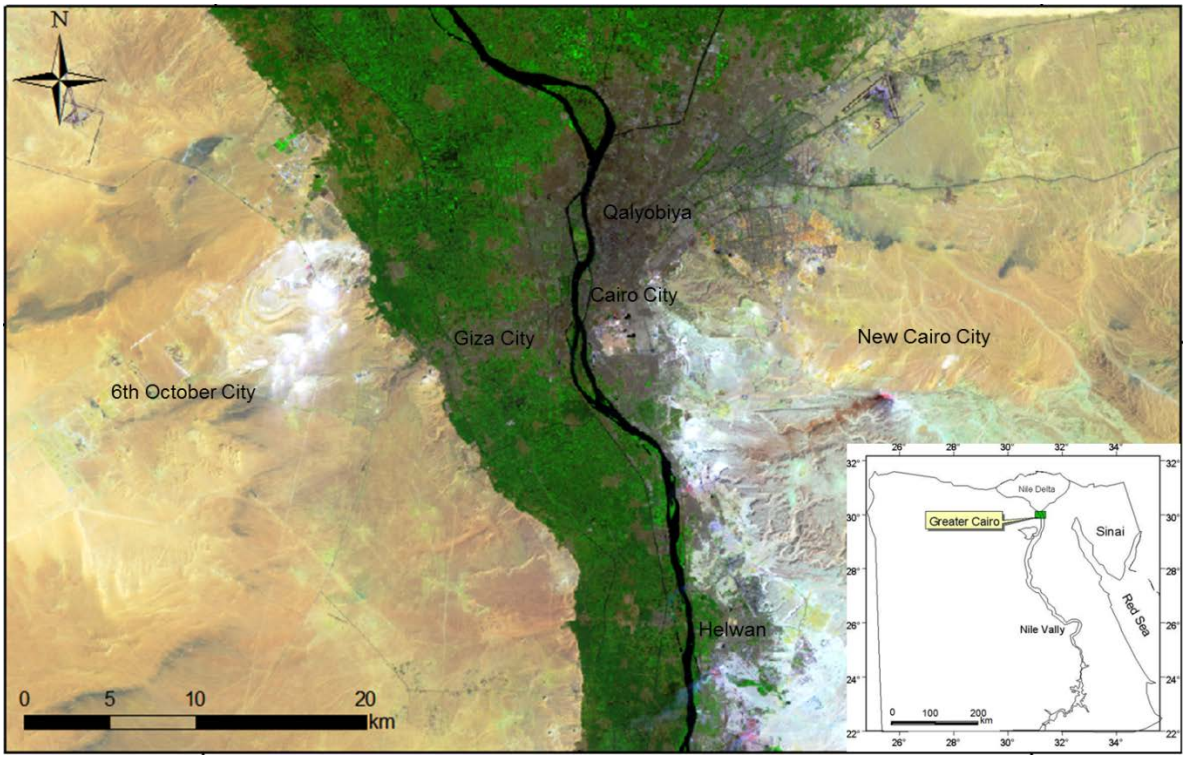


**Figure 2: The location (small map) and boundary of the study area (whole map) based on a TM-Landsat scene of 1984**

The Greater Cairo Metropolis (GCM) is a vast agglomeration that encompasses major parts of the governorates of Cairo, Giza, Qualyoubia, 6th October City, New Cairo City and Helwan-15th May City. The Nile River forms the administrative division between these governorates, with Cairo, Qualyoubia, New Cairo and Helwan on the east bank of the river, and Giza and 6th October city on the west bank (Fig. 2 and 3). The area is dominated by three zones, which are core, periphery, and backyard (hinterland) (Fig. 3). The core is represented by the old Cairo and Giza cities, which are located in the center of the study area. The periphery is represented by the area extending east and west from the core to the hinterland or desert area, but to the north and south the ring road and the 15th May road delineate it. The hinterland is mostly dominated by desert area surrounding the urban GC megacity and it hosts most new cities constructed during the last three decades.

The main roads that serve GCM (Fig. 3) are the ring road which spans an area of approximately 30 km around greater Cairo, 15th May, Autostrad, and the highways connecting the Cairo region with other cities such as Alexandria, Suez-Sinai, Ismailia, Fayoum, Baharyia Oasis, delta cities, the Upper Egypt region and the Red Sea. Since the beginning of the 1990s, the transportation network of GC has been supported by the first metro line (Fig. 3), which has its starting point at Helwan in the south and ends at Marg in the north.

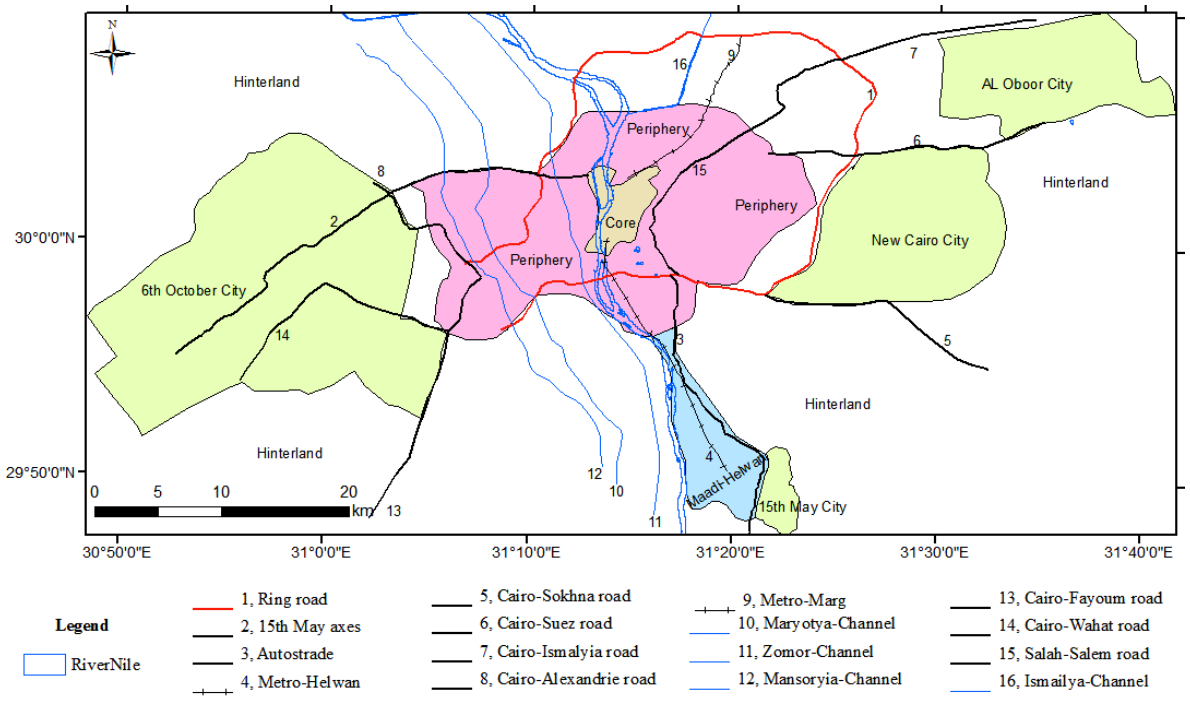


**Figure 3: The GCM sectors, main roads, metro lines and water channels (the map based on ETM 2006)**

The main water resource in GCM is the Nile River and its tributaries and channels (Fig. 3). The latter mostly supply the GCM with drinking water and irrigation water (El Arabi 1999).

GCM has encountered rapid urban development and population growth in the last 20 to 30 years. The present population of the whole GCM is approaching 20 million (UN-Habitat 2013). Nevertheless, the most recent census conducted by the Central Agency for Public Mobilization and Statistics (CAPMAS) in 2006 found that the total population of the GC governorates had reached 17.5 million and it could be more than 20 million by 2030 with a population density then to be about 39,000 persons per one square kilometer. These differences in calculation might be due to the city-user effect. This means that many people come from the countryside to the administration center and ministries in Cairo city every day to access services, and then go back to their cities. That puts more pressure on the infrastructure of the city. Therefore, it is not easy to calculate the exact population for the whole metropolitan area. However, the CAPMAS censuses show that the population of GCM represents about 20-25% of the total population of Egypt, and almost half of the Egyptian urban population. Recently, the Egyptian population reached about 82 million with the rate of growth declining from 1.9% in 2003 to 1.7% in 2008 based on CAPMAS census data (Fig. 4 and 5). Regarding the GC governorates, the population of Cairo city is about 8.7 million, Giza city is about 3.15, Qualyoubia is about 4.64 million, Helwan about 1.87 million, and 6$^{th}$ October city about 3.06 million (CAPMAS 2011).

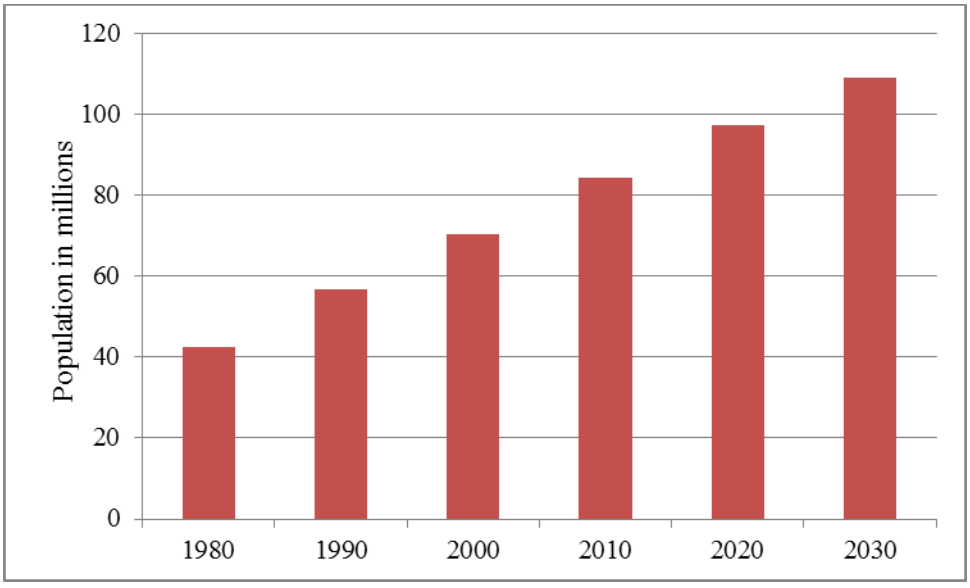


**Figure 4: The population of Egypt in millions (Source: CAPMAS)**

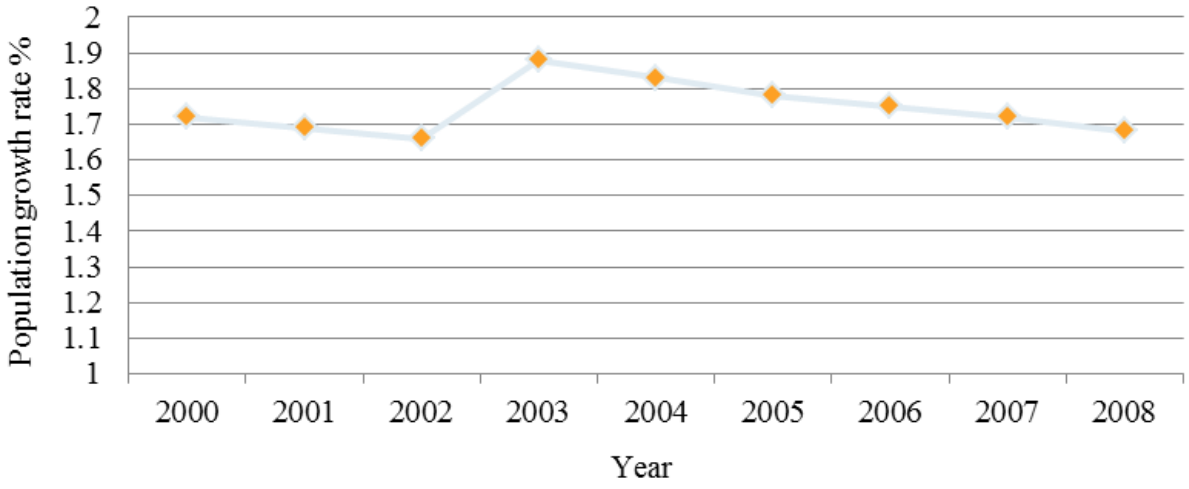


**Figure 5: The annual rate of population growth of Egypt (Source: CAPMAS)**

GCM has suffered not only from the global economic crisis of 2008 but also from some economic trends such as privatization that have accelerated urban growth during the last two decades. The latter led to an increase gap between people's incomes (Fahmi and Sutton 2008; and World Bank 2011). According to the World Bank report of 2013, Egypt's economy is still suffering from a severe downturn and the government faces numerous challenges as to how to restore growth as well as market and investor confidence. Political and institutional uncertainty, a perception of rising insecurity and sporadic unrest continue to have a negative effect on economic growth. The growth of Gross Domestic Product (GDP) slowed down to just 2.2% per year in October-December 2012/13, and investments declined to 13% of GDP in July-December 2012 (World Bank 2013). These figures show the challenges that the big metropolitan city of Greater Cairo is facing. Another challenge is the massive emigration of people seeking work to GCM from the countryside and rural areas (Fig. 6) (Bienen 1984 and Fahmi and Sutton 2008).

**Figure 6: The city users and workers coming from the countryside and rural areas are descending from the ring road . Photo captured (2010) via the ring road, SE-Cairo.**

Due to the diversity of cultures and cultural heritages inside and around Greater Cairo, a large number of tourists and students visit the city to learn the history not only of Egypt but also of other countries in the world. There are four civilizations recorded which have had a great impact on the city's culture; the culture of the Pharaohs, Roman culture, Christian (Coptic) culture, and Islamic culture. Moreover, nowadays Cairo is influenced by the modern globalized culture which is shown for example in the famous building "Cairo-tower". The most famous remains of the era of the Pharaohs are the Pyramids and the Sphinx in Giza, and invaluable parts are preserved in the Egyptian Museum in Cairo city. The Romanic remains are not so plentiful and the main place to find them is close to a pyramid plateau in Giza. While the old Coptic churches mainly dominate the area south of the old Cairo city (core), old mosques, religious schools and houses represent the Islamic settlements, which are located mainly in the core of GCM (old Cairo). Because of the impact of extensive urban growth in the GCM, views on landscape and ancient quarters and the cultural heritage sites often are misty and dazzling (Fig. 7), which means that they lose some of the touristic fascination and value. However, the negative influences of urban sprawl and the rapid development of Greater Cairo on most heritage sites have received attention by the United Nations (UN) and its branches, which fund some projects to mitigate the dangers such as the rise of the ground water level and the instability of some buildings (UN-Habitat 2004 and Amedi et al. 2010).

**Figure 7: Misty view on Cairo city from El Mokattam. On clear days the pyramids could be seen on the opposite shore of River Nile valley. Photo due West captured 2009**

The weather and climate information based on data of the Egyptian Meteorological Authority (EMA 2013) for GCM is summarized as follows. The GCM is characterized by a Mediterranean, arid to semi-arid climate with two main seasons: the first one, humid and fresh; extends from October to April, when 85% of total precipitation falls with an average yearly precipitation of about 20mm, and the average temperature is about 18ºC; the second one, dry and very warm, from May to October, has an average temperature of about 25ºC. Maximum and minimum temperatures registered in GCM are about 40ºC and about 7ºC respectively. The main wind blows from northwest to southeast.

Furthermore, air pollution in greater Cairo is a matter of serious concern. Greater Cairo's volatile aromatic hydrocarbon levels are higher than in many other similar climatic cities (ex. Upper Egypt Cities). Air quality measurements in Cairo have also recorded dangerous levels of lead, carbon dioxide, sulphur dioxide, and suspended particulate matter concentrations due to decades of unregulated vehicles emissions, urban industrial operations, and chaff and trash burning (Egyptian Environmental Affairs Agency (EEAA) 2011, and El-Metwally et al. 2010). Greater Cairo produces 10,000 tons of waste each day, 4,000 tons of which are not collected or managed (Megcity Project 1998). This represents another huge health hazard that the Egyptian Government is seeking to combat. The city also suffers from water pollution, as the sewer system tends to fail and overflows occur regularly (El Arabi 1999). Occasionally, sewage has spilled onto the streets and created a very serious health hazard. It is hoped that this problem will be solved with a new sewer system able to cope with the demand of the city funded by the European Union (Neill 2000).

The geological setup is one of the driving forces which could help to control the growth of cities. In this thesis, the geological setting and physiography of GCM are therefore studied and described in detail in Chapter Two.

## 1.6 State of the art

In this study, I deal with GCM not only as a complex system but also as a land mass, and seek to understand which factors define its characteristics and influence its evolution. It will be important to single out the factors that would help us to provide sustainable planning and environmental management at all levels of the city's development. All processes inside that complex system, such as social, economic, cultural and ecological, have an influence on land use and land cover, and affect the landscape of the city. Thus, understanding the land will lead to understand the system.

The definition of land, according to the FAO (1976, pp 70-80), is "an area of the earth's surface, the characteristics of which embrace all reasonable stable, or predictable cyclic, attributes of the biosphere vertically over and under this area, including those of the atmosphere, the soil and the underlying geology, the hydrology, the plant and animal populations, and the result of present and past human activity, to such an extent, that those attributes exert a significant influence on present and future uses of land by man". Only recently have researchers focused on management schemes that take a systems approach to understanding ecosystems and on new strategies for sustainability which include social parameters. This development in scientific thinking reflects the need to understand complex issues such as urban growth and the bidirectional interactions with global environmental changes, particularly in the developing world. Moreover, sustainable development requires sound planning and land-use management, supported by a framework of analysis for spatial conditions and processes of change, as well as their interactions with the used space and its management (Selman and Paul 2000). Seto (2011) concluded that drivers of growing mega regions must be understood in the context of the underlying factors and spatial inequalities of development. Urban planners and administrative bodies require reliable information to assess the consequences of urbanization, to ensure a sustainable functioning of cities, and to minimize the negative impacts of rapid urbanization. Urban expansion in the developing world often takes place in an unplanned manner and administration is unable to keep track of growth-related processes (Griffiths et al. 2009). Data should be presented within a framework that helps us to unpack the demographic and economic land use changes that take place in a megacity (e.g. Mexico City) (Aguilar and Ward 2003). Therefore, I want to introduce a monitoring system by using a certain framework for land

use land cover change (LULCC) data analysis. Consequently, in this study the DPSIR conceptual model was used to create a workflow, which has never been used before for spatial analysis of GCM. The European Environment Agency recommends this concept which distinguishes between driving forces (D), pressures (P), states (S), impacts (I), and responses (R) to develop a strategy for integrated environmental assessments. In this study, the DPSIR model is used to identify and to determine a framework to find and describe the development indicators of GC megacity in relation to its ecology and environment, and to provide a deduction of main transformer indicators in Greater Cairo.

GIZ (2010) concluded at the end of a development project that the Cairo experience was extraordinary in many regards. In the project GIZ developed valuable capacities in order to deal successfully with the multiple challenges. Working as consultants in a real world context and therefore being exposed to multiple actors, stakeholders and interests requires to focus on various perspectives at the same time in order to be able to develop strategies and plans in a sensitive political context. I introduce here the DPSIR framework from the view of a target-oriented-workflow that supports the interests of different stakeholders. This work provides some orientation concerning the most pressing subjects for stakeholders, which could be used for an advanced planning strategy including the geo-setting of the city.

Most studies explain the problems of GCM in terms of the rapid rate of urbanization and population growth, and study their impacts on the quality of air, water, transportation and traffic congestion, health hazards, waste accumulation, growth trends, etc. (Rashed et al 2001; Yin et al. 2005; Kahdr 2009; Piffer 2009; Jenerette and Potere 2010; Shaker et al. 2011; Taubenböck et al. 2012; and others). Moreover, most studies argue that the main challenge of urban planning is how to provide services over a large geographical area. Additionally, this study focuses on the impact of rapid development over time on spatial growth and spatial resilience based on selected system components (e.g. geological ground, land use).

## 1.7 General research approach of the study

The concept, materials, and methods used in this study are described in detail in Chapter 3.

To facilitate understanding, I will now lay out how I carried out my work.

The work was divided into three distinct phases: pre-processing, processing, and post-processing which are described in detail in the following sections (Table 1).

**Table 1: Research approach of this study**

| Pre-processing | Processing | Post-processing |
|---|---|---|
| Literature and data collection | Georeferencing and enhancement (pre-processing) | Data management and interpretation |
| Field observation | Data processing and classification | Dissemination of processed data |
| Conceptual model | Post-classification (assessment) | Stakeholders interaction |

### 1.7.1 **Pre-processing steps**

The preliminary work focused on collecting the low- to high-resolution time series of Landsat thematic mapper (TM and ETM) and SPOT satellite images, and a digital elevation model (DEM) (together with some ancillary data, such as topographic and geological maps, and bibliographical information). To understand the area of study and its problems, I felt that it was important to obtain real information from the field. This step was followed by the implementation of the conceptual model to define the workflow.

### 1.7.2 **Processing and analysis of data**

The detection, monitoring and analysis of rapid development problems was carried out using a multi-temporal series of Landsat images which were analyzed with advanced remote sensing techniques (pixel-based and object-based classification). The land use land cover (LULC) was classified into several classes based on the land units identified during the pre-processing step. The classification was then refined and dynamic changes were detected.

### 1.7.3 **Post-processing and dissemination of information**

In this phase, the results were analyzed and interpreted. Finally the dissemination of digital data is recommended by using modern technologies such as open source web maps or smart display tools.

## 1.8 Outline of study

Chapter 2 focuses on the geological and physiographic setting of Greater Cairo metropolis and introduces a geo-map of the whole study area based on remote sensing applications. Therefore, the rock cover types are differentiated and the topographic relief dominating Greater Cairo is described. In Chapter 3, the concept and methodology of this study are described in detail. The DPSIR model is used and its looping process is modified for GCM monitoring and analysis. In addition, the remote sensing techniques and satellite data applied for change detection and spatial resilience are identified and discussed. Chapter 4 is concerned with the monitoring and analysis of the LULCC (land use/land cover change) to capture and define the state of spatial resilience of the whole GCM based on time series of TM and ETM satellite images, and the examination of pixel-based versus object-based classifications. The selected time span coincides with the economic reform that took place during the last three decades. For a higher level of monitoring, Chapter 5 deals with the further analysis at different levels of classification based on high resolution SPOT-satellite data and object based image analysis (OBIA). The classification is guided by three developments, which are the first metro line at Helwan, the ring road, and New Cairo city. The impact of these developments is recognized in three different zones selected for examination. Consequently, in Chapter 6, the main results are interpreted. The most affected areas in GCM are detected and the growth is explained. The trapping effect is used here for the first time and the response priorities are introduced.

The last chapter not only provides the conclusions of the study but also makes some recommendations. Therefore, I suggest how to disseminate the results so that they are easily available and can support planners, and also recommend an incubation strategy to reduce the stress on GCM.

# 2 Geo-cover of Greater Cairo

## 2.1 Introduction

Nowadays, many cities in developing countries are striving for reconstruction and sustainable growth after a long time of corruption and conflict. Hence, the planners of different disciplines need to access different types of information easily and to work confidently with modern technology. This chapter therefore aims to present the geological and physiographic setting of Greater Cairo metropolis and introduces a modified general rock cover scheme of the whole area. To do so, remote sensing techniques to differentiate the rock cover types and describe the topographic relief of the area dominating Greater Cairo are applied. The classification and nomenclatures used were based on field observations that take into consideration the previous geological studies published on the area and its neighborhoods.

## 2.2 Remote sensing and geology

Generally, the applications of techniques in order to obtain information about an object without touching the object itself are widely and extensively used in geological investigations. These techniques are mainly geophysical tools (e.g. electromagnetic induction, ground penetration radar, aeromagnetic, etc.) and satellite sensors. These were located far apart hence, the distance between the object and sensor is several kilometers or hundreds of kilometers (Gupta 2003). In the recent past, the remote sensing technique played a very important role in geological mapping, starting from the interpretation of aerial photographs and ending in the sophisticated enhancement, processing, and interpretation of images acquired by space satellites. These are able to show features and patterns which may not be distinguishable in aerial photographs due to the lack of color information (aerial photographs) (Ibrahim and Johari 1997). Therefore, the remote sensing techniques used allow not only geological mapping but also lithology and mineral differentiation and exploration on small and large scales respectively. Accordingly, the use of satellite images for geological mapping and for exploring economic resources is becoming an increasingly important issue for earth scientists.

Furthermore, 3D or elevation remote acquisition data provide mitigation and hydrological investigation for geo-hazards rather than topographic and relief description and measures. The latter proved that the application of digital elevation model analysis (DEM) is a potentially efficient,

reliable, reproducible and effective technique for undertaking geological terrain mapping. Abd Manap et al. (2010) concluded that the advantage of the 3D visual technique over conventional stereoscope interpretation is that the geological terrain features such as hillcrest, side slope, foot slope, straight slope, concave slope and convex slope can be observed not only from the normal vertical view but also according to different scales, orientations and perspectives.

A study conducted by Nalbant and Alpiekin (2010) showed that thematic mapper (TM) imagery can be used as a valuable tool together with field studies for geological mapping and structural patterns. This procedure can save an appreciable amount of time, money and manpower compared to the efforts exerted by earth scientists. It is also useful in undertaking geological terrain mapping, especially in inaccessible areas. The US Geological Survey carried out a research program in 1985 to produce 1:250,000-scale land-cover maps for Alaska using Landsat MSS data (Patrick et al. 1987). Sulatn et al. (1986) and Gad and Kusky (2007) demonstrated that TM data can be used to distinguish mineral potential from surrounding rocks in arid regions and to generate detailed maps over wide regions by using quantitative, reproducible mapping criteria. In addition, possibilities for locating suture zones in the less well known parts of arid continents are clear.

Ingram et al. (2008) evaluated the relationships between the geology, land use, and elevation parameters in north Mississippi, and discovered a strong correlation between the different rock formations and slope degrees. Therefore, land use information was extracted from satellite imagery, topographic parameters were derived from elevation data, and textural characteristics were generated from these datasets to provide a basis for surface mapping. However, integrated GIS (Geographic Information System) and remote sensing techniques which can be used effectively to develop a more comprehensive geological database to facilitate geological field studies have been occurring for large areas.

Most geological studies describing Greater Cairo do not apply remote sensing techniques in an advanced way. Hence, most work deals with raw image data by using color combination of multispectral satellite images to prepare preliminary maps regardless of the georeference, radiometric character or spectral analysis. Also, most maps were traced based on Thematic Mapper (TM) and Enhanced Thematic Mapper (ETM), which are now freely available from many open sources. Such studies conducted by some geologists (e.g., Osman 2010) who modified the geological map of Eastern Greater Cairo area based on false color composite and utilization of band combination 7, 4, and 2 for the red (R), green (G), and blue (B), respectively, that is the best visualization for the general lithological discrimination in the study area.

## 2.3 Materials and techniques

### 2.3.1 Data availability

Because of the rapid development and extensive human activities in the area around the Nile valley in Greater Cairo (hinterland and/or Nile valley terraces), the data selected are characterized by less cover of land use for a better discrimination of the rock units. Accordingly, I used Landsat 5 TM image data acquired in 1984 with seven bands (three invisible wavelengths, four in infrared), most of which have 30-meter resolution, except band six with 120 m resolution. Then, to increase the spatial accuracy of the TM-5 image, I merged the moderate resolution panchromatic image with 10m pixel resolution acquired in 1997 by Spot-2 sensor (TT station). The high resolution (5 m pixel resolution) of multispectral Spot-5 images acquired in 2006 by Spot-5 is available too for a good and accurate picture of surface exposures in the study area. Moreover, there is another sort of satellite data with elevation information that have been used to construct 3D visualization for the entire area of interest. This elevation data are obtained from ASTER GDEM, which is generally characterized by 30 m pixel resolution at 95% confidence horizontally and about 10 m at 95% confidence vertically. Furthermore, ancillary data such as scanned topographic sheets and geological map of scale 1:100,000 are utilized for the required nomenclatures and location detection.

### 2.3.2 Methodology

In this study, the work procedure is based on different techniques of image processing to extract geological and physiographic features. First of all, all satellite images and scanned sheets are georeferenced to UTM Zone 36 North projection with WGS-84 datum. Moreover, TM and Spot satellite data are enhanced to ensure radiometric balance between individual scenes, and the DEM data were mosaicked to cover the study area. This step was followed by a fusion technique to increase the pixel size and resolution of all TM image bands (Fig. 8) and thereby to obtain more spatial information of surface exposures. However, the maps that were produced based on TM reached a scale of 1:100,000, but the maps based on merged images reached a scale of 1:32,000 without remarkable pixels.

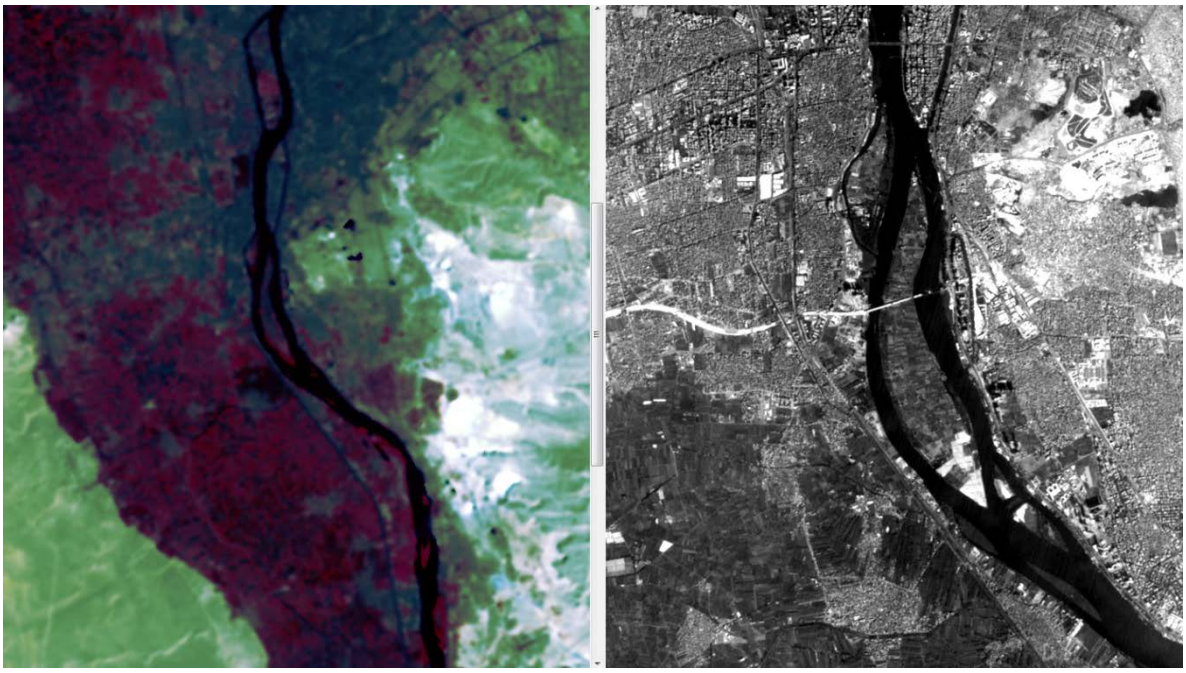

**Figure 8: TM image (1984) (left) and Panchromatic Spot band (1997) (right) represent low and high resolutions respectively**

The fusion process occurred by using the sharpen module which is provided with different merge algorithms in Erdas Imagine software. Therefore, I used the subtractive resolution merge algorithm in this study. Consequently, I tested the different band combinations for preliminary results of lithology discrimination. So, the combination between bands 7, 4, and 2, and 5, 3, and 2 were reviewed in RGB false color and presented the best image composites in the study area.

The principal component analysis (PCA) used in this study to reproduce the merged high resolution image allows inordinate and excessive data to be computed into fewer bands (ERDAS Guide 2010). In addition, Principal component algorithms are image enhancement techniques to visualize the maximum spectral contrast from many spectral bands to three primary display colors (Robert, 1997). These lead to a stretching of the pixels to differentiate different rock types. Furthermore, the bands of PCA data are non-correlated and independent, and are often more interpretable than the source data (Jensen, 1996). The PCA technique was applied separately to two different kinds of multispectral satellite data: TM with 7 bands and Spot with 3 bands. The difference after the removal of redundancy information showed that differences exist between the different bands of each image. Because of the wide range of spectral wavelength of TM data which have seven channels, I preferred to merge the enhanced 7 bands TM image with the coarse resolution SPOT band in rock discrimination, that is to compose a geo-digital thematic map rather than the multi-spectral Spot data which have only three channels.

Consequently, I found that the first principal component channel (PC1) has the largest possible variance, while the next two PC channels (PC2 and PC3) contain all other interband variations. Therefore, each one of the components from 3 to 7 in TM merged image are comprising less than 1.3% of information and seems unnecessary in lithological information (Fig. 9).

Therefore, in the classification process, I mainly used the first three principal components, calculated from preferred and enhanced TM merged image beside the field observations and experiences.

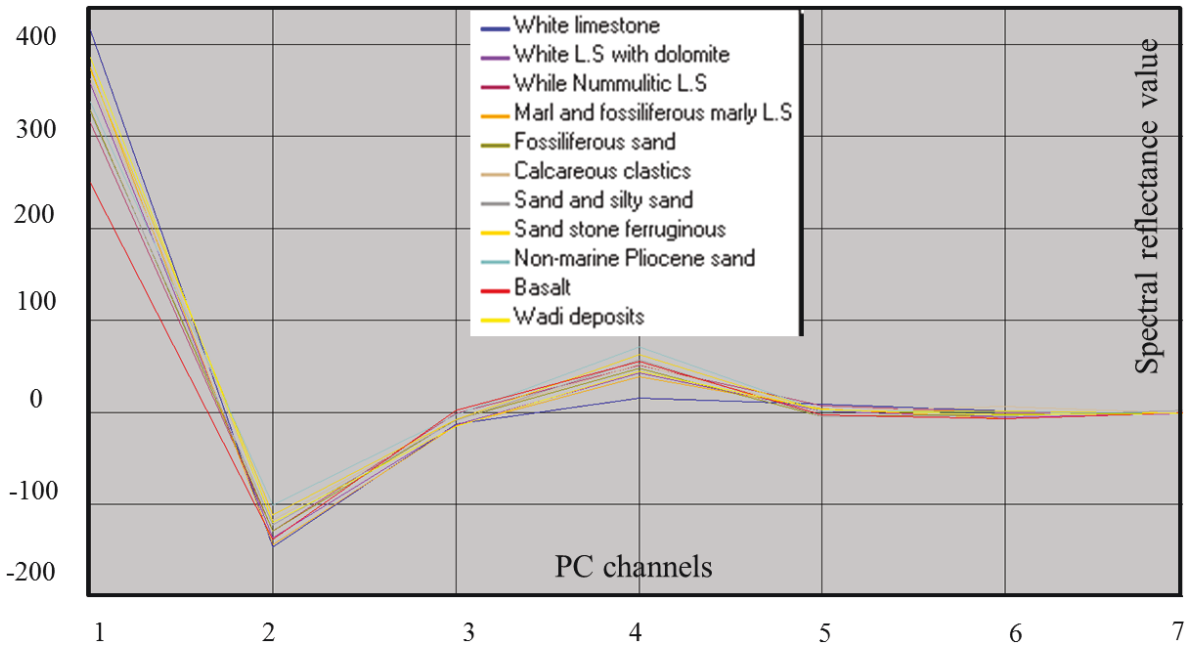


**Figure 9: The spectral reflection of the classified rock types based on PC channels (Erdas Imagine Software)**

The classification step is provided by the supervised classification method which assembles the surfaces that have similar spectral signatures. Once signatures have been examined, the classifier then attaches labels to all image pixels according to the trained samples (ground truth points). The procedure of supervised classification was carried out by using maximum likelihood algorithm, which assumes that each spectral class can be described by a multivariate normal distribution (Richards 1999). In spite of that, one of the objectives of this study is to increase the accuracy of assessment; but there are many control points acquired from the ground and estimated by the GPS used and interpolated in the process of classification to enhance the pixel selection and refine the rock type identification.

Finally, I extracted the morphological information and topographic features from the mosaic of digital elevation model (DEM) available (Fig. 10 and Fig. 11).

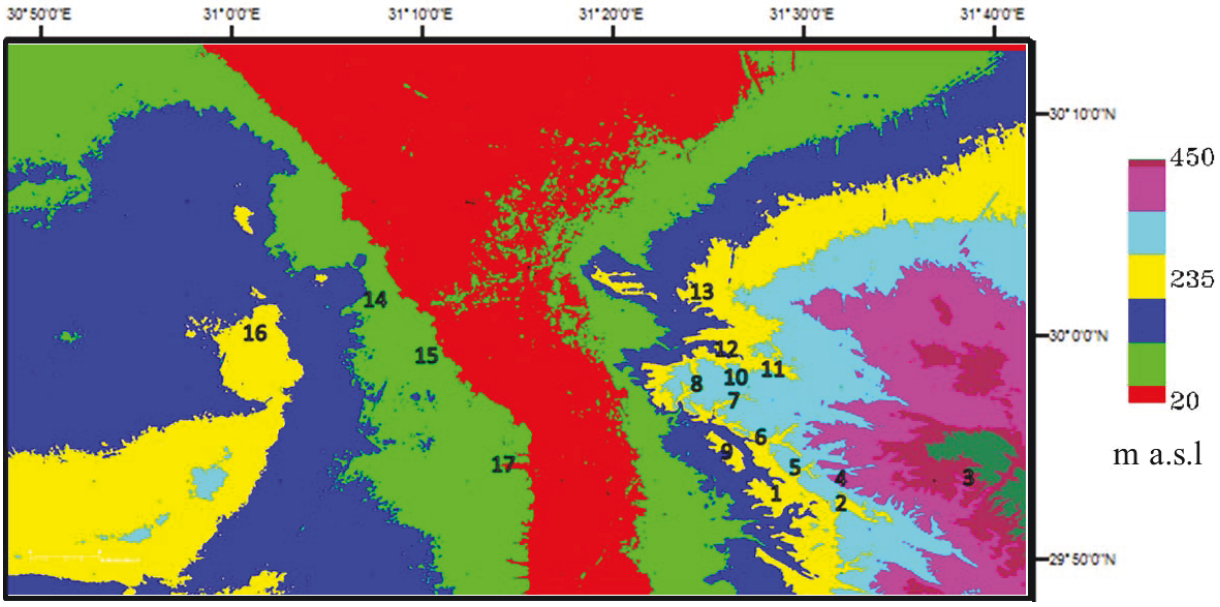


**Figure 10: Colored DEM of the Greater Cairo area based on ASTER GDEM data**

**1-15th May city, 2-Wadi Garawi. 3-El Halawana Height. 4-El Qurn Height. 5-Wadi Gibbu, 6-Wadi Abu Silli. 7-Wadi Hof. 8-Gabal Hof 9-Obesrvatiory Plateau. 10- Wadi Abu El Rokham. 11-Wadi Degla. 12-Wadi El Tih. 13-El Mokattam Plateau. 14-Abu Roach. 15-Pyramids Plateou. 16-6th of October City.17-Wadi El Tafla.**

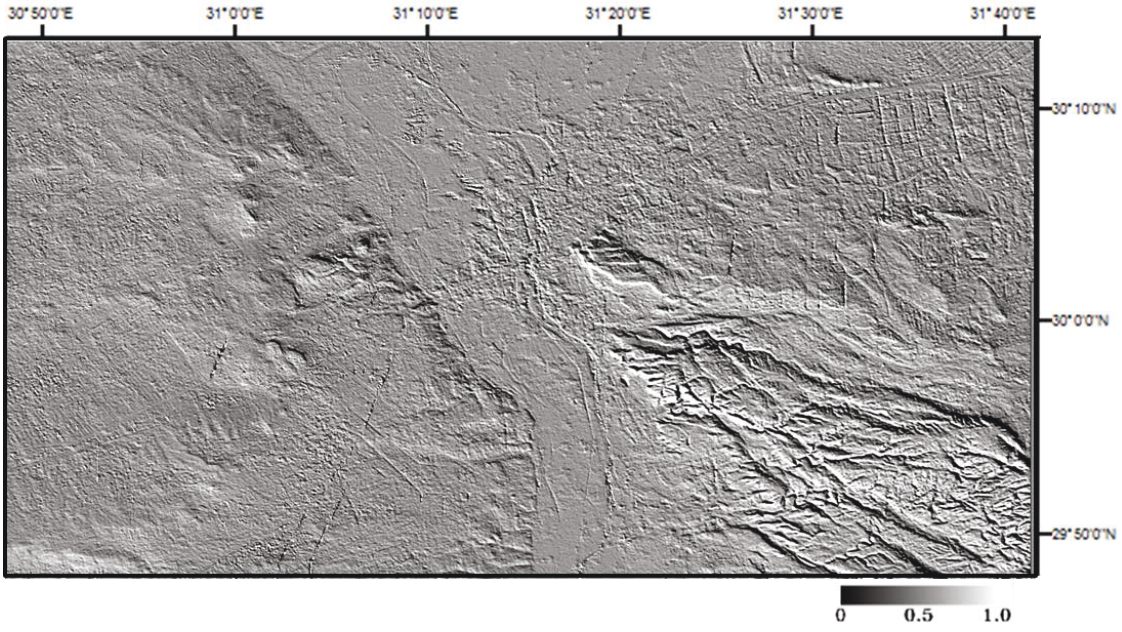


**Figure 11: Shaded relief (hill shading) of the Greater Cairo area based on ASTER GDEM data**

The techniques used to obtain and analyze the elevation information are principally supported by ENVI 4.7 software. Also, the digital maps produced could be scaled from 1:75,000 to 1:50,000.

## 2.4 Geology of GCM

### 2.4.1 Rock types

Many authors have studied the different time rock units cropping out in the eastern and western sides of Greater Cairo and have produced geographical maps and geological correlations (e.g., Frag & Ismail 1956; Said 1962; Abdel Khalek et al. 1989; Moustafa 1988, Moustafa et al. 1991 and 2003; Swedan 1991; Sehim 1993; and Osman. 2010).

The present application of remote sensing image processing techniques and field observation supplemented with the previous geological studies and nomenclatures in West-and-East Greater Cairo came to subdivide the rock exposure of the study area into the eleven rock types. Besides that, two dominating classes of the fertile Nile valley area are concerned too. One of them represents the urban materials and roads, and the other one is concerned as a mix class representing the green cover and water bodies.

Moreover, the spectral analysis of the exposed rocks in the area of interest is summarized and reported to show the relation between each band of PC (principle component) image and reflectance spectrum of selected pixels for classification (Fig. 9).

In short, the eleven litho-types covering the study area are mainly dominated by 1-white limestone (Chalk), 2- white limestone with dolomite, 3- white Nummulitic limestone, 4- marl and fossiliferous marly limestone, 5- sands and fossiliferous sandstone, 6- calcareous sandstone and/or eroded surface 7- sand and silty sand with subordinate clay intebeds, 8- sand stone (Ferruginous) with Gravels, 9- non-marine Pliocene sand, 10- basalt, and 11- Wadi deposits (Fig. 12).

These exposed rock successions range in age from Upper Cretaceous to Quaternary (Fig. 13).

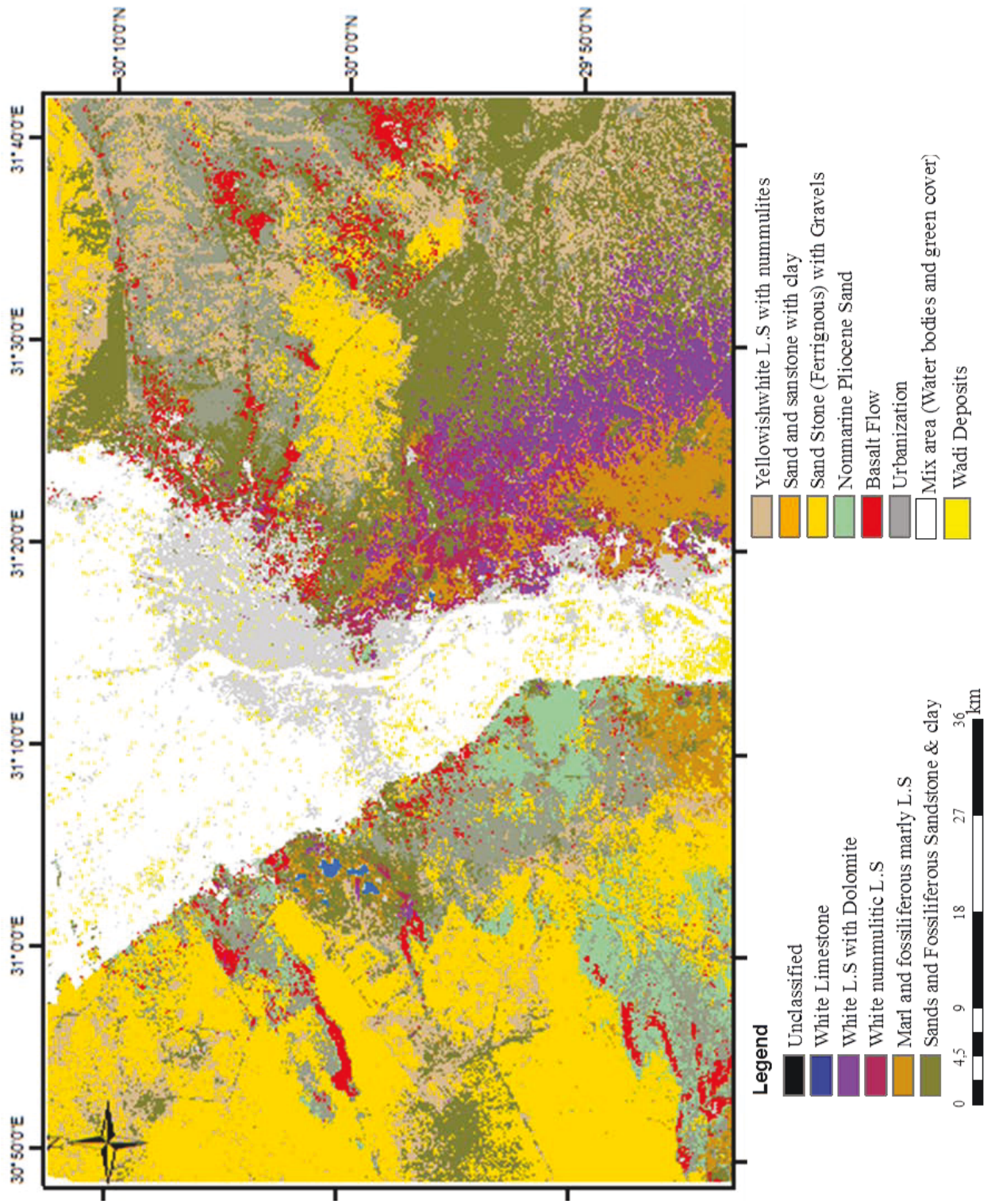


**Figure 12: Rock cover classification based on PCA**

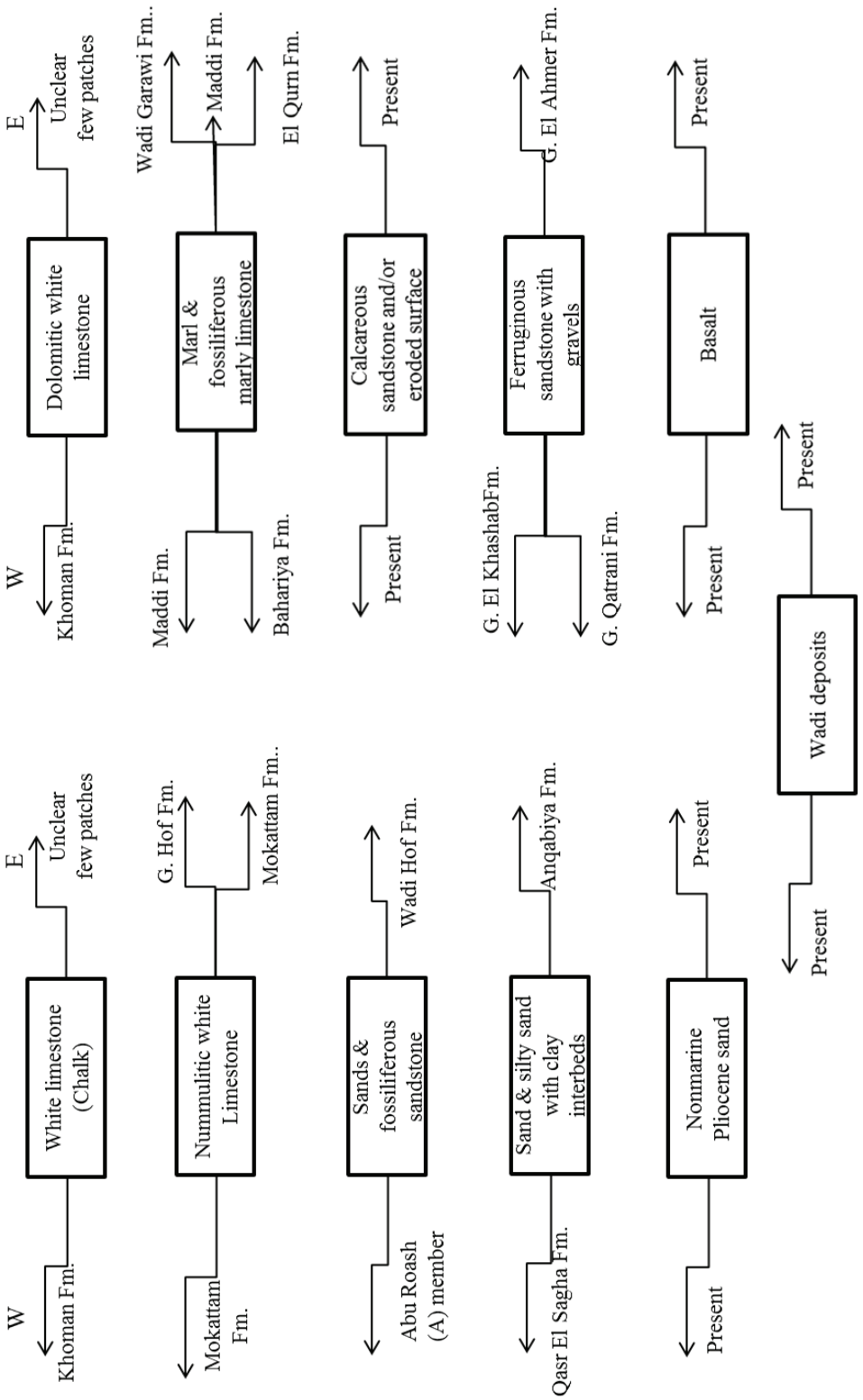


**Figure 13: Rock type scheme shows the rock types in east and west side of GCM and their different names**

1) White limestone (L.S)

The white limestone or chalk unit is distinguished by the first appearance of snow-white massive thick bedded chalk, with thin chert bands and nodules (Fig. 14). The chalk is exposed only in the Western part of the study area and mainly in Hassana Dom. According to Said (1962), the age of the chalk unit ranges from Campanian to Masstrichtian with a maximum exposed thickness of about 78 m. In the western part of the desert, this formation belongs to the Khoman Chalk and Senonian age (Norton 1967).

2) White limestone with dolomite

The white limestone contaminated with dolomite and / or marl is represented in the eastern part of the study area and mainly by Observatory Formation and slightly by Abu Roach Formation or Abu Roach "D" member in the Western part (Fig. 15).

The Observatory Formation belongs to the Middle Eocene and comprises the bedrock of the northern eastern part of 15th of May city and its northern extension (Osman 2010). Swedan (1991) has said that the formation is composed of white to yellowish white, marly and chalky limestone, intercalated with several interbeds of hard, grey, dolomitic limestone. The type section of this rock unit measured by Frag and Ismail (1956) in the northeast of Helwan below the Observatory establishment is about 77 m thick.

The Abu Roach Formation or "D" member (Abdel Khalek et al. 1989) is dominated mainly by white to yellowish white, dolomitic limestone with large amounts of large fauna (e.g. Acteonella). Said (1962) named the Turonian-Santonian beds in many parts of northern Egypt (including the study area) as Wata Formation, commonly used in Sinai.

3) White Nummulitic limestone

The white Nummulitic limestone class refers to the beds built up mostly of grayish-white, slightly chalky beds rich in Nummulites gizehensis, Nummulites beaumonti, N. subbeaumonti, Schizaster africanus, and Turbinella frequens (Farag and Ismail 1956). These beds are exposed from the Eastern part to the North of Helwan province, which are represented by the upper part of the Gabal Hof Formation. The former was named and subdivided into two units (up to 80 m in thickness) in its type locality at Wadi Abu Rakham by Frag and Ismail (1956). This formation is equivalent to the Middle Eocene rock unit cropped out at the escarpment of El Mokattam Plateau, east of Cairo city.

Along the western side of the Nile, the spectral analysis of this rock type does not show any good and/or obvious cover except in the area of the Pyramid plateau.

**Figure 14: Chalky limestone (Khoman Fm.) observed in the western part of study area (6th October City). Photo captured 2010**

**Figure 15: Well bedded limestone at Gabal Hof Fm. Photo captured (2010) at E Cairo city**

4) Marl and fossiliferous marly limestone

The marl and/or fossiliferous marly limestone are essentially represented in the eastern side of the study area by Upper-Middle to Upper Eocene time unit of El-Quran and Wadi Garawi Formations in southeast part and Maadi Formation in northwest part. Osman (2010), Frag and Ismail (1956), and Swedan (1991) have observed that the El-Quran Formation is mainly composed of about 70 m thick marl, marly limestone with thick gypsum veinlets, and hard dolomitic bands. In addition, they have stated that the Wadi Garawi Formation is very similar to the Maadi Formation, which is dominated by Carolia Placunoides, Plicatula polymorpha, Ostrea reili, Nummulites beaumontai, and N. striatus.

In the Western side of the study area, this rock class is recorded southwest and west of the Pyramid plateau with a maximum thickness of 154 m measured by Frag and Ismail (1956) and named Maadi Formation. To the north of the Pyramid plateau, this unit cropped out at the flanks of the macro structure of El Hassana Dom. In contrast, this class has built up of marl and fossiliferous marly limestone units which intercalates with sand and shale in the small part of the core of Abu Roach structure (Fig. 16). These units belong to the Cenomania (Lower Cretaceous) Baharyia Formation (Said 1962).

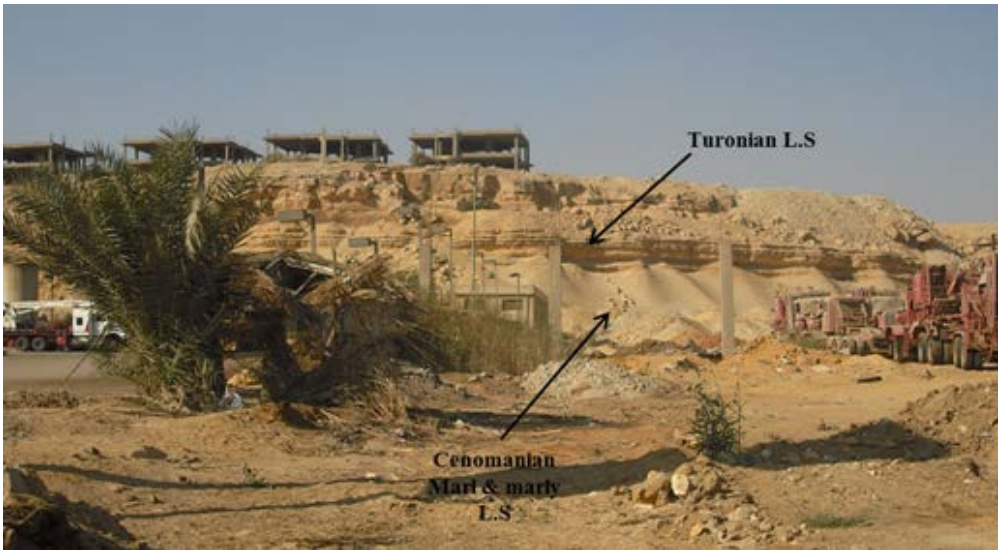


**Figure 16: The core of Abu Roach structure shows the marl and limestone rock units. Photo captured (2010) at W Giza city**

5) Sands and fossilifereous sandstone

The sandstone facies cover a large area east and west of Greater Cairo and comprise the bedrock of many parts of the new cities such as New Cairo, and 6th of October City. This rock type is mainly composed of sandstone, marl, yellowish green clayey marls, sandy limestone and bioturbated marly limestone. According to the descriptions of Frag and Ismail (1956), Moustafa et al. (1991), and Swedan (1991), the spectral signature of this class could be represented by Late Upper Eocene of Wadi Hof Formation and Anqabiya Formation in the eastern side of the Nile valley. On the other side of the Nile valley, this rock unit belongs to the upper part of Qasr El Sagha Formation. This formation concerned by Said (1990) and Swedan (1991). The upper most part is of the Eocene age and consists of poor fossiliferous clay and channel deposits with a minimum thickness regarding the original thickness. Also, this signature reflected the Coniacian-Santonian beds exposed in some areas at El-Hassana Dom.

6) Calcareous clastics and/or eroded surface

The spectral reflectance of this rock unit is very ambiguous all over the study area, but the field check oriented to identify it to be under the erosional surfaces of clastics and calcareous-clastics outcrops, in addition to some eroded Nummulitic limestone with clay contamination.

7) Sand and silty sand with clay

The exposed part of this rock type is found mainly in the Gabal El Mokattam area eastwards and very close to the area west to southwest of the Pyramids Plateau composed mainly of fine grained calcareous sand stone, grading upward silty sand and shale (Sewadan 1991; and Osman 2010). The unit could be represented in the Anqabiya Formation due east of the study area and some upper Eocene and Oligocene units due west (Qasr El sagha Formation). Generally, the pixel reflectance of this unit represents the unconsolidated sandstone and silt to shale outcrops in many parts of the study area.

8) Sandstone (ferruginous) with gravels

This exposure is widely distributed in the study area, especially to the east of the El Mokataum plateau including the East of Cairo (Nasr City), New Cairo City, and protected areas (forest of petrified wood) along the Cairo-Red Sea highway. This rock exposure belongs to the Gabal Ahmar Formation. Otherwise, this rock cover mainly dominates the region of 6th of October City and belongs to Gabal Qatrani Formation and Gabal El Khashab Formation (1991). However, Skukri (1954) and Said (1990) have stated that this formation comprises the extension of a narrow belt of

Oligocene-Miocene age from Suez via Cairo and onward into the north western desert, which is essentially dominated by distinct red bed sequences with coarse-grained sand and gravels with large amounts of petrified wood separated by basaltic sheets in between (Fig. 17).

9) Non-marine Pliocene sand

This rock unit in the area of interest consists mainly of fine to coarse friable sands and conglomerate sandstone of yellowish to brownish-white color (Said 1990; and Sewadan 1991). Its spectral reflection appears on the western side of GC, obviously accompanied by basaltic sheets, rather than on the eastern side (Fig. 18).

10) Basalt

The distribution of Oligo-Miocene deposits was governed by the volcanicity and tectonic activity which affected the Red Sea regions and the high belt between the stable and the unstable shelves in Egypt during the Oligocene (Said 1990). Therefore, the basaltic sheets in the study area were recorded within the sandstone beds of Oligo-Miocene beds in 6th of October City towards the west and the New Cairo area towards the east.

11) Wadi deposits

In the study area this rock unit is filled with recent fine clastics, deposits mainly of clay, which is often being reworked by eolian processes and stream deposits near the River Nile bank.

**Figure 17: Petrified wood forest at Gabal El Khashab, West of GCM. Photo captured 2009**

**Figure 18: Non-marine Pliocene caped by basaltic sheet, West of GCM. Photo captured 2009**

### 2.4.2 **Physiography**

Topographically, the study area can be divided into three parts, the first is represented by the lowest elevation corridor of the River Nile valley, the second is dominated by two plateaus detached by

two low areas on the eastern side of the area under investigation, and the third being the western side which is represented by topographic features and that form an almost featureless plain with the exception of some small structure-related heights.

Based on the analyzing and slicing of the digital elevation model (DEM), the elevation information, and slope degradation maps were extracted (Figs. 10 and 11).

Therefore, the area around the Nile River is mainly occupied by different human activities such as agriculture, housing, and industries with elevations ranging from 20 to 100m above sea level (asl).

The topographic features on the east side of GC are characterized by moderately rough relief and formed by soft rocks ranging in age from Middle Eocene to recent.

The highest elevation is recorded about 450m above sea level (asl) east of the El Halawana Height. In general, the landscape in the study area is characterized by numerous rugged and isolated hills mostly made up of hard Eocene limestone beds. Those are arranged from the south (close to 15$^{th}$ of May City) to the north (El Mokattam plateau), e.g. El Qurn Height (~270m asl), Observatory table land (~175m), Gabal Hof (~330m asl), and El Mokattam Plateau and New Cairo area (maximum ~287m asl). The wadies are usually controlled by different faults, directed N-E to N-S and E-W to ENE (Fig. 10). These wadies are generally of dendritic and sub-parallel types. The main wadies traversing the study area are:

Wadi Garwi to the southeast from 15$^{th}$ of May City,

Wadi Gibbu and wadi Abu Silli, which dissect 15th of May City and Helwan area towards due West, to North of Helwan area which present Wadi Hof which extends ESE-WNW and joins with Wadi Abu El Rakham at Gabal Hof area,

Wadi Degla, which is the most important protected area and the largest drainage line on the east side of GC delineating the southern scarp of El Mokattam plateau, and due North of the Wadi Degla is a small stream called Wadi El Tih bounding the New Cairo from the south.

Most of the surface of the West GCM area is covered with very gently dipping Tertiary-Quaternary strata including 6th of October City. However, the area in some parts is characterized by different topographic features mainly consisting of Giza Plateau (~120m) and small folded and faulted Abu Roach complex and El Hassana Dom to the north of the Giza pyramids (Fig. 19). That is highly manifested and controlled by both the lithologies and structures. The drainage lines have a very low degree of shaded relief (hill shading) (Fig. 11) on the western side of the GC and only Wadi Tafla south of the Pyramid could be detected.

**Figure 19: Hassana Dom in the Abu Roach area, West of GCM. Photo captured 2009**

## 2.5 Recommendation for future work

The Object Based Classification technique would be used with customized algorithms to refine the map produced. Hence, the spectral information is extracted from a group of pixels (object) rather than one pixel. And, also, the membership relation between objects is provided to assign the most homogeneous object to one category. That can support the studies of landslide risks and suitability of rock cover for construction activities. Therefore, the spatial analysis framework of GCM would be provided with the more detailed of advanced geo-environmental studies for geo-hazards mitigation.

# 3 Concept, Methodology and Materials

## 3.1 Concept

### 3.1.1 Spatial resilience definition

The term "resilience" and its definition have been the subject of debate amongst scientists. Recently, the resilience of a system has been defined by the resilience alliance (http://www.resalliance.org/index.php/key concepts date accessed: August 2010) as the ability to absorb disturbances, to be changed and then to re-organize and still have the same identity (retain the same basic structure and ways of functioning). Also, it includes the ability to reduce the magnitude of internal disturbances and absorb external shocks. Moreover, most applications of the resilience concept by environmentalists, planners, and sociologists seek to identify and assess the vulnerability, stability, robustness and diversity of socio-ecological systems (e.g. cities) (Lintz et al. 2012).

Furthermore, Cumming et al. (2005) have defined a resilient socio-ecological system as consisting of actors, components, and interactions. And system identity lies in maintaining these elements through space and time. The state of susceptibility to harm from exposure to stress associated with environmental and social change is seen as "vulnerability" by Adger (2006). Regarding system sustainability and environmental changes, Norberg and Cumming (2008) defined them as "the equitable, ethical, and efficient use of natural resources".

Many researchers have used the concept of spatial resilience to describe the relation between space and time with regard to the resilience of landscapes, resources and land use (Nystrom and Folke 2001; Peterson 2002; Evans et al. 2008), Cumming (2011) has described the different uses of the concept as follows:

- To cope with disturbances and avoid shocks thresholds at scales larger than the individual ecosystem.
- To indicate the vulnerability and resilience of landscapes to change.
- To include large scale functions and processes beyond the boundaries of an ecological unit.

"Spatial resilience" can be defined as the capacity of socio-ecological systems to make their own strategy choices to protect area-bounded, socio-economic and ecological functions and services against internal and external elements; these systems do so through adaptive forms of land use allocation, and integration across multiple spatial and temporal scales (Resilience Alliance 2010 and Cumming 2011).

As spatial resilience is a dynamic concept that can not only be applied to specific properties of the system, but can also be used to understand socio-ecological change (Cumming 2011), the present study implemented the spatial analysis concept by using the conceptual framework and physical change detection tool (technique) (Fig. 20). This could provide the GCM system with general principles (components, relations, and functions) to understand the spatial aspects of growth and vulnerability to change (resilience) at different scale and time of information.

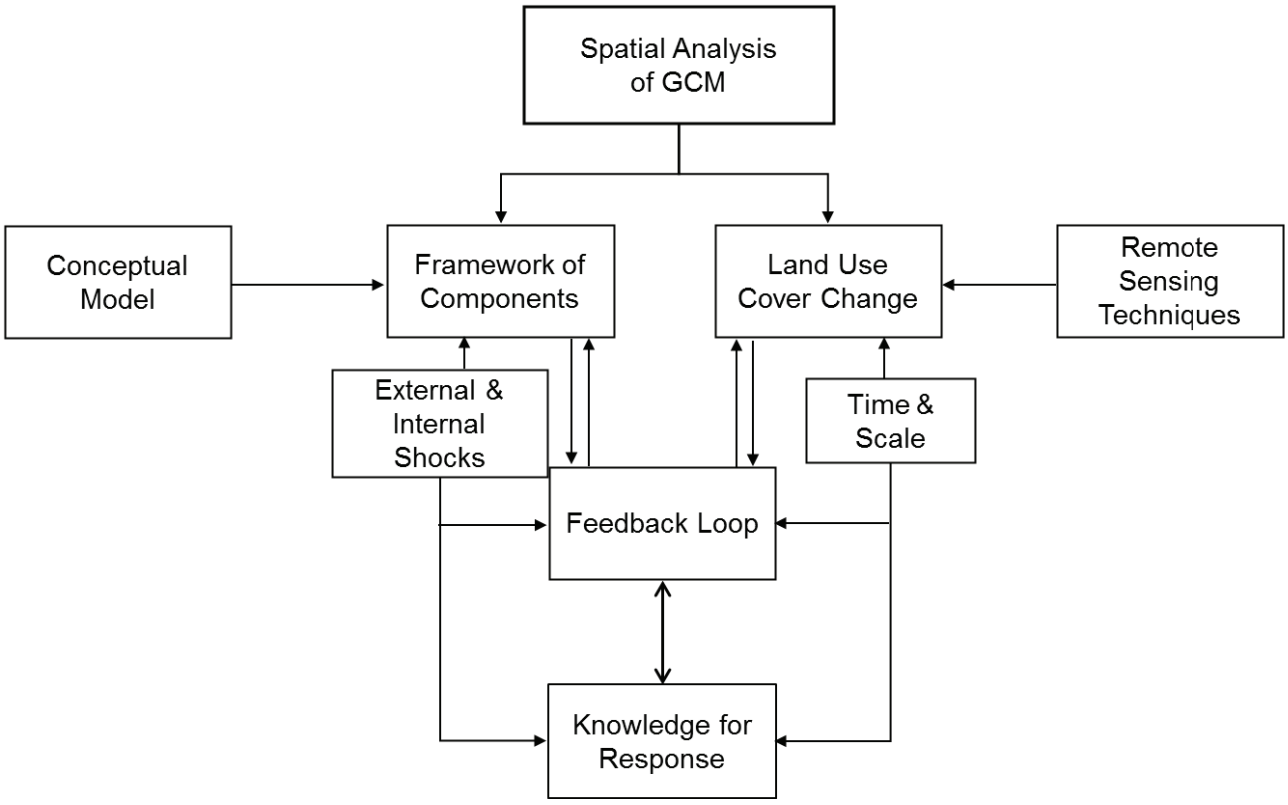


**Figure 20: Study concept for spatial analysis of GCM**

### 3.1.2 **Greater Cairo in the light of the DPSIR framework**

Landscape change is a highly complex process in terms both of the drivers affecting changes to natural and built environments and also of the outcomes or impacts of those changes (Evans et al. 2008). In addition, projects on megacities have shown that there is a need to develop a common set of definitions and working assumptions based on a conceptual framework (Perlman and Blueweiss 1990). Thus, understanding and analyzing challenges - such as rapid growth, rate of population growth and development, loss of fertile lands, urban sprawl, and lack of water in big cities in countries of global south (e.g. Greater Cairo in Egypt) are becoming complicated tasks in the environmental management approach (Fig. 21). This Chapter introduces a simple and flexible conceptual framework to extract and explore the drivers and components of spatial growth through complementation with change detection techniques. Hence, the relation between the different indicators, components, and affected elements are integrated and managed by applying the study concept (Fig. 20).

Therefore, a good starting point to understand the relevance of the internal and external dynamic components of a socio-ecological system is to introduce a conceptual framework (Anderies et al. 2004; and Houpin 2010). Additionally, Mourão et al. (2004) have stated that the determination of indicators is an excellent way to represent the environmental components while avoiding the measurement of too many parameters. Indicators are often adopted to avoid and reduce the complexity of environmental data.

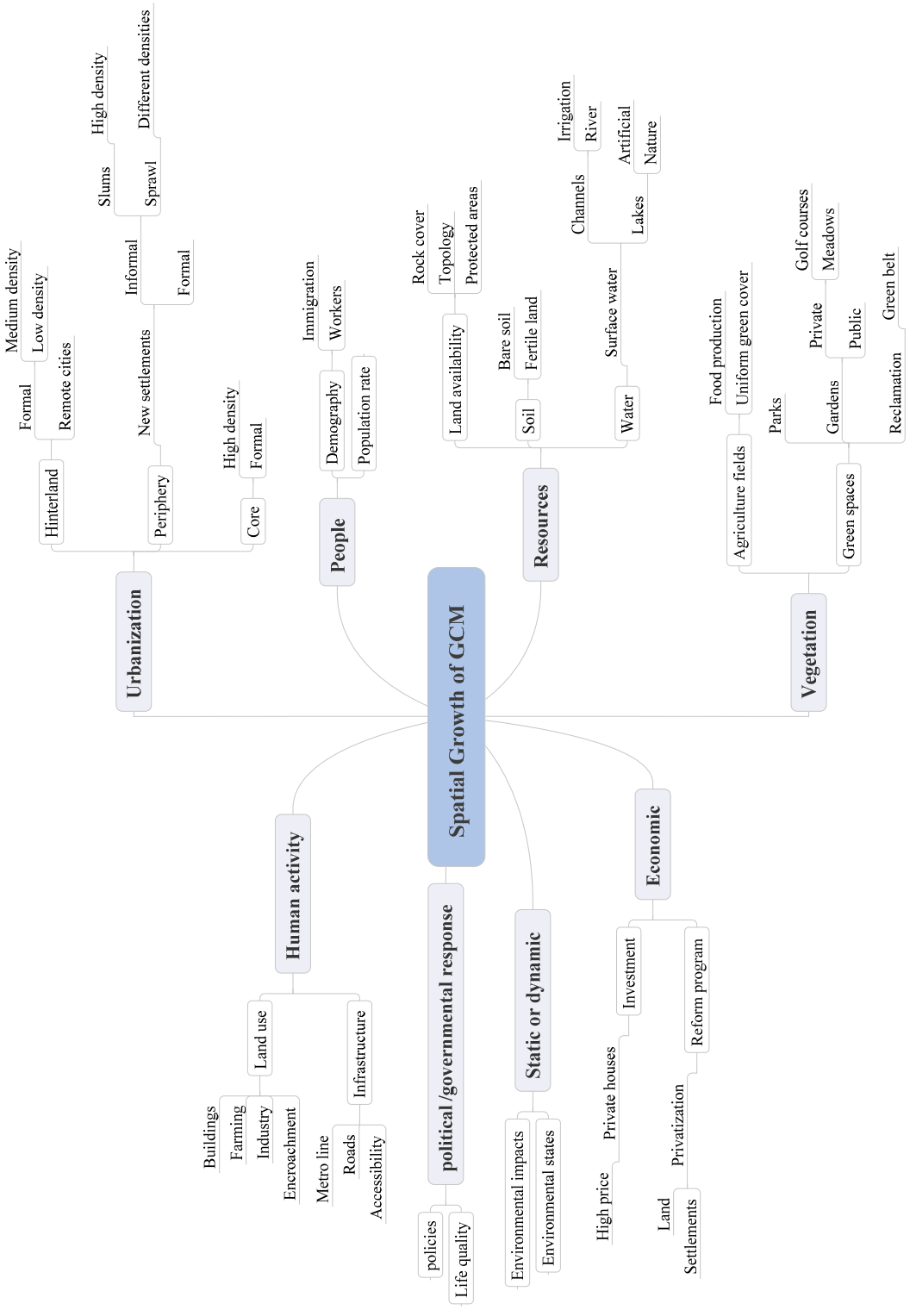


**Figure 21: The main components affecting the spatial growth of a complex system like Greater Cairo Metropolis**

Due to the spatial and temporal scope of the social ecological system (SES), change ranges from local to global over time that are relevant to the human use of natural resources (Pickett et al. 2007). Some authors have described and simplified the complex system of the real world to figure out key aspects of socio-ecological systems. Holling (1995) simulated the hierarchy of a complex system using the agent-based model, and he (2001) proposed that socio-ecological systems are composed of a series of interconnected adaptive cycles of interaction at different scales. Moreover, Kay and Boyle (2008) introduced a hierarchical model of structures and processes which focuses on flows, feedbacks, and thresholds based on the self-organization of resource dissipation (energy). And Ostrom (2009) divided the socio-ecological system (SES) into four interacting levels: resource units, a resource system, a governance system, and users. She aimed to identify relevant variables and provided a common set of variables to compare similar SESs. Also, Houpin (2010) developed monitoring and assessment tools which are dedicated not only to the basic indicators of urban mobility (travel, reasons, distance, time, cost), but also to other economic, social and environmental factors in order to assess the sustainability of urban development (network congestion, urban attractiveness, local accessibility, impact on public health, energy dependency). Hence, planners and urban designers could adopt a conceptual model to promote ecosystem resilience when planning new urban areas, such as in the support of "response diversity" among functional species groups, and in the support of ecosystem services (Colding 2007).

However, most of the conceptual models are complicated and analyze ecosystems in only one direction; for example, from top to down (i.e. hierarchy framework), using key comprises that do find links and relations between elements, and also fuzzy models which are changed core and fuzzy boundaries of a system. Here I tried to find and use a useful analytical tool to show back-forward relations between elements and to get a feedback mechanism (loops) that can provide support for monitoring and decision analysis processes of spatial resilience of GCM.

Therefore, in order to develop a strategy for integrated environmental assessment, the European Environment Agency (EEA) recommended a concept developed by the OECD (Organization for Economic Co-operation and Development 1993) which distinguishes between driving forces, pressures, states, impacts, and responses (DPSIR) (Fig. 22).

The DSPIR concept has been described by Kristensen (2004) and Camarrota and Pierantoni (2007) as the logic that helps to detect relations and causal links between the bulk of socio-environmental components: there are 'driving forces' (functions and activities that exert pressures on the

environment), 'pressures' (act of driving forces on the environment), 'states' (influence of acting pressure on the environment) 'impacts' (the reactions of the environment to changes of states), and finally social and political "responses" (laws, prioritisation, target setting, effective indicators, etc.). The strength of the DPSIR model is that it seems to show in a simple way the important connections between human needs and the state of the socio-ecological system. Also, it seems to help different disciplines, researchers, policy makers and stakeholders to communicate (Potschin 2009).

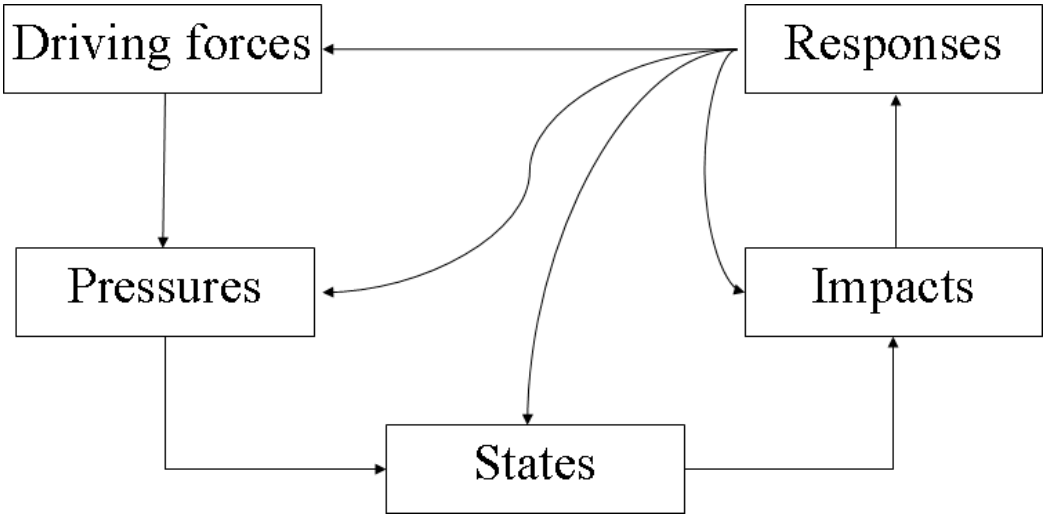


**Figure 22: DPSIR scheme (After: EEA 2007)**

Although planning is the function between human needs and natural resources with reference to the future (Prenzel 2004), few scientific analyses exist of how different land uses can be configured for greater support of ecosystem services (Colding 2007). Similarly, to understand and contribute to the spatial planning response of intricate megacity systems, this study mentioned that the complex function between human needs forces and the land states has to be easily translated to different levels of disciplines by flexible reporting system (framework).

Thus, in this study, I used the DPSIR model to conceptualize the main spatial components which affected the growth of GCM. Therefore, on the one hand, I have identified the causal relation between the different indicators and drivers, and on the other, I had explored the sequence of spatial change detection process in a monitor framework to deduct the main transformer indicators in GCM (Fig. 23).

However, population size is used as the primary criterion for the inclusion of megacities rather than a city's importance as a major communication node in the world hierarchy of cities (Friedman 1986). Indeed, population growth represents the main driving force behind environmental and spatial changes in land uses and planning. So, the conceptual model used in the present study assumed that population growth is the initial actor for growth but it is not represented in classification processes of LULC.

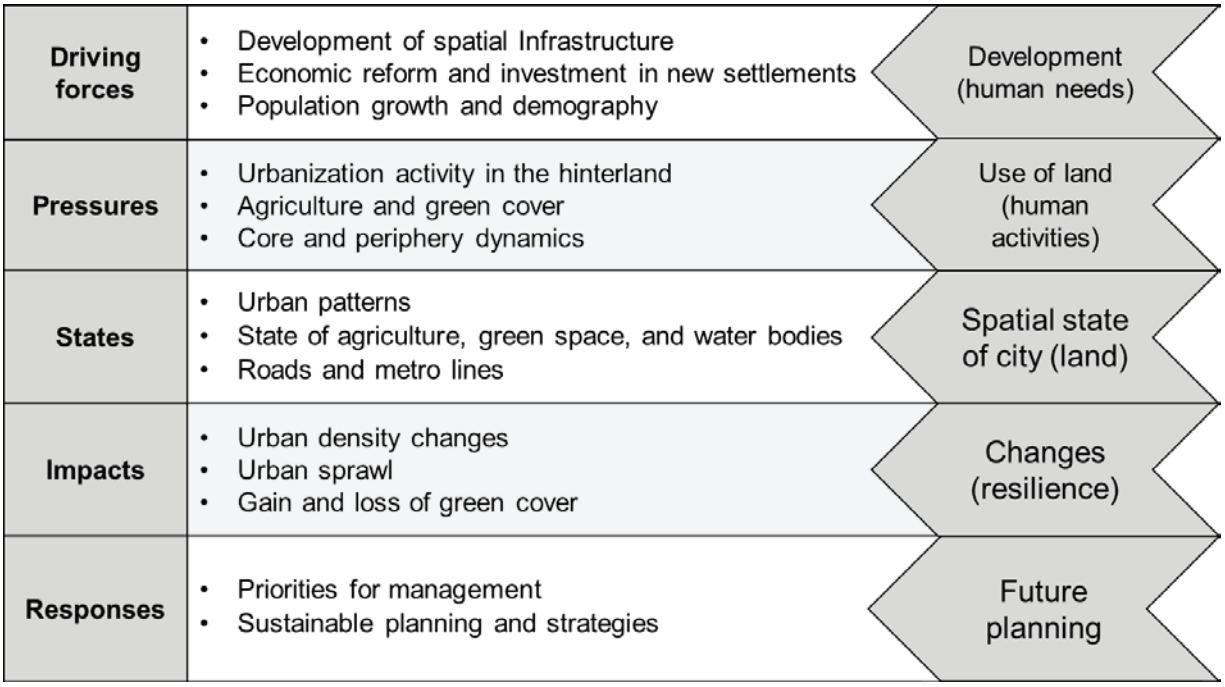


**Figure 23: Generic DPSIR scheme for spatial resilience analysis in GCM**

The components of the generic DPSIR concept illustrated above were focused on the causal link between the different aspects which could change the spatial pattern of GCM. Also, the relationship between the driving forces and the dynamic process of land use were linked for GCM.

Generally, the driving forces represent the human needs, capital potential and the development aspects and trajectories of the mega metropolis. In the present study these forces are starting from the reform of economic policies to the nature of land and its suitability for human activities through investment orientations and the problem of population growth.

These exert pressure on the land (city), which is explicitly reflected in urbanization, cultivation activities, space use, and resources (e.g. water). As a result of pressure on the land, the states of

main spatial indicators are affected, where the distribution and growth of the various spatial compartments (urbanization, green cover, desert, water, bare soil, etc.) in different scales of time and space are detected.

Consequently, the dynamical state of each component can be analyzed to find out the spatial and environmental impacts on the resilience of GCM. Spatial monitoring was applied to determine what and where the most degraded areas were, and also to put into place responses and plans.

Due to the exerting pressure on the land, the states of urbanization and losses of fertile land will be used in this study as major transformer indicators implemented and linked between dynamic processes through the DPSIR chain. Moreover, spatial monitoring is applied to determine what and where the effect of the failures were and to put into place responses to manage these changes. One of the benefits of using DPSIR has been mentioned by many authors (Mourão et al, 2004; EEA 2007; Potschin 2009): namely, that the response can take into account any indicator from driving forces, pressure, state and impact. In addition, I suggested that the work under subsidiary DPSIR can be expressed by the condition of the change detection process and its related criteria; such conditions as, the change in time scale and/or resolution and type of spatial data, target of analysis, and objective of stakeholder. Such work mechanism would be adding value to the function of DPSIR assessment framework and provide the feedback loops of monitoring process. Accordingly, the relationship between human activities (society) and the dynamic processes (spatial) of land-use-cover-change has been understood and implemented into the framework for response and system management.

### 3.1.3 **Change detection by using remote sensing techniques**

Remote sensing can be defined as the collection of information about an object, area or phenomenon without coming into direct contact with that object, area or phenomenon (Reddy 2001; Gupta 2003; Lillesand et al. 2003; Prenzel 2004). Thus, remote sensing has a wide range of applications and serves different kinds of disciplines in earth science, environmental and social science and even in economics. Images of space and identities represent an important part of common social memory for locally committed actors and form an important context of orientation for human land use (Schmidt 2012).

There are different sensors available that provide an opportunity to increase the area and frequency with which users are able to monitor the earth's surface with different spatial data resolutions ranging from fine (e.g. Landsat TM and ETM) to very high resolution data (VHR) (e.g. SPOT, IKONS, etc.). That is done by sensing and recording reflected or emitted energy and processing, analyzing and applying that information (Woodcock et al. 2001) (Fig. 24). Different satellite systems have different characteristics (Table 2), i.e. resolutions, number of bands, and therefore have their own importance for different applications.

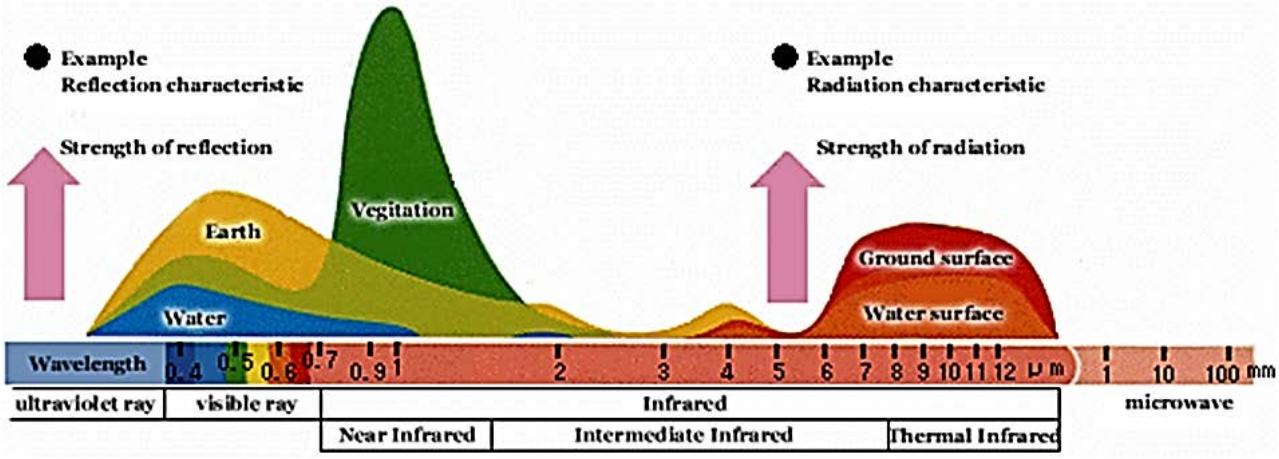


**Figure 24: Strength of reflection and radiation of electromagnetic waves from plants, earth and water in each wavelength (From: JAXA 2003) (please consider the mistake from the source in typing of vegetation word)**

Most planners and administrative bodies of large cities now require reliable information to assess the consequences of growth, to ensure a sustainable functioning of cities, and to minimize the negative impact of environmental degradation. Moreover, spatial expansion in the developing world often takes place in an unplanned manner, and administrations are unable to keep track of growth-related processes (Griffiths et al. 2010). So, information based on remote sensing is one of the most important resources to support urban planning and administration in megacities (Maktav et al. 2005). Additionally, satellite imagery provides a synoptic view of the urban mosaic and remote-sensing data can complement limited in situ measurements in urban areas (Rogan and Chen 2003; Kwarteng and Small 2010).

Because of the lack of information and difficult ground accessibility in some areas, the use of information gained through remote sensing is of particular relevance in the world's developing countries (Miller and Small 2003).

**Table 2: Some major satellite systems and their characteristics, Source: http://geoportal.icimod.org/ (date accessed: Sep. 2009)**

| Satellite Systems | Spatial Resolution | Type | Number of Bands | Launched by |
|---|---|---|---|---|
| LANDSAT-TM | 30m | Multi-spectral | 7 | USA |
| LANDSAT-ETM | 30m + 15m | Multi-spectral | 8 | USA |
| LANDSAT-MSS | 80m | Multi-spectral | 4 | USA |
| SPOT-XS | 20m | Multi-spectral | 3 | France |
| SPOT-PAN | 10m | Panchromatic | 1 | France |
| IRS-1C PAN | 6m | Panchromatic | 1 | India |
| LISS-III | 24m | Multi-spectral | 4 | India |
| WiFS | 188m | Multi-spectral | 2 | India |
| SPIN-2 | 2m | Panchromatic | 1 | USA/Russia |
| IKONOS | 1m | Panchromatic | 1 | Canada |
| IKONOS | 4m | Multi-spectral | 4 | Canada |
| ADEOS-AVNIR M | 16m | Multi-spectral | 4 | Japan |
| NOAA | 1.1Km | Multi-spectral | 5 | USA |
| MOS | 50m | Multi-spectral | 4 | USA |

Remote sensing data can help us to address both time and space considerations on a wide range of scales (Prenzel 2004). Moreover, extracting information on change is an extension of this basic remote sensing paradigm in that a temporal component is included (Quenzel 1983). So, remote sensing data have been used to examine the possibilities of multi-temporal imagery for mapping and monitoring changes in land cover and environmental change (Curtis et al. 2001; Sobrino et al. 2000). Also, remote sensing can reveal spatial-temporal growth trajectories of cities, which allow a thorough understanding of the impacts of urbanization on ecosystems and ecosystem services (Griffiths et al. 2010).

Recently, several remote sensing satellite sensors (described above in Table 2) have enabled the detection of change to a particular object between two or more time periods. This availability of different resolutions of satellite images, which launched by different sensors in different dates, has encouraged many spatial and environmental planners to specify different applications to improve spatially and spectrally historical data and collected information of the land. Hence, analyzing the spatial-temporal patterns of land use or land-cover (LULC) is the basic premise of the monitoring and driving forces analysis, and can even lead to more precise predictions of regional land use-cover-change (LULCC) (Deng 2002). Based on that, land use-cover-change on a large scale is a key aspect of global environmental change, and indicates the influence of human activities on the physical environment (Lei et al. 2005).

LULCC can be reduced to three tasks: the dynamic analysis of process, the detection of driving forces, and the global and regional modeling of LULCC (Li 1995). Moreover, monitoring information can then be combined with different layers to help to predict which areas were affected in the past and which could be at risk in the future, allowing secure decisions to be taken where they are needed most. Therefore, the successful utilization of remotely sensed data for land-cover and land-use monitoring requires careful selection of an appropriate data set and image processing techniques (Lunetta 1998). Consequently, Landsat TM and ETM+ provide an opportunity to extend the area and frequency with which we are able to monitor the earth's surface on large geographical scales (e.g. megacities) (Curtis 2001). Curtis (2001) claims that monitoring LULCC for large cities could provide fast and preliminary spatial information of alternative elements which could be dynamically and rapidly transformed. So, in this study I used the time series of Landsat TM and ETM for change detection analysis of the whole area of GCM.

Further, planners and land managers require spatial data of high resolution to represent land-cover and land-use problems at higher thematic levels, and therefore high resolution space-borne images are required (Rogan and Chen 2004). Accordingly, the higher level of change detection analysis has occurred based on medium to high resolution data acquired by SPOT satellites.

## 3.2 Materials and methods

### 3.2.1 Methodology framework

In order to achieve the study goals, satellite images with different dates and types were collected and used, as well as topographic sheets (scale 1:100,000 and 1:50,000) and geological maps of Greater Cairo (scale 1:250,000 and 1:100,000) constructed by the Geological Survey of Egypt.

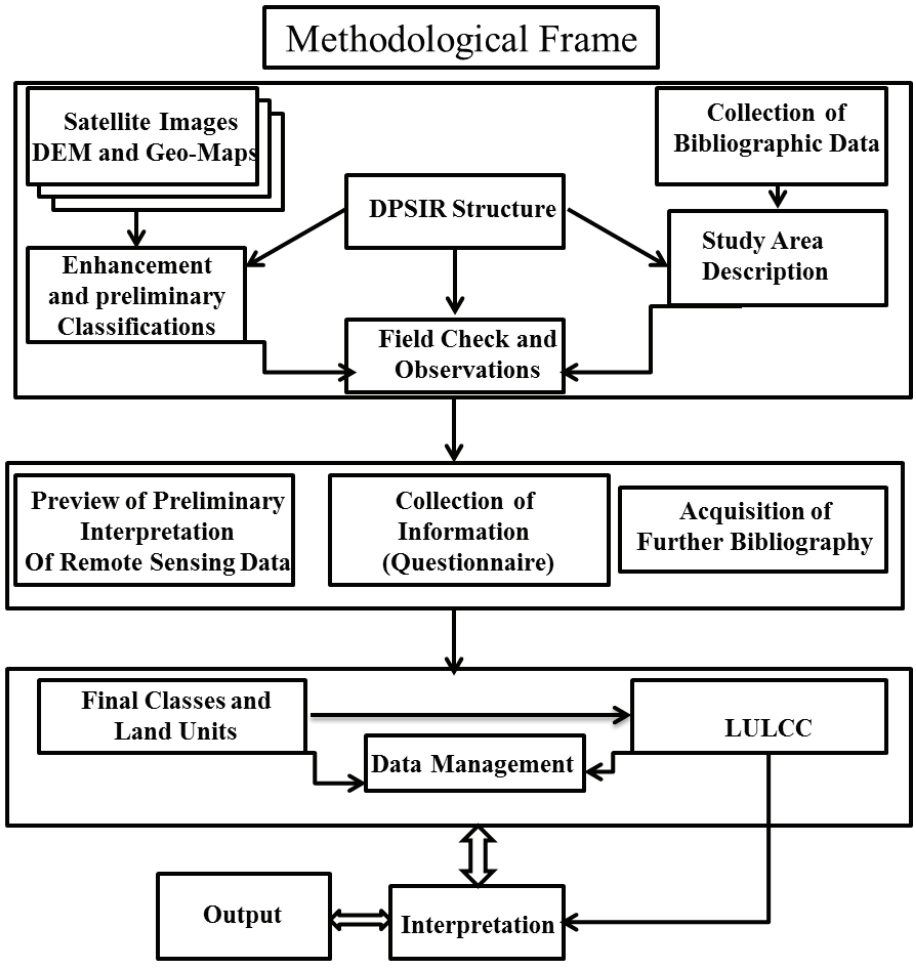


**Figure 25: The methodological framework of the study**

The latter was followed by field observations and validation, which were carried out during field trips extended for about eight non-consecutive weeks. In the third step, undertaken after the fieldwork, the final LULC and LULCC multi-temporal maps and its legend were defined and the export data stored and analyzed. The multi-temporal layer was organized and managed by using the

geographical information system (GIS) ArcGIS.10 software and then the interpretation of land changes was performed and a final output of the whole work was created. There are two programs mainly used for data processing and classification; ERDAS IMAGINE 9.1 and 9.10, and eCognition Develpoer 8.4 and 8.64. This methodological framework and the phases of the work are shown in Figure 25.

### 3.2.2 **Satellite images**

This study is based on time series of Landsat TM & ETM images (path 176, row 39), from 1984 to 2006 (the image of 1984 is considered as the reference year for the other images) (Table 3). These images are orthorectified Landsat imagery provided by the Global Land Cover Facility (GLCF; http://glcf.umiacs.umd.edu/).

**Table 3: Description of Landsat image data used in the study (modified after: http://landsat.usgs.gov/index.php (date accessed: Sep. 2009))**

| Reference year | Sensor resolution | Path/Raw |
|---|---|---|
| 1984 | Landsat 5 TM 30m | 176/39 |
| 1990 | Landsat 5 TM 30m | 176/39 |
| 2006 | Landsat 7 ETM+ 30m | 176/39 |

The main differences between Landsat 5 and Landsat 7 are the ETM+ instrument, with an eight panchromatic band, and the thermal IR channel with 120m spatial resolution for Landsat 5 and 60m for Landsat 7 (Table 4).

**Table 4: Radiometric characteristics of Landsat images (after: http://landsat.gsfc.nasa.gov/, date accessed: Sep. 2009)**

| Satellite instrument | Spectral Resolution (µm) | Bands | Spatial resolution |
|---|---|---|---|
| Landsat 5 TM | Band 1: 0.45 – 0.52 | Blue | 30 |
| | Band 2: 0.52 – 0.60 | Green | 30 |
| | Band 3: 0.63 – 0.69 | Red | 30 |
| | Band 4: 0.76 – 0.90 | Near IR | 30 |
| | Band 5: 1.55 – 1.75 | Mid IR | 30 |
| | Band 6: 10.4 – 12.5 | Thermal | 120 |
| | Band 7: 2.08 – 2.35 | Mid IR | 30 |
| Landsat 7 ETM+ | Band 1: 0.450 – 0.515 | Blue | 30 |
| | Band 2: 0.525 – 0.605 | Green | 30 |
| | Band 3: 0.630 – 0.690 | Red | 30 |
| | Band 4: 0.760 – 0.900 | Near IR | 30 |
| | Band 5: 1.550 – 1.750 | Mid IR | 30 |
| | Band 6: 10.40 – 12.5 | Thermal | 60 |
| | Band 7: 2.080 – 2.35 | Mid IR | 30 |
| | Band 8: 0.52 – 0.92 | Pan | 15 |

Landsat spectral feature space is limited for assessing land features (Herold et al. 2002, Phinn et al. 2002). I therefore used coarse resolution SPOT images (Table 5) to improve understanding of land-cover changes and the means to observe them in more detail. Hence, the use of SPOT images led me to investigate both the patterns and processes of land-cover and land-use change at another level of classification. A variety of more detailed maps have also been produced. For instance, this study includes change and differentiation in vegetation cover and change in urban densities that required coarse satellite images. The spectral characters of the images acquired by SPOT Earth observation satellites are presented in Table 3.4, which is a source of information for studying, monitoring, forecasting and managing natural resources and human activities on our planet.

**Table 5: SPOT spectral bands and resolutions. Source: (http://www.spotimage.com/web/en/172-spot-images.php (date accessed: Feb. 2010))**

| Sensor | Electromagnetic spectrum | Pixel size | Spectral bands |
|---|---|---|---|
| SPOT 5 | Panchromatic | 2.5 m or 5 m | 0.48 - 0.71 µm |
| | B1 : green | 10 m | 0.50 - 0.59 µm |
| | B2 : red | 10 m | 0.61 - 0.68 µm |
| | B3 : near infrared | 10 m | 0.78 - 0.89 µm |
| | B4 : mid infrared (MIR) | 20 m | 1.58 - 1.75 µm |
| SPOT 4 | Monospectral | 10 m | 0.61 - 0.68 µm |
| | B1 : green | 20 m | 0.50 - 0.59 µm |
| | B2 : red | 20 m | 0.61 - 0.68 µm |
| | B3 : near infrared | 20 m | 0.78 - 0.89 µm |
| | B4 : mid infrared (MIR) | 20 m | 1.58 - 1.75 µm |
| SPOT 1 | Panchromatic | 10 m | 0.50 - 0.73 µm |
| SPOT 2 | B1 : green | 20 m | 0.50 - 0.59 µm |
| SPOT 3 | B2 : red | 20 m | 0.61 - 0.68 µm |
| | B3 : near infrared | 20 m | 0.78 - 0.89 µm |

The SPOT images span a time period of approximately fourteen years (1994-2008) (Table 6) and were acquired from different SPOT sensors. This study was provided with these images by SPOT IMAGE FRANCE within their Planet action program.

**Table 6: SPOT scenes of Greater Cairo used in this study, (http://www.spotimage.com/web/en/172-spot-images.php (date accessed: Feb. 2010))**

| Reference year | Sensor resolution | Code |
|---|---|---|
| 1997 | Spot 1-3: 10 m panchromatic | SCS21R20A |
| 1999 | Spot 4: 10 m color | SCSH1R20N |
| 2008 | Spot 5: 5 m color | SCS61R20N |

The digital elevation model (DEM) that covered the area of interest has been cut and separated from ASTER GDEM (http://www.gdem.aster.ersdac.or.jp, Access date: Oct. 2010). The ASTER Global Digital Elevation Model (ASTER GDEM) is a joint product developed and made available to the public by the Japanese Ministry of Economics, Trade, and Industry (METI) and by the United States National Aeronautics and Space Administration (NASA). It is generated from data collected from the advanced spaceborne Thermal Emission and Reflection Radiometer (ASTER), a spaceborne earth-observing optical instrument. That DEM is utilized to obtain information concerning elevations and to describe the physiography of GCM in a geo-setting study (Chapter 2). The ground information and location names are taken from topographic sheets printed by the General Authority of Egyptian Survey.

### 3.2.3 **Image processing**

A series of processing operations were performed on the acquired images whether SPOT or Landsat. Most of these processes were carried out by using ERDAS IMAGINE software (versions 9.3 and 2010) and the following description of modules is mainly based on the user guide of ERDAS IMAGINE.

For georeferencing, all images used in this study were re-projected using Universal Transverse Mercator (UTM) map projection for zone 36 and WGS84 datum.

A pre-classification enhancement was undertaken to prepare the raw image for classification. A number of modules and techniques were chosen, which I shall now describe.

Radiometric correction was used to compensate the effects of the atmosphere. Radiometric correction can be achieved through many functions such as detailed correction of atmospheric effects, calibration to surface reflectance, and bulk correction of atmospheric effect. Although the study area is located in an arid region and most of the available images have zero cloud cover, some radiometric corrections were performed to confirm the processes of change detection. Such processes started from simple contrast and remove strip lines (for TM and ETM+ images), through linear stretching, haze reduction, and histogram matching.

To be sure that the images used for change detection have the same resolution in all subsets of time series images, the spatial resampling module was applied. Therefore, the Landsat images were

resampled to 30 m for the bands 1, 2, 3, 4, 5, 7, to 15 m for panchromatic and to 60 m for thermal bands using the nearest neighbor algorithm. The spatial resampling tool was utilized on the SPOT subsets, which were resampled to 10 m by 10 m and 5 m by 5 m for SPOT4, and SPOT5 respectively.

Furthermore, the subset images were tested by using the AutoSync function in ERDAS IMAGINE to be geometrically corrected and edge matched. This application seems to be obligatory for applications such as change detection, resolution merge (pan sharpening), mosaic, and even simple layer stacking. That is to avoid the shifting between overlapped layers (Fig. 26).

IMAGINE AutoSync uses an automatic point-matching algorithm to generate thousands of tie points, and produces a mathematical model to tie the images together (Fig. 26). The resulting workflows significantly reduce or sometimes completely eliminate manual point collection. The output should be generally equal or better in accuracy in comparison to the raw subset images (ERDAS user guide 2010). In some cases, the Gamma method was applied to SPOT images in particular to increase the surface reflection of concrete areas, green cover, and water rather than the desert and rocky cover.

In order to produce a test area for the band selection, different band combinations were tested, and alternatives of false color composites were displayed to select the best possible outcome. Accordingly, false color composites from TM and ETM+ bands (RGB 7, 4, and 2) and (RGB 4, 3, and 2) were used to show the best quality for separating the available land use/land cover features, while all of the six bands (ETM+ bands 1, 2, 3, 4, 5 and 7) were used for pixel and object based classification. From my point of view, it should be noted that standard RGB 4, 3 and 2 band combinations provide very useful information for land use mapping and a false color composite of RGB 7, 4 and 2 is particularly suitable for providing useful information for land cover in the periphery and desert areas (Fig. 27).

**Figure 26: Pre-classification synchronizing process to match the used images to detect dynamic changes. Left: two images before synchronizing. Right: after synchronizing process (Erdas Imagine)**

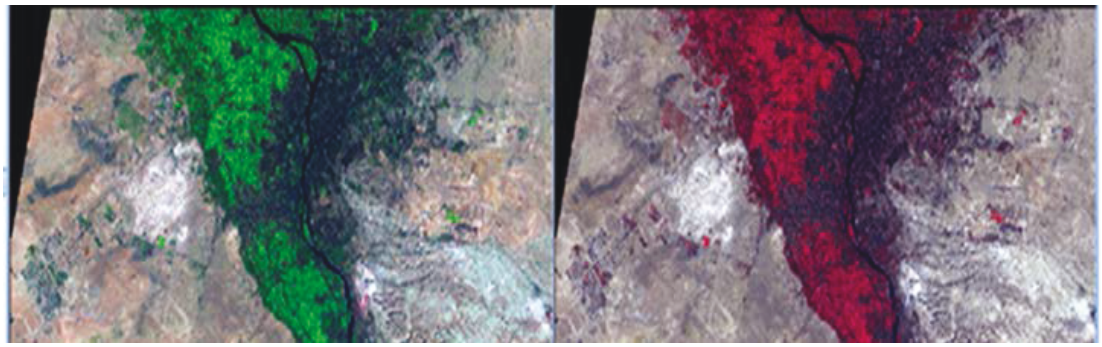

**Figure 27: Two different band combinations of Landsat ETM+; the right image shows RGB 4, 3, and 2, and the left shows RGB 7, 4, and 2 (Erdas Imagine)**

In a similar way, false color composites from SPOT 4 and 5 bands (RGB 1, 2, 3 and RGB 2, 1, 3) were constructed to show best quality for separating the available land use/land cover features, while all of the three bands (Spot 4 and 5 bands 1, 2 and 3) were used. What can be noted is that standard RGB 1, 2 and 3 band combinations provide very useful information for land use mapping and a false color composite of RGB 2, 1 and 3 is particularly suitable for providing useful information for land cover in the periphery and desert areas. Additionally, a subset of spot images mosaic of the study area was compiled to cover the whole of the study area, which was used mainly for the soft method of object-based classification (Fig. 28).

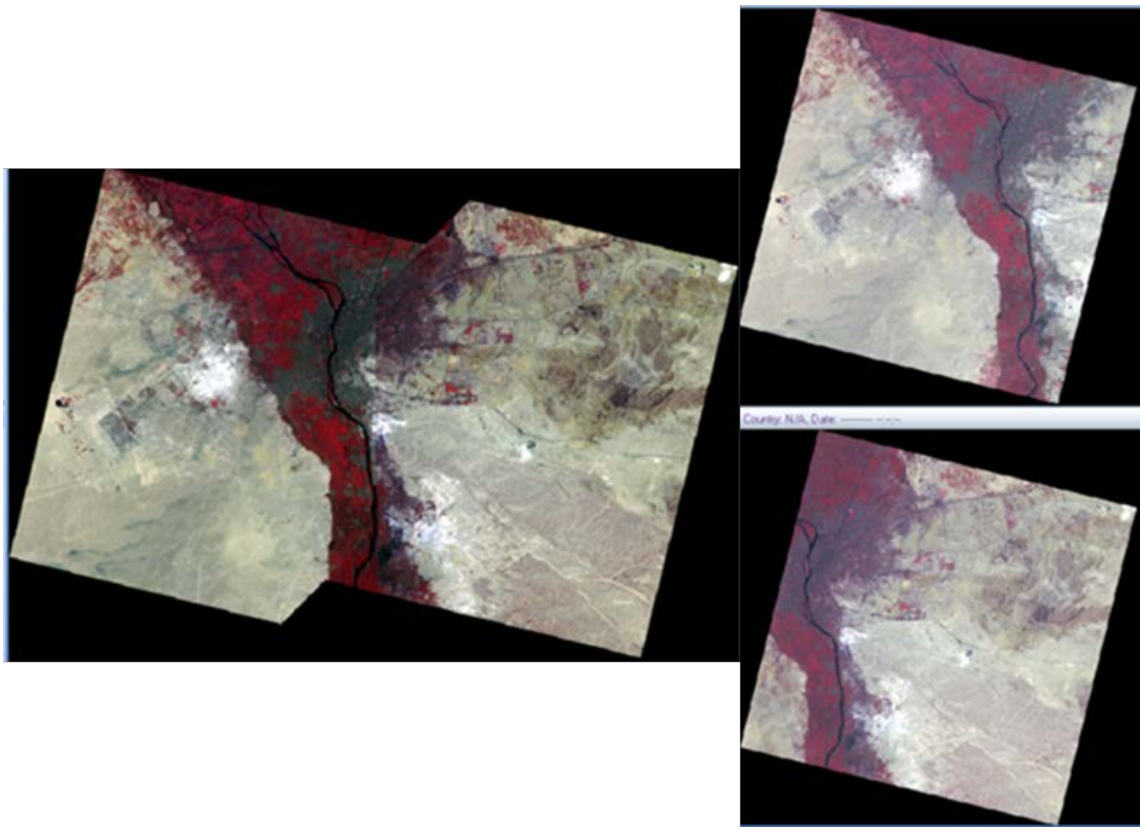

**Figure 28: Mosaic compiled for SPOT-5 images. Right: view of two different scenes (East and West Greater Cairo) Left: view of resulting mosaic (Erdas Imagine)**

### 3.2.4 **Classification**

A more significant issue is the fact that an ideal classification approach for a large area, using multiple images and a land cover mapping application, has not yet been developed (Franklina and Wulder 2002). Therefore, this study examined the two most common remote sensing techniques used in image classification. The classical one is the pixel-based classification and the more advanced one is the object-based classification. The applicability of pixel-based analysis in complexly structured land-use and land-cover (LULC) areas is limited because the semantic information necessary to interpret an image is usually not represented in single pixels. Therefore, both pixel and object based approaches were used and compared. This involves a certain trade-off between the richness of detail of medium to high resolution (MHR) remote sensing imagery such as the SPOT image used here and the generalizing nature of low to moderate resolution (LMR) sensors such as the 30 m spatial resolution of Landsat TM and ETM+ used in this study, too. Furthermore, the pixel-based approaches use conventional statistical techniques, such as supervised and

unsupervised classification. When the image is analyzed in supervised classification, the pixel categorization process is "supervised" by specifying numerical descriptions of the various land cover-types presented in a scene using the computer algorithm. This approach has shown good accuracy for images acquired by little coarse resolution sensors, while in the case of MHR images it was considered that the spectral mutability increases within a particular class, making the extraction of thematic information more difficult (Foody 2002). Accordingly, various new techniques were taken into account besides the spectral data, namely the texture features of the image were used as an additional layer in the classification process (Puissant et al. 2005).

The advances of object-based classifications are examined here for city land use/land cover classifications. Hence, object-based analysis facilitates work with meaningful image objects and their mutual relationships (Matinfar et al. 2007). Moreover, there are many algorithms and indices which were applied mainly by using object-based techniques to differentiate between the classified units and to refine the classified results (Table: 7).

**Table 7: Land-use-land-cover indices used in this study**

| Indices | Equation | Reference |
|---|---|---|
| Land water mask (LWM) | ([Mean Layer 3NIR]) / ([Mean Layer 1Green])*100 | Carroll et al. 2009 |
| Normalized difference moisture Index (NDMI) | (NIR-IR) / (NIR+IR)<br><br>Modified by author for SPOT to (R-IR)/(R+IR) | Skakun et al. 2003 |
| Normalized difference vegetation index (NDVI) | ([Mean Layer 3NIR]-[Mean Layer 2red])/([Mean Layer 3NIR] + [Mean Layer 2red]) | Rouse et al. 1973 |
| Green normalized difference vegetation index (GNDVI) | (NIR-green)/(NIR+green) GNDVI= (NIR-Green)/(NIR+Green) | Giltelson et al. 1996 |
| Ratio vegetation index (RVI) | NIR/Red. | Birth and McVey 1968 |

**Pixel-based (PB) classification**

Supervised classification was performed using TM and ETM+ bands. The following basic steps were taken: (1) select training samples which are representative and typical for that information class; (2) perform classification after specifying the training samples set and classification algorithms of ERDAS IMAGINE software. Training samples were selected according to ground truth points. The pixel related to the training sample was assigned to reference land unit in the image to create a class.

The selected algorithm for performing the supervised classification is characterized by minimum-distance classification, thereby determining the mean spectral value in each band for each class. The degree of compactness of each class could be estimated from the standard deviation for each feature of the pixels making up close affiliation to training sample for a given class.

Generally, most classification methods are based on per-pixel information, a pixel-based method is associated with the mixed-pixel problem because of the heterogeneity of landscapes as well as the limitation in spatial resolution of imagery. The problems are common particularly in medium and coarse spatial resolution (Castelli et al. 1999; Walter 2004; and Robertson and King 2011).

**Object-based (OB) classification**

In complexly structured land-use and land-cover (LULC) areas, pixel-based analysis is limited because the semantic information necessary to interpret an image is usually not represented in single pixels and also because the statistical independence assumption for pixel-based classifications involves the digital number of reflection (DN) values individually without considering the neighborhood pixels (Castelli et al. 1999). Thus, the image segmentation approach was used for object-oriented analysis and classification. This approach segments the pixel images into homogeneous objects based on the spectral and spatial features of neighboring pixels. A classification is then made based on objects, instead of individual pixels (Lu and Weng 2007). Segmentation is the main and initial process in the object-based classification technique in eCognition Developer software and any other software supported by that module which aims to create meaningful objects. This means that an image of an object should ideally represent the pattern of each object in question. This pattern, combined with further derivative color and texture properties, can be used initially to classify the image by classifying the generated image objects.

Thereby, the classes are organized within a class hierarchy and rule set structure. With respect to the multi-scale behavior of the objects to detect, a number of small objects can be aggregated to form larger objects constructing a semantic hierarchy (Matinfar et al. 2007). In performing the segmentation of the SPOT images, four and three spectral bands (5 m and 10 m resolution 1, 2, 3, 4) were taken in the segmentation process with full weight. The biggest benefit of the applied OB classification by eCognition software is the ability to use the membership function module which helps us to overcome and/or deal with the fuzzy relationship between classified units.

### 3.2.5 **Accuracy assessment**

The accuracy assessment has been done here not only to compare the classification results and ground truth, but also to evaluate the classification processes and results that have been done by using PB and OB classification techniques. The PB accuracy assessment was achieved by using ERDAS IMAGINE software and ground truth point. There were about one hundred GPS points (geographical position system), which were essentially used with some random point and used to evaluate the classification processes. The total accuracy and kappa (K) statistics indicated that the accuracy of PB classification ranged from 60% to 72% and from 0.5 to 0.6 respectively for classified images (Fig. 29).

ACCURACY TOTALS

| Class Name | Reference Totals | Classified Totals | Number Correct | Producers Accuracy | Users Accuracy |
|---|---|---|---|---|---|
| Unclassified | 0 | 0 | 0 | --- | --- |
| | 0 | 0 | 0 | --- | --- |
| Bare soil | 1 | 3 | 1 | 100.00% | 33.33% |
| Semi-urban (Urb | 21 | 15 | 6 | 28.57% | 40.00% |
| | 0 | 0 | 0 | --- | --- |
| Water | 1 | 1 | 1 | 100.00% | 100.00% |
| Desert area | 65 | 74 | 62 | 95.38% | 83.78% |
| Urban area | 15 | 5 | 3 | 20.00% | 60.00% |
| Cultivated land | 9 | 14 | 7 | 77.78% | 50.00% |
| Totals | 112 | 112 | 80 | | |

Overall Classification Accuracy = 71.43%

----- End of Accuracy Totals -----

KAPPA (K^) STATISTICS

Overall Kappa Statistics = 0.5032

Conditional Kappa for each Category.

| Class Name | Kappa |
|---|---|
| Unclassified | 0.0000 |
| | 0.0000 |
| Bare soil | 0.3273 |
| Semi-urban (Urban to Cultivated | 0.2615 |
| | 0.0000 |
| Water | 1.0000 |
| Desert area | 0.6136 |
| Urban area | 0.5381 |
| Cultivated land | 0.4563 |

----- End of Kappa Statistics -----

**Figure 29: Accuracy assessment of PB classified TM image (1984) (screen shot after Erdas Imagine)**

The results of the OB classification were evaluated by using the accuracy assessment based samples module in eCognition software. The evaluation process considered the object (group of pixels) rather than one pixel. That led me to use fewer training samples and to provide more spectral information. The total accuracy of classified images exhibited ranged from 78% to 90%, and the kappa statistics ranged from 0.77 to 0.8 (Fig. 30 and 31).

| User Class \ Sa... | Water84 | Vegitation Cover... | Baresoil84 | Urabanarea84 | Desert84 | Losse urbanizati... | urabna-cultivate... | Basalt84 | Sum |
|---|---|---|---|---|---|---|---|---|---|
| **Confusion Matrix** | | | | | | | | | |
| Water84 | 7 | 0 | 0 | 0 | 0 | 0 | 0 | 0 | 7 |
| Vegitation Cover84 | 0 | 12 | 0 | 0 | 0 | 0 | 0 | 0 | 12 |
| Baresoil84 | 0 | 1 | 4 | 0 | 0 | 0 | 0 | 0 | 5 |
| Urabanarea84 | 0 | 0 | 0 | 10 | 0 | 0 | 0 | 0 | 10 |
| Desert84 | 0 | 0 | 0 | 0 | 48 | 3 | 1 | 2 | 54 |
| Losse urbanization... | 0 | 0 | 0 | 10 | 0 | 0 | 0 | 0 | 10 |
| urabna-cultivated84 | 0 | 0 | 1 | 0 | 0 | 0 | 12 | 0 | 13 |
| Basalt84 | 0 | 0 | 0 | 0 | 1 | 0 | 0 | 2 | 3 |
| unclassified | 0 | 0 | 0 | 0 | 0 | 0 | 0 | 0 | 0 |
| Sum | 7 | 13 | 5 | 20 | 49 | 3 | 13 | 4 | |
| **Accuracy** | | | | | | | | | |
| Producer | 1 | 0.923 | 0.8 | 0.5 | 0.9795918 | 0 | 0.923 | 0.5 | |
| User | 1 | 1 | 0.8 | 1 | 0.8888889 | 0 | 0.923 | 0.6666667 | |
| Hellden | 1 | 0.96 | 0.8 | 0.6666667 | 0.932 | 0 | 0.923 | 0.5714286 | |
| Short | 1 | 0.923 | 0.6666667 | 0.5 | 0.8727273 | 0 | 0.8571429 | 0.4 | |
| KIA Per Class | 1 | 0.914 | 0.7908257 | 0.452 | 0.9612245 | -0.09615384615 | 0.9131759 | 0.4864865 | |
| **Totals** | | | | | | | | | |
| **Overall Accuracy** | **0.8333333** | | | | | | | | |
| **KIA** | **0.777** | | | | | | | | |

**Figure 30: Accuracy assessment of OB classified TM (1984) (eCognition Developer)**

| User Class \ Sa... | Water08 | Vegetation08 | AgricultureFields... | Lessdense vege... | Urbanization08 | Medium density ... | low density dens... | Very High densit... | Rocky and hinte... | Bare soil2008 | Sum |
|---|---|---|---|---|---|---|---|---|---|---|---|
| **Confusion Matrix** | | | | | | | | | | | |
| Water08 | 12 | 0 | 0 | 0 | 0 | 0 | 0 | 0 | 0 | 0 | 12 |
| Vegetation08 | 0 | 2 | 0 | 0 | 0 | 1 | 0 | 1 | 0 | 0 | 4 |
| AgricultureFields08 | 0 | 1 | 12 | 0 | 0 | 0 | 0 | 0 | 0 | 1 | 14 |
| Lessdense vegeta... | 1 | 6 | 0 | 22 | 1 | 2 | 0 | 0 | 0 | 0 | 32 |
| Urbanization08 | 0 | 0 | 0 | 0 | 8 | 3 | 0 | 1 | 0 | 0 | 12 |
| Medium density ur... | 0 | 0 | 0 | 0 | 2 | 28 | 1 | 0 | 0 | 0 | 31 |
| low density density... | 0 | 0 | 0 | 0 | 6 | 3 | 17 | 1 | 1 | 0 | 28 |
| Very High density08 | 0 | 0 | 0 | 0 | 0 | 1 | 1 | 53 | 2 | 0 | 57 |
| Rocky and hinterla... | 0 | 0 | 0 | 0 | 0 | 0 | 3 | 0 | 28 | 0 | 31 |
| Bare soil2008 | 0 | 2 | 1 | 2 | 0 | 0 | 0 | 0 | 0 | 11 | 16 |
| unclassified | 0 | 0 | 0 | 0 | 0 | 0 | 0 | 0 | 0 | 0 | 0 |
| Sum | 13 | 11 | 13 | 24 | 17 | 38 | 22 | 56 | 31 | 12 | |
| **Accuracy** | | | | | | | | | | | |
| Producer | 0.923 | 0.1818182 | 0.923 | 0.9166667 | 0.4705882 | 0.7368421 | 0.7727273 | 0.9464286 | 0.9032258 | 0.9166667 | |
| User | 1 | 0.5 | 0.8571429 | 0.6875000 | 0.6666667 | 0.9032258 | 0.6071429 | 0.9298246 | 0.9032258 | 0.6875000 | |
| Hellden | 0.96 | 0.2666667 | 0.8888889 | 0.7857143 | 0.5517241 | 0.8115942 | 0.68 | 0.938 | 0.9032258 | 0.7857143 | |
| Short | 0.923 | 0.1538462 | 0.8 | 0.647 | 0.381 | 0.683 | 0.5151515 | 0.8833333 | 0.8235294 | 0.647 | |
| KIA Per Class | 0.919 | 0.1677721 | 0.9182477 | 0.9036585 | 0.4423529 | 0.6972407 | 0.7422793 | 0.9294643 | 0.8886627 | 0.9106335 | |
| **Totals** | | | | | | | | | | | |
| **Overall Accuracy** | **0.8143460** | | | | | | | | | | |
| **KIA** | **0.7857671** | | | | | | | | | | |

**Figure 31: Accuracy assessment of OB classified SPOT (2008) of metro-autostrad sector (screen shot after eCognition Developer)**

## 3.3 Conducting a field check and observation

A field check of the results was conducted in order to compare the results obtained from the accuracy assessment report with the actual situation on the field and landmarks (buildings, cultivated land, water bodies, etc.). The field work was carried out during several visits to the study area in 2009 and 2010 with the purpose of assessing the agricultural land, hinterland and the urban environment. It was found that the cultivated-urban (CU) class is more difficult to separate accurately by spectral and even texture analysis because of the fine resolution of Lands SAT images. However, by using the medium to high resolution SPOT images, this difficulty was reduced with the exception of some urban-green areas (e.g. El Maadi). The bare soil (BS) class, on the other hand, offered an even more complicated problem, because large bare land has limited spatial distribution and is usually affected by the neighborhood objects of vegetation or urbanization. Thus,

the field observations revealed that most CU objects dominated different size areas of bare soil. On the one hand, the urban areas ranged from high density to low density which explored five patterns that could not be differentiated by using a pixel-based module and fine data, while the object-based analysis showed some success in recognizing the sub-class of loose urbanization. On the other hand, using SPOT images helped to differentiate the density of urbanization into high, medium, and low, with the limitation of pattern identification which was verified by field observations. In general, the desert showed high accuracy in both techniques with little confusion in low density areas (new settlements).

## 3.4 Implementation of DPSIR into LULCC analysis

Using an appropriate spatial methodology, we can hope to discover the true underlying relationships between system components and indicators (Anselin 2001). Therefore, the application of the DPSIR model with remote sensing data can provide an empirical monitoring system (spatial resilience framework) on different levels. These levels increase with an increasing reflectance and spatial resolution, as well as ground information. At any level of monitoring, sublevels can be included which are oriented to obtain a specific response for a specific indicator or component which provide the feedback (looping) mechanism inside the system. Based on the data available, the present study examined two monitoring levels (Fig. 32).

Therefore, the DPSIR schemes were introduced here to guide and describe the position and the role of the derived indicators through the framework of monitoring process that determines the spatial changes at different levels and scales of time and space.

Generally, the fine satellite data used here to classify and detect the dynamic change of the whole study area were the first level of information extracted and implemented by using the DPSIR scheme (Fig. 23 and 32). On that level, it has been assumed that the land use and land cover were represented in the DPSIR scheme by the driving forces that exerted a pressure on the land, and their indicators were classified to show the state of classified indicators under a specific time (year). Accordingly, the states of the selected year were analyzed and interpreted in order to determine the degree of spatial changes over the time span at that level of classification (Fig. 33).

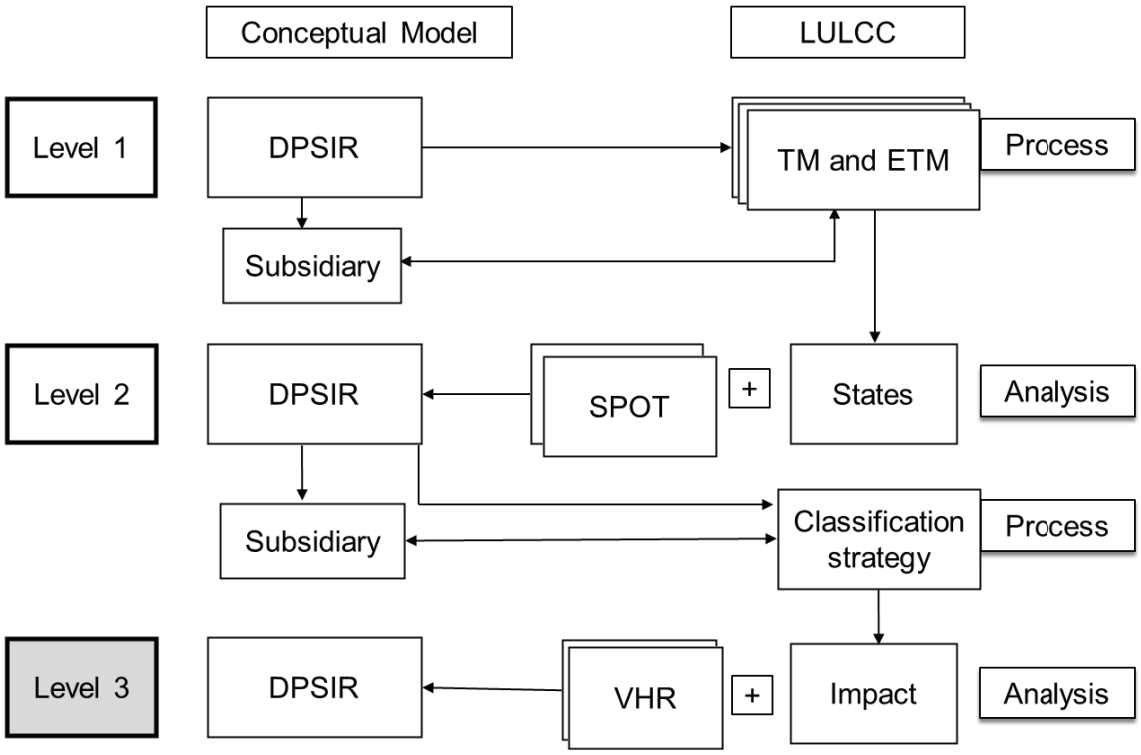


**Figure 32: The monitoring framework used to analyze the spatial resilience of GCM at different levels**

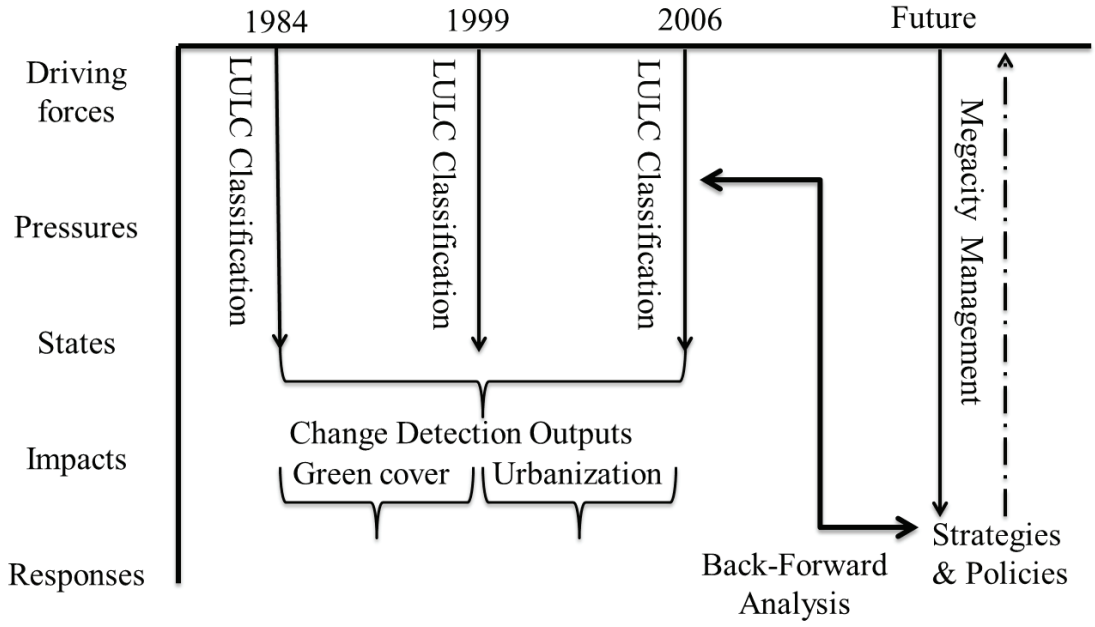


**Figure 33: Implementation of LULC analysis on DPSIR at first spatial resilience level of GCM**

The framework models mentioned above are mainly mono-analytical (i.e. from top to bottom), while the DPSIR could be modified to describe the spatial resilience by reworking the analysis of any key elements based on the data available and stakeholder requests through the conceptual framework. For example, the DPSIR scheme showed that the states of LUC over the time series could have been impacted by urbanization and green cover in GCM (Fig. 33) and the changes detected. Within this framework, the analysis and conceptualization of the resilience of one object could be possible by using a subsidiary DPSIR model which leads to a specific response for a specific object (Fig. 34).

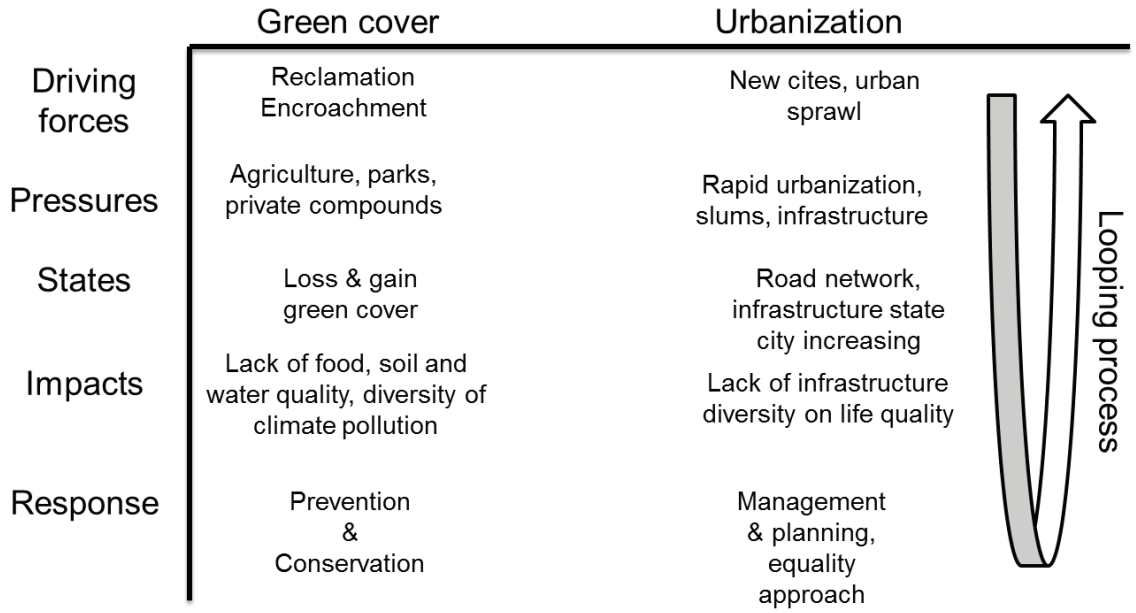


**Figure 34: Back-forward process analysis (Looping mechanism) of changed indicators by using DPSIR for GCM**

The back-forward mechanism permits us to reselect elements (objects) within the system and repeat the analytical process through the monitoring system. This process provides the feedback mechanism through the DPSIR monitoring framework which might be described as "Forked and Manifold Looping Mechanism" of spatial resilience analysis.

In this study, the back-forward (Looping Mechanism) works two ways regarding new information coming from the change of time span and/or spatial resolution of images. For example, a classification by using SPOT images and applying an object-based classification approach that could be implemented with DPSIR to represent the other (second in current study) level of spatial dynamic analysis which is provided with advanced technique and more details of spatial

information. At that level, the classification strategy performs a stepwise extraction of the indicators into classes that are arranged in a hierarchical structure and rule set which are complemented by the DPSIR framework (Fig. 35).

The conceptual framework, and the classification rule set associated with it, can be applied to produce the system of monitoring based on the affected elements coming from inside or imposed from outside the framework. This system would assist the stakeholders by feedback mechanisms to understand the system resilience and find suitable responses.

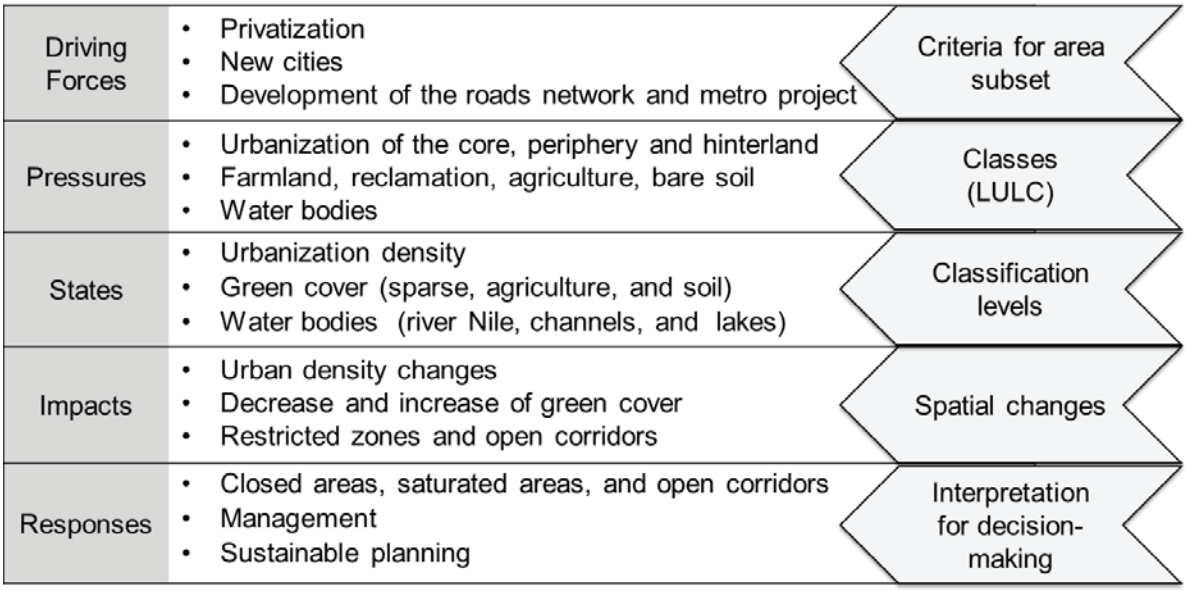


**Figure 35: Implementation of DPSIR on second level of LULC classification strategy**

# 4 Land Use/Land Cover (States)

## 4.1 Introduction

To examine the first level regarding the whole area of GCM (Fig. 36), I monitor and analyze in this chapter the LULCC of the whole GCM. This led me to define and analyze the state of and impact on six main LULC classes (urbanization, cultivated land, surface water, desert (hinterland), cultivated-to-urban, and bare soil).

Furthermore, at that level, I used and evaluated the fine-to-medium resolution time series of TM and ETM+ satellite images (1984, 1990 and 2006), and also pixel-based versus object-based classifications.

Moreover, I investigated the benefits of the techniques used to understand and determine the criteria of more affected areas (hot spots) for further processing and estimation of the change levels.

As mentioned in Chapter 3, there is a need to create a conceptual model in order to explore key aspects of human-environment relations in such a complex system as Greater Cairo. Therefore, the first implementation of the DPSIR model to clarify the mechanism between different stages in this model and the land use land cover state regarding the back-forward mechanism would be confirmed. Thus, this study assumed that the land classes or indicators in the terms of land use/cover classification represent the spatial driving forces, exerted pressures, and affected states of increasing or decreasing Greater Cairo. The indicators used are defined either as anthropogenic, such as urbanization, cultivation, and artificial water bodies, or natural, such as natural surface water and geo-cover. The impact of human activity could then be reanalyzed and conceptualized in a sub-scheme of DPSIR.

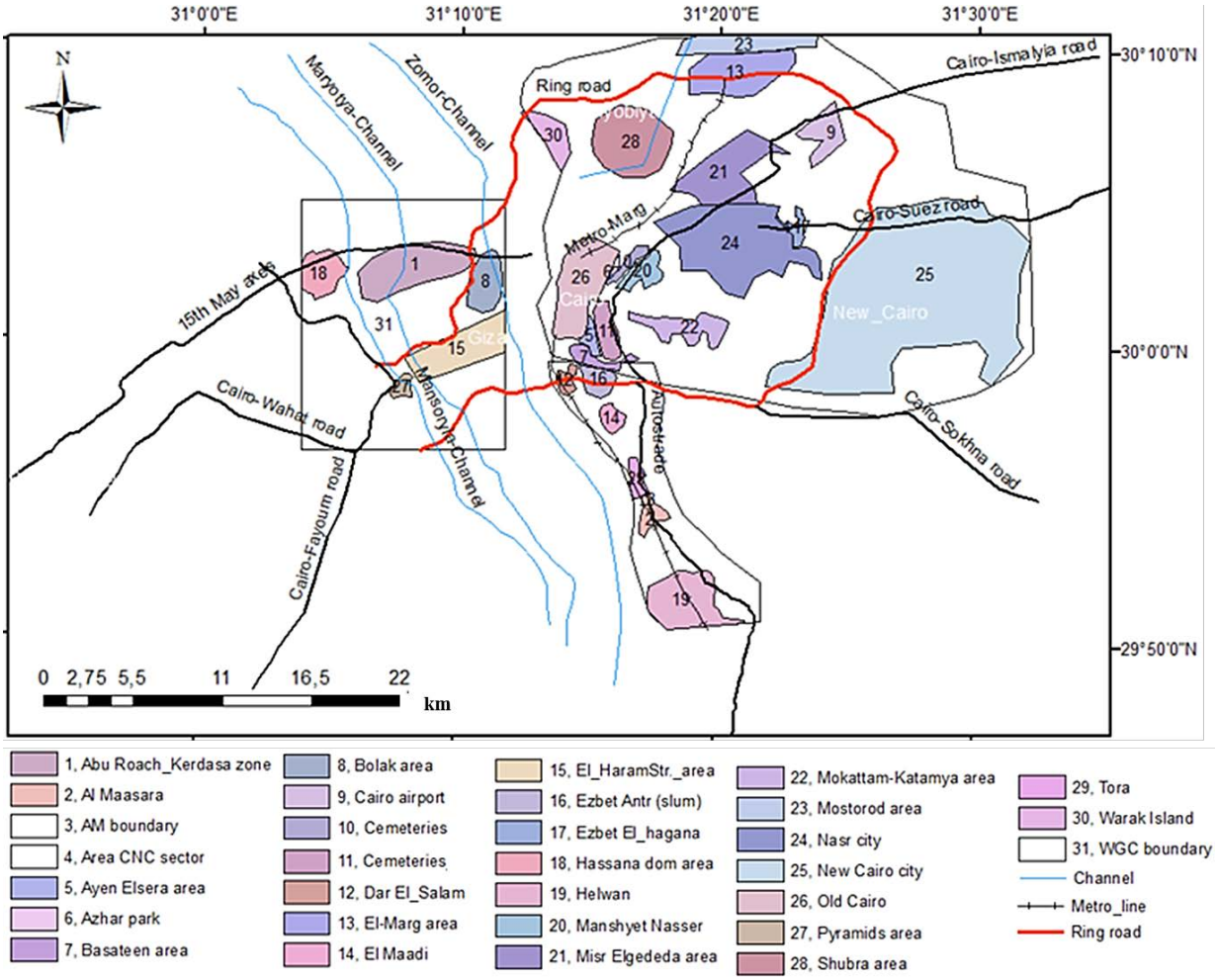


**Figure 36: Names of areas and roads used in the present study of GCM (map based ETM 2006 and field information)**

## 4.2 Time span choice

This part of my study deals with the selection of satellite data and their acquisition date concerning two phases of economic reform GCM. To classify the whole area of GCM, between the end of open trading time and post privatization economic program, I used the low-to-medium resolution images of Thematic Mapper (TM) and Enhanced Thematic Mapper Plus (ETM+) with a pixel size of approximately 30 m.

Change detection researchers have become interested in the close relation between land use / cover changes and economic growth. Luc (2001), for example, has argued that a spatial econometric

approach is not exclusively a consequence of the nature of the data, but may also be required to quantify the "spatial" components.

Kozova and Finka (2010) have also concluded that current trends in management and planning processes show the growing importance of landscape planning that reflects social change and the emphasis on the link between land use and civil requirements. Also, Latocha (2010) has studied rapid development and its impact on the environment in City of Sudety, Poland, and he argued that, in order to achieve a balance between the increasing socio-economic needs and the need to preserve and maintain the harmony, culture, and landscape patterns of the region, sensible planning is required. In addition, Scrieciu (2007) has recognized the link between economic growth and spatio-temporal monitoring in large areas. Through a regression analysis based on a panel dataset of fifty tropical countries over an eighteen-year period, he studied on a macro scale the economic determinants in the depletion of global forest as a variable in land cover changes.

I therefore chose the three different time periods corresponding to the economic changes beginning in 1984 (which is considered as the reference year for the other images), and continuing to 1990 and 2006. The time span from 1984 to 1990 represents the phase of market economy introduced by Sadat at the end of the 1970s (http://www.mideastweb.org/egypthistory.htm). From 1991, Mubarak introduced a number of important laws and decrees which significantly changed the domestic economic program to reduce the size of the public sector and expand the role of the private sector (IDRC report 1996). This is called privatization and has been represented here spatially by the 1990-2006 time span. This time span had a great impact on the socio-environmental system of the whole country generally and on the capital in particular. According to the World Bank, about 18% of the Egyptian population now live below the national poverty line, this figure rising to 40% in rural areas; moreover, an additional 20% of the population have been at risk of experiencing poverty at some point during the last decade, heightening a sense of social vulnerability and insecurity (http://www.worldbank.org/en/country/egypt/overview). The impact of privatization therefore led dramatic changes in society and precipitated the 2011 revolution.

Environmental to planners are increasingly evaluating landscape diversity and degradation in different time periods in connection with economic processes. For example, Xie et al. (2005) have argued that the promotion of rapid economic growth in China in the mid-1990s led to the loss of farmland, and the use of paddy fields for non-agricultural purposes in Wuxian City. They also showed that continued rural to urban migration, rural economic development and rapid urban expansion represent the primary forces of spatial resilience.

Similarly, Jian-fei et al. (2007) compared quantitative and qualitative changes to cultivated land and analyzed the proximate causes and the driving forces behind such changes over time. The results suggest that similar land-use changes can occur in different regions as the regions pass through comparable stages of economic development at different times.

Moreover, Matelas et al. (2011) have stated that, in order to determine urban growth in Athens City, various aspects concerning the quality of life, socioeconomic and cultural conditions should be analyzed not only for sustainable but also for desirable planning.

However, I assumed that these two time spans (1984-1990 and 1990-2006) represent the dynamic changes and socio-spatial inequalities caused by the drivers like economic reform and trends of investment in the Greater Cairo metropolis. Furthermore, the better accessibility and infrastructural development led to increasing human activities such as urban activity. These activities result in conversions of one specific type of LU and/or LC into several others (Cassidy et al. 2010). For instance, during the period of economic reform the government realized the building of the ring road and the metro lines that influenced the spatial growth of GCM.

## 4.3 Classification processes and technique benefits

There are many methods available to classify land cover-land use based on multispectral satellite data. However, this chapter will test only two of them. The first is supervised pixel-based classification while the second is multi-algorithms object-based classification. I differentiate between the techniques available and investigate the advantages and disadvantages of their respective algorithms. Moreover, the field experiences and checked ground points and some ancillary data were played an important role for sample selection and pixels affiliation. There are six land use/land cover (LULC) classes which represent the first level of change in the main DPSIR scheme.

These classes are as follows: Urban areas (U), Cultivated Land (CL), Cultivated to Urban (confusing and fuzzy area) (CU), Desert (D), Bare Soil (BS), and Water Bodies (WB). These six classes are used for both pixel- and object based classification.

### 4.3.1 Supervised pixel based classification

The supervised pixel based classification was applied after pre classification processes (Chapter 3) and examined in the three time periods (1984, 1990, and 2006). Because pixel-based classification

is described as a traditional and unsophisticated way of classification (Flanders 2003), this classification represents the main part of the preliminary work in this part of the study. Hence, the LULC knowledge will be extracted from the satellite images by using the spatial and spectral information per pixel. The selected training pixels (samples) of each class are coincided and supported with the ground and marker points which have been chosen from published maps and field observations., besides that, the histograms of training pixels have been a unimodal and relatively have a narrow range of values (i.e. low standard deviation). After selection of training samples, the class´s signature were evaluated by comparing between a spectral information of a single class signature which composed from different group of pixels and spectral information coming from primitive reference pixels (training pixels) of this class. The previous step has been taking an effort especially in using of low to medium resolution images for big areas. The condition of supervised classification was applied in the same manner for all three used images.

The resulting classification images are illustrated in Figures 37 and 38 and summarized in Table 8, which show the LULC transition rates among land cover-use types in the whole GCM area. The classes that changed most are urban and cultivated lands, where the percentage rose from 4% in the reference year 1984 to 7% in 1990 and to 17% in 2006. In contrast, the proportion of cultivated land showed no change between 1984 and 1990, and decreased by about 20% between 1984 and 2006. This loss of fertile land occurred mostly in favor of CU areas, the latter gradually becoming informal settlements over time. Therefore the spectral reflectance diagram showed the semi-coincidence between the CU and U classes (Fig. 39). Therefore, the rate of change of mixed land (confusing or fuzzy area) CU showed little change over time where decreased by 1% between 1984 and 1990, increased by 1% between 1984 and 2006. The spatial transformation of the CU class is clear on the classified maps in many areas. This showed that the growth of urban areas occurred at the periphery of GCM in favor of CU areas. Moreover, the rocky cover (desert) areas representing the hinterland and its total area decreased by 2% between 1984 and 1990, and then by 9% between 1984 and 2006. The classification of bare soil (BS) was hard, because the scarcely spatial distribution of its land and miss definition of its pixels by using low resolution images. Surface water class WB (water bodies) was represented on classification maps by surface river Nile (N-S blue channel), lakes called “Ayen El-Sera” due east of the GC core, and uncovered channels for irrigation of cultivated land. Water bodies represent a very small proportion of the total area (1%).

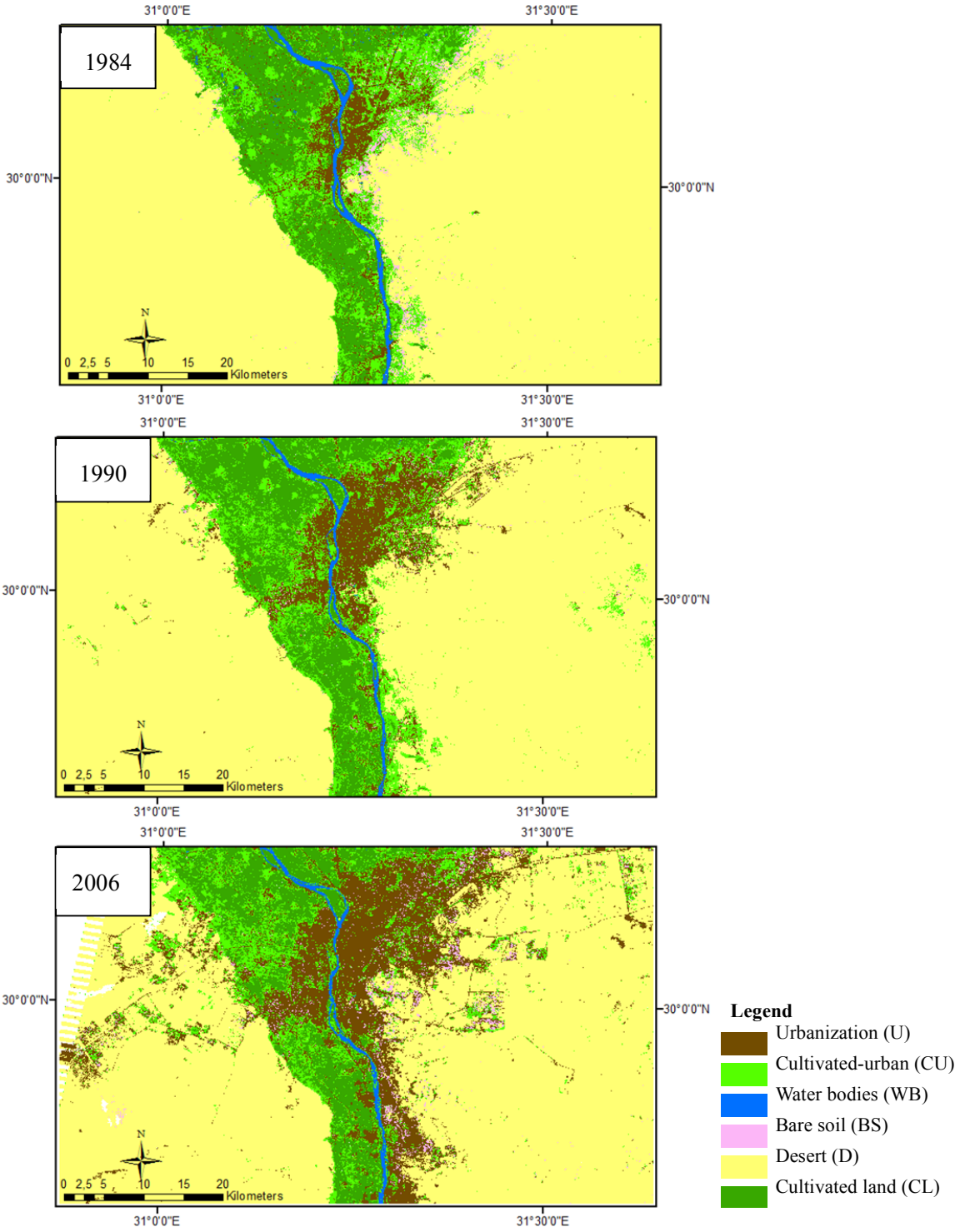


**Figure 37: Classified LULC time series maps per-pixel based remote sensing technique**

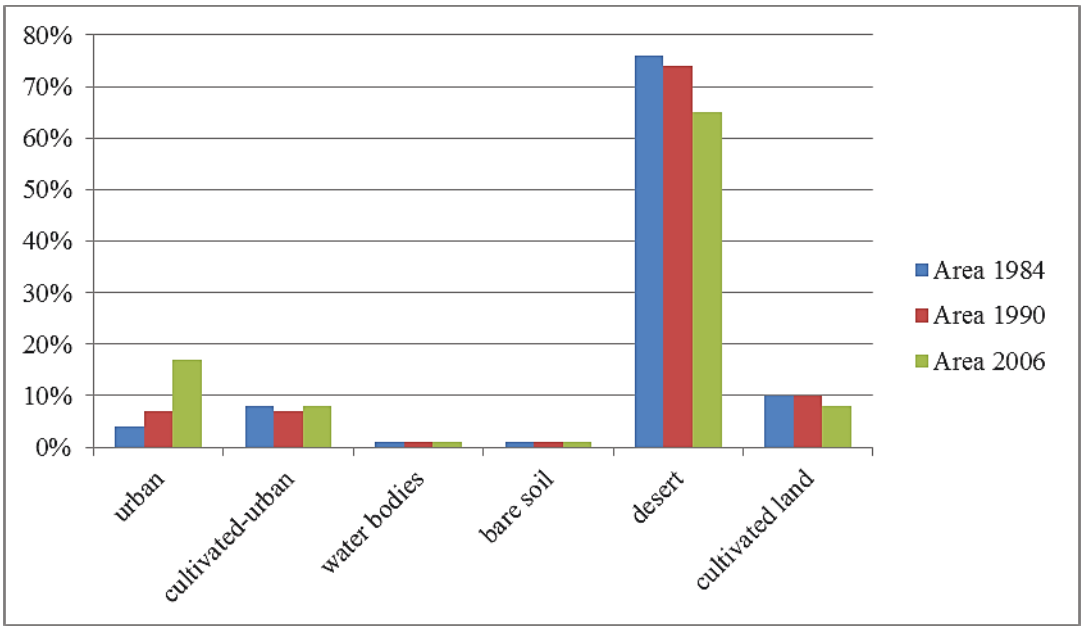


**Figure 38: Changes in land use of GCM from 1984 to 2006**

**Table 8: Percentage of LU/LC classes in the study area (see abbreviations at Fig. 38)**

| LU/LC classes | 1984% | 1990% | 2006% |
|---|---|---|---|
| U | 4 | 7 | 17 |
| CL | 10 | 10 | 8 |
| CU | 8 | 7 | 9 |
| D | 76 | 74 | 65 |
| BS | 1 | 1 | 1 |
| WB | 1 | 1 | 1 |

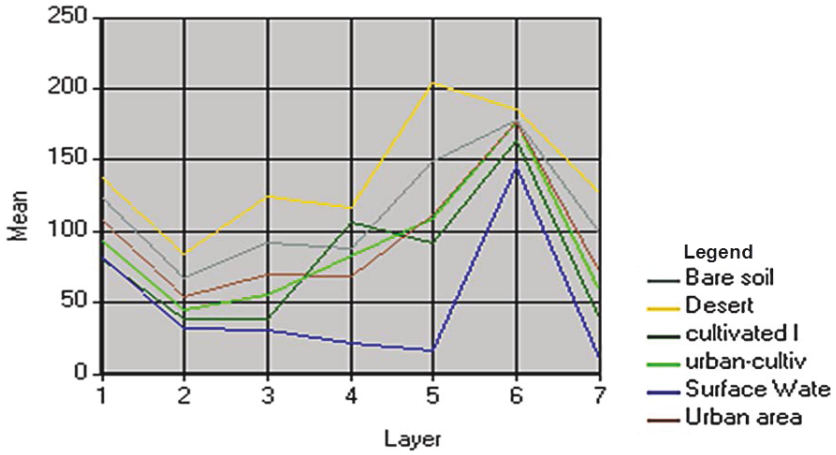


**Figure 39: The graph shows the signature mean relation between each class and 2006 image bands (Erdas Imagine)**

#### 4.3.1.1 Ground truth and accuracy assessment

More than one hundred distributed points on the image were used for calculating the accuracy of the classifications (Tables 9, 10, and 11). Some of the points were positioned at the edge of the image, so these points were left out of the actual points.

**Table 9: Total accuracy of 1984 (see abbreviations at Fig. 38)**

| Class Name | Reference Totals | Classified Totals | Number Correct | Producers Accuracy | Users Accuracy |
|---|---|---|---|---|---|
| BS | 1 | 3 | 1 | 100.00% | 33.33% |
| Cu | 21 | 15 | 6 | 28.57% | 40.00% |
| WB | 1 | 1 | 1 | 100.00% | 100.00% |
| D | 65 | 74 | 62 | 95.38% | 83.78% |
| U | 15 | 5 | 3 | 20.00% | 60.00% |
| CL | 9 | 14 | 7 | 77.78% | 50.00% |
| Totals | 112 | 112 | 80 | | |
| Overall Classification Accuracy = **71.43%** | | | | | |

**Table 10: Total accuracy of 1990 (see abbreviations at Fig. 38)**

| Class Name | Reference Totals | Classified Totals | Number Correct | Producers Accuracy | Users Accuracy |
|---|---|---|---|---|---|
| BS | 5 | 9 | 3 | 60.00% | 33.33% |
| CU | 24 | 17 | 7 | 29.17% | 41.18% |
| WB | 3 | 5 | 2 | 66.67% | 40.00% |
| D | 67 | 76 | 63 | 94.03% | 82.89% |
| U | 20 | 7 | 5 | 25.00% | 71.43% |
| CL | 11 | 15 | 8 | 72.73% | 53.33% |
| Totals | 130 | 130 | 88 | | |
| Overall Classification Accuracy = **67.69%** | | | | | |

**Table 11: Total accuracy 2006 (see abbreviations at Fig. 38)**

| Class Name | Reference Totals | Classified Totals | Number Correct | Producers Accuracy | Users Accuracy |
|---|---|---|---|---|---|
| BS | 11 | 10 | 7 | 63.00% | 75.00% |
| CU | 21 | 19 | 11 | 36.67% | 53.33% |
| WB | 10 | 12 | 8 | 77.00% | 91.00% |
| D | 34 | 33 | 33 | 92.31% | 98.16% |
| U | 16 | 18 | 13 | 44.29% | 80.00% |
| CL | 20 | 20 | 15 | 87.00% | 50.00% |
| Totals | 112 | 112 | 87 | | |
| Overall Classification Accuracy = **61.29%** | | | | | |

Therefore, the actual points used for the per-pixel of about 112, 130, and 112 for 1984, 1990, and 2006 respectively. I found that the classified map of 1984 has a better overall accuracy of classification (71.43%) than the maps of 1990 (67.69%) and 2006 (61.29%). Moreover, the overall

Kappa statistics were 0.5032, 0.5052, and 0.4963 for the maps of 1984, 1990, and 2006 respectively.

However, the accuracies for the desert found by producers accuracy as well as users accuracy in the three maps resulted in more than 90%. The cultivated land and water body classes then showed an average accuracy ranging from 60% to 70%. The urban and urban-cultivated classes had producers accuracy ranging from 20% to 44% and users accuracy ranging from 60% to 80%. Also, the field observations (Fig. 40) and mean spectral diagram (Fig. 39) revealed the close relation between these two classes and difficulties in distinguishing between them at the current level of classification. Because there is only a small number of bare soil class and because of the small size of the areas the classifier assigns them to the nearest neighbor pixels hence the class mean distance is larger than the user-defined threshold distance.

The overall accuracy of PB classification of a large area such as GCM through fine TM and ETM satellite data showed that the classification results did not assign the pixels to their classes by high percentage correctly.

**Figure 40: Cultivated land and cultivated-urban in transformation process in favor of urbanization, in an area located due north of GC periphery**

#### 4.3.1.2 Evaluation of pixel-based technique

The application of pixel based classification technique used in this part of my study to detect the multi-temporal changes explored that:

- Field observation before and after the classification process should be obligatory, because of limitations regarding the spectral separation of classes.
- The statistical calculation of spectral information involves the digital number (DN) values individually without considering the neighborhood pixels (Castelli et al. 1999).
- Land cover maps derived from the classification of images usually contain some sort of error due to several factors; for example, the classifier is not supported by multi-algorithms which can prove class identification, and the resolution of satellite data also plays an important role in the accuracy of classification. Hence, the evaluation of classification results is an important part of the process of classification.
- The accuracy of classified maps resulting from the pixel based approach still requires more advanced technique for satisfying results.

### 4.3.2 **Object based image analysis (OBIA)**

The more advanced classification technique used in this study is Object-Based Image Analysis (OBIA), which is commonly called object-oriented classification. This technique has been developed to divide the landscape into LULC types by using any type of geometric shape (e.g. a polygon) rather than individual to distinguish contiguous forms of land use. This would lead logically to more accurate classifications of land use (Burnett and Blaschke 2003).

The classification process of the three selected times has been done simultaneously by using only one process tree. This process tree contains three main steps: image segmentation, classification and refining classification. Field experience and observation have also been been taken into consideration here in assigning the origin of segments and also during the refining process. This work has been carried out by using mainly eCognition 8.64 software and ArcGIS.10 software.

#### 4.3.2.1 Image preparation

The satellite images for the three time periods (1984, 1990, and 2006) were used and stored in one project. Hence, all input and output information which expressed the image analysis could be easily

accessed (Fig. 42). In spite of the color weight of image channels (red, green and blue) can be defined by increasing or decreasing their intensity, but I preferred to use the default weight equal one for all bands (Fig. 43).

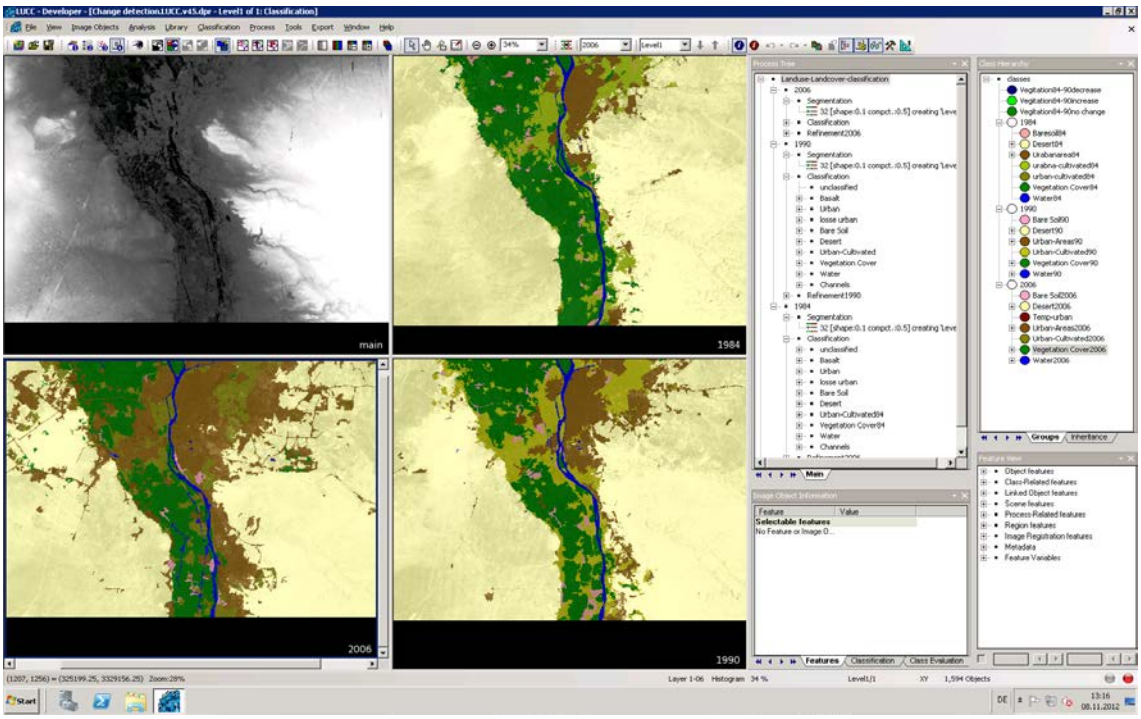


**Figure 41: Side by side view shows the capacity to classify different images simultaneously (eCognition Developer)**

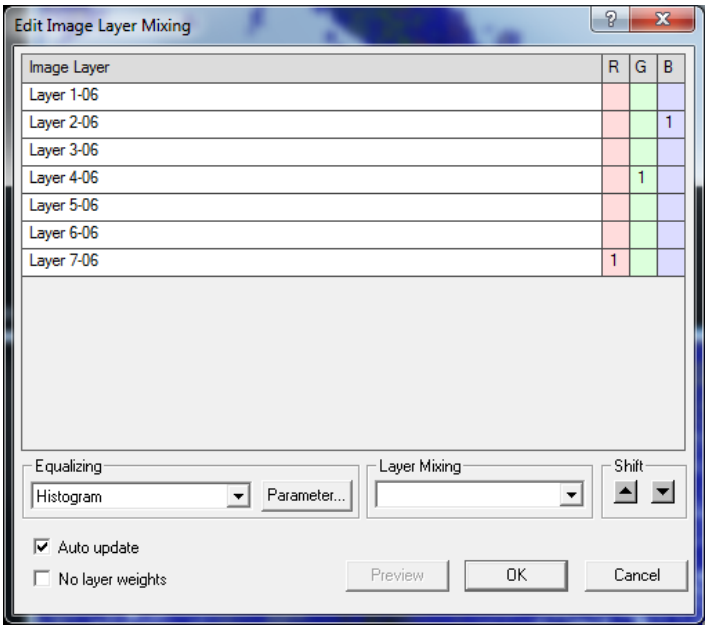


**Figure 42: The channel weight of image layers displayed in the classification process (eCognition Developer)**

#### 4.3.2.2 Segmentation

The segmentation process is the first and most important part in the technique of OBIA. Hence, the levels of classification and degree of accuracy are based on the type and criteria of segmentation. There are two principles of segmentation (eCognition handbook): top-down segmentation to cut something large into smaller pieces, and bottom-up segmentation to join small pieces to obtain something larger. The segmentation process in this study was based on the bottom-up type. This means that the image pixels were grouped to represent the primitive image objects. Therefore, the multi-resolution segmentation algorithm is applied to all images used for classification. The multi-resolution segmentation algorithm consists of many parameters and criteria, which I identify below (eCognition user guide 2009) (Fig. 43 and Fig. 44).

Level: To determine at which level the new image objects created by segmenting will be stored. The LULC segmentation-classification here has been stored at level 1, which is above the level of image pixels.

Weight: Also, the multi-resolution segmentation view is supported by an option to allow the user to select the layers and weight of channels for the segmentation process. All the supported layers of the image under examination were selected and given equal weight.

Scale parameter: The scale parameter is chosen according to the objective of classification and the needs of object homogeneity. Small-scale parameters result in small objects, while larger-scale parameters result in larger objects. Therefore, for the current images, the values between 10 and 50 were tested to select the most suitable object size for class's identification. As a result, after testing all three images were segmented with a scale value of 32 and used for the classification procedure.

Shape and compactness: These represent the composition of homogeneity criteria. Shape is opposed to color and is calculated from compactness and smoothness, since the higher the color the less the criterion of shape influences the size of the image object. The shape value used here is 0.1 with a compactness of 0.5.

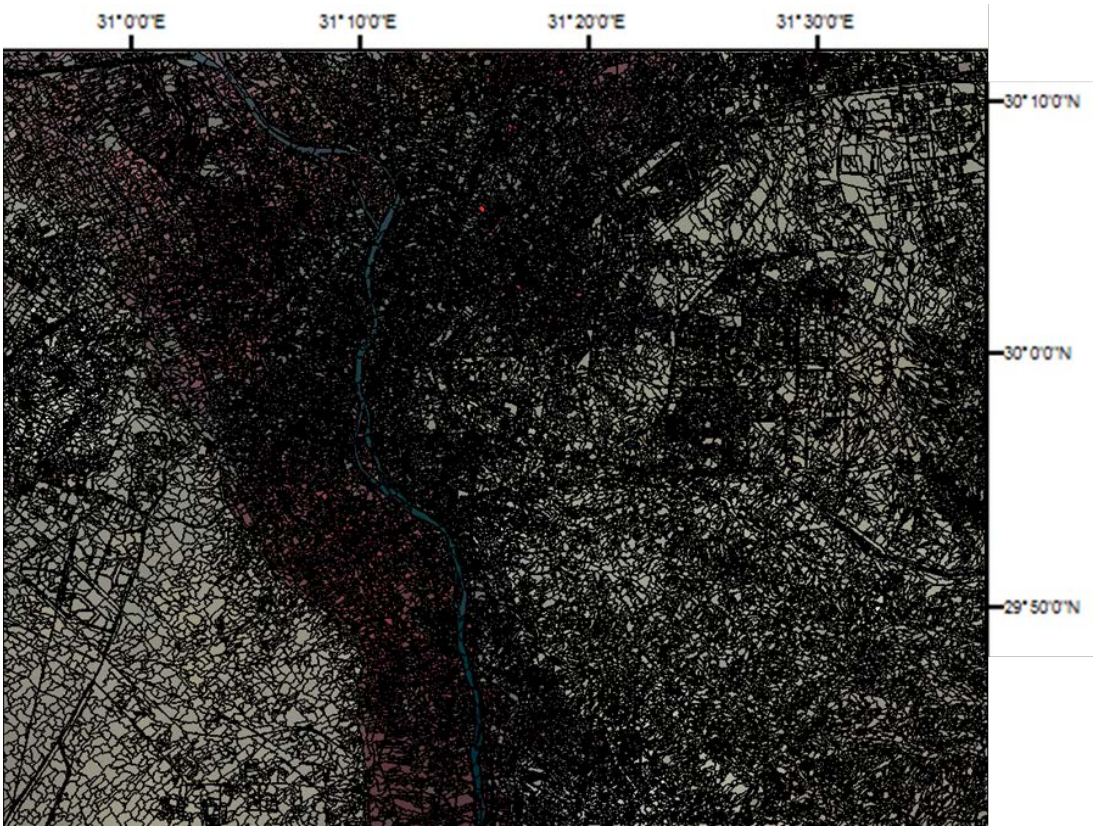


**Figure 43: Result of the multi-resolution segmentation with scale parameter 10 (eCognition Developer)**

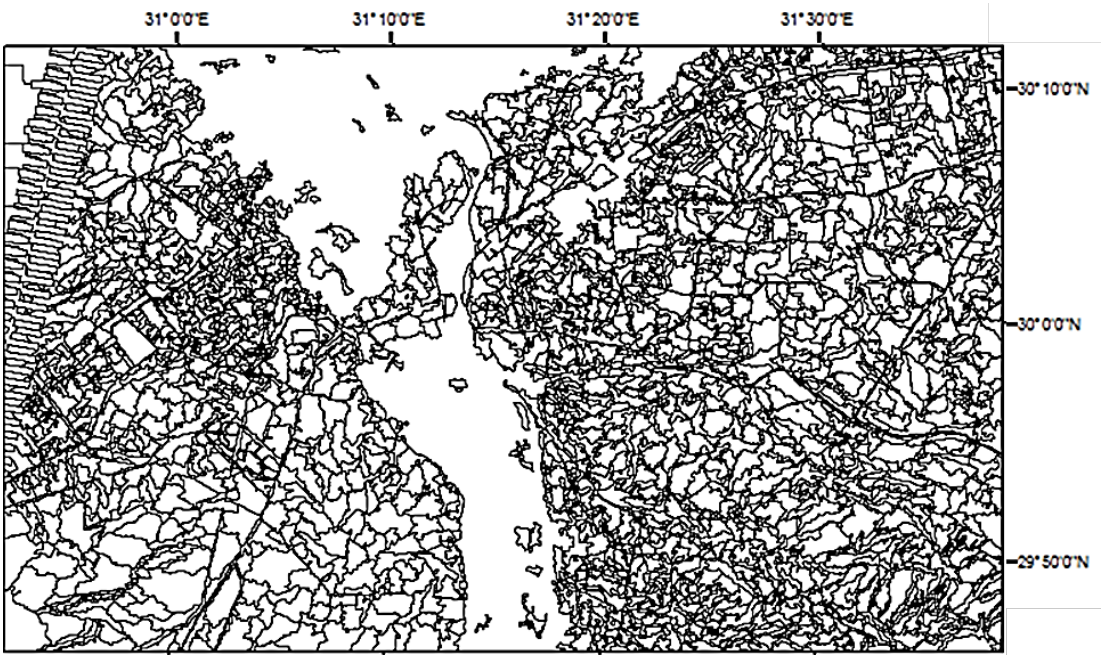


**Figure 44: Result of the multi-resolution segmentation with scale parameter 32 used for TM and ETM images**

4.3.2.3 Classes

After the segmentation process, I assigned the objects to several classes based on their specific spectral information, shape, and texture which were provided by the ground truth points. Furthermore, the brightness relationship between adjacent image objects was worked out explicitly and the relationships between objects were established. As a result, the six spatial indicators for classification are determined more accurately than pixel-based classification. In this case, some of these classes could be differentiated into sub-classes as an urban area class.

*1-Urban areas (U)*: represent any houses and settlements in the study area. This class can evolve into sub-classes of loose urbanization based on the object features.

*2-Bare soil (BS):* is any non-sealed fertile land which is not covered with vegetation. However, in the sampling step, the field experience played a major role alongside identification algorithms.

*3-Green Cover (CL)*: contains agricultural fields and reclaimed land and any other green space in the study area.

*4-Water body (WB)*: is represented by surface water that contains the River Nile, some channels and small lakes.

*5-Cultivated-urban (CU)*: is represented here by the areas that have more vegetation than buildings; hence, the degree of brightness has played an important role in determining this class.

*6-Desert (D)*: is hinterland area and here the basaltic cover has been specified and reported as a sub-class of the desert.

#### 4.3.2.4 Classification and Process Tree

The object-based classification procedures started with the creation of classes and identified their possible position in the class hierarchy (Fig. 45). This was followed by work on the process tree, which dominates the classification rule set and responses to its functions such as execute, modify, add, and delete (Fig. 45). Because the area under concern is large and the images used were with low to moderate spatial resolution, the separation between objects is a little complicated, the fuzzy classification based mostly on membership functions is recommended and applied. Therefore the classes can be separated from one another by one or few features used. However, the application of different algorithms and functions can reduce the overlap between classes and provide accurate descriptions of objects. Most features are supported by eCognition Developer software 8.46, and others can be calculated and used as customized arithmetical features. In this part of my study, the most commonly used features are:

*Object features:*

- Customized algorithms: by using this feature, I calculated the Normalized Difference Vegetation Index (NDVI) and Land Water Mask (LWM) to discriminate the vegetation cover, and water and soil respectively.
- Layer values of image bands such as brightness, which are used mainly to discriminate between objects.
- Geometrical features such as area, length/width and main direction, which are mainly used to identify the shape of objects.
- Texture, e.g. GLCM Statistics and Layer value texture are partially used for layer-7 and layer-6 to examine the homogeneity of objects (e.g. basalt sub-class).

*Class-related features:*

- Relations to classification; e.g. membership and classification value, which are used to adjust the object assignation and class affiliation.

*Scene features:*

- Class-related; this algorithm is used to calculate the number of classified objects, area and area percentage.

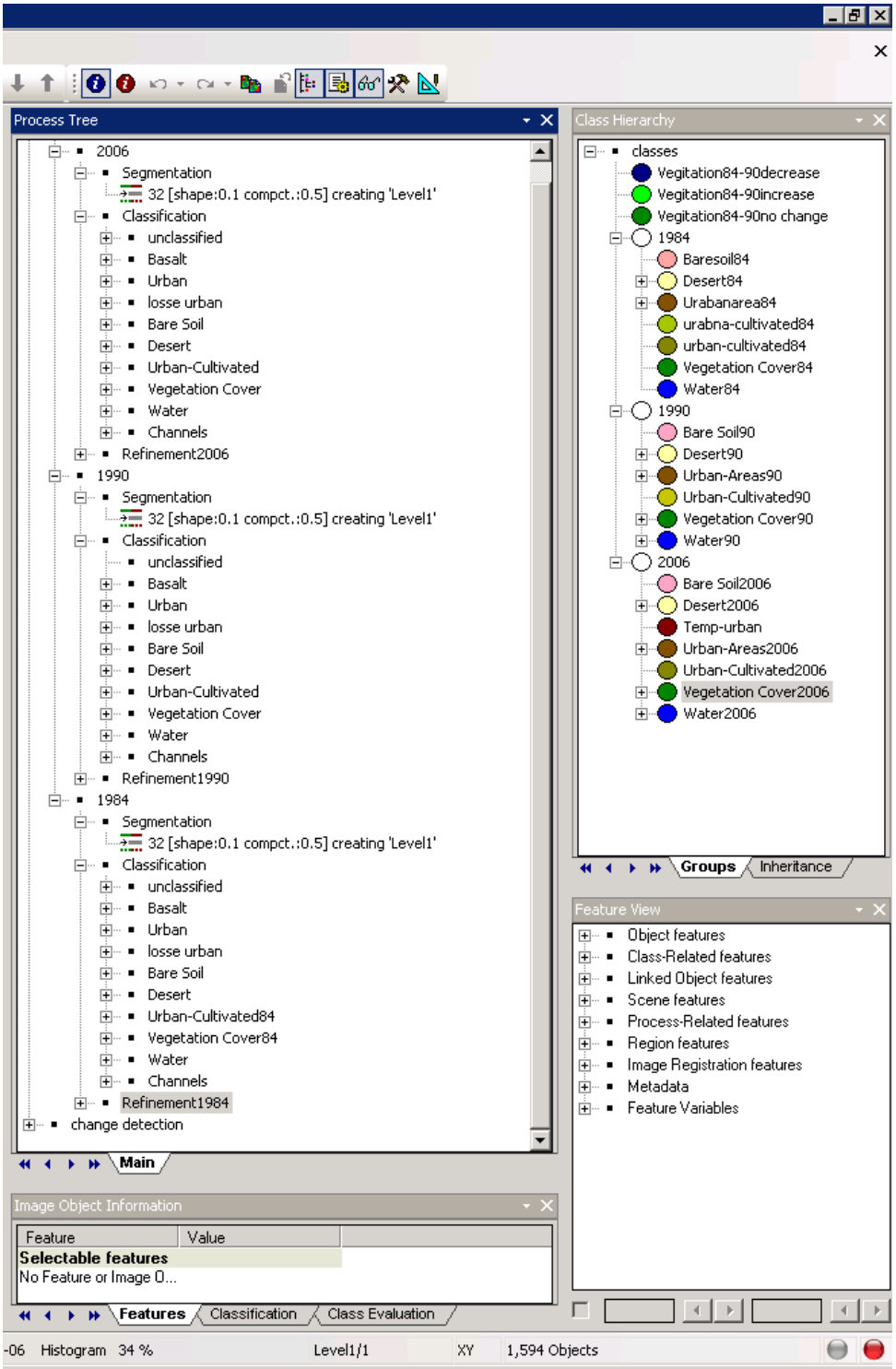


**Figure 45: The rule set and class hierarchy view used for object based classification (eCognition)**

#### 4.3.2.5 Refining the classification

There are some steps that should be added and applied to the classification rule set to refine the classification. In this study, refining the classification was carried out through the extensive application of membership function (Fig. 46 and Fig. 47) and through the reshaping of objects manually and automatically based on the ancillary data. The algorithms most used are "find enclosed by", "remove objects", "merge region" and "assign class" to refine primary results. Additionally the manual editing to cut or merge or reshape objects was partially applied.

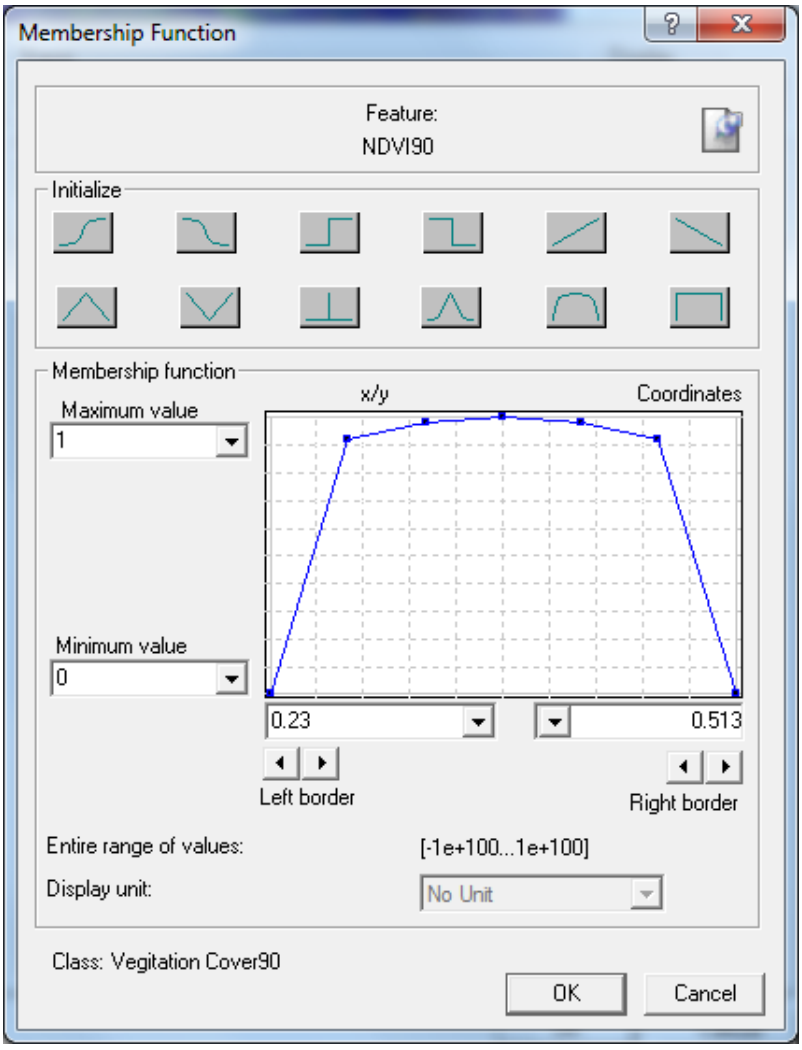


**Figure 46: The membership function applied to define the fuzzy range of NDVI (eCognition)**

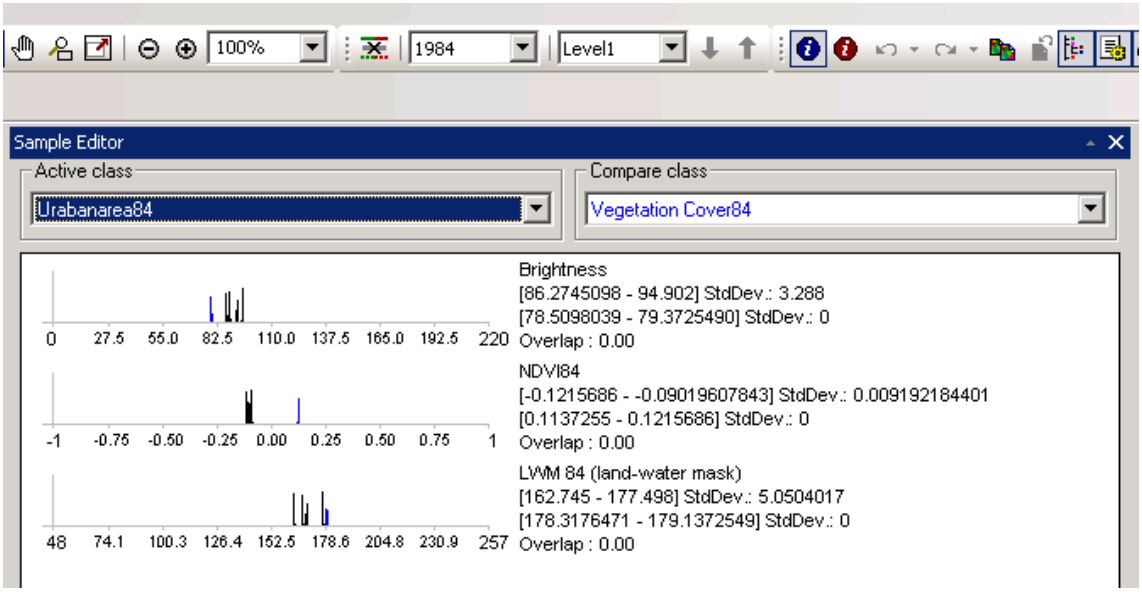


**Figure 47: Features histogram to compare between two classes (eCognition Developer)**

4.3.2.6 Resulting maps and export results:

The area under study here covers GCM and most of the new cities established in the hinterland of Greater Cairo. The LULC analysis of each time period describes the state of the most spatially distributed indicators covering the core, periphery and hinterland of GCM (Fig. 48 and Table 12).

The state of the 1984 classified image shows that urbanization represents about 4% of the total area, which is mainly concentrated in the core of the old Cairo city due east of the River Nile (RN) and surrounded by loose urban areas,. The cultivated urban (CU) class covers the most central part of Giza city and form a corridor extending due west of the pyramids plateau. Moreover, the CU was mainly limited to areas north to northeast of the Cairo core and distributed partially in the Helwan and Maadi areas. Generally, the total amount of CU areas reaches 4%, which indicated to the transformation process from rural and cultivated land to settlements. That revealed to a strong impact on the environment during the period of capitalism and free trading policies. Furthermore, the desert at this time was rarely used for development, and the bare soil was nested with cultivated land. The surface water body represented by the Nile and its tributaries and by the small lakes to the east called Ayen El-Sera accounts for about 1% of the total area.

1990 saw the visible appearance of the new cities established in the hinterland (desert). There were three corridors considered low-density and loose-urban areas: the first, due east-northeast comprised of Nasr, Salam cities and the Mokattam plateau; the second due south-southeast comprised of 15$^{th}$

May City; and the third, due west of the pyramid plateau and comprising 6th October City. These new remote cities and the low density urban areas at the periphery of the GC core jumped from 1% in 1984 to about 4% of the total classified area in 1990. Urbanization with high density dominated most areas of the old Cairo city, including the southern part of El-Qualyoubia city and Giza center, with a percentage of 6%. It is quite clear that the cultivated-urban land very close to the urban areas in the Nile valley represents about 8% of the total area under concern. Therefore, the difference between rural areas and CU is very difficult to calculate and is beyond the scope of this part. The cultivated land and the bare soil are very close to each other, since the bare soil represents the key element of misuse of fertile land with area percentage reached to 1% of the total classified areas. The green cover mainly exists in the Nile valley and is represented by the agriculture fields with about 10% of the total classified area.

Focusing on 2006, we can see that urbanization has spread randomly and that GC can be described as a shapeless metropolis. Urbanization covered an area of about 22% of the total region and was concentrated extensively in the area parallel to the east bank of the River Nile. That dominates the peripheral zone and some parts in Helwan and Maadi sectors. On the other side, the corridor from Giza center to the pyramid plateau is saturated by dense urbanization (Fig. 49). In addition, the less dense urban areas distributed in the most of new settlements areas (Fig. 50) such as new Cairo city , 15th may city, most of 6th October city and other parts. The CU class accounted about 6% which mostly enclosed within an urban area in Nile valley and randomly distributed within cultivated land (Fig. 51).

In 2006, the vegetation cover represented about 11% and mainly occupied the north and south urban zone in the fertile Nile valley (Fig. 52). There were also a few scattered green spaces in the hinterland (desert), which would be one of the positive signs of development. The desert area amounted to more than 60% of the total area. The desert in 2006 showed extensive constructions and a wide distribution of buildings.

Work on the sub-level was also carried out here by classifying the basalt exposures as a subclass of the desert class (Fig. 48). All object-based classified images were exported to vector files and managed by using ArcGIS.10 software (Fig. 48).

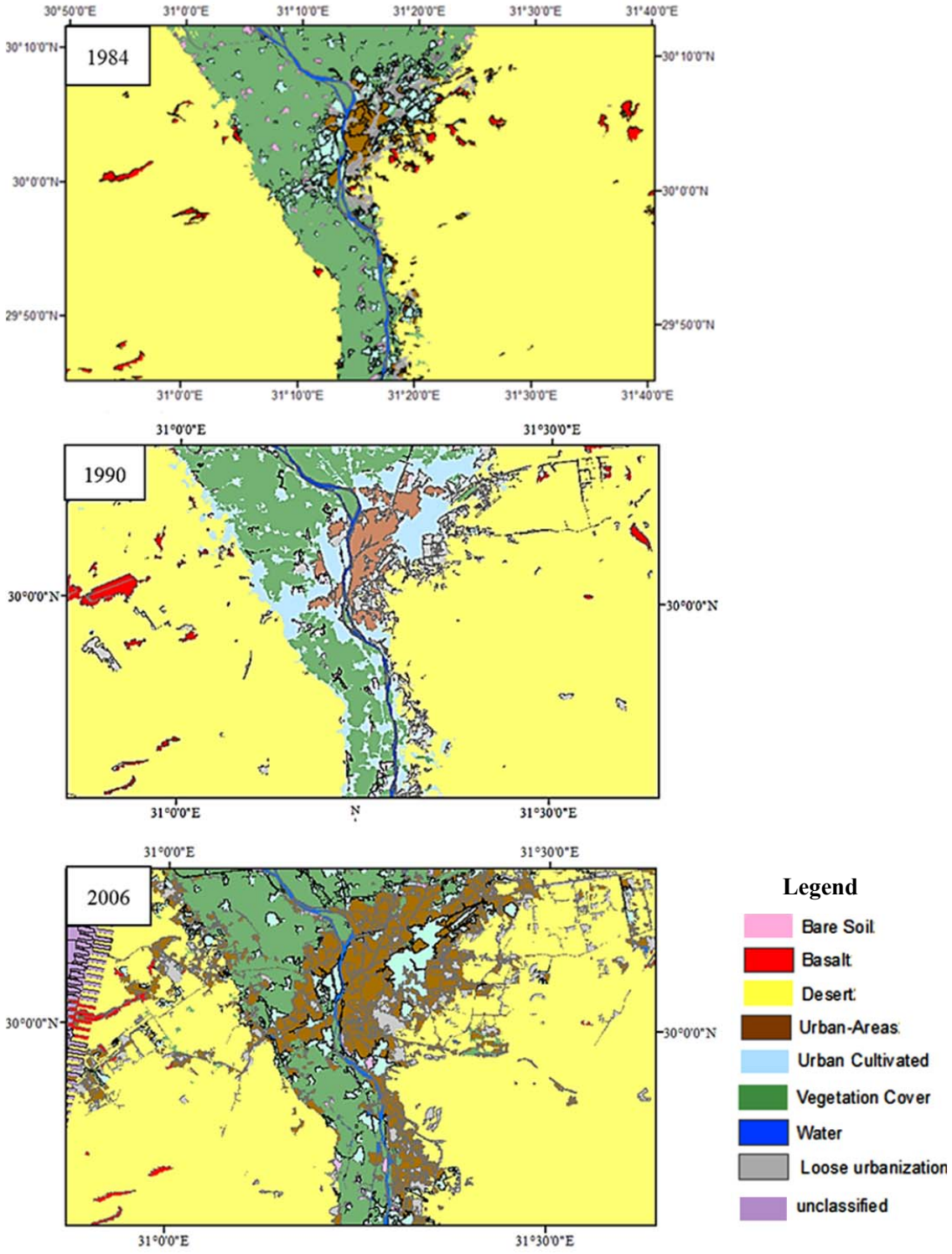


**Figure 48: LULC states of the classified three images per OB classification**

**Table 12: Total area percentage of LU/LC classified classes per OB classification (see abbreviations at 4.3.2.3)**

| LU/LC Classes | 1984% | 1990% | 2006% |
|---|---|---|---|
| U | 3 | 6 | 18 |
| CL | 14 | 10 | 11 |
| CU | 4 | 8 | 6- |
| D | 76 | 70 | 60+ |
| BS | 1 | 1 | 0+ |
| WB | 1 | 1 | 1 |
| LU | 1 | 4 | 4 |

**Figure 49: Dense urbanization at the core of GCM. Photo captured 2009**

**Figure 50: Less dense urbanization, the area located in the southern part of the new Cairo city. Photo captured 2010**

**Figure 51: The houses in rural areas resemble those in urban areas (north Cairo). Photo captured 2010**

**Figure 52: A very confusing area to classify located between Maadi and Helwan district east of the River Nile (RN). Photo captured 2010**

### 4.3.2.7 Accuracy assessment

eCognition software supplies a method to assess the accuracy by confusing (error) matrix including user and producer accuracy, and kappa based on ground truth (samples). Most ground points and landmarks used to evaluate the accuracy of classification per pixel were used to evaluate the results based on object-oriented classification. Because of some difficulties in exporting the accuracy outputs due to eCognition software, I have chosen to use snapshot views in Figures 53, 54, and 55.

**Error Matrix based on Samples**

| User Class \ Sa... | Water84 | Vegitation Cover... | Baresoil84 | Urabanarea84 | Desert84 | Losse urbanizati... | urabna-cultivate... | Basalt84 | Sum |
|---|---|---|---|---|---|---|---|---|---|
| **Confusion Matrix** | | | | | | | | | |
| Water84 | 7 | 0 | 0 | 0 | 0 | 0 | 0 | 0 | 7 |
| Vegitation Cover84 | 0 | 12 | 0 | 0 | 0 | 0 | 0 | 0 | 12 |
| Baresoil84 | 0 | 1 | 4 | 0 | 0 | 0 | 0 | 0 | 5 |
| Urabanarea84 | 0 | 0 | 0 | 10 | 0 | 0 | 0 | 0 | 10 |
| Desert84 | 0 | 0 | 0 | 0 | 48 | 3 | 1 | 2 | 54 |
| Losse urbanization... | 0 | 0 | 0 | 10 | 0 | 0 | 0 | 0 | 10 |
| urabna-cultivated84 | 0 | 0 | 1 | 0 | 0 | 0 | 12 | 0 | 13 |
| Basalt84 | 0 | 0 | 0 | 0 | 1 | 0 | 0 | 2 | 3 |
| unclassified | 0 | 0 | 0 | 0 | 0 | 0 | 0 | 0 | 0 |
| Sum | 7 | 13 | 5 | 20 | 49 | 3 | 13 | 4 | |
| **Accuracy** | | | | | | | | | |
| Producer | 1 | 0.923 | 0.8 | 0.5 | 0.9795918 | 0 | 0.923 | 0.5 | |
| User | 1 | 1 | 0.8 | 1 | 0.8888889 | 0 | 0.923 | 0.6666667 | |
| Hellden | 1 | 0.96 | 0.8 | 0.6666667 | 0.932 | 0 | 0.923 | 0.5714286 | |
| Short | 1 | 0.923 | 0.6666667 | 0.5 | 0.8727273 | 0 | 0.8571429 | 0.4 | |
| KIA Per Class | 1 | 0.914 | 0.7908257 | 0.452 | 0.9612245 | -0.09615384615 | 0.9131759 | 0.4864865 | |
| **Totals** | | | | | | | | | |
| **Overall Accuracy** | **0.8333333** | | | | | | | | |
| **KIA** | **0.777** | | | | | | | | |

**Figure 53: Figure 53: Screenshot of error matrix based on sample output of classified image 1984 (eCognition); note the effect relationof each class on the other classes**

Error Matrix based on Samples

| User Class \ Sa... | Water90 | Bare Soil90 | Desert90 | Urban-Areas90 | Urban-Cultivated... | Vegetation Cove... | losse90refine | Sum |
|---|---|---|---|---|---|---|---|---|
| **Confusion Matrix** | | | | | | | | |
| Water90 | 9 | 0 | 0 | 0 | 0 | 0 | 0 | 9 |
| Bare Soil90 | 0 | 2 | 0 | 0 | 0 | 1 | 0 | 3 |
| Desert90 | 0 | 0 | 42 | 0 | 0 | 0 | 1 | 43 |
| Urban-Areas90 | 0 | 0 | 0 | 8 | 0 | 0 | 0 | 8 |
| Urban-Cultivated90 | 0 | 2 | 0 | 0 | 17 | 1 | 0 | 20 |
| Vegetation Cover90 | 0 | 0 | 0 | 0 | 0 | 9 | 0 | 9 |
| losse90refine | 0 | 0 | 2 | 6 | 0 | 0 | 1 | 9 |
| unclassified | 0 | 0 | 0 | 0 | 0 | 0 | 0 | 0 |
| Sum | 9 | 4 | 44 | 14 | 17 | 11 | 2 | |
| **Accuracy** | | | | | | | | |
| Producer | 1 | 0.5 | 0.9545455 | 0.5714286 | 1 | 0.8181818 | 0.5 | |
| User | 1 | 0.6666667 | 0.9767442 | 1 | 0.85 | 1 | 0.1111111 | |
| Hellden | 1 | 0.5714286 | 0.9655172 | 0.7272727 | 0.919 | 0.9 | 0.1818182 | |
| Short | 1 | 0.4 | 0.9333333 | 0.5714286 | 0.85 | 0.8181818 | 0.1 | |
| KIA Per Class | 1 | 0.4846939 | 0.9208464 | 0.5345622 | 1 | 0.8003953 | 0.451 | |
| **Totals** | | | | | | | | |
| **Overall Accuracy** | **0.8712871** | | | | | | | |
| **KIA** | **0.8282987** | | | | | | | |

**Figure 54: Screenshot of error matrix based on sample output of classified image 1990 (eCognition); notify the effect relation of each class on the other classes**

Error Matrix based on Samples

| User Class \ Sa... | Urban-Cultivated... | Desert2006 | Bare Soil2006 | Urban-Areas2006 | Vegitation Cover... | Water2006 | Loose urbanizati... | Sum |
|---|---|---|---|---|---|---|---|---|
| **Confusion Matrix** | | | | | | | | |
| Urban-Cultivated2... | 20 | 1 | 0 | 1 | 0 | 1 | 0 | 23 |
| Desert2006 | 0 | 14 | 0 | 1 | 0 | 0 | 3 | 18 |
| Bare Soil2006 | 1 | 0 | 3 | 0 | 0 | 0 | 0 | 4 |
| Urban-Areas2006 | 6 | 1 | 3 | 42 | 1 | 0 | 2 | 55 |
| Vegitation Cover2... | 0 | 0 | 2 | 0 | 27 | 0 | 0 | 29 |
| Water2006 | 0 | 0 | 0 | 0 | 0 | 5 | 0 | 5 |
| Loose urbanization | 1 | 4 | 1 | 2 | 0 | 0 | 0 | 8 |
| unclassified | 0 | 0 | 0 | 0 | 0 | 0 | 0 | 0 |
| Sum | 28 | 20 | 9 | 46 | 28 | 6 | 5 | |
| **Accuracy** | | | | | | | | |
| Producer | 0.7142857 | 0.7 | 0.3333333 | 0.913 | 0.9642857 | 0.8333333 | 0 | |
| User | 0.8695652 | 0.7777778 | 0.75 | 0.7636364 | 0.931 | 1 | 0 | |
| Hellden | 0.7843137 | 0.7368421 | 0.4615385 | 0.8316832 | 0.9473684 | 0.909 | 0 | |
| Short | 0.6451613 | 0.5833333 | 0.3 | 0.7118644 | 0.9 | 0.8333333 | 0 | |
| KIA Per Class | 0.659 | 0.6564516 | 0.314 | 0.858 | 0.9551201 | 0.8272506 | -0.05970149254 | |
| **Totals** | | | | | | | | |
| **Overall Accuracy** | **0.7816901** | | | | | | | |
| **KIA** | **0.7198320** | | | | | | | |

**Figure 55: Sreenshot of error matrix based on sample output of classified image 2006 (eCognition); notify the effect relation of each class on the other classes**

When we consider the accuracy assessment tables, we can see that the classified maps of 1984, 1990, and 2006 have an overall accuracy of 83.4%, 87.1%, and 78.2% respectively. In addition, the overall Kappa indexes are 0.77, 0 82, and 0.72 for the maps of 1984, 1990, and 2006 respectively.

The greatest accuracy over the selected time span was for the water bodies (WB) class, with user and producer accuracy sometimes reaching more than 98%, while this class has a maximum 70% per pixel classification. For the desert (D) the producer accuracy is about 95% on average while the user accuracy ranges from 78% to 88%. This means that more than 95% of the desert is identified

correctly, while 78% to 88% of the area that was classified as desert is truly this category. The error matrix tables can be interpreted as showing that the D class is being confused with its sub-class (Basalt) and also with the loose urban areas which represent mostly the new settlements and remote cities. The cultivated land (CL) showed a high percentage in both user and producer accuracies in all classified images with an average of more than 90%. The CL is partly confused with the classes of bare soil (BS), urban (U) and cultivated urban (CU). Because CU is a mixed class, producer accuracy varies from 71% to about 99%, while user accuracy shows a more stable percentage ranging from 86% to 93%. The U class exhibited strong relation with its loose urban sub-class, due to this relation the producer accuracy appears wide percentage range (55% to 91%) while the user accuracy appears high percentage reach to in some classified images to 100%. Generally, the U class has fairly relation with CU and D classes. The bare soil (BS) class is the most confusing class and shows a strong relation with the CU class and a partial relation with the CL and U classes. Both its user and producer accuracies show low overall accuracy with an average of about 60%.

The WB, D, CL and even U areas could be identified correctly by using image segmentation techniques which grouped the most spectral relative pixels into one object.

#### 4.3.2.8 Change detection and spatial impact

The green cover of the whole GCM decreased by 33% between 1984 and 1990, and then by 13% between 1990 and 2006, and between 1984 and 2006 increased by 36% (Fig. 56). Field observation proved that the loss of cultivated land was in favour of urban cultivated areas and urban sprawl. The change detection map (1984-2006) (Fig. 57) and ground information revealed that the green areas around the ring road and Helwan metro line represented an open corridor of fertile land that was lost. The vegetation change map between 1984 and 1990 showed extensive use of green areas in the area extending from the northeast to the west of Giza (Fig. 57).

There are some green patches appeared in desert area which confirmed in field observation and was assigned to reclamation activity. Such activity can interpret the increasing in vegetation cover area between 1990 and 2006 for about 15%. In general, there are two main forces that have impacted on the green cover: reclamation and encroachment.

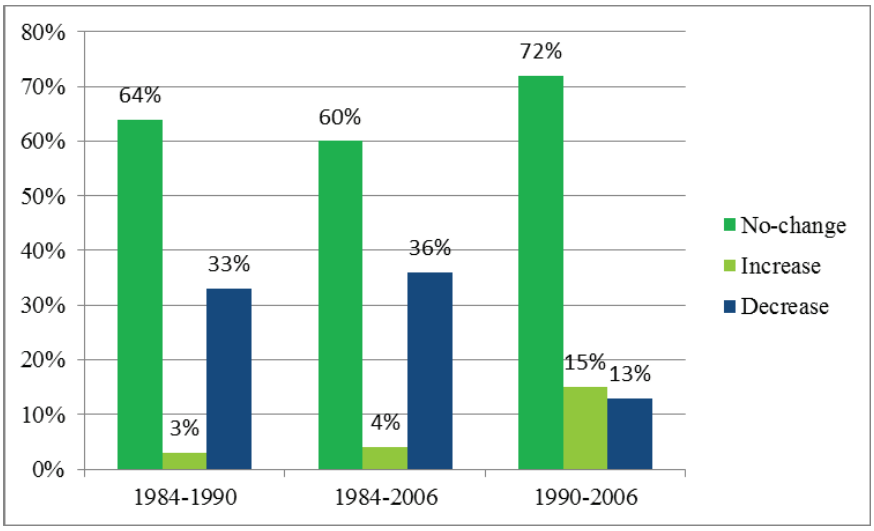


**Figure 56: The percentage of change in cultivated land**

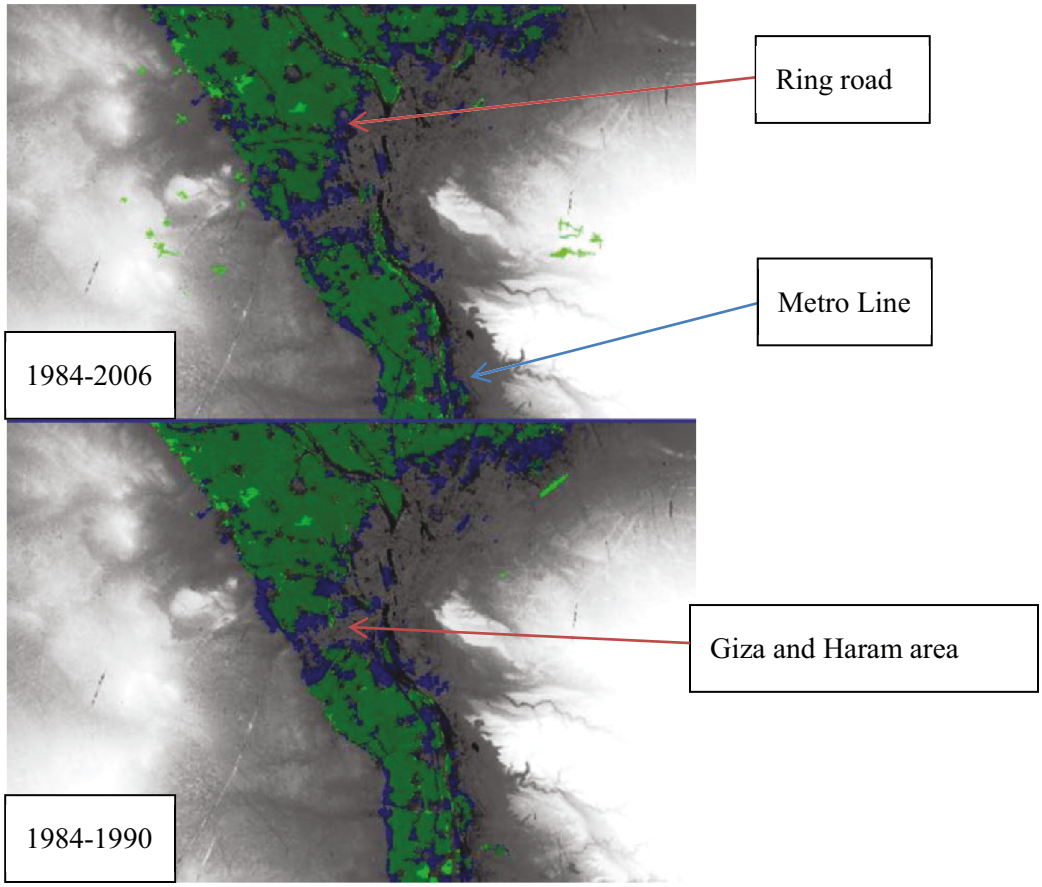


**Figure 57: Vegetation change between 1984 and 2006 (up), and between 1984 and 1990 (down) (eCognition), (for legend see Fig. 56)**

Change analysis of urbanization in the whole of GCM exhibited fast growth: from 57% between 1984 and 1990, to 83% between 1984 and 2006 (Fig. 58). The increase in urban activities could reflect the trend of investment over last three decades in Greater Cairo which touch all level of investors. On the one side, urban growth increased extensively between 1984 and 1990 due east of the GC core (Fig. 59), when slums appeared and informal building work was carried out in different parts at the periphery. In addition, there are some patches mostly due west of the study area (hinterland) representing the first new settlements in the desert area (6$^{th}$ October City). On the other side, the change detection map between 1984 and 2006 showed settlement saturation in the northeast to west Giza corridor and also at some areas around the metro line in Maadi-Helwan area. Besides that, the large part of desert used for new cities establishment. Furthermore, most of cultivated-urban land (CU class) was transformed to urbanization. Therefore, the new patches of urban class appeared close to ring road, and also appeared in the west boundary between the vegetation cover and hinterland (Fig. 60 and 61). Furthermore, the spatial distribution of CU in hinterland indicated to the increasing of the urban green areas that explores the raising of life quality in these areas (Fig. 62).

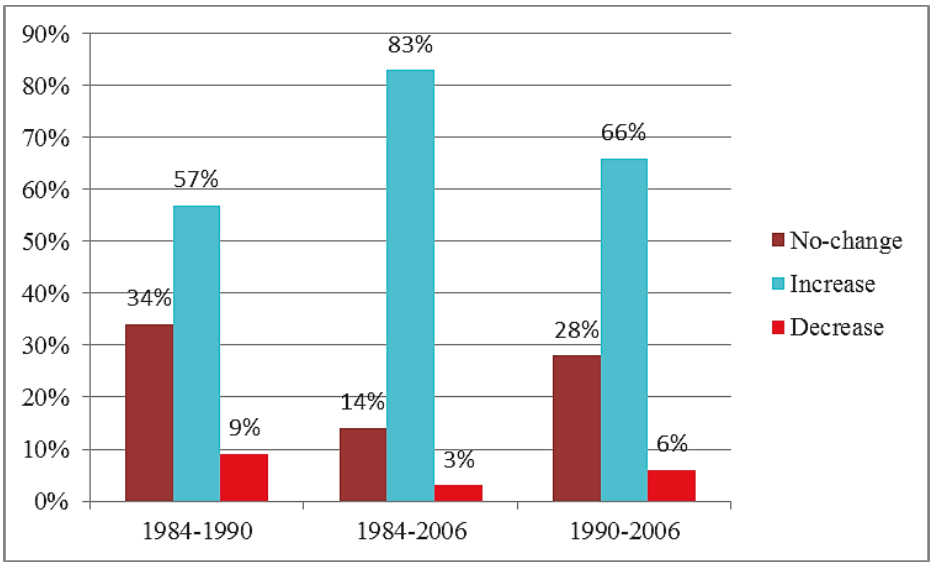


**Figure 58: The percentage of change in urbanization**

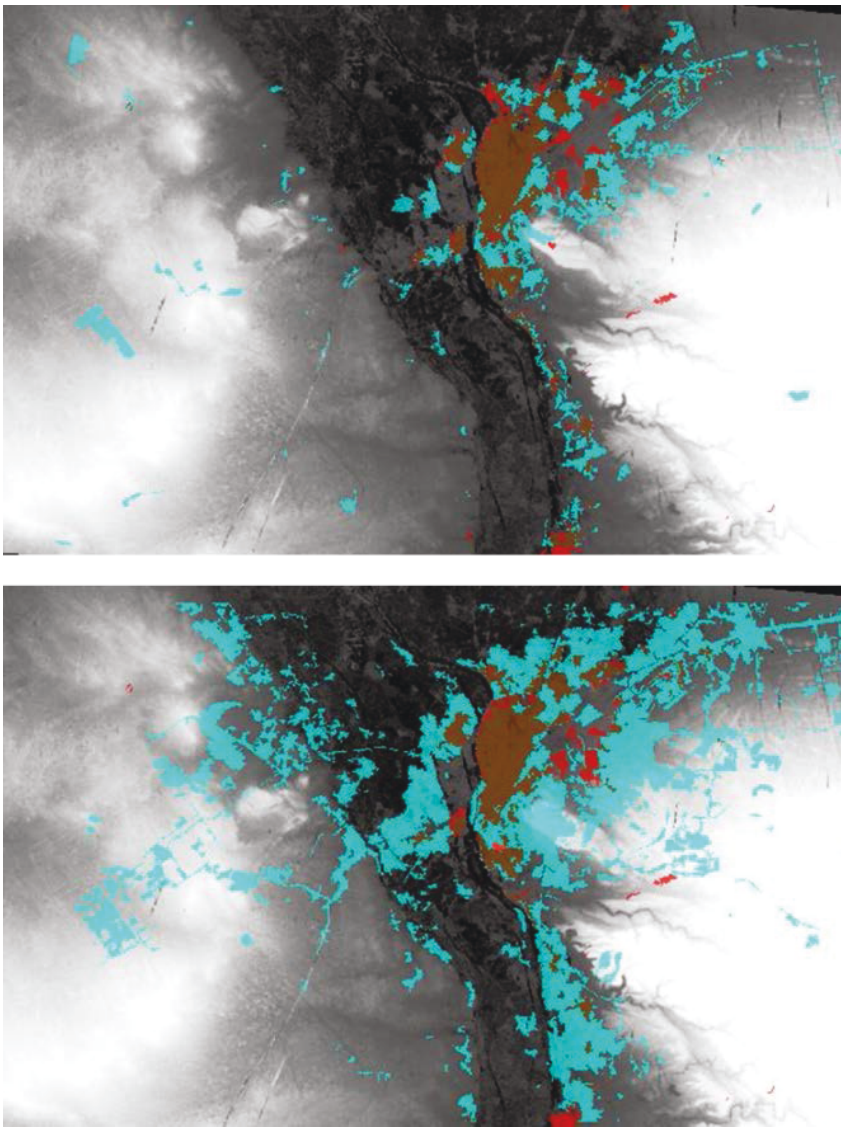

**Figure 59: Urbanization change between 1984 and 2006 lower, and between 1984 and 1990 upper (eCognition), (for legend see Fig. 58)**

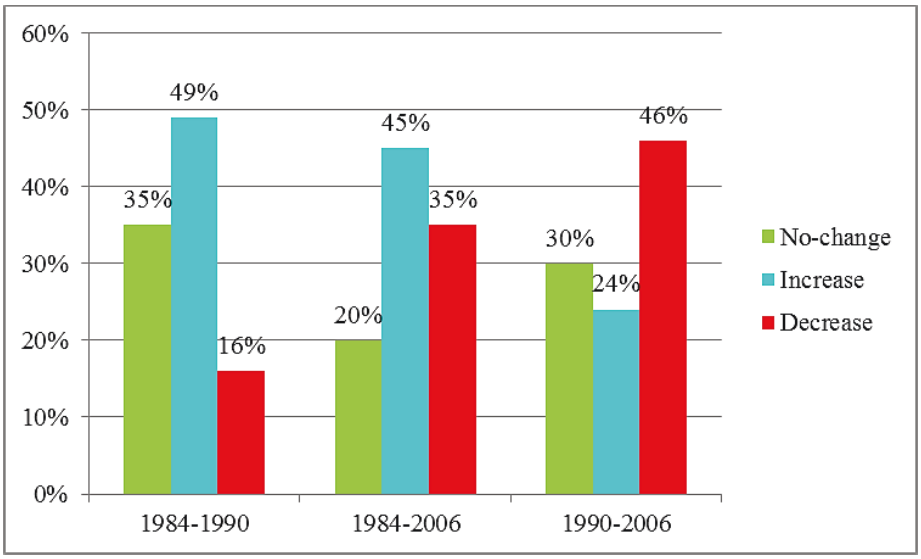


**Figure 60: The percentage of change in the cultivated-urban class**

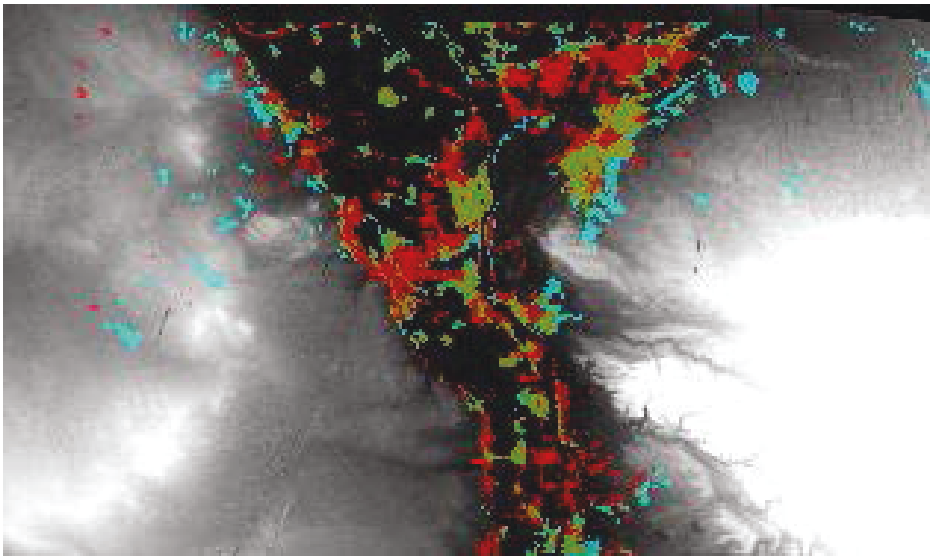

**Figure 61: Urbanization change between 1990 and 2006, (for legend see Fig. 60)**

**Figure 62: Green space in new cities (Photo taken east of new Cairo city). Photo captured 2010**

## 4.4 Subsidiary DPSIR and feedback mechanism

At the first level of monitoring which was examined here, there are some driving forces to be deducted which impacted on the LULC state and spatial growth of GCM. For example, people in the new cities established in the desert need green spaces, which was reflected in the cultivation activity in the desert, the use of water, and how it attracts the medium to high class dwellers. That puts pressure on fertile land on the Nile Wadi and the use of food production fields. These components could be conceptualized at the same level of the monitoring framework by creating a specific subsidiary DPSIR for green cover which will contribute to response for a specific system (Fig. 63). The understanding of green cover of GCM at that sub-level can play a feedback role which linked with the main DPSIR (Fig. 23 and 33). This kind of process is called "feedback mechanism" or "self-organization process" (Cumming and Norberg 2008, and Cumming 2011).

To understand urbanization resilience, I created subsidiary DPSIR schemes at sub-level and conceptualized the urbanization system indicators for further monitoring and analysis processes and then that can link to the main framework (Fig. 63). The monitoring process which might provide the subsidiary level could involve climate change or poverty. Such feedbacks and iteration processes are very interesting in the study of complex systems because they create the possibility for alternate stable states, regimes, and regime shifts (Cumming 2011).

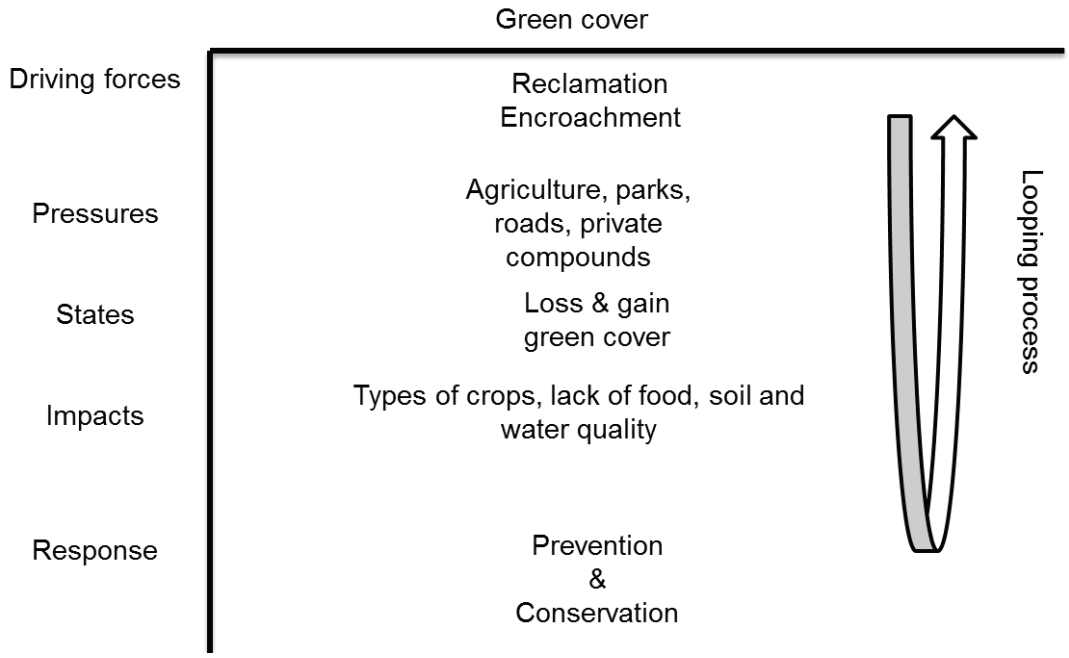


**Figure 63: Subsidiary green cover DPSIR scheme**

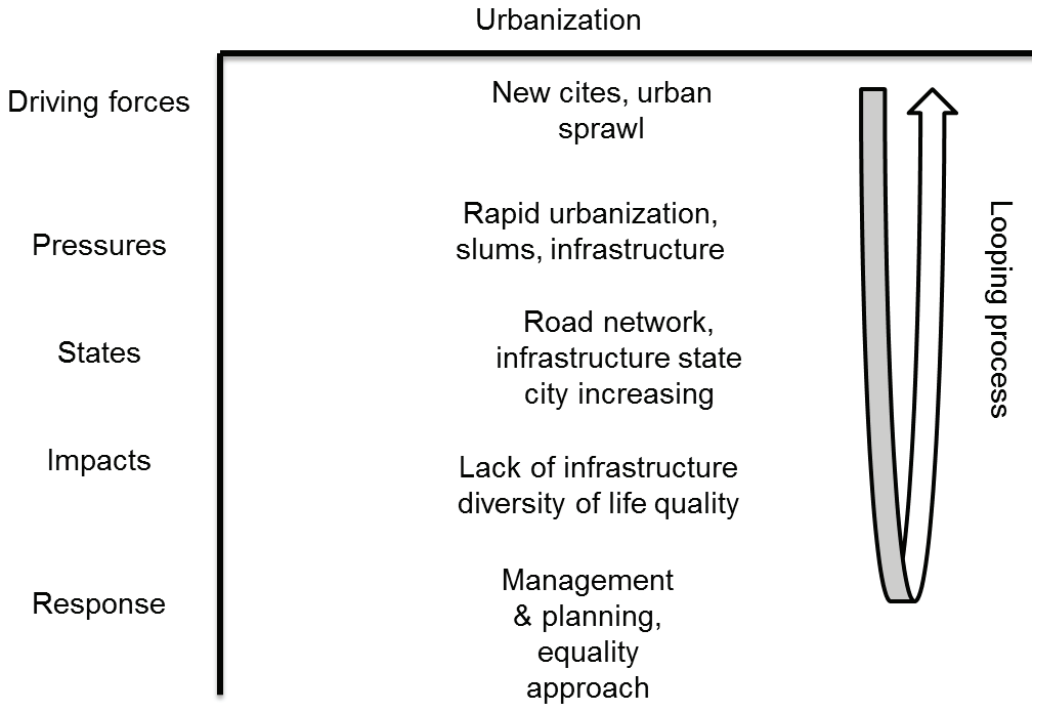


**Figure 64: Subsidiary urbanization DPSIR scheme**

Regarding the GCM case study and the objective of understanding the spatial dynamics, the second level of change detection process has been taken place in next chapter (five). That level was created based on two parameters; first is the spatial information deduced from change detection analysis at the first level examined in this Chapter, second the availability of coarser satellite data (ex. SPOT). At that level, the question of how and what is the impact of some spatial development elements such as the construction of new settlements in hinterland, roads network, and metro lines beside the economic reform (privatization) on the spatial growth and the LULC state of GCM (Fig. 35). The ability to segment the satellite image using OB classification technique (e.g. by using eCognition Developer) helps to differentiate the one class into sub-classes and work on different levels. Such technique approach could be integrated with the DPSIR scheme to determine the framework of spatial analysis (Fig. 35). Therefore, the strategy of analysis was fabricated to understand the causal relation and interaction between the examined elements and indicators.

Moreover, if I could have used very high resolution (VHR) of satellite data, I would have the higher level (third) of monitoring frame work by using DPSIR (Fig. 32). Such level could explore in detail the socio-ecological and spatial information of specific target (object).

## 4.5 Benefits of object-based classification

The analyses of LULC in the three time periods for the GC region were carried out using pixel- and object-based methods (Fig. 65). What arose from this is that OBIA (object based image analysis) has many more benefits than the pixel-based method, some of which are described below:

- Simultaneous classification of time series images by using the same classification procedures.
- The object size can be controlled by scale parameters, which increases the performance of the selected object for the classification.
- The discrimination between classified indicators and the ability to work on sub-levels have been achieved by OBIA rather than the pixel based method. For example; in the identification of the basalt exposures, OBIA has more refined processes than those described in Chapter 3.
- The pixel-based classification technique requires many separate steps to analyze and apply different types of algorithms, but the object-based classification technique can apply many algorithms within only one rule set and image view (e.g. for vegetation analysis).

- The OBIA classification process could be called multi-algorithm classification, because many features and functions are used to refine the classification.
- With both DPSIR and OBIA, we can work at different levels simultaneously, which means that using the DPSIR model and the classification tree designed by eCognition OBIA as rule-set supports the system of spatial monitoring of big cities and complex systems like Greater Cairo. Therefore, DPSIR is used not only as a reporting framework but also as an analytical system of the monitoring workflow. Consequently, that integration can add value to the application of the DPSIR which mainly used to identify the character relation of environmental indicator (Hains-Yound 2007) rather than to design causal framework of the complex system like megacities.
- Furthermore, some criteria (development elements) could be derived from classification results and can be implemented by the conceptual model (DPSIR) to put in the subsidiary and/or high level of DPSIR which support the stakeholder needs.

## 4.6 Technical disadvantages

There are, though, some technical problems when working with a large set of satellite data for large areas such as mega cities. The first is the capacity of the software´s cache memory to deal with sophisticated classification rule set which may comprise of hundreds of processes, which takes a long time and sometimes has to be discontinued. The second is that the export of some results, such as accuracy assessment, still needs to be improved.

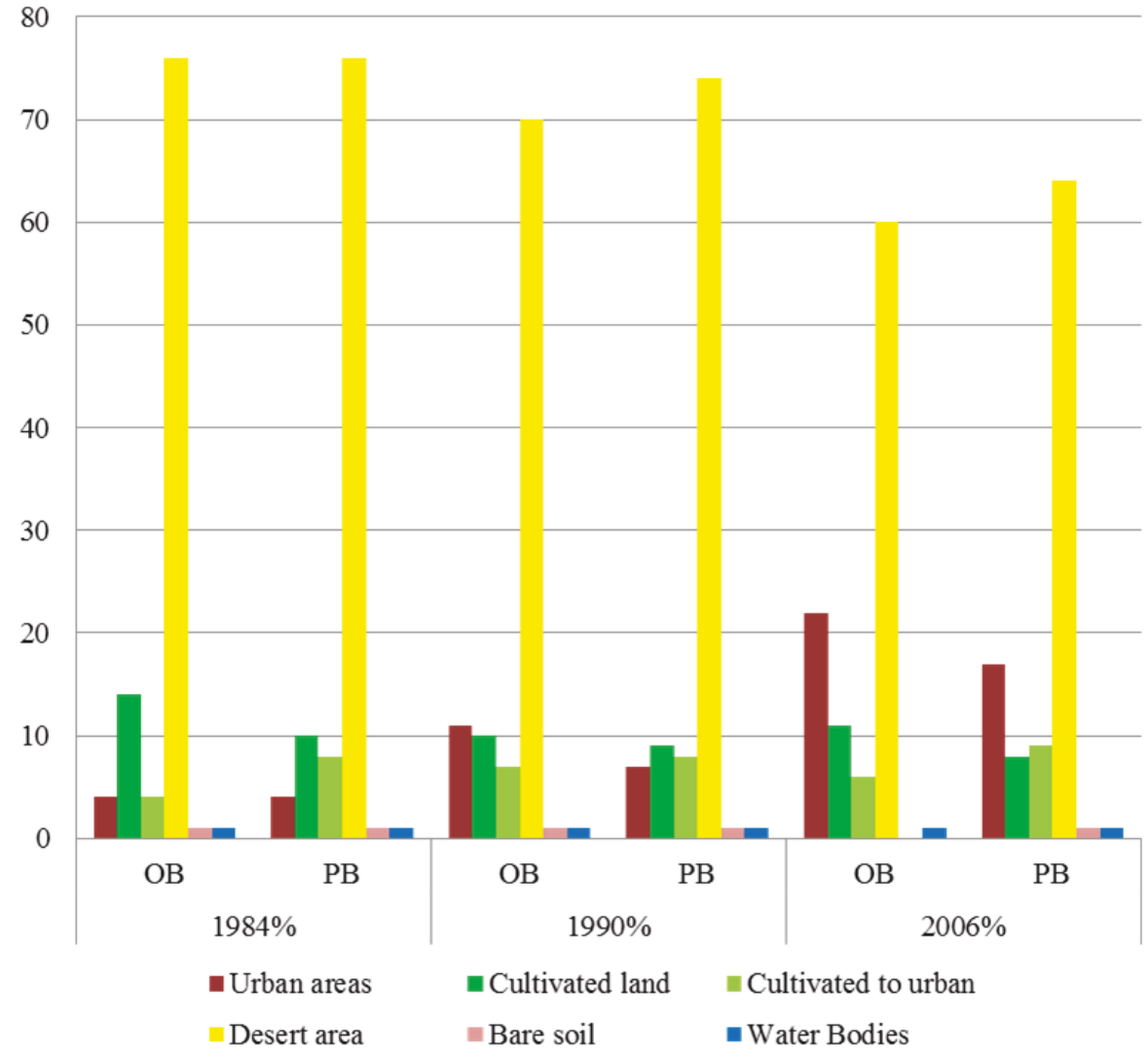


**Figure 65: Comparison of OB and PB classification methods**

# 5 Spatial Changes (Impacts)

## 5.1 Introduction

In this chapter I continue to analyze the spatial resilience of GCM in different timescales and data resolutions. That shows the second level of change detection chain (monitoring framework) and the spatial impact of developmental elements (e.g. ring road, metro, and new cities) on the period of privatization economic program harvest (Figs. 32 and 66). This chapter is divided into three parts, with each part dealing with a sector of Greater Cairo (*metro-autostrad, core-new, and west GC (ring road-Giza sectors)*) which is affected by one or more of the developmental elements. These elements or criteria derived based on the first classification occurred for the whole study area in Chapter four and implemented with the DPSIR framework (Fig. 66).

Abu-Lughod (1969) has stated that implicit in earlier ecological research was the idea that the spatial pattern of a city was embedded in objective reality and would be revealed almost automatically once a sufficient number of sensitive indices were gathered and processed.

Li et al. (2010) have concluded that, in China's economic development, roads and highways are planned on the basis of environmental impact assessment. Also, they recommended that evaluation of environmental indicators should be integrated into road-system planning at various scales, from the national scale to the smallest planning units. The neo-liberal economic as well as broader regional shaped the megacity of Calcutta in India, which influenced the spatial structure of the metropolitan core by developing several secondary cores over time to support the expanding function of the city (Haque and Bandyopadhyay 2012). In GCM, the link between environmental degradation, economic reform and transportation evolution besides urban expansion still need to be integrated spatially to support the master plan of the Metropolitan. The classification process was made according to the DPSIR scheme (Fig. 35), which is integrated with the object-based approach to define the spatial indicators to be classified at different levels (at least two in this study).

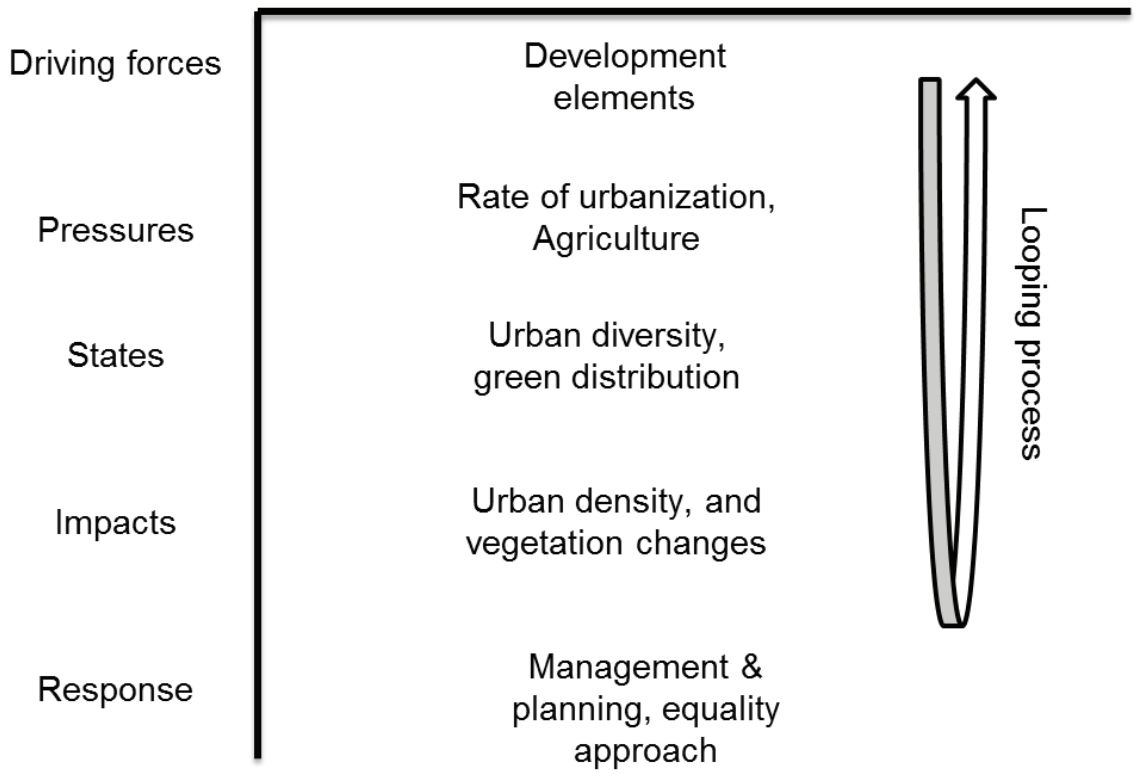


**Figure 66: Implementation of the DPSIR model to understand influences of developmental and infrastructural elements on spatial resilience in GCM**

## 5.2 Privatization program

The privatization program has been controversial ever since it was announced in 1991. The program started slowly in 1993, but then accelerated until 1999. The first actual privatization took place in 1996 and its effect on Egyptian society is undeniable (PCSU 2002). PCSU 2002 also concluded that all Egyptians benefit from the improved services and products, and sometimes lower prices resulting from liberalization policies that encourage subsector competition, new entrants and innovation. The resulting expansion is likely to create more jobs than those lost through the privatization process. In contrast, the Deputy Prime Minister and supervisor of Egypt's sell-off of state enterprises, Ali Al-Selmi announced after the 2011 uprising that Egypt's "unfair privatization program" will be cancelled, sparing the country's last 147 public companies. An early-retirement scheme put in place to reduce the number of factory workers which was aimed at facilitating the selling of overloaded public enterprises was severely criticized when it affected around 500,000 people (http://english.ahram.org.eg/News/16923.aspx). Therefore, this chapter is concerned with the

impact of the privatization program on the dynamic pattern and spatial structure of GCM in the selected time periods.

## 5.3 Spatial infrastructures (developmental elements)

The most recent transportation infrastructure built over the past twenty years are the metro project and ring road, the 15th May axis, and Autostrad road (motorway) that, combined with improvements to most highways, connected GCM to Egypt's countryside (Fig. 3). The main characteristics of the first line of Cairo's metro system are internal width of 8.7 m, internal height of 6.0 m, and a total length of 45 km from Helwan to El-Marg (http://www.ace.com.eg/transportation-rail-cairo1.htm). The ring road was completed in the late 1990s, and aimed to serve the new settlements (new cities) and to relieve traffic congestion inside the city (Suttan and Fahmi 2001, DRTPC 2009). In the meantime, the autostrad road and 15th May axis were constructed to link Helwan and Cairo, and the new cities to the west with Cairo, respectively. This chapter also is concerned with the spatial impact of metro line and autostrad road in the south east of GC and of the ring road-15th May axis west of the River Nile.

## 5.4 New cities

The master plan for new cities is aimed at saving the fertile land, especially by encouraging urban development in new cities dominated by the desert area (Fouad 1980). Though expansion into desert land is certainly preferred to expansion into prime agricultural land, rampant expansion into the desert will need to be controlled (Yin et al. 2005). Wherever private development rather than public building has occurred in the new towns, the social objectives of the master plan have not been met, either (Suttan or Fami 2001). This chapter therefore shows how the new towns influenced the spatial pattern and urban density and diversity in GCM, and examines and analyzes the sector from the core of Cairo east towards new Cairo city.

## 5.5 Materials and methodology

### 5.5.1 Materials

Because the target of analysis in this chapter is based on different levels of time and resolution, the Spot images with two different time series have been used. The images acquired in 1999 and 2008

by Spot satellites 4 and 5 with a resolution of 10 and 5 meters respectively were selected to show the changes since the establishment of GCM development projects. These images are characterized by high resolution with a short range of spectral information and few band channels. Therefore, the classification applied here by OBIA (Object Based Image Analysis) concerns not only the spectral character of the object but also the physical character which is mainly used during the refine step of classified indicators. Accordingly, the classifier features were applied like shape, texture appearance and so on accompanied by ground observations and check points. All images were enhanced by using spectral contrast, haze reduction and synchronize are utilized (Chapter 3). Each image was subdivided into three similar subsets while the classification was carried out on each sector with approximately the same conditions.

### 5.5.2 **Classification rule set**

A classification rule set created with various algorithms and features was used for both selected years and their subsets. The rule set is explored by three classification trees, two of which represent the two years and the third represents the change detection processes.

The classification processes differentiated the land use and cover of the areas of interest according to five main: settlements (low, medium, high densities), vegetation cover (agricultural fields (dense-uniform, and sparse), water bodies, bare soil, and desert (rocky cover) (Fig. 35).

As usual, segmentation is the first process to identify the characters of the objects, and we used the scale parameter equal to twenty after testing scale parameters of 100, 50, 30, and 10. Consequently, we found that the scale parameter between 20 and 25 is suitable for medium-to-high resolution data for a large area.

### 5.5.3 **Classes and features**

The selected range of indices and algorithms are mainly based on the field and ground information, which lead to a stability of classification and help us avoid the complexity of accuracy assessment methods.

#### 5.5.3.1 Indices formula applied on SPOT images

Land water mask (LWM) = ([Mean Layer 3NIR]) / ([Mean Layer 1Green])*100

The Normalized Difference Moisture Index (NDMI) = (NIR-IR) / (NIR+IR), but this index (NDMI) was modified in this study for Spot bands to be (R-IR)/(R+IR).

Normalized difference vegetation index (NDVI) = ([Mean Layer 3NIR]-[Mean Layer 2red])/ ([Mean Layer 3NIR] + [Mean Layer 2red])

Green normalized difference vegetation index (GNDVI) = (NIR-green)/(NIR+green) GNDVI= (NIR-Green) / (NIR+Green)

Ratio vegetation index (RVI) = NIR / Red.

#### 5.5.3.2 Water bodies (WB)

This class represents here the surface water which mainly dominates the River Nile, canals, natural and artificial lakes, and large swimming pools.

The WB class is identified for both Spot images of 1999 and 2008 by using features such as brightness and indices such as LWM.

Brightness applied to image99 ranges from 15 to 20 for NIR and SWIR bands, while for image08 it ranges from 20 to 25 for all bands. The LWM was used to define unclassified water bodies and enhance the brightness of classified water bodies. The LWM formula was applied for both images and showed that the water bodies are mainly represented by an average value of more than 200.

We realize that the LWM is better for water discrimination than brightness, with a reflectance of more than 200 for Spot4&5 images.

The classification of water in 1999 which has 10m resolution is difficult because the channel in some areas is covered by Hyacinth Flowers (Ward El-Nile) (Fig. 67) which affected spatial reflectance. However, in 2008, with 5m resolution, the spatial reflectance of this plant was reduced.


**Figure 67: Water channel covered in some parts with Hyacinth Flowers (Ward El-Nile). Photo captured 2009**

5.5.3.3 Bare soil and/or wet land (BS)

I mean here by bare soil any fertile land uncovered by vegetation and any land no longer used for any agricultural activity – land which is left by people for a period of time in order so that it is ready for building activity.

Many algorithms are used to identify the bare soil and wet land in the areas under concern; basically, the NDMI index was used and supported by GNDVI and RVI for further enhancement. For both images, the NDMI ranges in value from 0.0 to 0.01 for primary results of this class (bare soil and wet land) which is provided by check point from field 2009 and 2010.

The GNDVI is also used for the further identification and enhancement of the bare soil, which mostly ranged from -1 to -0.15, while the RVI is mainly applied with a range of between 1.1 and 1.15.

Most bare soil and wet land areas classified are in a stage of transformation and indicate spatial change behavior.

5.5.3.4 Desert (rocky cover and hinterland) (D)

This class represents here the land covered by rock and the hinterland, and is described in detail in Chapter 2 of this study.

However, the desert class (rocky and hinterland) is differentiated correctly by using three different algorithms; these are NDMI, NDVI and RVI. For image99, desert class is represented by NDMI ranging from 0.08 to 0.15, NDVI of less than -0.08; and RVI of less than 0.86. In addition, the GNDVI and LWM showed less accuracy regarding desert. Furthermore, this class for image08 was also represented by the same three algorithms applied to image99 but with little change in spectral reflectance numbers due to the difference in resolution. Moreover, the indices like NDMI of more than 0.02, NDVI of less than -0.08, and RVI of less than 0.86 were used to discriminate the desert class. And LWM was used here to separate the desert correctly by using membership function ranging from 0.07 to -0.02 for refining process.

#### 5.5.3.5 Vegetation cover and cultivated land (CL)

The vegetation class described here has many different nomenclatures such as green cover, cultivated land, and fertile land. There are two other classes (sub-classes) belonging to the green cover class: agriculture or dense vegetation (AG), and less dense and / or sparse (SV) areas. The dense vegetation is represented essentially by agricultural fields and some wide and dense cultivated areas. The less dense (sparse) areas are mostly comprised of fertile land with less dense vegetation, open space, and urban-green areas (fuzzy objects).

The most common greenness vegetation indices used to discriminate the green cover are NDVI, RVI, and GNDVI.

Generally, the RVI with more than 1 represents the green cover for both images (image99 had a range of 1.01 to 1.25 and 1.01 to 1.2 for 2008).

Besides, the NDVI was used not only to identify the general green cover but also to differentiate the dense areas from the less dense to sparse areas. Hence, the NDVI value with a range of 0.03 to 1.1 represented the dense green cover and / or trees and a value of more than 1.1 represented the other vegetation covers that applied to overcome the confusing differentiation (fuzzy relationship) of its sub-classes.

GNDVI is used to differentiate the agricultural fields from other types of vegetation cover. For most subsets using the range from -0.06 to 0.009 for agriculture fields identification, and applying range from 0.07 to 0.09 to differentiate the disperse vegetation areas.

The NDMI was used to enhance the dense and less dense objects classified in some cases.

5.5.3.6 Urbanization (U)

As the separation between urban and rural area is fuzzy and their boarder cannot be delineated, we used urbanization to refer to any buildings and settlements in classified sectors of GCM.

The urbanization classification is based on ground observations, and uniformity of buildings that dominated the objects. Accordingly, the urban areas and settlements are classified and differentiated into a few sub-classes, such as: high density (HDU), medium density (MDU), and low density (LDU) based on shape and textures.

Most of the indices customized here were examined to classify urbanization beside with many algorithms (features) of eCognition software. However, the brightness and LWM are used extensively to differentiate the urban densities.

The brightness of green, red, and near infra-red band combination of used images was applied to represent loose urbanization in a range from 97 to 101, medium density urbanization in a range from 97 to 87, and high density urbanization in a range from 68 to 87, while the formal dense urbanization was identified in a range from 77 to 88 and the informal in a range from 77 to 67.

By using LWM, the very high density urban areas range from 103 to 109, medium density from 103 to 97, and low density from 93 to 97, while the very low are less than 93. The latter ranges were applied for most subsets with some little modification from image to image guided by the ground sample.

The first refinement of the urbanization classification was performed by utilizing the GNDVI that can discriminate the fuzzy areas (green-urban areas). For example, the highly dense urban areas were represented by a range from 0.01 to 0.06, medium urbanization from -0.01 to 0.01, low from -0.02 to -0.01 and low density of fuzzy areas (green-urban) from -0.19 to -0.065. The relation between density and brightness has been examined by Lenaa et.al (2006) (Fig. 68).

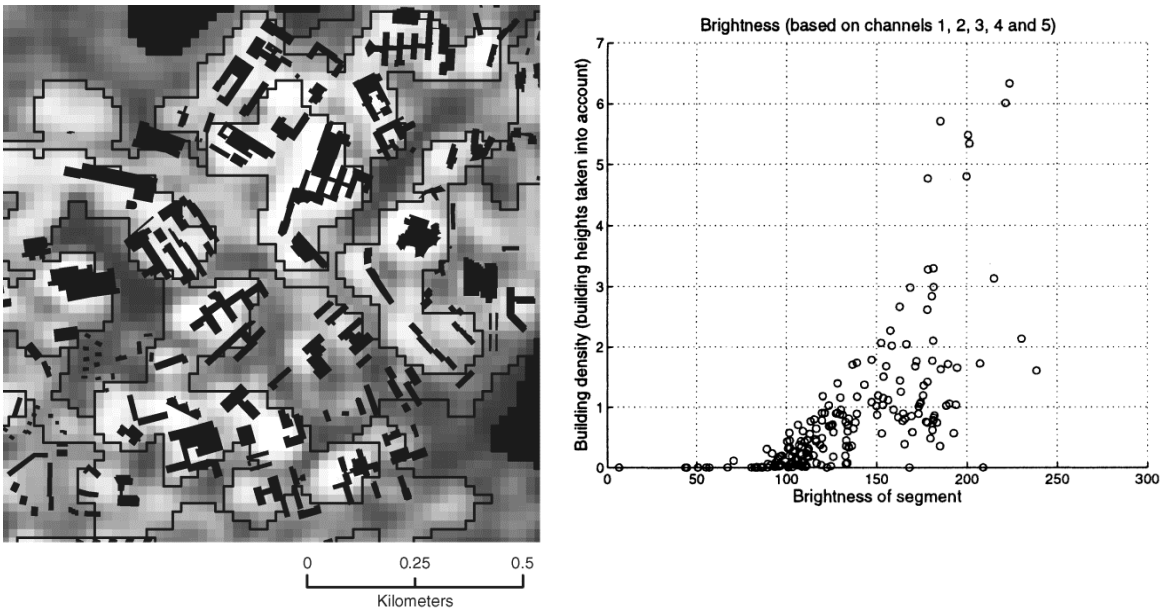


**Figure 68: Illustrations of the relation between brightness and building density (after Matikainen et.al, 2006: 44). "Building polygons overlaid on the segmentation result (left), and scatter plot showing the relationship between the brightness of segments and building density (right)".**

### 5.5.4 **Refining classification**

Classification was refined in two different ways. First, by using multiple algorithms and repetition of the classification process and applying the membership functions module witch support the classifier to overcome the fuzzy and confusing objects identification. Second, by using some algorithms to merge, identify, and cut classes based on some criteria such as length, number of pixels per object, and area.

These steps were followed by manual enhancement based on field observations and selected samples so as to enhance the obscure classified objects.

### 5.5.5 **Accuracy assessment**

Accuracy assessment was carried out based on the ground points for the three classified sectors by using the error matrix based sample option in eCognition software (Tables 13, 14, and 15). The tables that resulted show the confusing matrix, accuracy of producer and user, overall accuracy, and kappa index.

**Table 13: Accuracy assessment of classified metro-autostrad sector SPOT2008 (after eCognition)**

| User Class \ Sample | Water | Vegetation | Agriculture fields | Sparse vegetation | Urbanization | Medium density | Low density | High density | Desert | Bare soil | Sum |
|---|---|---|---|---|---|---|---|---|---|---|---|
| Water | 12 | 0 | 0 | 0 | 0 | 0 | 0 | 0 | 0 | 0 | 12 |
| Vegetation | 0 | 2 | 0 | 0 | 0 | 1 | 0 | 1 | 0 | 0 | 4 |
| Agriculture fields | 0 | 1 | 12 | 0 | 0 | 0 | 0 | 0 | 0 | 1 | 14 |
| Sparse vegetation | 1 | 6 | 0 | 22 | 1 | 2 | 0 | 0 | 0 | 0 | 32 |
| Urbanization | 0 | 0 | 0 | 0 | 8 | 3 | 0 | 1 | 0 | 0 | 12 |
| Medium density | 0 | 0 | 0 | 0 | 2 | 28 | 1 | 0 | 0 | 0 | 31 |
| low density | 0 | 0 | 0 | 0 | 6 | 3 | 17 | 1 | 1 | 0 | 28 |
| High density | 0 | 0 | 0 | 0 | 0 | 1 | 1 | 53 | 2 | 0 | 57 |
| Desert | 0 | 0 | 0 | 0 | 0 | 0 | 3 | 0 | 28 | 0 | 31 |
| Bare soil | 0 | 2 | 1 | 2 | 0 | 0 | 0 | 0 | 0 | 11 | 16 |
| Sum | 13 | 11 | 13 | 24 | 17 | 38 | 22 | 56 | 31 | 12 | 0 |
| | | | | | | | | | | | |
| **Overall Accuracy** | **81.43%** | | | | | | | | | | |
| **KIA** | **0.788** | | | | | | | | | | |

**Table 14: Accuracy assessment of classified core-new Cairo city sector SPOT2008 (after eCognition)**

| User Class \ Sample | Water | Vegetation | Agriculture fields | Sparse vegetation | Urbanization | Medium density | Low density | High density | Desert | Bare soil | Sum |
|---|---|---|---|---|---|---|---|---|---|---|---|
| Water | 18 | 0 | 0 | 0 | 0 | 0 | 0 | 0 | 0 | 0 | 18 |
| Vegetation | 0 | 4 | 0 | 1 | 0 | 0 | 0 | 0 | 0 | 0 | 5 |
| Agriculture fields | 0 | 0 | 13 | 0 | 0 | 0 | 0 | 0 | 0 | 0 | 13 |
| Sparse vegetation | 0 | 0 | 1 | 27 | 0 | 1 | 0 | 0 | 0 | 0 | 29 |
| Urbanization08 | 0 | 0 | 0 | 1 | 3 | 35 | 1 | 0 | 0 | 0 | 40 |
| Medium density | 0 | 0 | 0 | 0 | 0 | 0 | 0 | 0 | 0 | 0 | 0 |
| Low density | 0 | 0 | 0 | 1 | 0 | 1 | 12 | 0 | 0 | 0 | 14 |
| High density | 2 | 0 | 0 | 0 | 0 | 1 | 0 | 26 | 0 | 0 | 29 |
| Desert | 0 | 0 | 0 | 0 | 0 | 0 | 0 | 0 | 77 | 0 | 77 |
| Bare soil | 0 | 0 | 0 | 0 | 0 | 0 | 0 | 0 | 0 | 3 | 3 |
| Sum | 20 | 4 | 14 | 30 | 3 | 38 | 13 | 26 | 77 | 3 | 0 |
| | | | | | | | | | | | |
| **Overall Accuracy** | **80.26%** | | | | | | | | | | |
| **KIA** | **0.765** | | | | | | | | | | |

**Table 15: Accuracy assessment of classified ring road-Giza sector SPOT2008 (after eCognition)**

| User Class \ Sample | Agriculture fields | Sparse vegetation | Urbanization | Medium density | Low density | High density | Desert | Bare soil | Sum |
|---|---|---|---|---|---|---|---|---|---|
| Agriculture fields | 55 | 2 | 0 | 0 | 0 | 0 | 0 | 0 | 57 |
| Sparse vegetation | 3 | 6 | 0 | 0 | 0 | 0 | 0 | 0 | 9 |
| Urbanization | 1 | 2 | 5 | 0 | 1 | 0 | 0 | 0 | 9 |
| Medium | 0 | 0 | 1 | 10 | 0 | 5 | 0 | 0 | 16 |
| Low density | 1 | 4 | 0 | 0 | 4 | 0 | 1 | 0 | 10 |
| High density | 0 | 2 | 0 | 3 | 0 | 34 | 0 | 0 | 39 |
| Desert | 0 | 0 | 0 | 0 | 0 | 0 | 42 | 0 | 42 |
| Bare soil | 0 | 0 | 0 | 0 | 0 | 0 | 0 | 2 | 2 |
| Sum | 60 | 16 | 6 | 13 | 5 | 39 | 43 | 2 | 0 |
| | | | | | | | | | |
| **Overall Accuracy** | **85.33%** | | | | | | | | |
| **KIA** | **0.814** | | | | | | | | |

If I consider the accuracy assessment tables, I can see that the overall accuracy of the classified results of the three sectors shows a high percentage ranging from 80% to 86%.

The water bodies (WB) class showed an average of producer and user accuracies of more than 95% in both MA and CNC sectors, while the water class in the third sector is mostly covered by vegetation or settlements constructions (e.g. bridges) (Fig. 69). In general, the WB class is seldom confused with the urban (U) and less dense (sparse) vegetation (SV) classes.

**Figure 69: Confusing classification of water channels west of GCM. Photo captured 2010**

For the desert (D) class, the producer and user accuracies have an average of more than 95% and it is seldom confused with urbanization classes. For the cultivated land (CL) class and its sub-classes (AG and SV), the information in accuracy tables exhibits a mix relation between the CL class SV that caused a reduction in the accuracy of the main vegetation class to reach a user accuracy of 50-80%. Regarding the AG class, the producer and user accuracies are more than 92% on average. The AG is well defined in all sectors due to its uniformity, but in some parts it shows confusion with BS, VS, and U classes. For the class SV, the producer accuracy is about 91% in sectors MA and CNC, and 31% in WGS, while the user accuracy in all sectors has an average of about 75%. The latter revealed that the SV class mixes with CL, LDU, and BS (Fig. 70). Moreover, the accuracy of the urbanization class and its sub-classes showed a strong relationship between each other and the

accuracy assessment of each sub-class exhibited in general a lower value of user accuracy than of producer accuracy. For the HDU class, the average of producer and user accuracies reached 95%, with an obvious confusion with MDU in some parts (Fig. 71). Similarly, the field observations confirmed the relation between medium and low density classes in many parts at the periphery of GC. This relation can be derived also from confusing matrix table of metro-autostrad (MA) sector. Therefore, the user and producer accuracies differ from sector to sector with a total accuracy of about 75% on average. For the LDU class, producer accuracy is about 81% on average, while user accuracy is about 60%, which is due to the difficulties in distinguishing between some urban areas dominated by green spaces on the one hand and sparse vegetation as well as low density urbanization on the other. The BS class has a satisfying overall accuracy of more than 90% (about 95% for producer accuracy and about 85% for user accuracy). Nonetheless, BS still needs higher resolution data to identify the small barren lands where the field observations indicated the difficulties of assessing the BS in the classification process.

**Figure 70: Mixed area between sparse vegetation (SV), bare soil (BS), and low urban density (LUD) NW GC's periphery (CNC sector). Photo captured 2010**

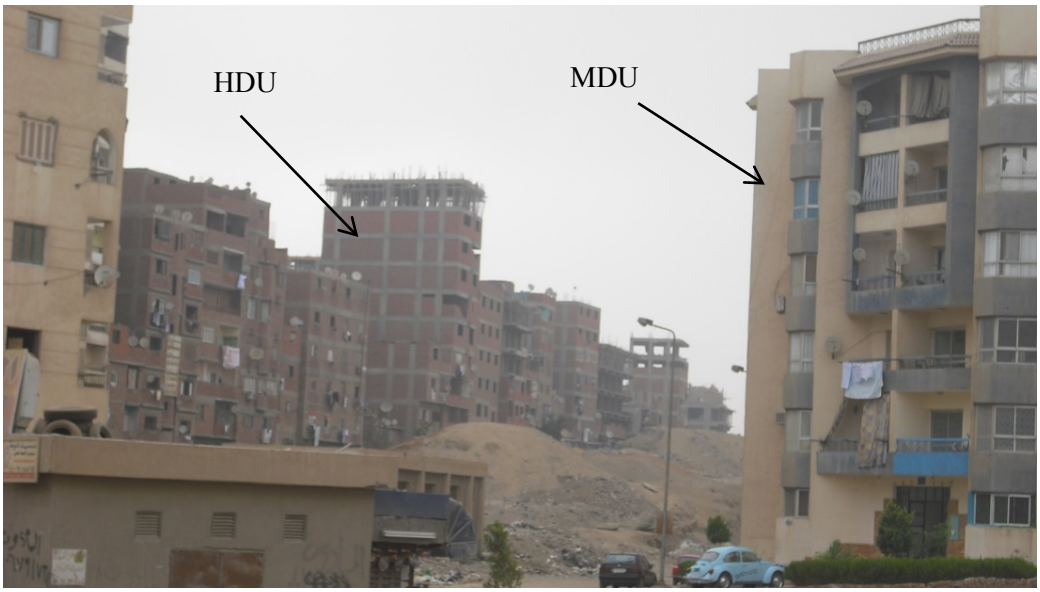


**Figure 71: Field observation of medium urban density (MDU) and high urban density (HDU) in east GC shows the close relation in spatial distribution arrows show the type of buildings used mainly in the two different classes. Photo captured 2010**

## 5.6 Results

The LULC maps of the three classified sectors of GCM for each selected year (1999 and 2008) have been analyzed and described. These are the metro-autostrad (MA) sector, the core-new Cairo city (CNC) sector, and the west ring road-Giza (WGC) sector. The classification has been done at different levels to differentiate the classes to sub-class which managed by the DPSIR framework

### 5.6.1 Metro-autostrad sector (MA)

The metro-autostrad sector is located in the SE of GCM and covers an area of about 82.5 square kilometers extending from Helwan to south and El-Maadi area to north (Fig. 72). This sector is dominated by two developmental elements: the first metro line, which extends for about 18.4 km due east of the River Nile, and the autostrad to the east of the metro line, which also extends from south to north. What, then, are the spatial influences of these two elements? This sector was divided into five main land use/land cover classes. It includes urban, cultivated areas, bare soil, rock cover (desert), and surface water bodies. Moreover, the land use land cover maps reveal that the spatial dynamic of the metro-motorway sector reflects the degree of activities of urbanization and cultivation. Thus, I created a sub-level of classification to deal with those two classes and thereby

detect the growth trends and understand the causal link between infrastructural projects in the AM sector and the spatial state of urbanization and green cover sub classes.

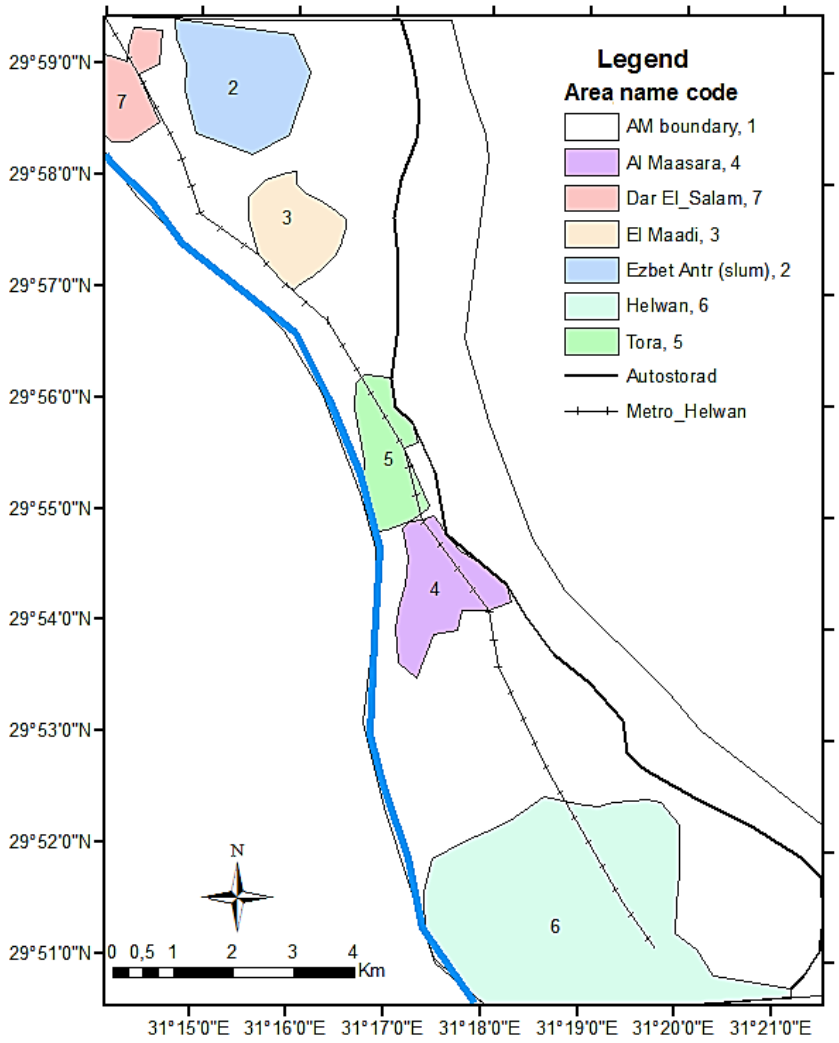


**Figure 72: The metro-autostrad sector (southeast GCM). Map based on SPOT image 2008**

### 5.6.1.1 LULC state

The classified land use and land cover map of 1999 shows that urbanization (Fig. 73) was the dominant LULC, accounting for about 40.98 $km^2$ (61%), followed by desert and rock-covered land with about 27.03 $km^2$ (21%), and green cover with about 10.69 $km^2$ (13%). The classes of bare soil and water bodies covered a small proportion of the study area (about 1.13 $km^2$ (1%) and 3.095 $km^2$ (4 %) respectively) (Table 16).

For the SPOT classified image of 2008 (Fig. 74), urban areas also comprised the dominant land use type, accounting for about 50.34 $km^2$ (61%), followed by desert and rock-covered land (hinterland), estimated at 17.12 $km^2$ (21%); cultivated land comprised a remarkable cover of about 11.27 $km^2$ (14%), which was an increase of about 1% on the area accounted for in the 1999 image. Surface water bodies covered an area of about 2.78 $km^2$ (3%), and bare soil represented a small proportion of the total area (about 0.96 $km^2$ (1%)) (Fig. 75 and Table 16).

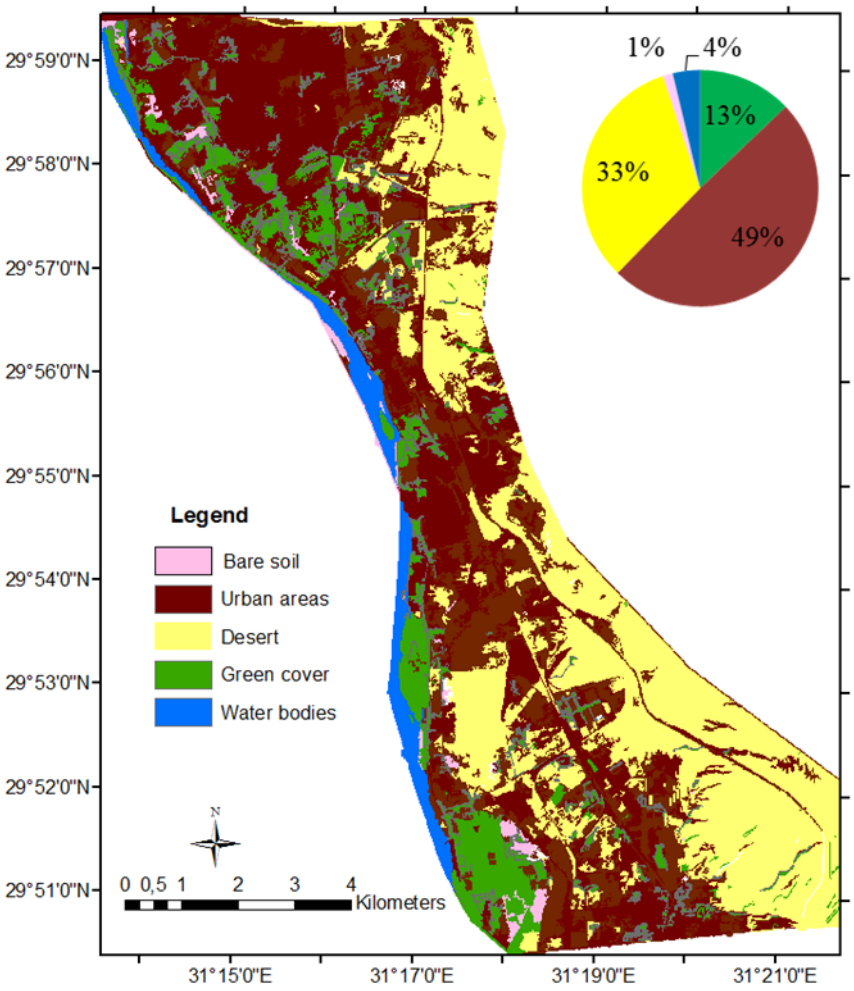


**Figure 73: LULC map of metro-autostrad sector for 1999**

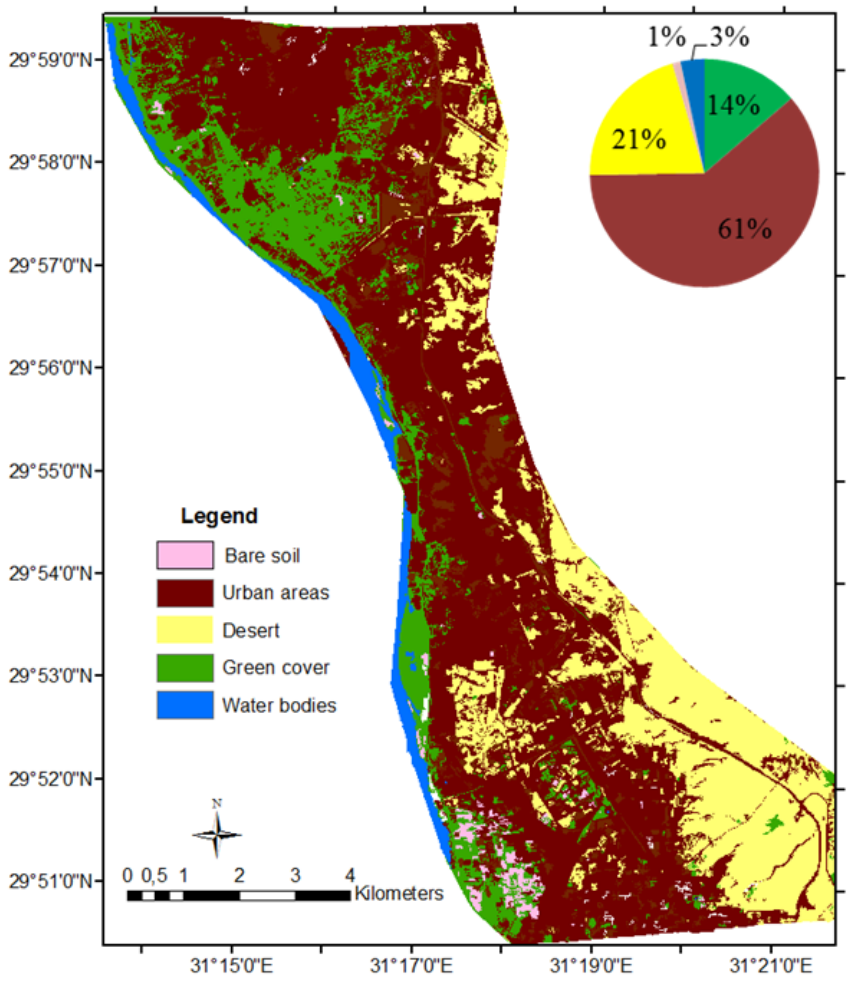


**Figure 74: LULC map of the MA sector for 2008**

The spatial distribution of urban areas and green cover in both images (1999 and 2008) shows that some areas like El Maadi are fuzzy areas, which is because separating urbanization from green cover still requires very high resolution satellite images and/or at least a refining of the current classification of images. To differentiate the classification of urban areas and vegetation cover, I bifurcated the classification tree into sub-levels and classes. It was at those levels that I then detected and analyzed the impact of spatial development on the distribution of urban densities and green cover forms.

**Table 16: Metro-autostrad sector statistics and percentage of the land use land cover units in 1999-2008 (see abbreviations in 5.5.3)**

| LULC Classes | 1999 | | 2008 | |
|---|---|---|---|---|
| | Area km | Area% | Area km | Area% |
| CL | 11.269 | 14% | 10.694 | 13% |
| U | 50.340 | 61% | 40.976 | 49% |
| D | 17.105 | 21% | 27.0287 | 33% |
| BS | 0.955 | 1% | 1.1272 | 1% |
| WB | 2.779 | 3% | 3.095 | 4% |

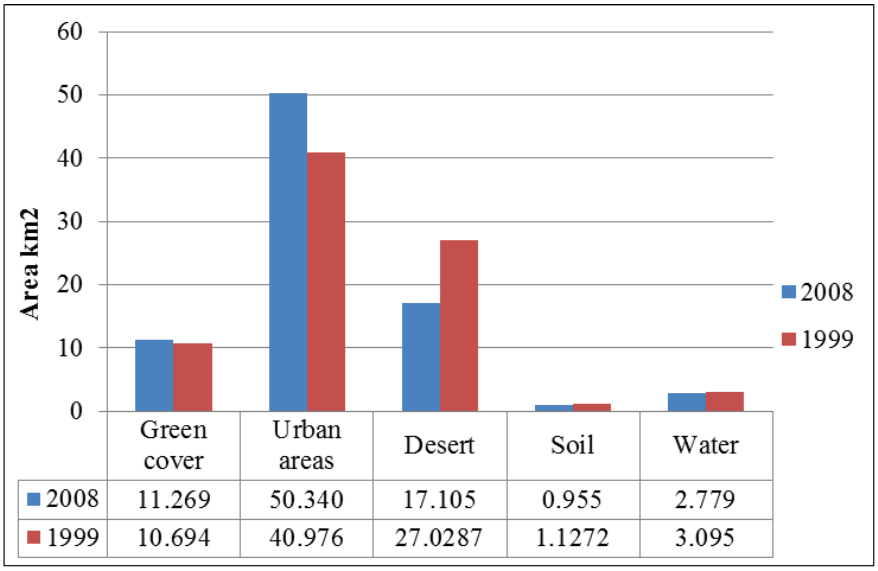


**Figure 75: Changes in land use land cover areas between 1999 and 2008 in metro-autostrad sector**

### 5.6.1.2 Urbanization

Due to the density of buildings, the metro-autostrad sector dominates the three main sub classes of urbanization. There are low, medium, and high density reflecting the spatial distribution of settlements and the impact of the metro project and autostrad high road on the density of buildings. In 1999, high-density urbanization accounted for an area of about 18.47 $km^2$ (22% of the total area

and 49% of total urbanization) located chiefly on the northern part of GCM (Dar-El_Salam and Ezebt Antr areas) (Figs. 73 and 76). These areas are characterized by very narrow streets and a random distribution of houses that are described as slums and informal buildings. In the middle of the study sector, a small sector of high-density urbanization is located to the west of the metro line and there is another small sector to the south.

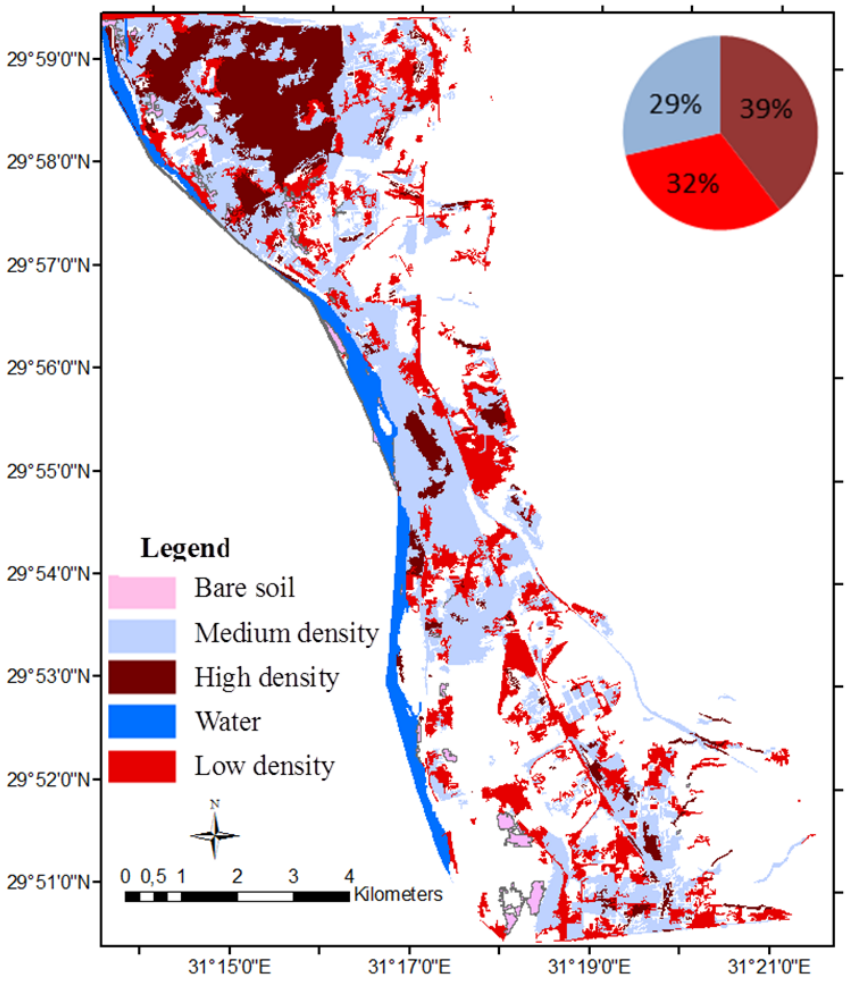


**Figure 76: Urban density classes in 1999**

In 2008 (Fig. 77), high density settlements covered the areas of north El Maadi and a large proportion of the middle part besides the areas around the metro line in the south. All of them estimated about 21.51 km$^2$ (26% of the total area and 39% of total urbanization), an increase of about 3.1 km$^2$ on 1999 (Fig. 78).

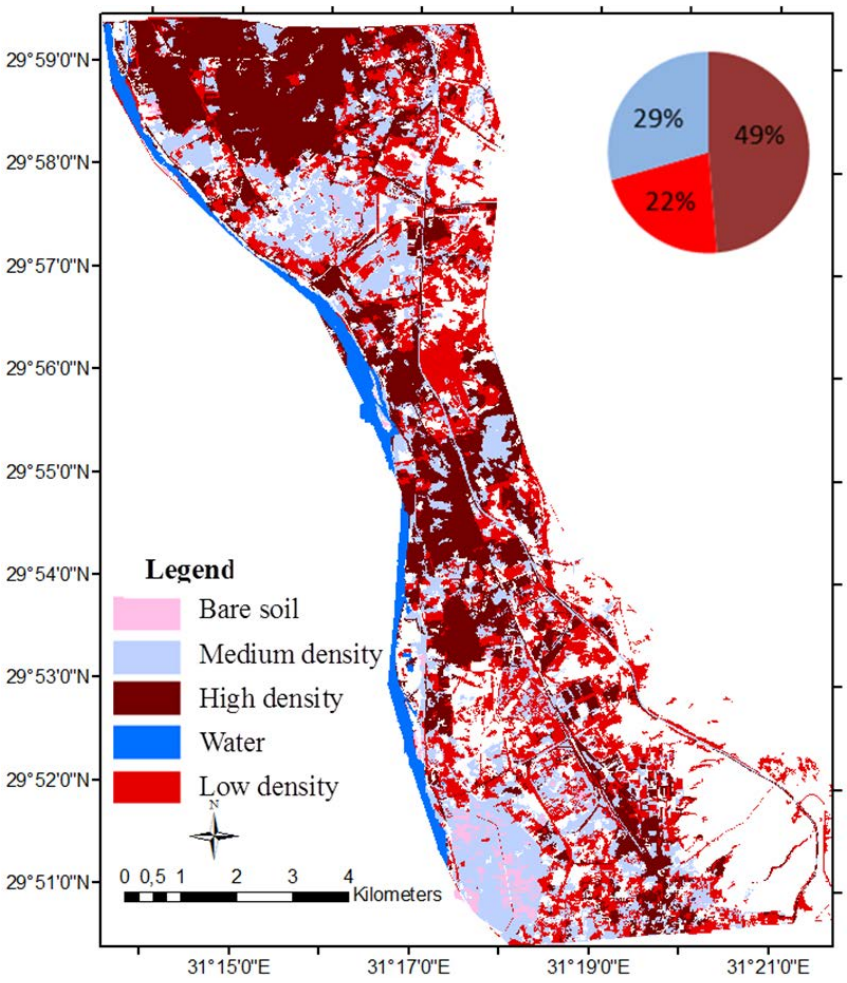


**Figure 77: Urban density classes in 2008 and their percentages**

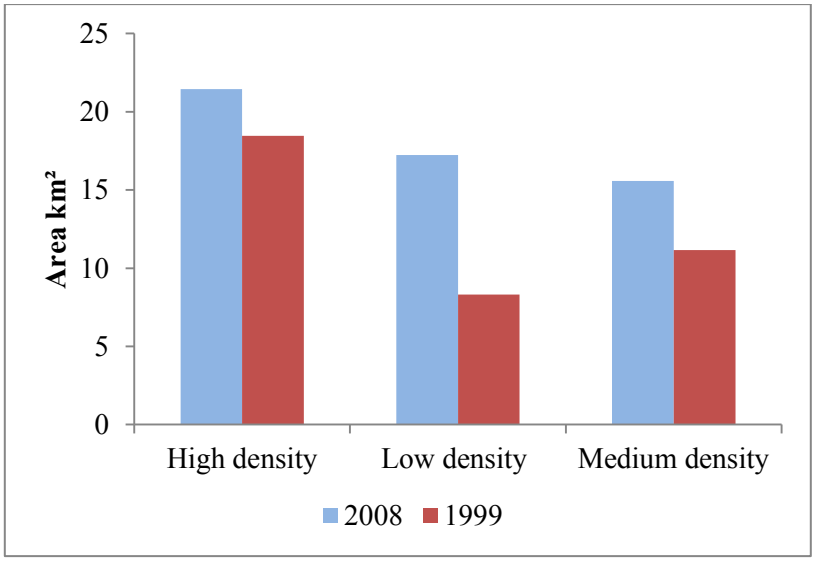


**Figure 78: Density classes of in 1999 and 2008**

In 1999, medium-density urbanization was established mainly in the areas between the River Nile and the metro line with an area of about 11.17 $km^2$ (14% of the total area and 29% of total urbanization). The objects categorized under medium density were represented the buildings with a uniform appearance and / or the distance between houses, which is quite easy to detect. Some of these buildings are formal, such as in east Helwan, and others are informal, such as in west Helwan (Fig. 76).

Medium-density urbanization accounted for about 15.6 $km^2$ in the classified map of 2008 (19% of the total area and 29% of total urbanization), which was focused mainly in the areas of Maadi due north and Helwan due south. These settlements also dominated the industrial areas to the central east of the metro line.

Low-density urbanization dominated the urban areas with distinct buildings set apart; such urbanization is distributed mainly around or close to areas of medium density and the hinterland (desert) to the east of the metro line. Spatially, low-density urbanization accounted for an area of about 8.32 $km^2$ (10% of the total area and 22% of total urbanization) in 1999. By 2008, its area had increased to 17.23 $km^2$ (21% of the total area and 32% of total urbanization), mostly at the expense of the desert due east and partially at the expense of cultivated land due west. Low-density buildings referred mostly to the new settlement projects which comprised of the area east of El-Maadi and east of the motorway. Most low-density urban areas included small public and private gardens like the area in to the northeast of El Maadi.

#### 5.6.1.3 Vegetation cover

I differentiated the vegetation cover here into uniform cultivated land (mainly agricultural fields), very loosely vegetated areas (sparse vegetation), and any other green cover (Figs. 79, 80, and 81, and Table 17).

The classified 1999 image reveals that the class of uniform cultivated land (agricultural fields) was present mainly in the area close to the River Nile (East Metro line) and was concentrated in the north Helwan and Al Maasara areas with some scattered fields due north-east of the MA sector. This class accounted for about 2.635 $km^2$ (3% of the total area and 23% of the total vegetation cover). By 2008, the proportion of agricultural land had decreased and covered an area of about 1.88 $km^2$ (2% of the total area and 17% of the total vegetation cover). Agricultural and uniform green cover are distributed indiscriminately along the green strip close to the River Nile, and there

is also some new uniform cultivated land due south-west that is reclaimed land around the new urban areas. In addition, the sparse vegetation recorded in some areas covered with public greens like Al-Maadi area (Fig. 81).

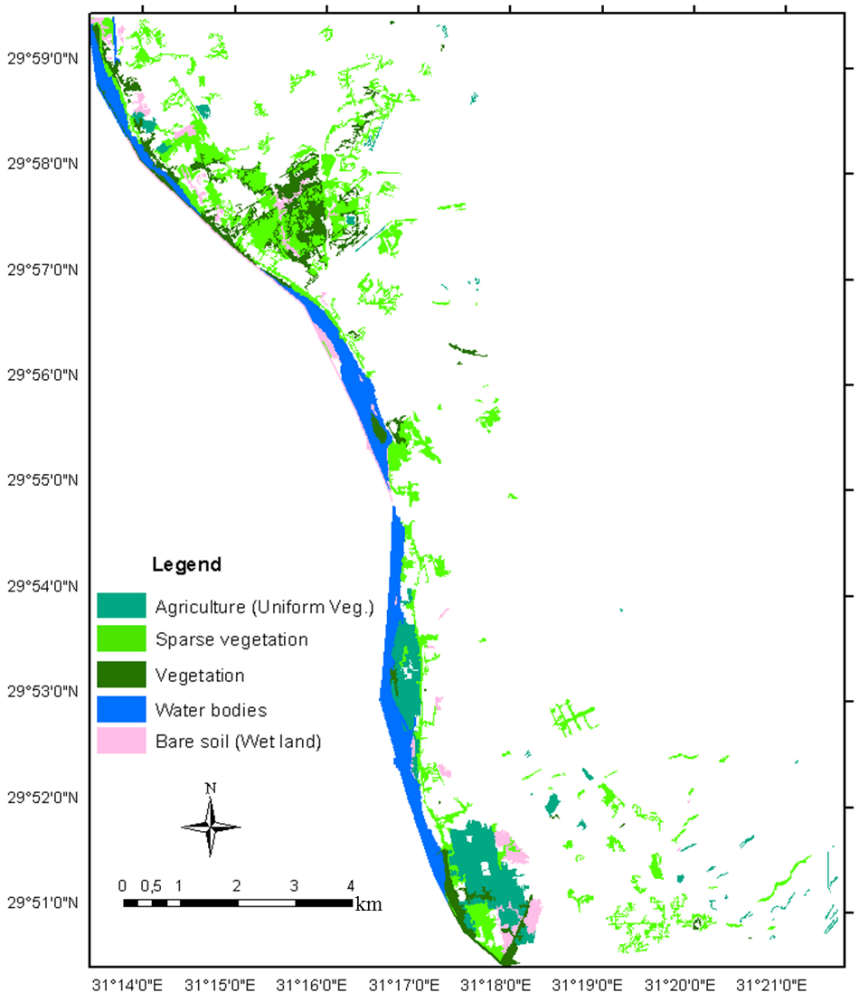


**Figure 79: Spatial distribution of classes of cultivated land in metro-autostrad sector in 1999**

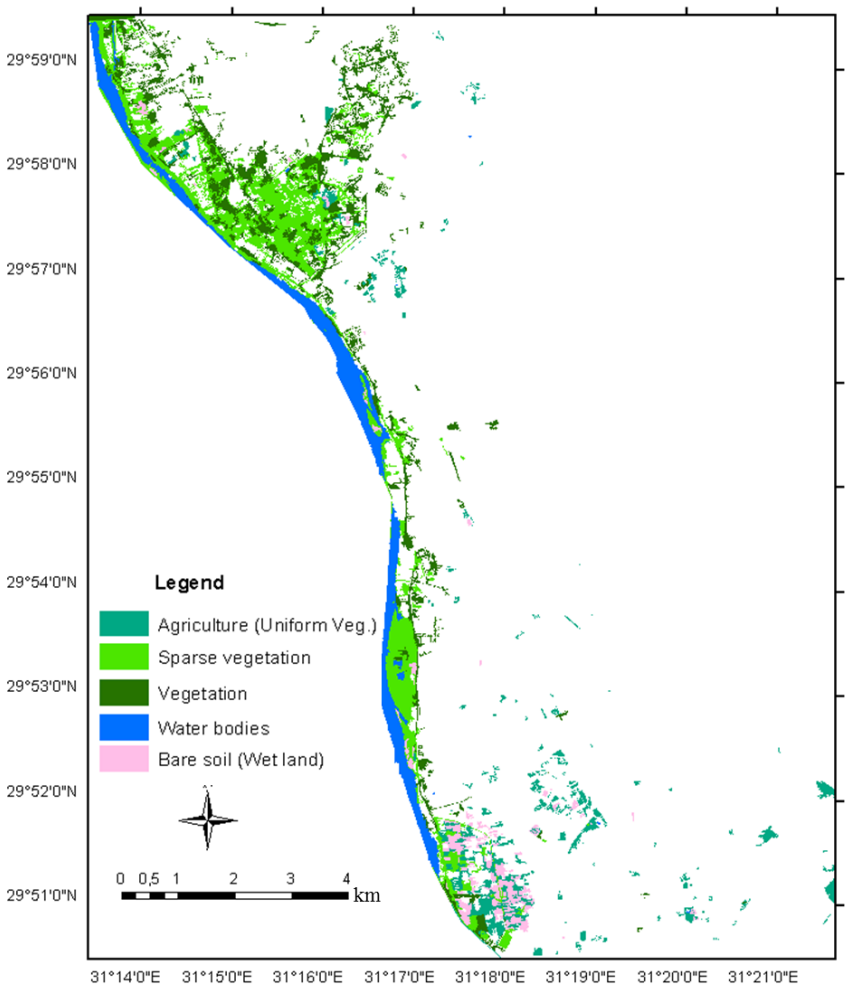


**Figure 80: Spatial distribution of classes of cultivated land in metro-autostrad sector in 2008**

Moreover, the classified map of 1999 shows that the areas of less dense or sparse vegetation cover were mainly concentrated in the urban areas of low to medium densities. This class accounted for an area of about 6.52 km² (8% of the total area and 56% of the total vegetation cover), while the less dense or sparse green cover was estimated in 2008 to account for about 5.2 $km^2$ (6% of the total area and 46% of the total vegetation cover) (Fig. 82). Most agricultural fields suffered from urban encroachment and appeared with less vegetation. In addition, the new urban areas of Al-Maadi and its surroundings due north-west and north-east are dominated extensively by sparse vegetation. Alternatively, the rest of green cover objects which classified in the first level and did not assigned to one of two sub-classes is categorized in this level of classification as vegetation-other sub-class. This sub-class covered an area about 2.52 $Km^2$ in 1999 (3% of total area and 22% of total

vegetation cover) while in 2008 it's represented by an area of about 4.21 km² (5% of total area and 37% of total vegetation cover) (Fig. 82).

**Table 17: Statistics on classes of cultivated land in metro-autostrad sector**

| CL classes | 1999 | | | 2008 | | |
|---|---|---|---|---|---|---|
| | Area km | Area km | Area% | Total | Area% | Total |
| AG | 2.63 | 1.87 | 17% | 2% | 23% | 3% |
| SV | 6.52 | 5.19 | 46% | 6% | 56% | 8% |
| V. others | 2.51 | 4.20 | 37% | 5% | 22% | 3% |

**Figure 81: Urban-vegetation in the Maadi area**

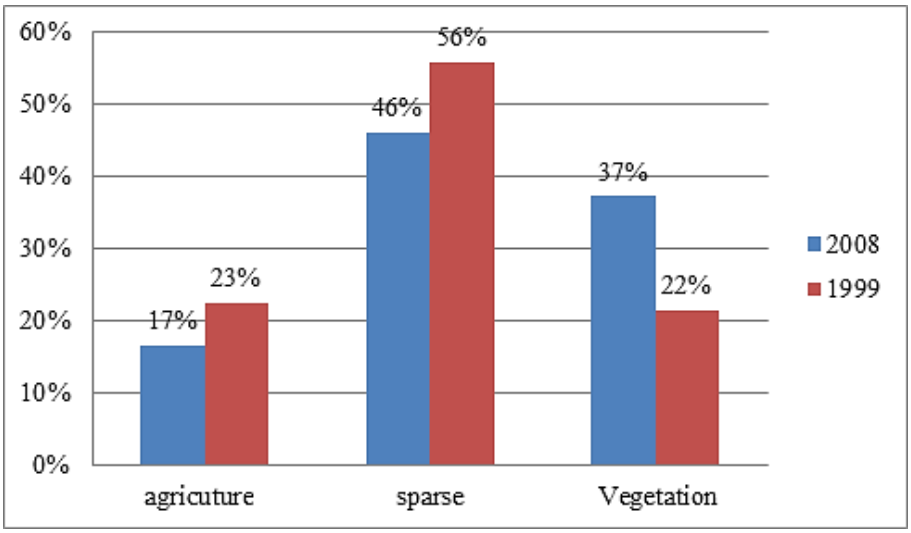


**Figure 82: Change of percentage in vegetation cover between 1999 and 2008**

#### 5.6.1.4 Change analysis

The change detection levels were added to the classification rule set to estimate the degree of change between the selected time periods (1999 and 2008). The resulting map shows the areas of change with regard to the selected classes. The spatial impact of the metro line and the autostrad on the growth of urbanization and vegetation, and their features is analyzed and demonstrated separately here (Figs. 83 and 84).

The urban areas increased by 21.19 $km^2$ (35% of the total urban objects) between 1999 and 2008, and the urban areas classified in 1999 as non-urban in 2008 are represented by a small proportion of 5.6 $km^2$ (9% of the total urban objects) (Fig. 84). The urban areas indicated to no changes were counted an area of about 33.34 $km^2$ (56% of the total urban objects). The decreasing urbanization might be revealed to the removal of old and/or temporary buildings used for a short time for construction activity or querying industry. The increasing urbanization mostly indicated that the construction of new houses and settlements are mainly established due northeast and southwest of the metro-motorway sector. Therefore, the impact of the metro line examined in the west area of Helwan, which changed dramatically from cultivation to urbanization. Nonetheless, the large proportion of no urban changes objects was classified over the time from lower density to higher one. The areas along the metro line from south Maadi to north (Dar El-Salam) showed increase in urban density from medium to high of the same area.

New classification level was created to detect the change on cultivated land by using the classified vegetation classes of 1999 and 2008. At that change level, the existence of vegetation classes over time was calculated (Figs. 85 and 86).

Between 1999 and 2008, about 5.823 km$^2$ (34% of the total green cover) of green vegetation cover was lost in the metro-motorway sector, while 5.3 km$^2$ (31% of the total green cover) of the landscape showed a positive change. About 5.85 km2 (35% of the total green cover) indicated that there was no change.

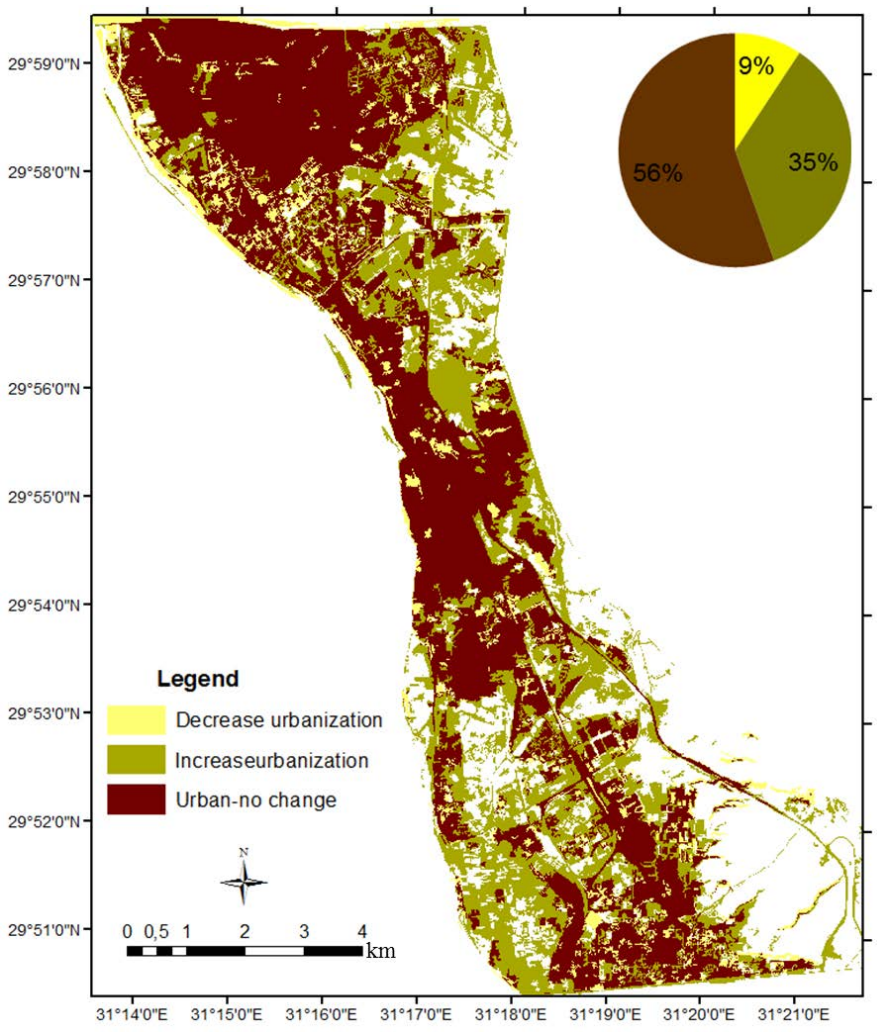


**Figure 83: Urban changes in the MA sector**

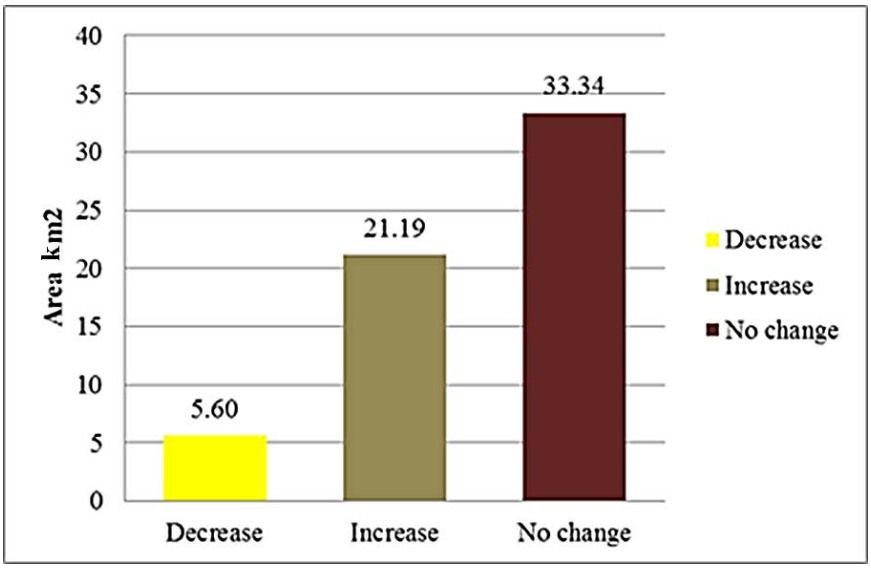


**Figure 84: Area estimated for changes in urbanization in the AM sector**

Thus, the southern part of this sector dominating the Helwan area is the most affected by the loss of green cover. The southwest areas showed an extensive loss of agricultural fields while the areas due south and southeast calculated a small proportion of non-existence of vegetation cover due to the increasing urban activity in the area. There is a substantial proportion of positive change of vegetation mainly on the most northeast and northwest parts. Besides that, there are scattered objects that represented an increase in green cover along the metro-line zone that usually indicated some cultivation activity in new settlement projects that might play a role in improving the living conditions and providing the urban areas with meadows and green spaces (Fig. 84). In addition, the classified image showed in the southeast (desert area) some scattered green cover that revealed that grassland partially grew over some valleys.

The existence of green cover objects with no change class between the time span studied did not reveal to the same sub-class of vegetation cover. In some areas the agriculture fields have been transformed to sparse vegetation. Some classified agricultural land in 1999 appeared as sparse vegetation in 2008 due to the urban sprawl, and this can be observed in the central part due west of the metro line along the River Nile in the Tora area (Fig. 85). Also, the urban area of El Maadi, which showed the most vegetation, experienced almost no change and partially increased its vegetation due to the trees which reached the roofs in some places and are quite near to the buildings of El-Maadi (fuzzy area) (Fig. 81). Thus, the classifier applied different algorithms that

provided membership functions; this was followed by manual classification based on ground truth to refine especially the indistinct parts.

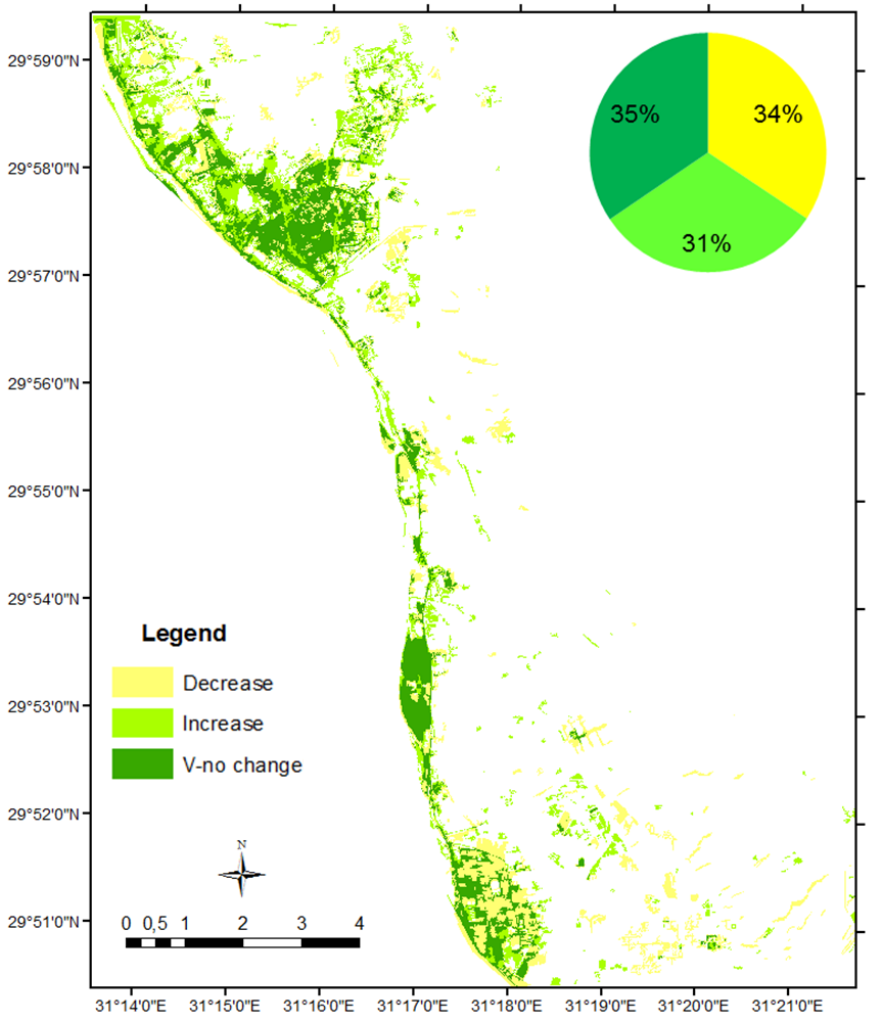


**Figure 85: Changes in vegetation cover in the MA sector**

The amount of surface water showed an ambiguous negative change of about 1%, which might be due to the extensive construction activity very close to the water channels (Nile River) and the dumping of some waste materials into the water.

The bare soil class occasionally gives an indication to process of the transforming land from agriculture to urbanization.

The desert area due east of autostrad road is mainly characterized by rough relief and is dominated by cement factories and carbonate quarries. Recently, the growth of urbanization extended to the areas located very close to these cement factories (Fig. 89) along autostrad road, which made it less easy to differentiate spatially between the urban types by using the current resolution of SPOT images.

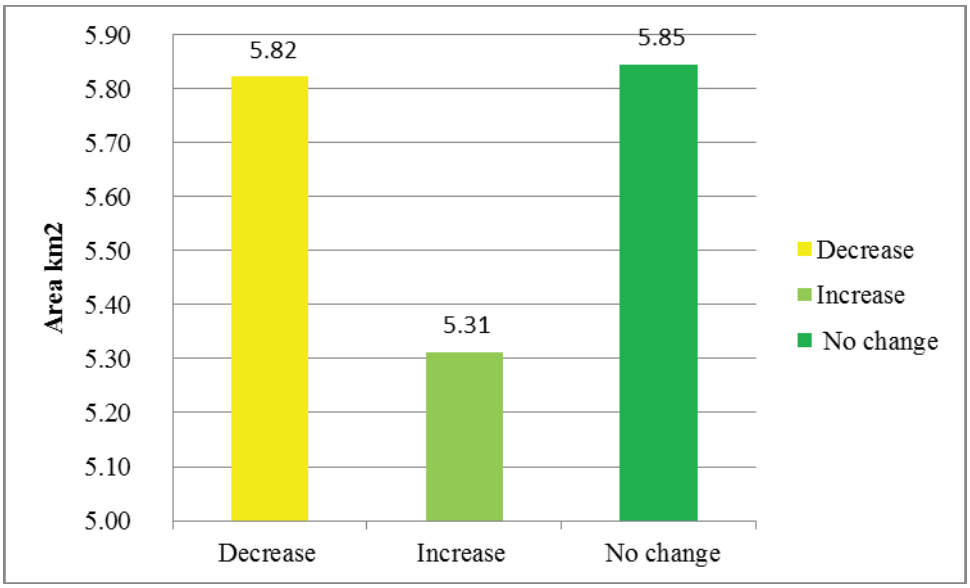


**Figure 86: Area estimated for changes in vegetation in the MA sector**

**Figure 87: Green spaces east of the Maadi area (MA sector). Photo captured 2010**

**Figure 88: Urban sprawl at northern Helwan area (Tora). Photo captured 2010**

**Figure 89: Cement factory along autostrad road close to recently settled areas. Photo captured 2010**

### 5.6.2 **Core-new city sector (CNC)**

The core-new city sector (CNC) is composed of the core of Cairo City and its periphery, as well as the most eastern hinterland of GCM with a total area of about 601.1 km2. This sector is dominated by some development, such as New Cairo City, El-Marg metro line, and the eastern part of the ring road (Fig. 90). In this part of my study, I present and analyze the spatial impact of the development of the city and the state of land use. To do so, I created a classification rule set and worked at different levels of segmented objects to define spatially the state of land use/land cover.

The five main classes (urban areas, green cover, water bodies, soil, and desert) at the first level of classification showed the state of land use/land cover (LULC) and the main changes to SPOT images between the selected time periods (1999 and 2008). The latter step are followed by inserting sub-levels into the process tree and applying the object features algorithms which are complemented by ground information to estimate the different urban patterns and green cover structures. In doing so, I hoped to grasp the causal link between spatial infrastructures (driving forces) and spatial resilience. I also analyzed and illustrated the degrees of physical change and the trends of growth.

#### 5.6.2.1 The state of LULC

The state of land units in 1999 (Fig. 92) shows that the desert and hinterland accounted for more than half of the total area (about 340.1 $km^2$ (56.57%)); the total urban area in CNC accounted for 192.8 $km^2$ (32.08%); the vegetation cover accounted for about 57 $Km^2$ (9.5%); bare soil and water bodies were estimated as accounting for a small proportions of the CNC sector (about 6.6 $km^2$ (1.09%) and 4.7 $km^2$ (0.78%) respectively).

The classified CNC image of 2008 (Fig. 93) illustrates that the class of desert (hinterland) accounted for an area of about 263.6 km2 (43.85%), a drop of about 13% compared to 1999; urbanization accounted for the largest area of land (about 289.4 $km^2$ (48.14%)), an increase of about 11% compared to 1999; the green cover covered about 37.4 $km^2$ (6.22%), a drop of about 3.26% compared to 1999; bare soil (uncovered fertile land) accounted for an area of about 4.7 $km^2$ (0.79%), which represented a drop, while water bodies increased with a total area of about 6 $km^2$ (1%).

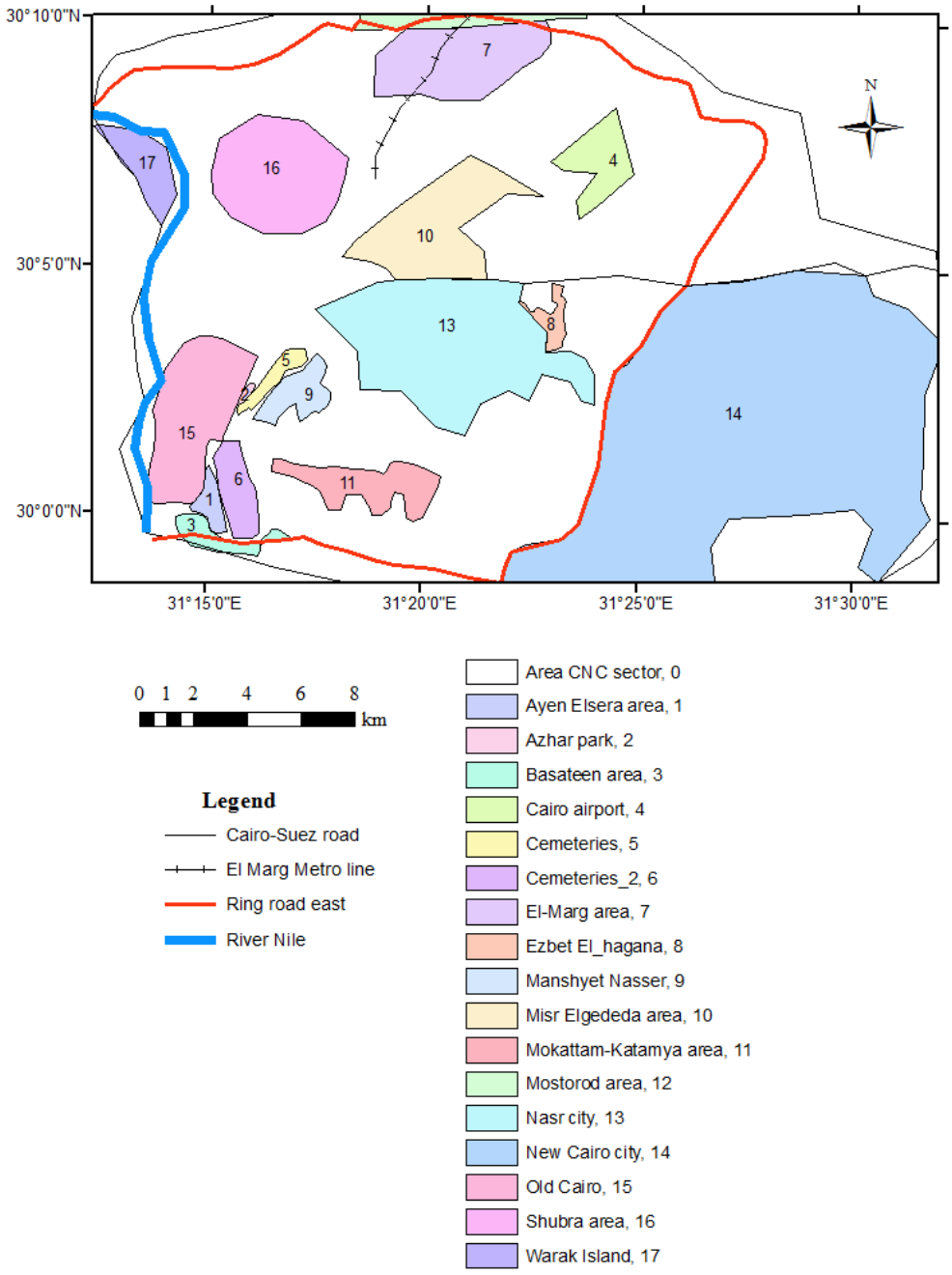


**Figure 90: Core-new city sector. Map based on SPOT image 2008**

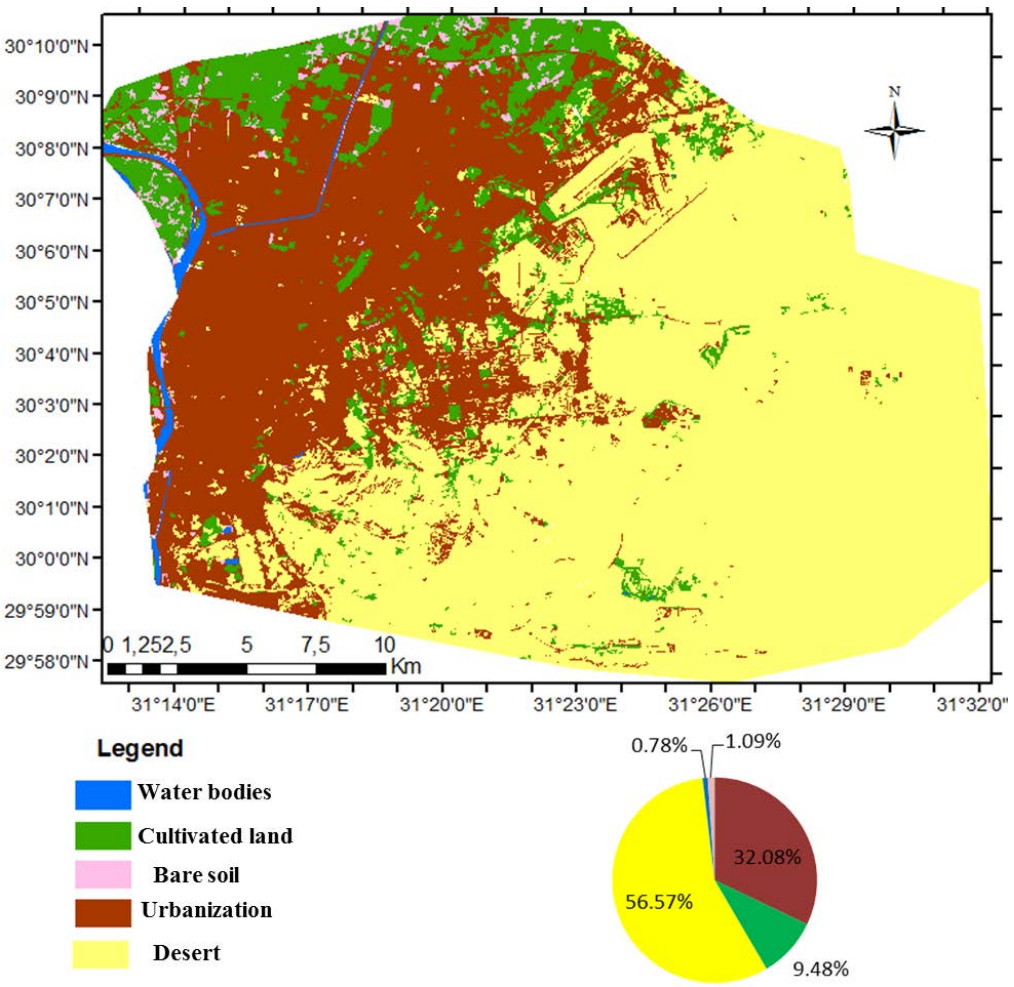


**Figure 91: LULC classification map of 1999 for the Cairo new city (CNC) sector**

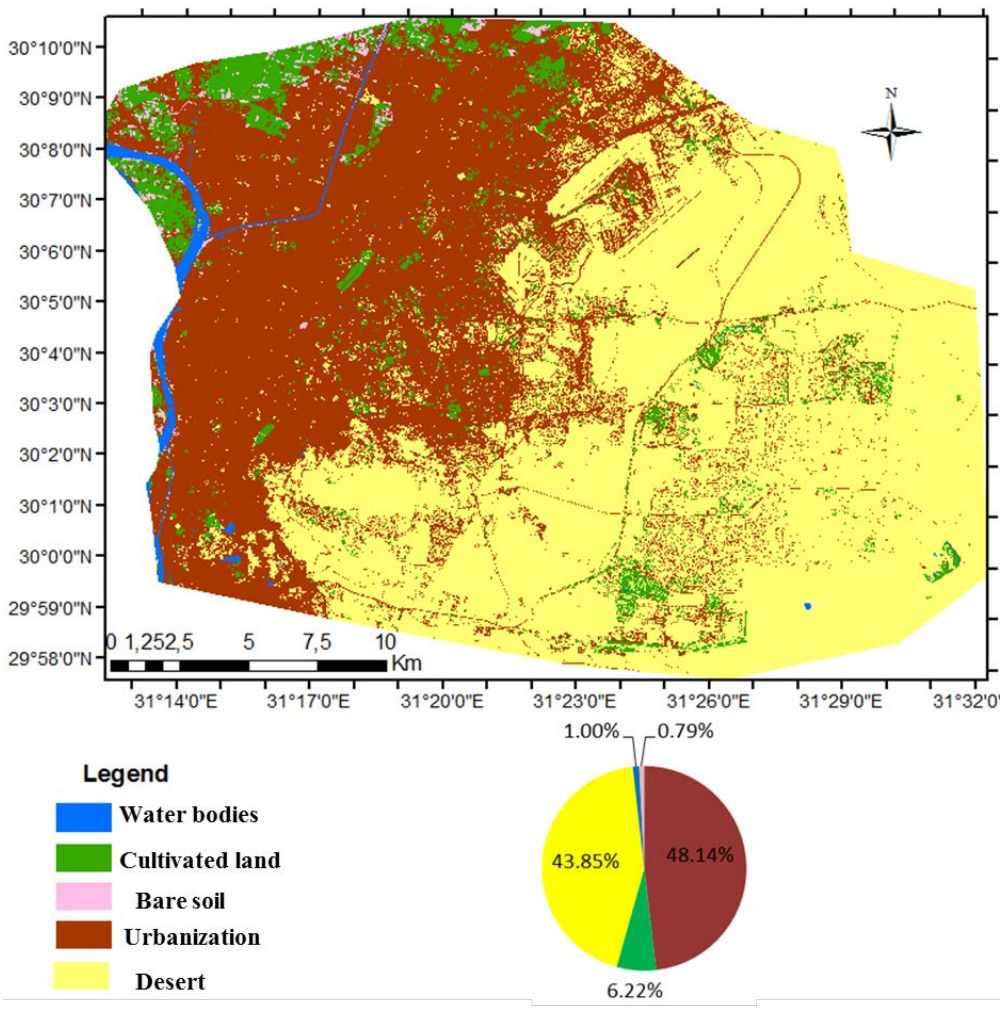


**Figure 92: LULC classification map of 2008 for the CNC sector**

The classified maps show that the desert area located to the east of the CNC sector is mostly used for new settlements to help release the pressure exerted on the core and periphery of Greater Cairo (GC). Moreover, I also investigated the urban patterns and densities to delineate the changes and spatial impact of using an extensive amount of land for building activities. The spatial distribution of small water bodies and green cover in areas where they had not previously observed are reflecting the manner of water use.

The green cover identified at the first level has been refined at other levels to lift the vague of cultivated land uses and determine their spatial features and structures. In spite of the general decrease in green cover in the time periods studied, the field observation revealed that there are different kinds of farming activity recorded especially in the hinterland of the CNC sector. I

described and analyzed the green cover classes to understand the diversity of human activities and their impact not only on spatial growth and resilience but also on the quality of life.

The statistical analysis of the state of LULC for both years is given in the following table (Table 18) and charts, showing the growth of some elements and the shrinkage of others.

**Table 18: CNC sector statistics and percentage of LULC in 1999 and 2008 (see abbreviations in 5.5.3)**

| LULC Classes | 1999 | | 2008 | |
|---|---|---|---|---|
| | Area Km. | Area% | Area km | Area% |
| U | 192.8 | 32.08% | 289.4 | 48.14% |
| CL | 57 | 9.48% | 37.4 | 6.22% |
| D | 340.1 | 56.57% | 263.6 | 43.85% |
| WB | 4.7 | 0.78% | 6 | 1.00% |
| BS | 6.6 | 1.09% | 4.7 | 0.79% |

5.6.2.2 Urbanization

I divided the urbanization class into three main sub-classes based on spectral reflectance and the texture of the settlement objects for the used images (SPOT 1999 and 2008) reflecting the spatial densities of urban areas (Figs. 93 and 94). These sub-classes are high, medium and low density; they changed year by year and showed the impact of rapid development on the spatial resilience on the core, periphery and hinterland (Table 19 and Fig. 95).

On the one hand, the high density class in the classified map of 1999 is dominated mainly by the old city areas (core) which extend to the north and northeast and cover the north of Cairo City (Shubra). At the periphery, there is some high density urbanization which represent mostly the slums due east of the core (Manshyet Nasser) and informal buildings due north of the Shubra area (Mostorad). The high density class accounted for an area of about 74.06 km2 (38% of the total urbanization and 12% of the total area) which are characterized by massive patches in classified images with undifferentiating streets and indistinct fabric of buildings. On the other hand, the high density class in the map of 2008 increased by about 4% of the total CNC sector but decreased by 4% regarding the total urbanization area, which covered an area of about 96.98 km2. The areas dominated by this class extended from the core to the north and northeast to the El-Marg area at the fringe of the ring

road, which indicated the influences of the metro line and the ring road. While the high density area due east (Manshyet Nasser) of the core is restricted to formal projects and private lands in the El-Mokattam plateau area, and also, the spatial distribution of the high density objects were increased due south of the city core along River Nile bank (Figs. 90 and 92). Generally, the high density of urbanization did not appear in the hinterland on either map.

The medium density class accounted for an area of about 107.34 km2 (56% of the total urbanization and 18% of the total area) in the map of 1999, and mainly dominated the periphery of the CNC sector. Based on the field observations and spectral character of its objects, this class explored to two types of urban pattern. Firstly, the formal and uniform buildings distributed mainly due east and east-north-east which dominate the Nasr City and Masr El-Gedida areas, and are also fairly common due southeast including the El-Mokattam area. Secondly, the areas of urban sprawl expanded due north of the Shubra area which is bounded by the ring road and restricted by Cairo airport in the east. There are a few patches representing medium density urbanization in the hinterland (desert), which indicates the first land use for urban activity and establishment of remote cities. Medium density urbanization in 2008 represented the largest proportion (about 154.69 km2 (53% of the total urbanization and 26% of the total area)). However, the classified image of 2008 shows that some patches of high density have appeared in the areas dominated by medium density in the map of 1999, the medium density buildings increased by 8% concerning the total area. Medium density urbanization is concentrated mainly in the periphery of the Cairo City sector and hinterland (desert), which is made up by urban encroachments due north and formal settlements due east. Consequently, the urban area to the north of the ring road (northern part of the CNC sector), which was used intensively for building activity, indicates the influences of infrastructural development on urban density (rate of urbanization).

Low density urbanization is represented in the map of 1999 by scattered segments mostly around the areas of medium density, and accounted for a small proportion of the CNC sector (about 11.45 km2 (6% of the total urbanization and 2% of the total area)). This class represents three patterns of urbanization: the informal houses representing the initial process of urban sprawl in rural (green cover) areas due north; some new construction projects located mostly due east-north east; and compound areas containing villas in the new cities in the hinterland. The proportion of low density urbanization changed in the map of 2008 (37.72 km² (13% of the total urbanization and 6% of the total area)).

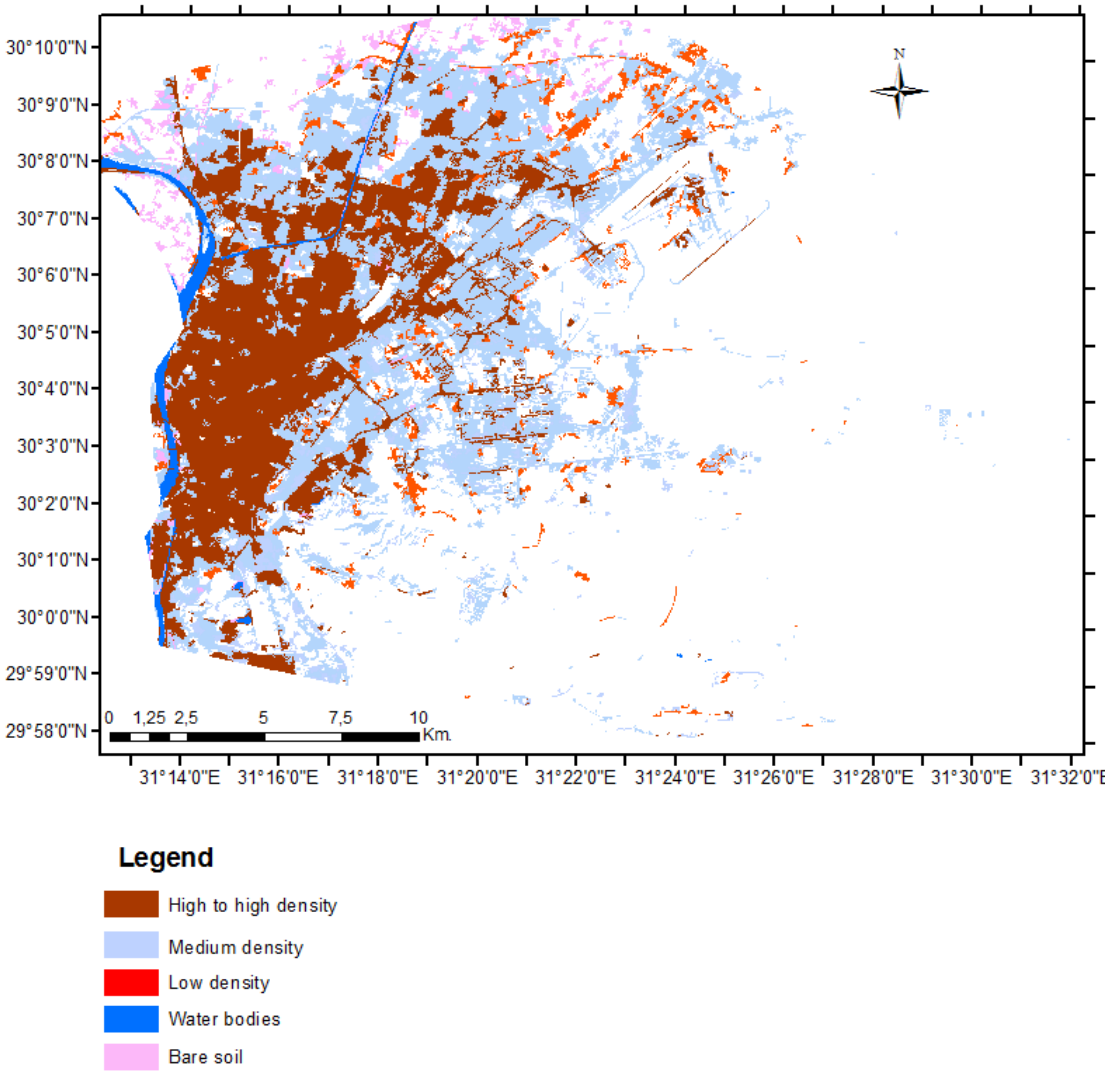


**Figure 93: Classes of urban density in 1999 in the CNC sector**

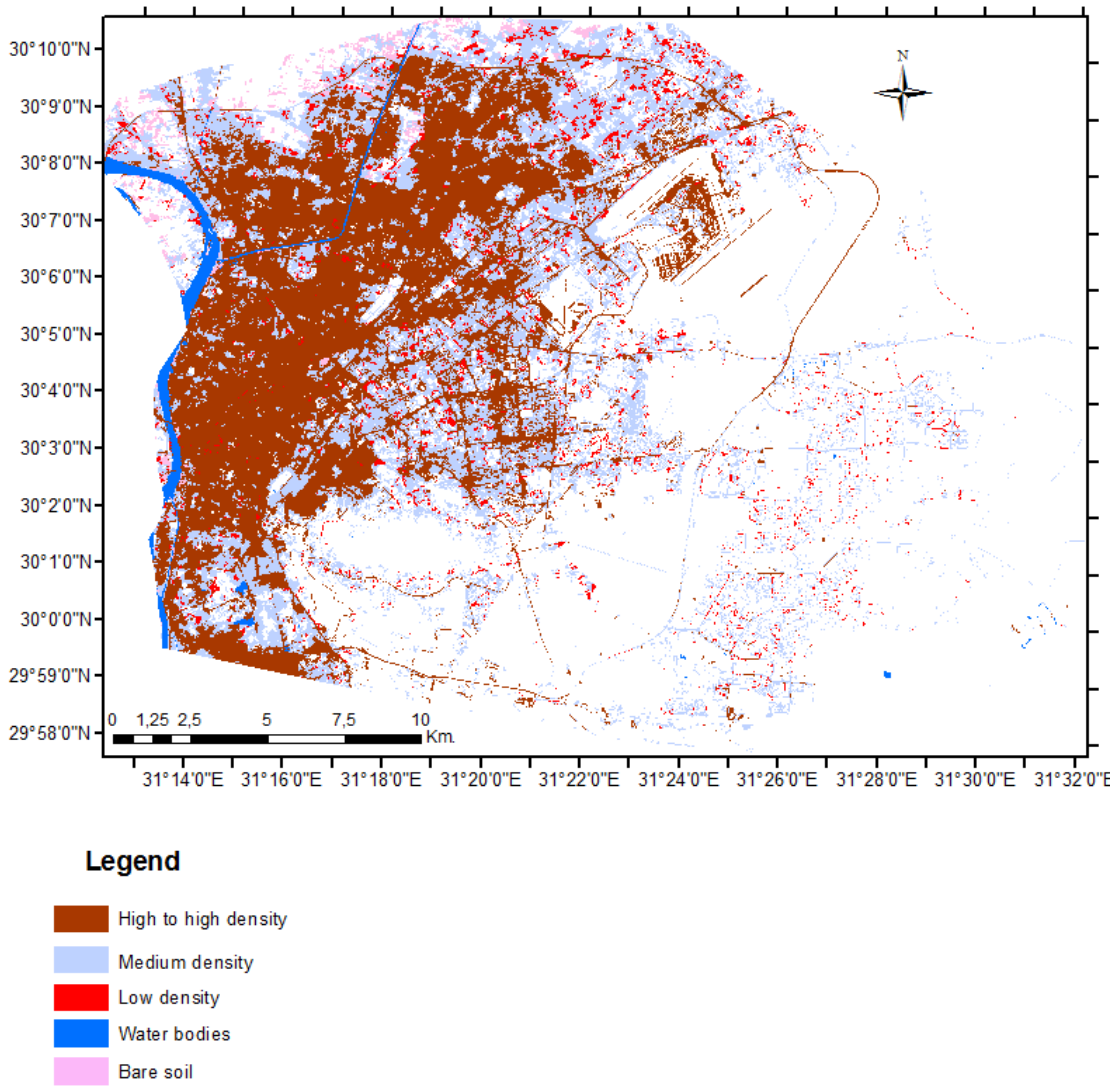


**Figure 94: Classes of urban density in 2008 in the CNC sector**

**Table 19: Analysis of urban classes in classified maps of 1999 and 2008 in the CNC sector (see abbreviations 5.5.3)**

| Urban classes | 1999 | | | 2008 | | |
|---|---|---|---|---|---|---|
| | Area km | Area% | Total% | Area km | Area% | Total% |
| HDU | 74.06 | 38% | 12% | 96.97 | 34% | 16% |
| MDU | 107.34 | 56% | 18% | 154.68 | 53% | 26% |
| LDU | 11.45 | 6% | 2% | 37.718 | 13% | 6% |

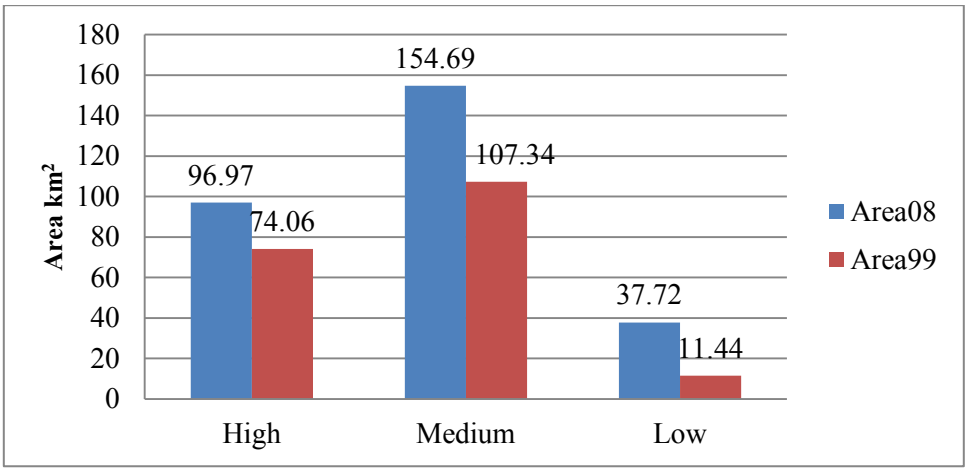


**Figure 95: Change in urban densities between 1999 and 2008**

5.6.2.3 Vegetation

The vegetation cover of the CNC sector was divided according to the spectral reflectance and geometry of the objects besides the ground check points into uniform with dense green cover, less dense green cover, and sparse. The rest of vegetation objects which haven't been classified under one of those sub-classes were categorized as "vegetation-other".

The classified map of 1999 (Fig. 96) shows extensive agriculture and uniform green parcels in the north and northwest part, and a small area spread mainly over the periphery of the CNC sector. The total area of this class accounted for about 23.92 $km^2$ (42% of the total vegetation and 3.98% of the total area); sparse vegetation is estimated to cover an area of about 22.63 $km^2$ (40% of the total vegetation and 3.76% of the total area), which is mainly distributed on the periphery and parallel to the east side of the ring road and which indicates the new cultivation activity on the desert (hinterland). This covers an area of 10.42 $km^2$ (18% of the total vegetation and 1.73% of the total area), and is spatially scattered all over the CNC sector.

According to the classification of 2008 (Figs. 97 and 98), agricultural land lost about 10 $km^2$, which indicates a rapid loss of sources of food in the area cut by the ring road (1 $km^2$ per year). This class accounted for 13.94 $km^2$ (37% of the total vegetation and 2.32% of the total area), and is spatially limited to the most northwest part of CNC. Furthermore, in this map, there are some cultivated lands transformed from uniform agricultural fields to sparse vegetation cover, especially at EL-Warak Island due NW and north of the El-Marg area. These changes mostly indicate the transition

step before the change in land use from cultivation to urbanization (Fig. 99). Additionally, the sparse objects appeared extensively in the hinterland (desert) and referred to the urban-green areas dominating the new Cairo city. The field observation found that the vegetation cover in new cities is composed of private gardens, open spaces and meadow, a green belt of trees around the city roads, and a few objects representing land reclamation for food production (Fig. 100). At the periphery, there are scattered objects classified as sparse green cover while this class at the core area is partially recorded. The objects of sparse vegetation accounted for an area of about 22.35 $km^2$ (60% of the total vegetation and 3.72% of the total area) with no apparent change to the area recognized by the map of 1999. The spatial distribution of the sparse class between 1999 and 2008 shows a rapid increase in the hinterland and north-northwest areas and a dramatic decrease at the periphery and in the northeast. The rest vegetation objects are estimated small proportion of about 1,125 $Km^2$ (3% of the total vegetation and 0.19% of the total area) which indicated mainly to green cover with fuzzy relationship.

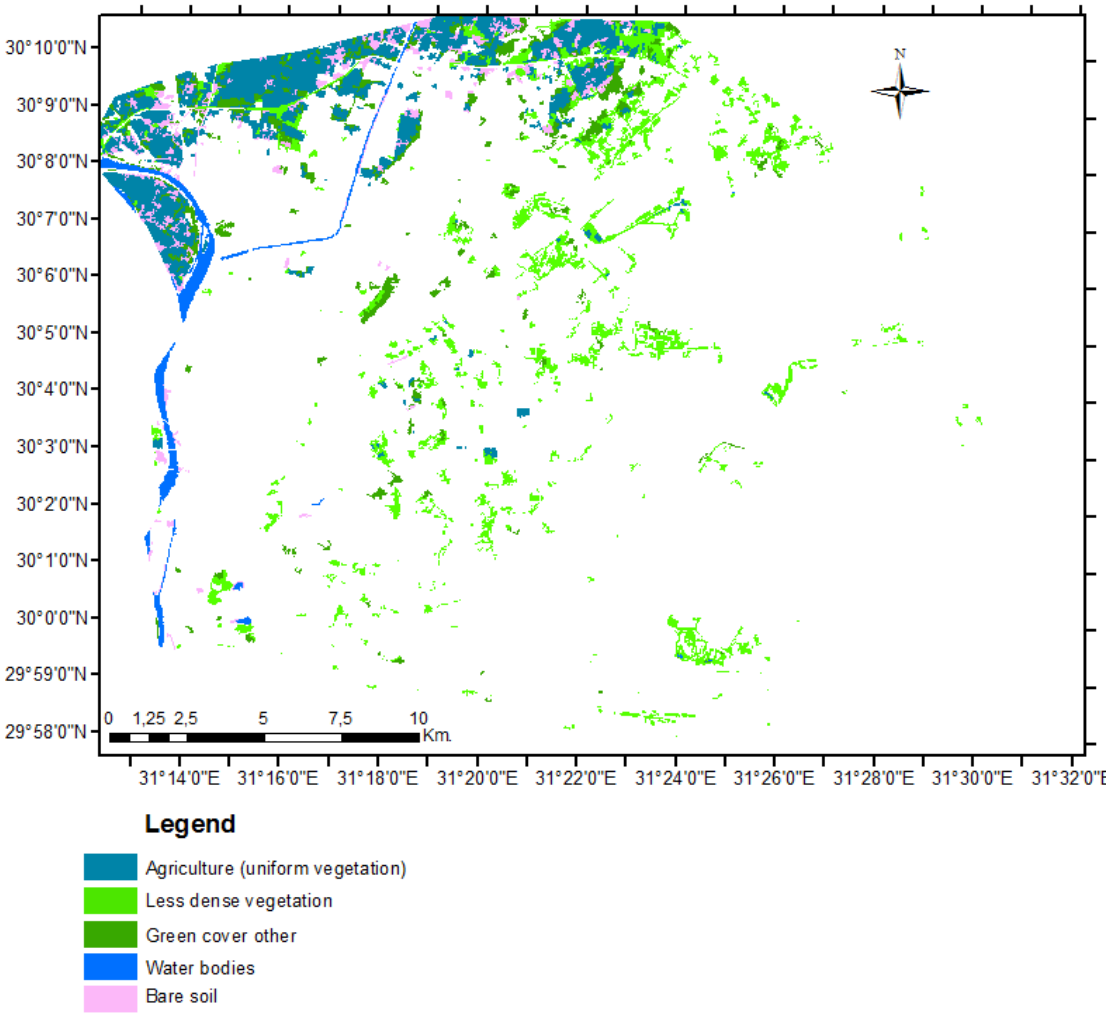


**Figure 96: Spatial distribution of classes of cultivated land in core-new-city sector in 1999**

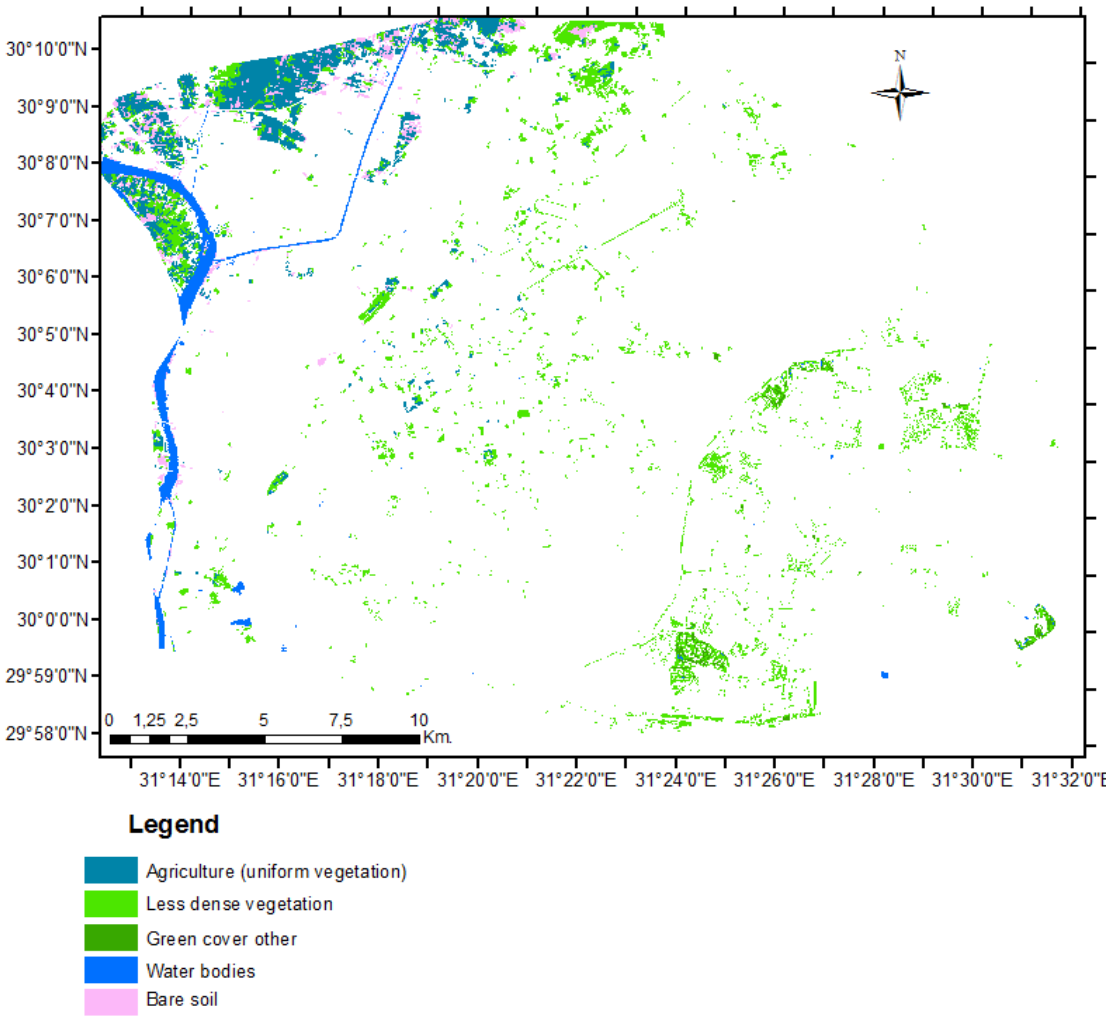


**Figure 97: Spatial distribution of classes of cultivated land in core-new-city sector in 2008**

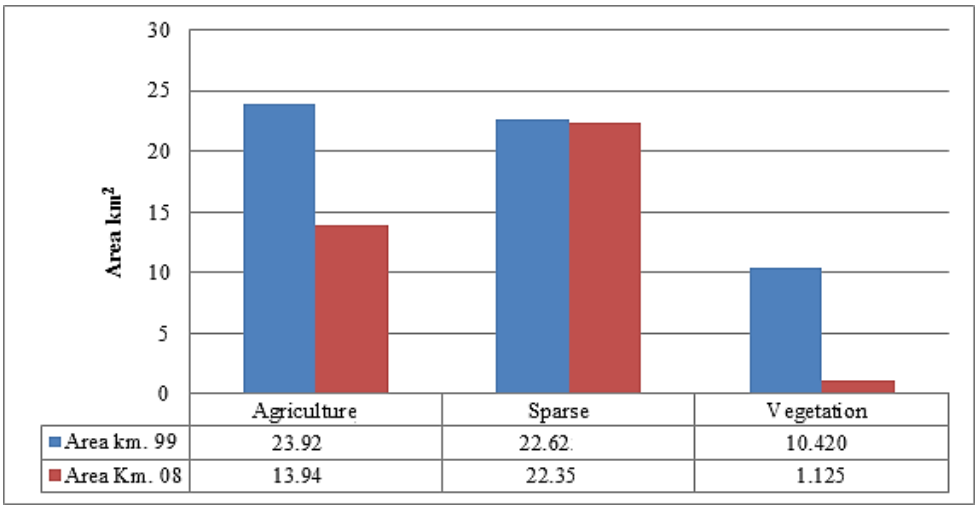


| | Agriculture | Sparse | Vegetation |
|---|---|---|---|
| Area km. 99 | 23.92 | 22.62. | 10.420 |
| Area Km. 08 | 13.94 | 22.35 | 1.125 |

**Figure 98: Changes in cultivated land between 1999 and 2008 in CNC sector**

**Figure 99: Urban sprawl over fertile land at the fringe of Al Warak Island (CNC sector). Photo captured 2010**

**Figure 100: Reclamation land north of new Cairo City (CNC sector). Photo captured 2010**

### 5.6.2.4 Change analysis

I analyzed the spatial impact of development (new cities, roads and metro line) by detecting the changes to the classified land units such as urbanization and vegetation between 1999 and 2008. The changes were categorized as being positive, no-change, and negative at the level of change detection at classification rule set. Thus, the presence of the urban areas recognized in 1999 classified level at the 2008 classified level was classified at the level of change detection (Figs. 101 and 102) and accounted for an area of about 183.32 $km^2$ (62% of the total urban objects); this was mainly concentrated in the core and periphery of the CNC sector and was classified as no-change. However, the urban density map between 1999 and 2008 shows that the no-change urban objects were exhibited transformation in urban density in some areas (e.g. from low to medium or medium to high). The new city areas and settlements were presented at level 2008 and indicated positive change with a large area of about 105.58 $km^2$ (35% of the total urban objects). The eastern part of the ring road separates the new cities established in the hinterland and the new buildings constructed on the core-periphery areas, comprises the part where the expansion of the old Cairo city. Therefore, the empty areas between new Cairo and old Cairo appeared as a target for urban activities initiated along the connected roads and will continue to cover the whole area. Thus, the boundaries of GCM seem to be becoming vague as a result of increasing urban activity. Moreover, the areas around the northern part of the ring road show urban sprawl especially in the area linking the end of Marg metro line with the ring road (Mostorod). The southern part of old Cairo shows a

positive growth of formal houses (around the Ayen El Sera area), which restricted the random growth of the most southern slums and informal areas (Establ-Anter and el-Basateen). The southern area of Cairo airport grew along the Cairo-Suez road and linked with the northern part of Nasser City, which limited the growth of the informal houses of the Ezbet El-Hagana slum.

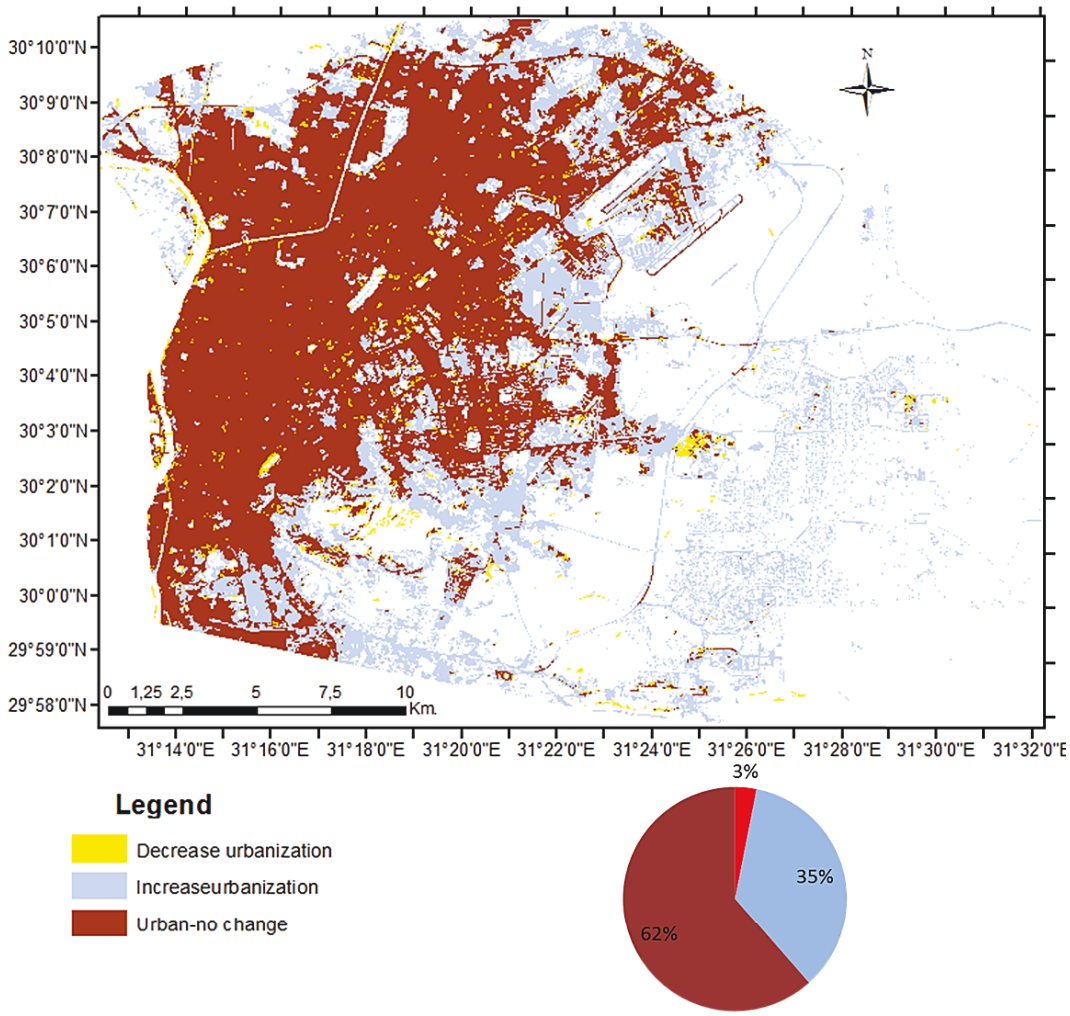


**Figure 101: Urban changes in the CNC sector**

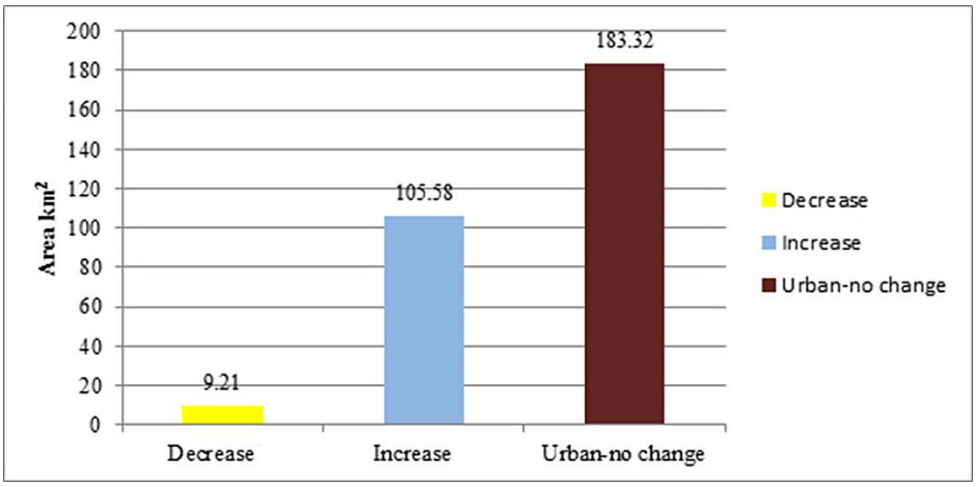


**Figure 102: Area estimated for urbanization changes in the CNC sector**

At the level of vegetation change detection (Figs. 103 and 104), vegetation cover with no changes between 1999 and 2008 accounted for an area of about 30.78 $km^2$ (31% of the total cultivation objects); the positive existence of green cover was estimated to occupy an area of about 21.78 $km^2$ (31% of the total cultivation objects), which indicates an increase of farming activity and a gaining of new cultivated land; the largest proportion of the CNC landscape showed no vegetation, which points to the loss of the vegetation cover (an area of about 43.47 $km^2$ (47% of the total cultivation objects)). The growth or contraction of the vegetation cover in the time periods do not indicate changes between dry and rainy seasons but are related to the extensive misuse of the fertile land in GCM due to the cultivation based on the River Nile. Furthermore, most agricultural land in the CNC sector is influenced by urban sprawl around the northern part of the ring road and the El-Marg-Mostorod area. There is some vegetation cover transformed from agriculture form to sparse vegetation form which can be observed for instance on El-Warak Island. The change detection map reveals that some green cover areas have been transformed into areas with no vegetation mainly on the eastern periphery of the CNC sector while the new Cairo City landscape is dominated by the newest cultivated lands that indication of the reclamation process in the desert areas simultaneously with the loss of fertile land of Nile delta.

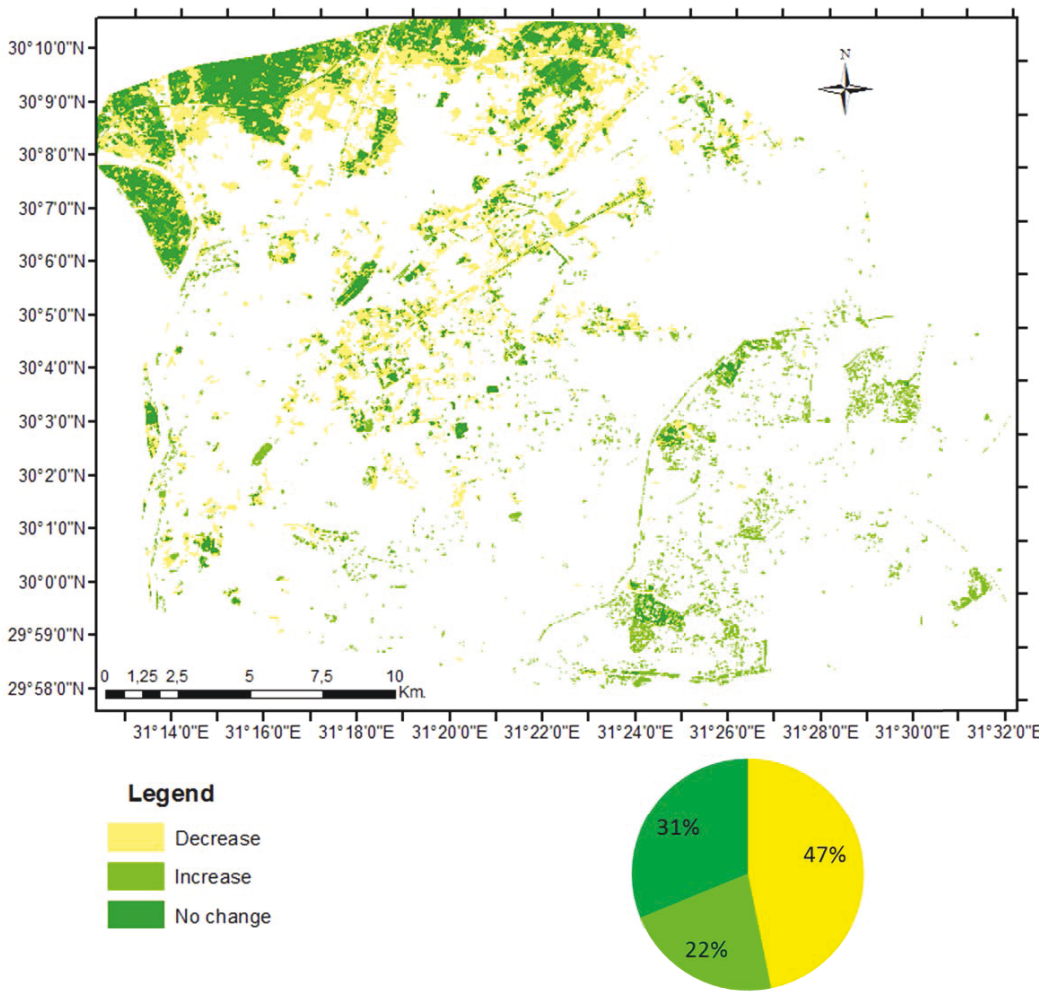


**Figure 103: Green cover changes in the CNC sector**

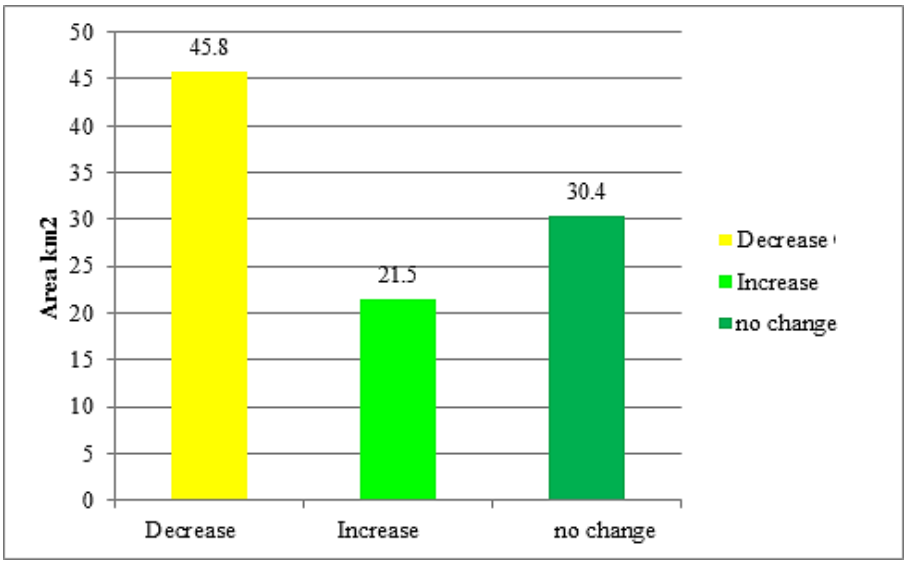


**Figure 104: Area estimated for the cultivated land changes in the CNC sector**

The less roughness and low relief properties of the desert and hinterland east of the CNC sector (see Chapter 2) drove the development planners to establish new settlements which used 86 $Km^2$ (13%) of the total desert area in the CNC sector between 1999 and 2008. Ironically, the water bodies (surface water) increased by 1.3 km2 (0.22%) between 1999 and 2008, and are located mainly in the new urban areas (New Cairo City). These water bodies are artificial and are composed of swimming pools, lakes for private compounds, and drainage lakes. The classified map of 1999 (Fig. 91) shows two distinct artificial lakes in the southern part of new Cairo City, a number that increased to more than ten in the classified map of 2008 (Fig. 92). These are spatially distributed inside the most vegetated areas in the hinterland and there are a few lakes which have been created in the low relief area due to the discharge of irrigated water used for golf courses, meadows, green belts, and gardens. These green spaces indicate to the intensive use and misuse of fresh water to improve the quality of life for high-income people in the new cities. However, the amount of irrigated water remained probably did not affected, due to the decrease in agricultural land (the food basket) between 1999 and 2008 (by about 10 $km^{2)}$, with this water being reused to irrigate the green cover (urban-green) in the desert. This emphasizes the impact of the development of new cities on different environmental indicators and proves the causal link between them.

### 5.6.3 **West Greater Cairo sector (ring road-Giza) (WGC)**

The WGC sector representing the large part of Giza Governorate, which dominates the EL-Haram area (pyramids), and the western part of the ring road and El-Mahor (axis road) (Fig. 105), has a total area of about 198 $km^2$. Despite the fact that it is called ring road the western side of the ring road ends in this sector and does not connect the ring due to the protection of the pyramid area.

I detected and analyzed the state of LULC in 1999 and 2008, and the influence of development work (roads) on the spatial resilience and the dynamic change of WGC. I also classified the urban areas, cultivated land, bare soil, and desert (LULC keys) at different levels to examine the mutual relation between sub-classes, and in particular between urbanization and vegetation. Where, the water bodies were observed as being very narrow canals, so, they were excluded from classification (Fig. 69).

#### 5.6.3.1 State of LULC

The classified image of 1999 (Fig. 106) shows that the vegetation cover represented the largest proportion of the WGC area (81.65 $km^2$ (41.3%)), while bare soil represented the smallest proportion (about 1.83 $km^2$ (0.93%)). The total urban areas accounted for about 54.04 $km^2$ (27.34%), and the hinterland (desert) located to the far west of the Nile River valley accounted for an area of about 60.2 $km^2$ (30.4%).

According to the LULC map of 2008 (Fig. 107), urbanization was the dominant land use and cover class (about 83.04 $km^2$ (41.9%)) while brae land covered a very small proportion of the WGC sector (0.53 $km^2$ (0.27%)). Furthermore, cultivated land accounted for about 60.6 $km^2$ (30.6%), and mainly covered areas to the north and south of the ring road; it is restricted in the west by hinterland (desert), which itself accounts for an area of about 54.04 $km^2$ (27.3%).

The statistical analysis of land use cover classes in Table 20 illustrates the increment of settlements (urbanization) and the reduction of green cover by 14.5% and 10.8% respectively, while the hinterland and bare soil show minor changes of 3.2% and 0.66% respectively.

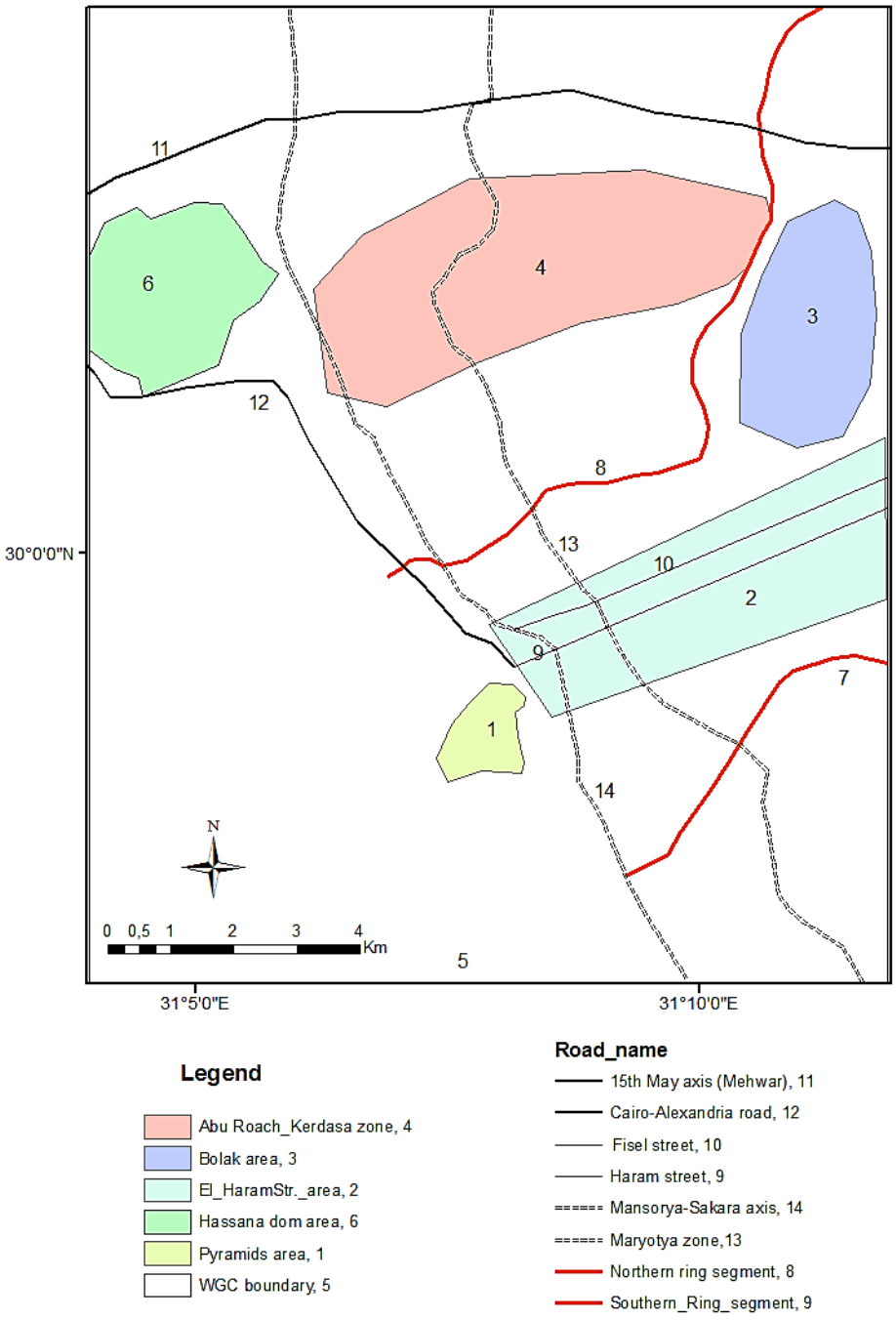


**Figure 105: Zones of the WGC (ring road-Giza) sector. Map based on SPOT image 2008**

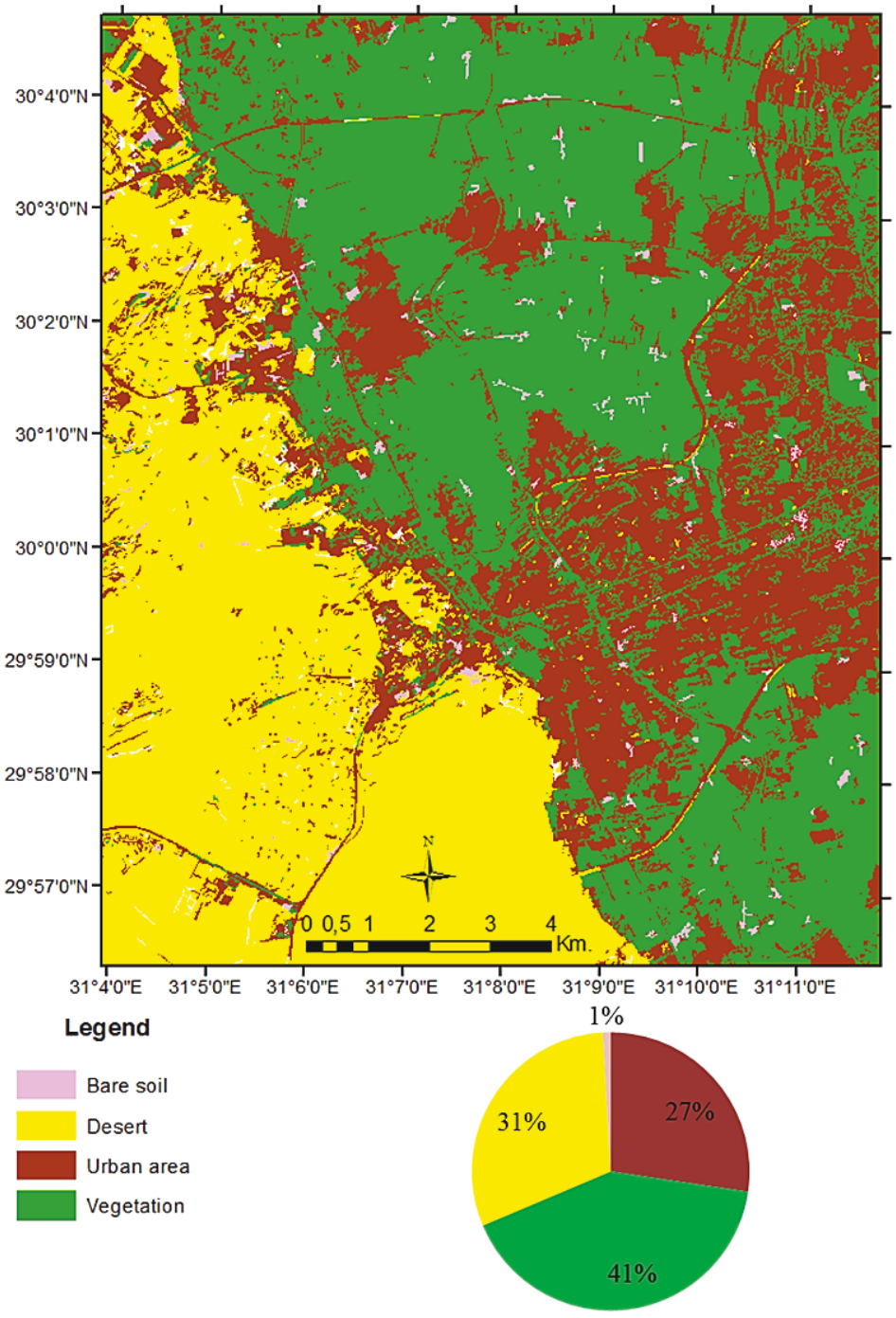


**Figure 106: LULC classification map for the WGC sector in 1999**

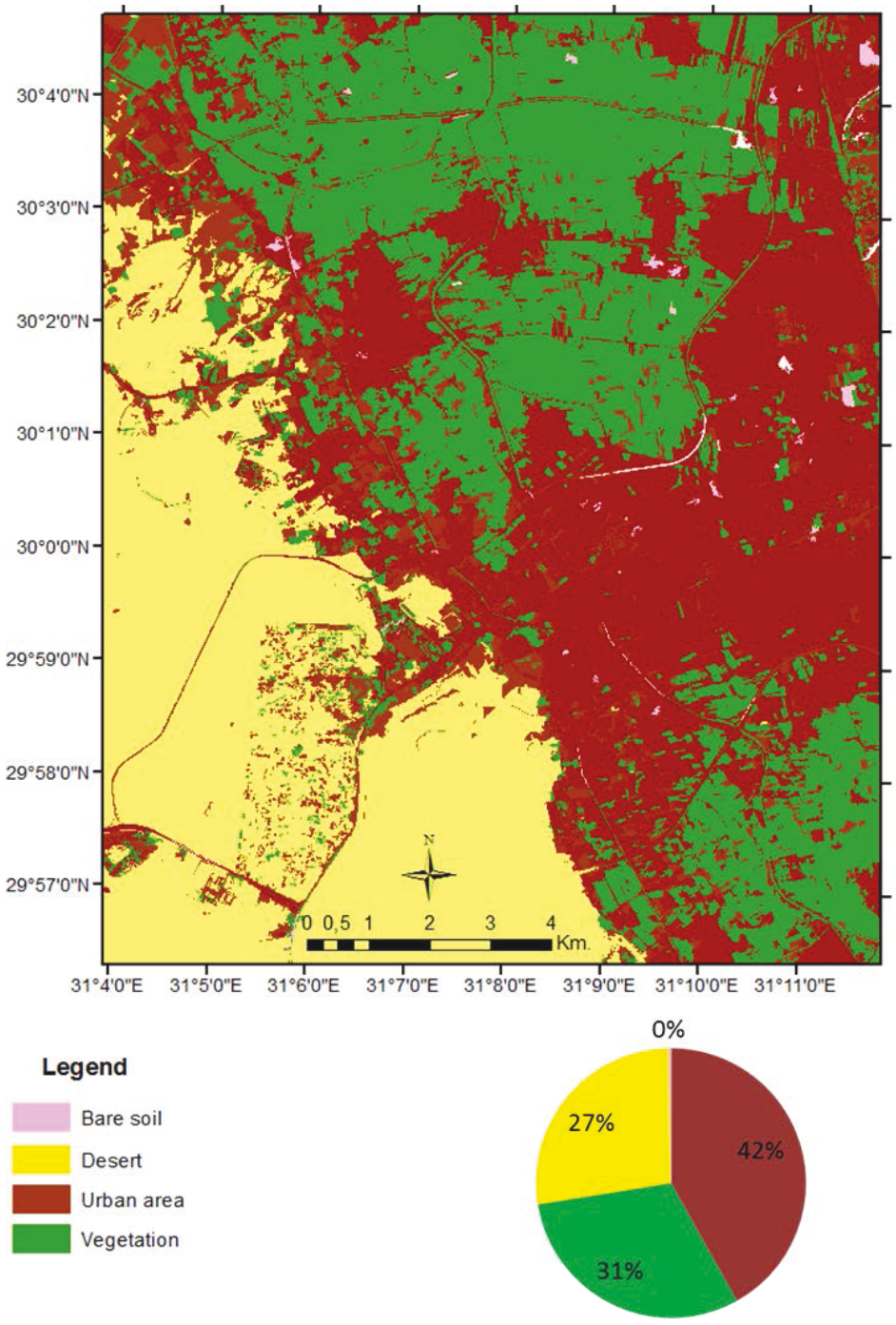


**Figure 107: LULC classification map for the WGC sector in 1999**

**Table 20: WGC sector statistics and percentage of LULC in 1999 and 2008 (see abbreviations in 5.5.3)**

| LULC Classes | 1999 | | 2008 | |
|---|---|---|---|---|
| | Area km | Area% | Area km | Area% |
| U | 54.042 | 27.34% | 83.04 | 41.89% |
| CL | 81.65 | 41.30% | 60.63 | 30.58% |
| D | 60.166 | 30.43% | 54.044 | 27.26% |
| BS | 1.831 | 0.93% | 0.538 | 0.27% |

5.6.3.2 Urbanization

I divided urbanization into three different sub-classes by using the object features and membership function. I identified high, medium, and low densities of urban areas to show spatial resilience not only horizontally (dynamic change) but also vertically (density).

The classified map of 1999 (Fig. 108) shows that high density urbanization accounted for an area of about 24.7 $km^2$ (46% of total urban area), which was distributed mainly along the Haram Street area and predominantly restricted between the southern and northern segments of the rind road. There are also some patches of high density urbanization in the rural areas located due north and south of the ring road segments, while this class scarcely appeared in the hinterland on the boundary zone between the Nile Wadi and desert area.

Medium density urbanization was mostly located in the areas (rural) due north and south of the ring road segments, and there are distinct patches located in the area between the two segments of the ring road practically at its fringe. The hinterland (desert) contained some urban objects of medium density, which are located mainly at the boundary with the Wadi. The total medium density objects accounted for an area of about 22.32 $km^2$ (41% of total urban area), which represented not only the uniform buildings but also some informal areas with fair separation between the houses.

Finally, low density urbanization was mainly represented in the newest urban areas established in the hinterland and concentrated at the boundary between it and the Nile Wadi. In addition, a small amount of low density urbanization can be identified in other parts of the WGC sector with distinct patches in the western part of the Haram Street area. The total area of the low density class in 1999 was 7.03 $km^2$ (13% of total urban area).

In the classified urbanization map of 2008 (Fig. 109), we can see that the high density urban areas increased dramatically by 16% in comparison to 1999, and covered a total area of about 51.48 $km^2$ (62% of total urban area) (Fig. 110). This class was spatially distributed not only in the area between the two segments of the ring road but also in some areas north and south of the ring road segments, which mainly indicated the change in the density of rural areas from medium to high. The field observations and ground truth points found that the increase in high density urbanization is usually due to using spaces in medium and low density areas as well as rapid urban sprawl over fertile land. The hinterland limited the expansion of high density urbanization, its being restricted by the Cairo-Alexandria desert road.

Furthermore, medium density urbanization accounted for an area of about 23.01 $km^2$ (28% of total urban area), which is distributed mainly in the western side of El-Haram Street and the boundary zone between the hinterland and the Nile Wadi. Although the medium density class showed little change between 1999 and 2008 (increasing by about 0.7 $km^2$), it underwent distinct spatial changes by transforming low density areas to medium density areas, and increasing the use of fertile land for urban activity, especially around the most western terminal parts of the ring road (Fig. 111).

Low density urbanization accounted for an area of about 8.55 $km^2$ (10% of total urban area) in 2008, this class being mainly located in the hinterland and representing the most uniform buildings (formal) all over the study sector. The area around the Cairo-Alexandria desert road showed many private urban projects which limited the random growth of informal building on the eastern side (Wadi side). Despite the fact that the area of the pyramids is protected from misuse and urban sprawl, the Hassana Dom protected area is being affected by the establishment of new official building projects.

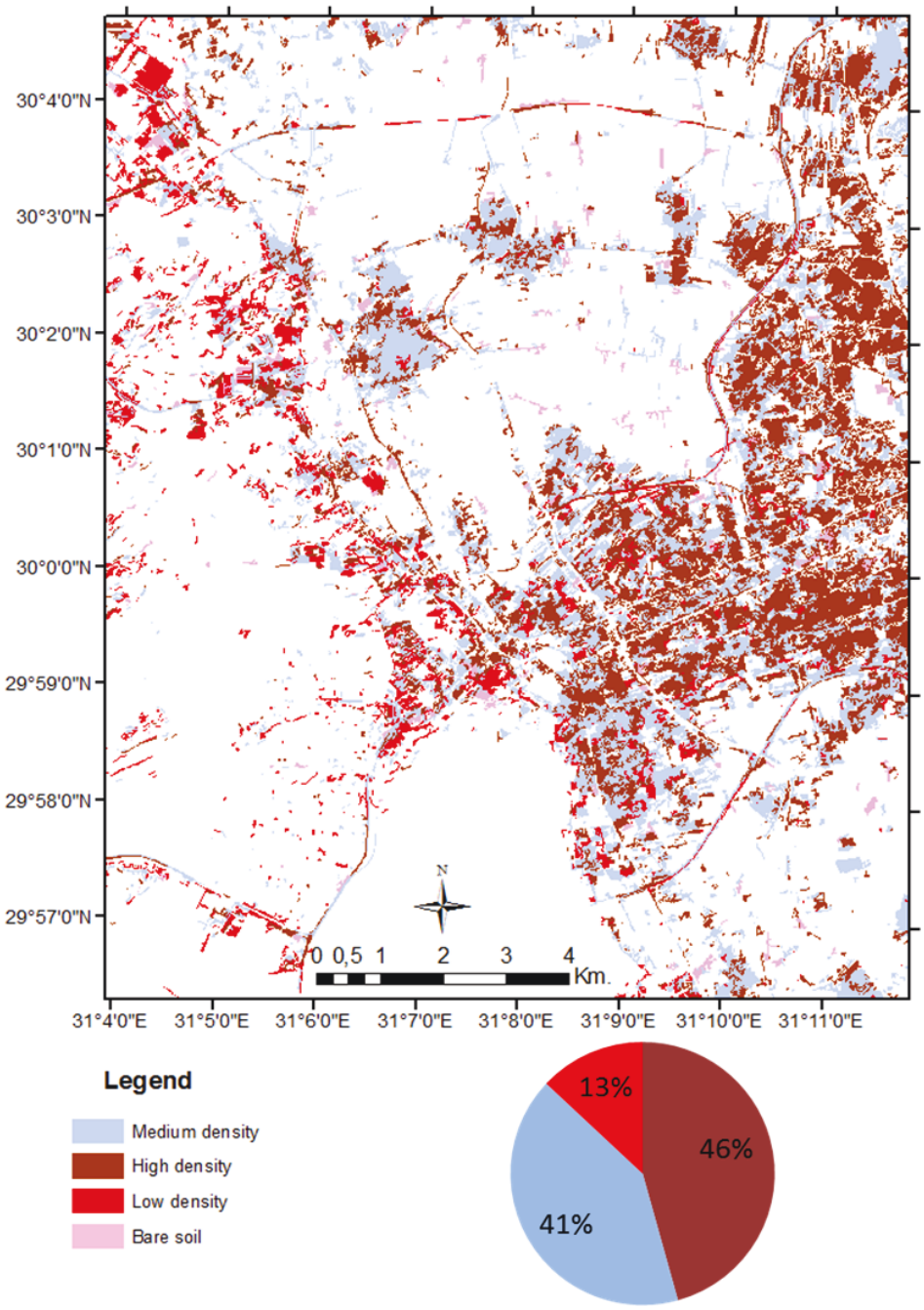


**Figure 108: Classes of urban density in the WGC sector in 1999**

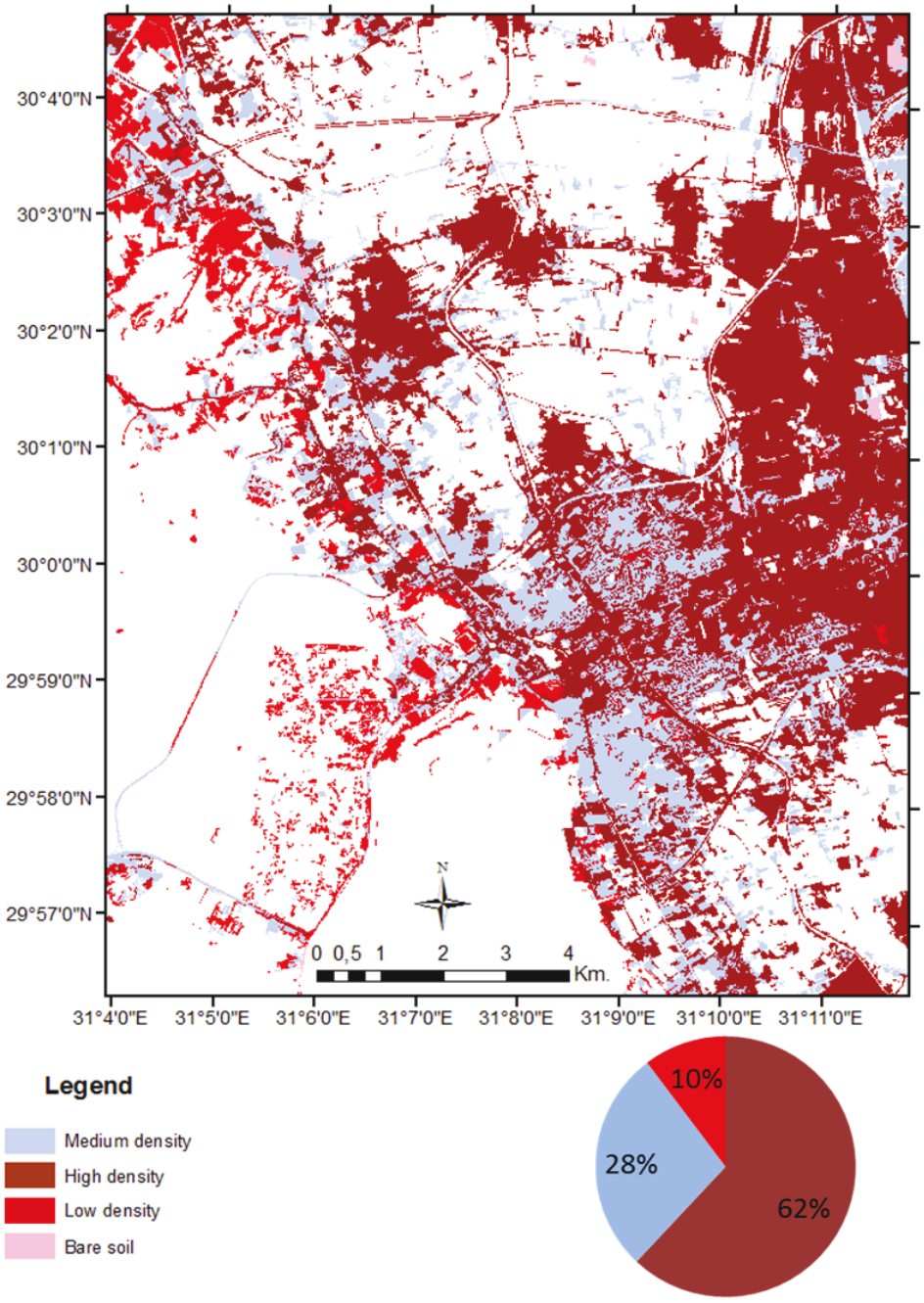


**Figure 109: Classes of urban density in the WGC sector in 2008**

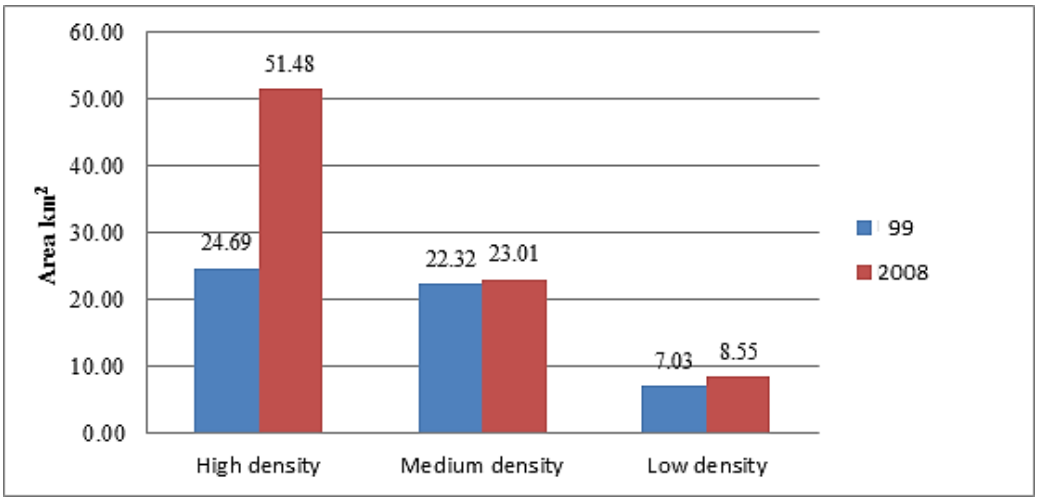


**Figure 110: Changes in urban density in WGC between 1999 and 2008**

**Figure 111: Urban encroachment close to the ring road. Photo captured 2009**

### 5.6.3.3 Vegetation

In both classified maps of 1999 and 2008 (Figs. 112, 113, and 114), the vegetation cover was differentiated into three sub-classes: uniform (agriculture), sparse vegetation, and other vegetation cover.

There is a large amount of cultivated land in the WGC that consists of mainly agriculture fields (uniform-massive vegetation). Additionally, there are parts of sparse vegetation (less dense) objects which are composed of public green spaces, meadows, and private gardens, golf courses.

In 1999, agricultural land accounted for an area of about 52.5 $km^2$ (64% of total cultivation) while in 2008 it accounted for an area of about 45.85 $km^2$ (76% of total cultivation). Most agricultural land is located to the north and to the south of the ring road segments which is historically dominated the old rural areas that transformed to urban pattern because of the intensive use of concrete materials for building activity.

In 1999, sparse green cover was spatially distributed all over the Wadi areas and partially appeared in the hinterland with a total area of about 22.96 $km^2$ (28% of total cultivation). The classified map of 2008 shows a reduction in this class of about 50%, with the total area accounting for about 11.61 $km^2$ (19% of total cultivation). The areas most affected are located between the two segments of the ring road (El-Haram, Bolak, etc.), and the area at the fringe between the Nile Wadi and the desert (east of the Cairo-Alexandria desert road). This rapid change of sparse vegetation shows the progress of the process of urban sprawl over the green cover and also indicated to the most affected areas and referred to the hot spots which should be taken into consideration to preserve the fertile land and green cover. Controversially, the hinterland showed increasing green patches within the new urban areas, which were merely used to enhance life quality rather than food production.

Few rest green cover areas classified at the first level have no affiliation to one of the two sub-classes; it represented the fuzziest classified objects. This fuzzy objects accounted for an area of about 6.22 $km^2$ (8% of total cultivation) in 1999, and 3.17 $km^2$ (5% of total cultivation) in 2008). I have classified these objects as “other vegetation cover”. More division of the study area and the use of very high resolution satellite images will be necessary to define that class more precisely.

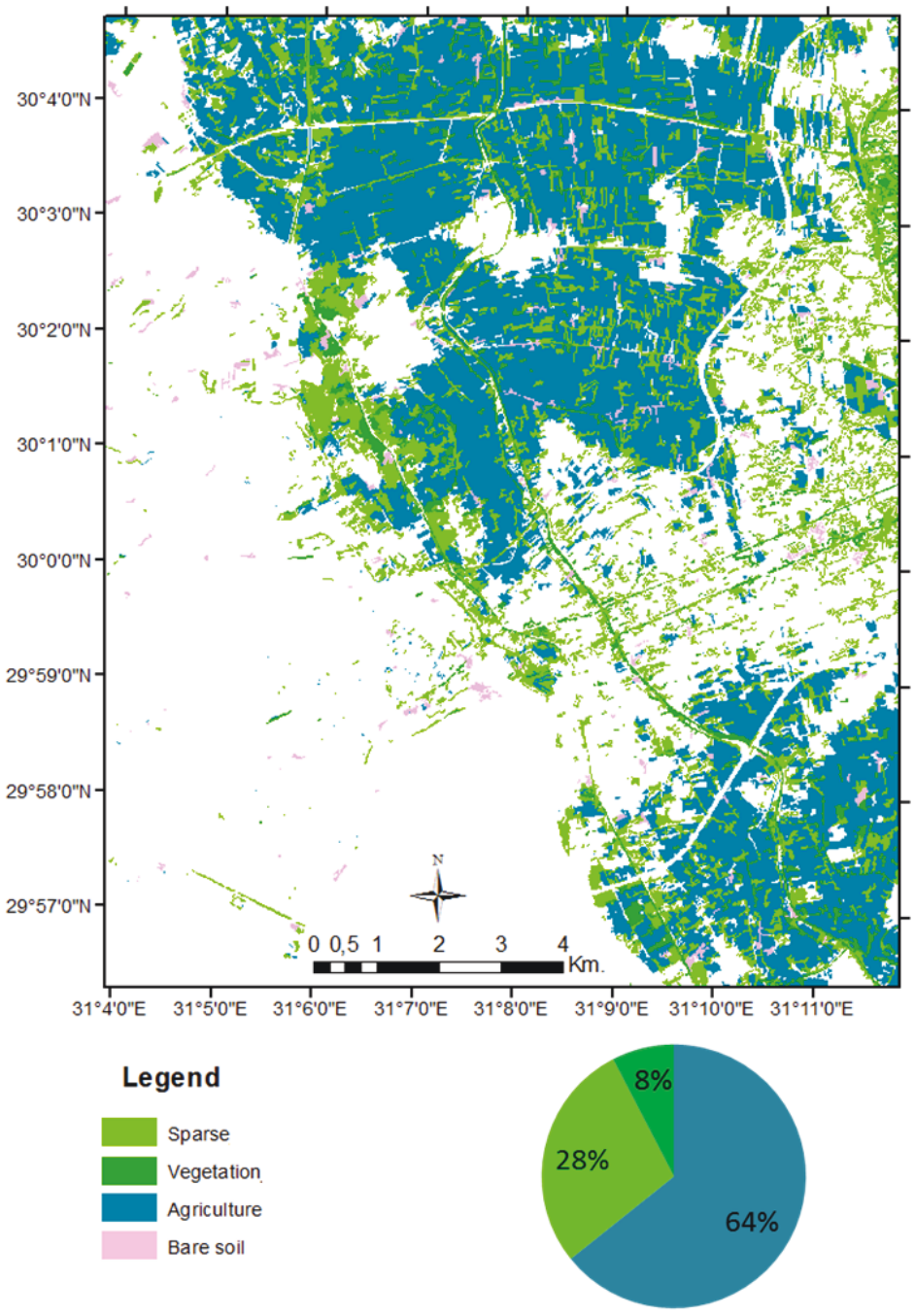


**Figure 112: Spatial distribution of CL classes in the WGC sector in 1999**

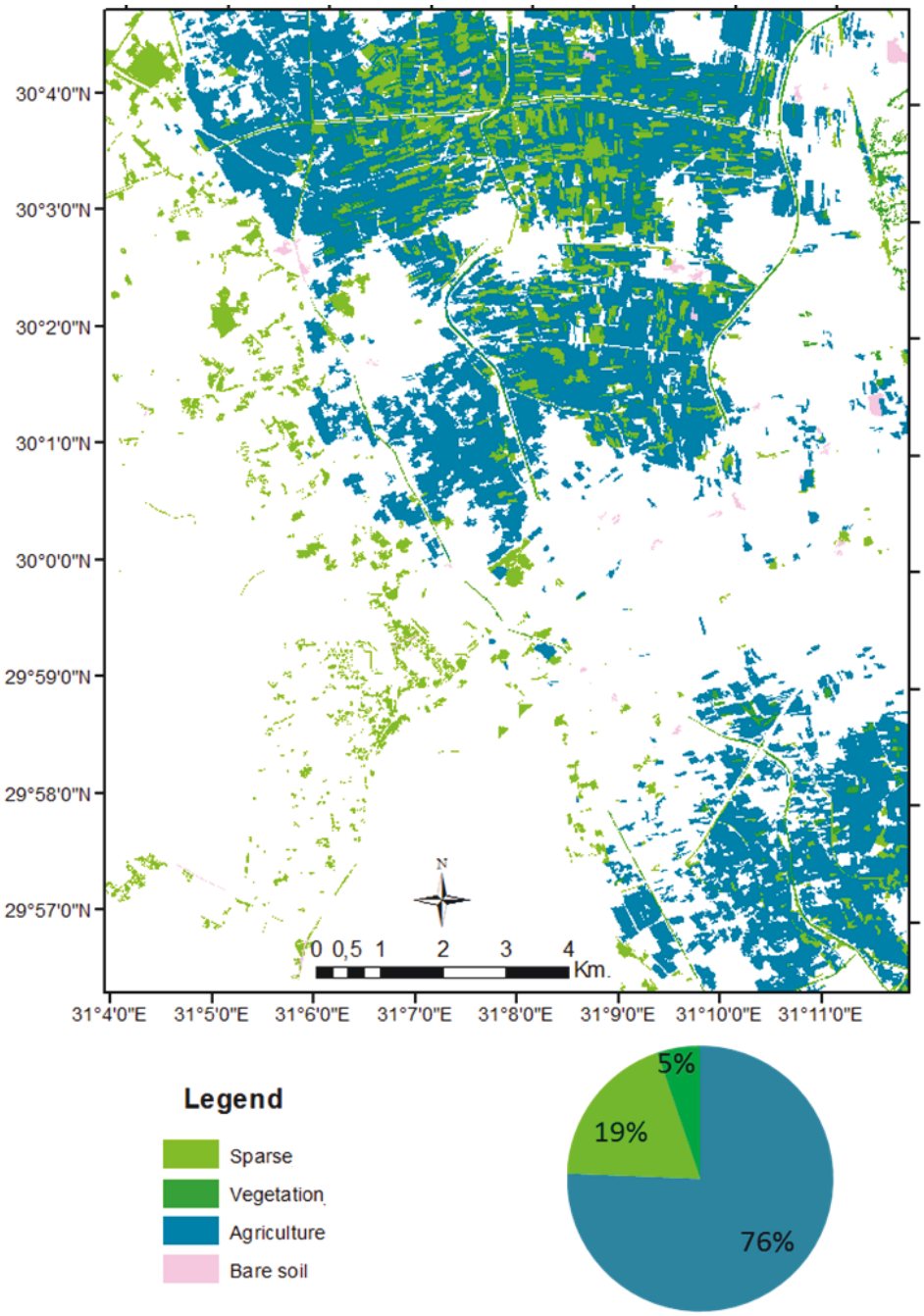


**Figure 113: Spatial distribution of CL classes in the WGC sector in 2008**

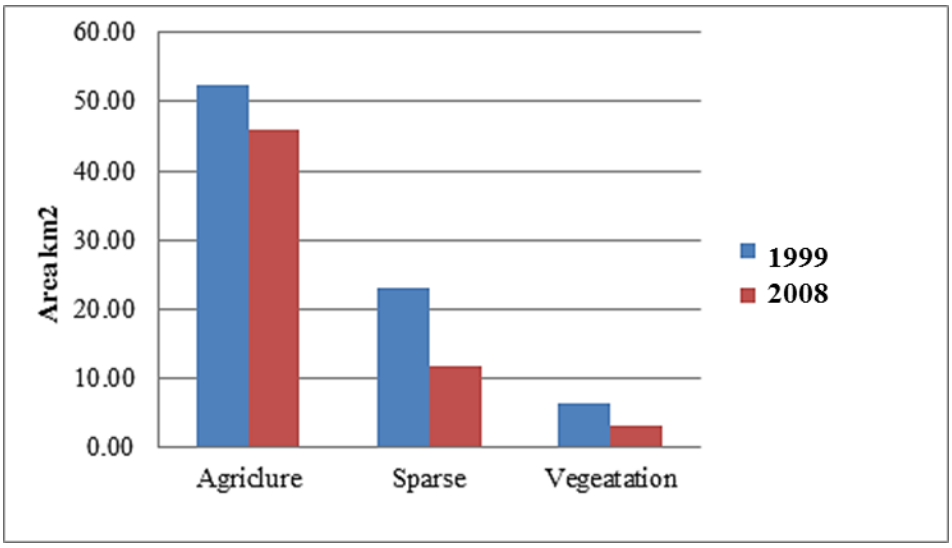


**Figure 114: Changes in cultivated land classes in WGC between 1999 and 2008**

### 5.6.3.4 Change analysis

To analyze spatial growth and detect dynamic changes in the WGC sector, there is an algorithm within eCognition software that allows to created levels of changes that includes the multitemporal assessment using the classification rule sets.

My calculations and analysis show that the total urban areas increased between 1999 and 2008 (Fig. 115) by about 42% (38.98 $km^2$) while 6% (5.66 $km^2$) of urban objects indicated negative changes. The largest proportion was assigned to no-change class in urbanization and estimated about 52% (48.51 $km^2$) (Fig. 116).

The spatial distribution of urban growth, shown in the change detection map (Fig. 115) shows that most new settlements in the contact zone between the Nile Wadi and the hinterland (Cairo-Alexandria road) builds up are mainly characterized by low to medium urban densities. The areas around the ring road segments in the western part show an increase in urbanization in different orientations. Most of these new buildings sprawl over fertile land.

The new urban areas, established under legal development plans, are located mainly in the desert and represent the most uniform-formal urban patterns with low and medium urban densities.

In spite there seems to be no change in the urbanization classes between 1999 and 2008 it could happen that at a more detailed scale there was some change e.g. between low or high density pattern. At least it was not possible to calculate these changes for the whole research area. But the urban density maps show a change in order of densities. Thus the high density urbanization classified in 1999 mostly showed no-change in 2008, while the main urban change happened in the medium and low density urban areas. Furthermore, the urban areas located between the north ring road segments and the axis road (El-Mahwar) have been affected by density transformation. There are urban areas located around and inside the zone between northern and southern ring road segments (e.g. El-Hrama, Dokki, and Bolak areas) that also show no-change in the urbanization class while density of its subclasses changed from low to medium or from medium to high. .

At the level of vegetation change (Fig. 117), the positive existence of green cover is estimated at 4% (3.29 $km^2$), a drop of 34% (28.68 $km^2$), and the existence of cultivated land with no-change is estimated at 62% (53.08 $km^2$) (Fig. 118). The negative change in green cover has occurred mainly on the cultivated land close to the urban areas and particularly around and inside the zone between the two ring road segments and the arc parallel to the eastern side of the Cairo-Alexandria desert road and the terminal of the Axis road (El-Mahwar). In addition, the change map showed that some villages such as which located in the Abu Roach-Kerdasa zone influenced by decreasing of vegetation cover around their rims. The maps of vegetation types show that most change happened to the sparse vegetation type which mostly increased close to farmland and decreased in the urban areas. That could indicate the misuse of fertile land and the debasement of the quality of life. Controversially, the green cover which increased in the hinterland, combined with the new formal building projects, might indicate the rise of green-urban spaces which impacted on the quality of life.

At that level of monitoring framework, the dynamic change of bare soil is slightly contributed to spatial growth and resilience analysis of the WGC sector. Generally it accounted a very small proportion and represented the uncovered fertile land. The increase of sparse vegetation in the desert between 1999 and 2008 is compatible with a decrease of bare soil in the same areas.

The use of the hinterland in the WGC sector could reflect the role of desert development on spatial resilience. Thus, the main informal growth of the urban areas (high density) in the WGC periphery was occasionally controlled due west by formal development projects (privatization) and protected areas (pyramid zone).

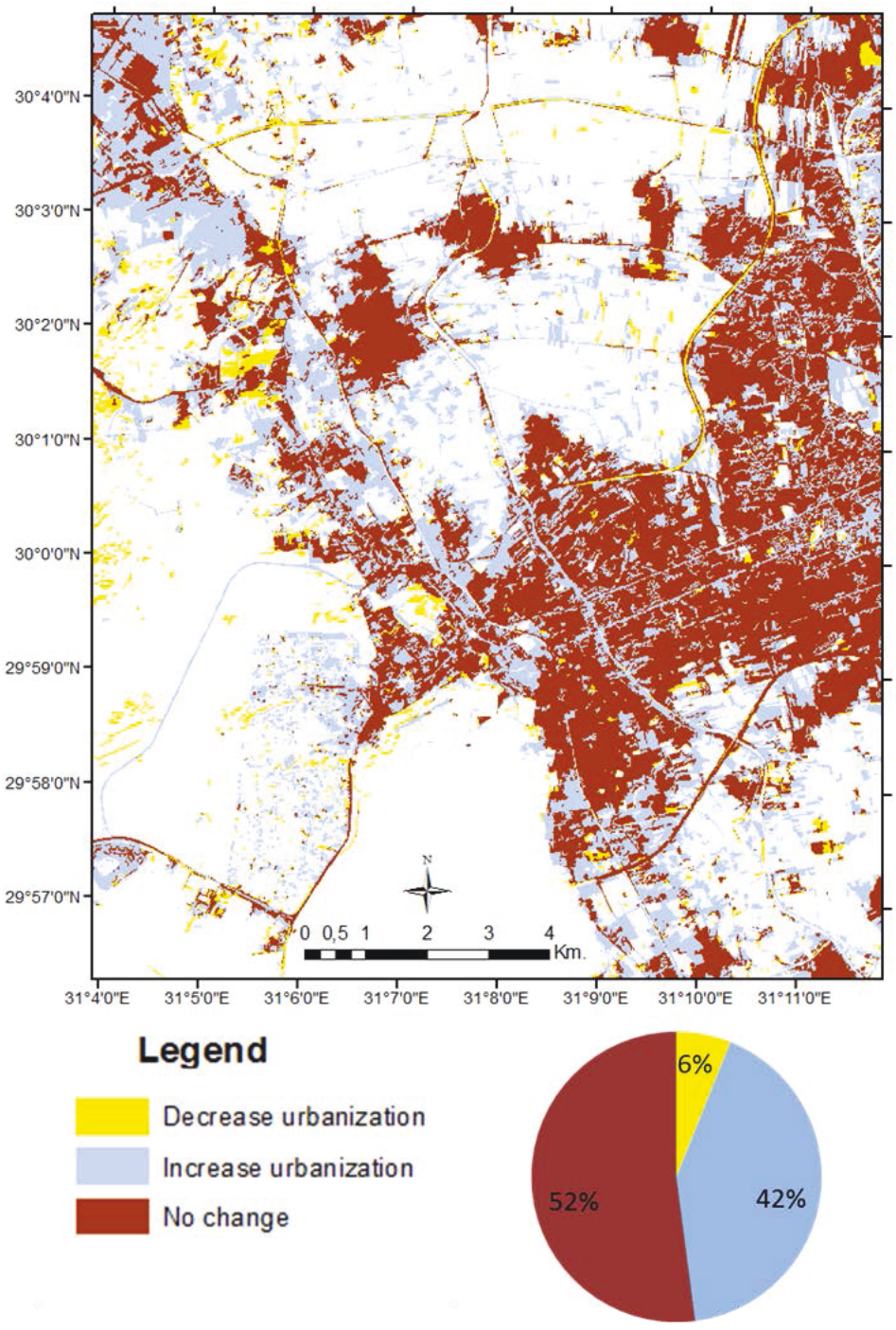


**Figure 115: Urban changes in the WGC sector**

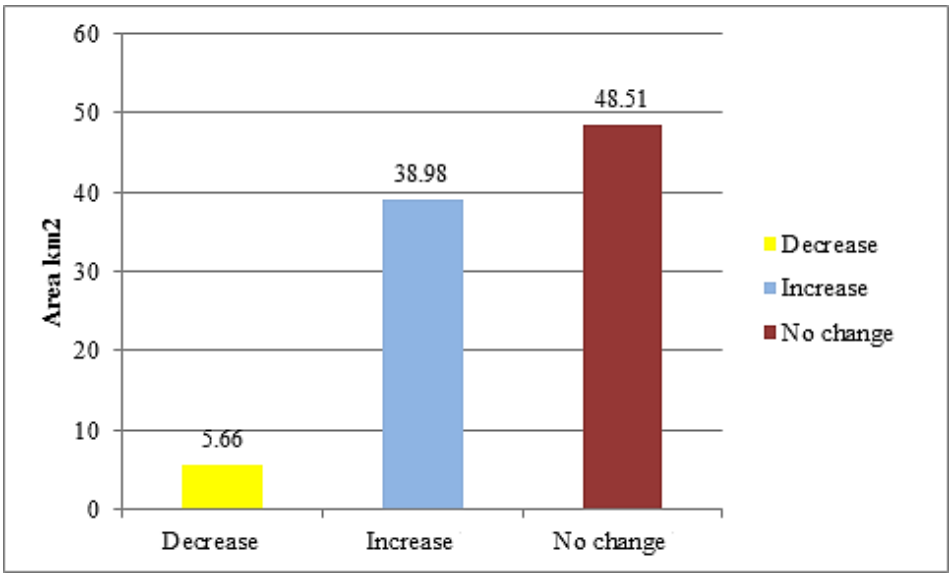


**Figure 116: Area estimated for urbanization changes in the WGC sector**

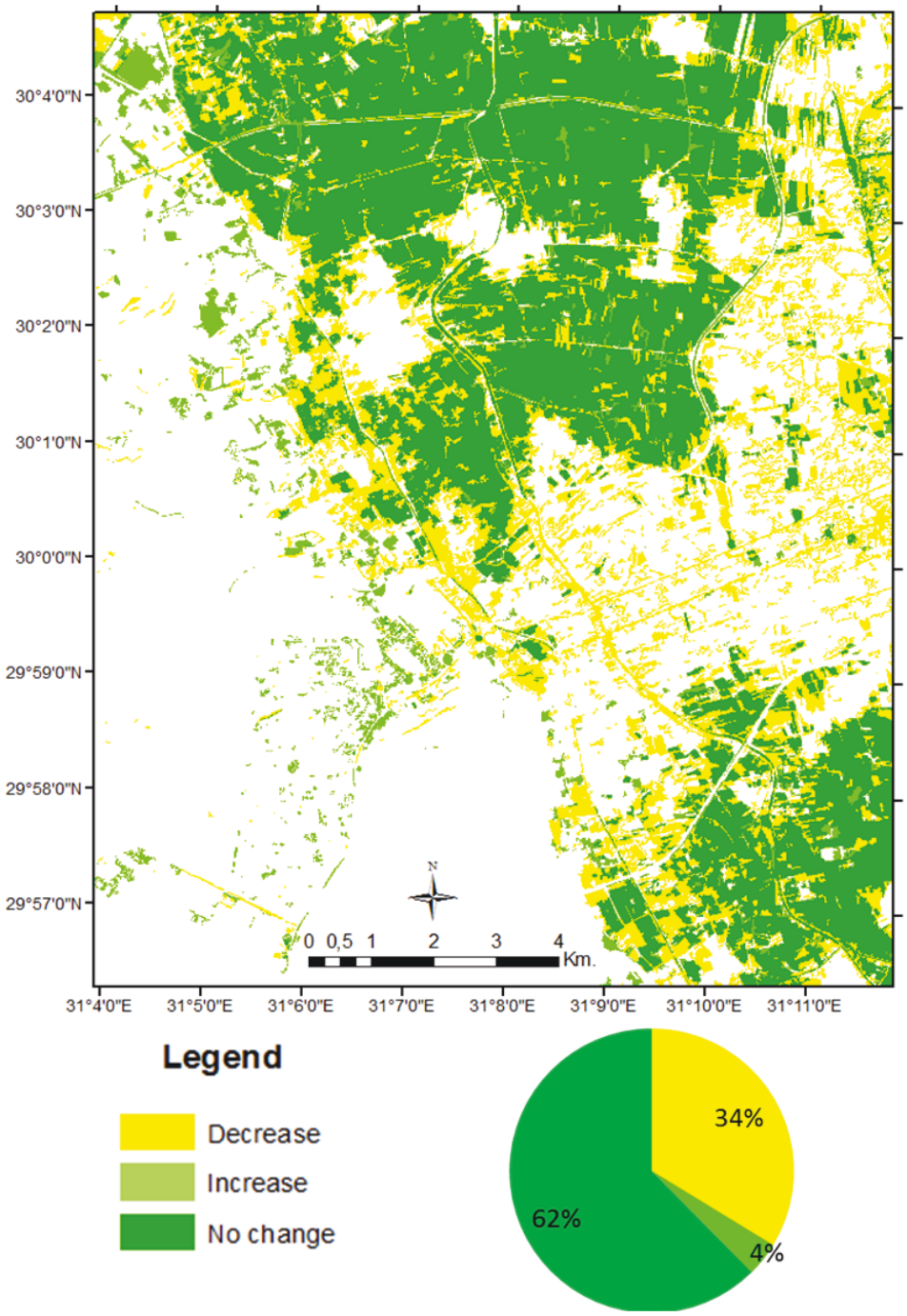


**Figure 117: Cultivated land changes in WGC sector**

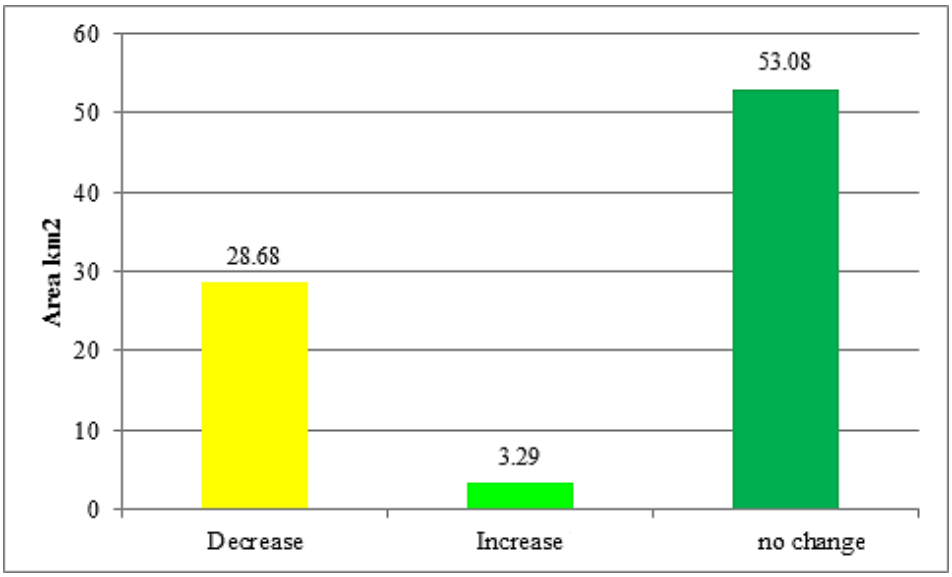


**Figure 118: Area estimated for cultivated land changes in WGC sector**

# 6 Analysis and Interpretation (Response priorities)

## 6.1 Urban density and diversity

The urban densities classified and detected in the last chapter can be used to understand spatial growth and spatial resilience of urban areas in GCM. GCM showed three different urban densities referring to five urban patterns verified from field work: core-old pattern, slums, urban sprawl over fertile land, new cities, and villas and compounds. The slums and urban sprawl areas are usually described as informal buildings, while new-city constructions including villas and compounds are defined as formal buildings (Fahmi and Sutton 2008, and Khalifa, 2010).

All over, the classified time series data have shown the change in urban densities from lower order to higher which were triggered in most GCM areas by the building and infrastructure elements and the economic reform program.

### 6.1.1 High density pattern

The urban areas of high density dominate most of the core-old pattern and informal buildings which extended in the peripheral lands. The core-old pattern is mainly dominated by old buildings, heritage areas, multistory buildings close to the Nile River, and center markets (Fig. 119). In spite of what some authors mentioned that the build-up surface in the core area being unchanged during the last three decades (Yin et al. 2005; and Fahmi and Sutton 2008), others have recorded and interpreted the change in the urban pattern over time by showing how the old buildings and villas have been replaced by modern multistory blocks (Ehlers 1989, Meyer 1990, and Khadr 2009). This reflects the increasing density in some core areas of GCM (e.g. Masr EL-Kadyma or Ayen El-Sera) between 1999 and 2008 from medium to high, which has been verified from field observations in this study (Fig. 120).

**Figure 119: High density urban area in GCM core showing heritage buildings. Photo captured 2010**

**Figure 120: New towers on the Nile River show the replacement process and the transformation of urban patterns. Photo captured 2010**

Moreover, the high density urban areas at the periphery are mostly made up of squatter settlements at the fringe of the core-desert (slums) and of urban sprawl or urban encroachment as informal sectors expanded into fertile land. The definition of slums and informal buildings is a matter of controversy (El Araby 2002, Khadr et al. 2009 and Khalifa 2010), but they are generally characterized by an absence of public land management, and the presence of low to middle-low income dwellers (Fekade 2000, El Araby 2002, and Khalifa 2010). In this study, the informal settlements exhibited the most changeable areas concerning urban density and urban built surfaces between 1999 and 2008, which reflects the intense pressure exerted on the peripheral land.

The most distinctive high density slums were located on the eastern side of GCM, such as Manshyet Nasser and Estbal (Ezbet) Antar-Basateen-Dar El Salam (Fig. 121). At the fringes of the core area, there is little change in built-up surface and a remarkable increase in low and/or medium density to high density urban areas. Most of the slums which were formed in different parts of the El-Mokattam plateau have been established in past time by squatter on land. These areas of increased urban density, with their lack of drainage and sewage systems, concentrated sources of environmental pollution, and a large number of illegal workshops and small factories, have been categorized as unsafe by Khader et al. (2010).

Spatially, the slums showi no dominant urban core and consist of undefined streets; they are also surrounded by planned areas for private projects or by uniform medium density settlements. For instance, the Manshyet Nasser area is surrounded by formal Nasser City and El Mokattam formal buildings. Furthermore, Establ-Antr-Basateen slum is bounded by El Maadi formal buildings from the south and east and by Nile Cornish buildings from the west, while the northern part is connected with old Cairo through the cemetery area.

Studying high density slums has clarified the point that most of the land is already used for urban activity and the few remaining parts are located in the riskiest geographical areas or areas evacuated by the government after a disaster (e.g. the rock fall of 2008 in east Cairo), suggesting that the dynamic growth in the future of such slums could be restricted as their spatial area might be trapped by their surrounding forms.

**Figure 121: Establ Antr-Dar El Salam informal houses (east GCM). Photo captured 2010**

The high density informal areas represented by the process of urban sprawl onto agricultural land indicate not only the rapid dynamic changes in GCM but also the impact and intensity of the pressure created by the increased urban density in the core and the restriction of informal urban expansion (slums) on the suburban desert fringes. For instance; although the ring road was constructed to connect the new cities with other parts of the metropolis, to confine the periphery of GCM, and to restrain Cairo's urban sprawl (Stewart 1996), it has also increased urban density around it and its related axes (e.g. El Mehwar and Autostrad), showing that the ring road accelerated the urbanization process at the periphery, which then extended in some parts to connect villages and merge them with the rural land (Fig. 111).

Similarly, the change in urban density maps showed a distinctive transformation of low density urban areas around the metro line turning it into a high density urban area. For instance, the urban densification was occurring through the northern parts (El-Marg and Shubra area) and the southern parts (Helwan- Maadi area) (Fig. 122).

Furthermore, some uniform and/or planned areas, such as Nasser City, north Helwan and Haram street sector, also showed increases in density rates reaching high density levels. This is due to changes in the urban fabric through filling up, condensation and densification of land spaces. Therefore, continuing such phenomena in such areas will decrease the uniformity of buildings and increase the informal features.

### 6.1.2 **Medium density pattern**

The resulted maps of urban sub-classes showed that the medium density category contains the most changeable objects due to the densification of most of its categorized informal areas and particularly in the areas dominated formal buildings. The medium density pattern was present mainly on the peripheral zone and in the new cities. On the east and west peripheral zones, it was represented by formal built-up areas (e.g. Nasser City, El-Mokattam, Haram Street, and the Cairo Alexandria road) and by informal built-up areas to the north and south of the peripheral area (e.g. El-Marg and Mostorod aresa).

However, one of the large slums (Ezbet El Hagana) in the north-east of Nasser City (Figs. 36 and 90) experienced little change in terms of both urban density and built-up areas between 1999 and 2008. That could be interpreted in several ways. Firstly, the area is located far away from the high density core area; secondly, the social bond between residents is stable as the area was initially established as a settlement for the families of soldiers based in the vicinity (Khalifa 2010), which caused difficulties for other people who emigrated from the country side to use free land; and, thirdly, the effect of the location is important because the area is surrounded by formal buildings, military locations, and the Cairo-Suez highway, all of which have limited the expansion of the Ezbet El Hagana slum (Fig. 122).

In most of the new cities, urban density increased from low to medium. These cities were occupied by people with medium to high incomes, while people with low incomes and young people could not afford to live there due to the high cost of buying or renting a property and the lack of transportation services (Stewart 1996 and Fahmi and Sutton 2008).

According to Portnov and Pearlmutter (1999) and Fekade (2000), one of the criteria in the development process undertaken by informal areas is the presence of spatial isolation of low density and medium density clusters around a distinctive agglomeration of high urban density. This phenomenon was also observed in some areas of GCM.

Under such conditions, such as the evolution of development elements and connection services, the isolated urban clusters have been growing much more, leading to an increase in built surface and density. One example is the area surrounding the terminal of El Haram Street, where the development elements and connection services (metro, roads, etc.) accelerated the urbanization process and increased urban density especially in the north and the south of the GCM. Most villages on the fringe of the periphery were influenced by the saturation of the core and the blocking of the growth of the slums through using the surrounding land and increasing the urban built-up surface.

### 6.1.3 **Low density pattern**

The low density urban areas are represented by the scattered groups of buildings which take different urban patterns in different places, referring to the most recent urban development activity and trends of the growing city. The spatial distribution of low density patches shows that the hinterland and the periphery are dominated mostly by these urban patterns, and the time series layers point to the rapid increase in the number of new settlements and to the influence of land privatization on investment trends.

The low urban density on the fringes of the northern and southern parts of the GC periphery represents the initial urban encroachment onto the agricultural land through the transformation of some of the fertile land into barren land (or, in other words, into building land), which marked the first stage in the building of the clusters of informal concrete settlements. In contrast, the low density areas located mainly on the fringes between the desert and the GC periphery represent the beginnings of formal settlement projects. It is also worth noting that some of these projects bounded the slums located in the east of GC from one or more sides, which constrained the continued building of informal houses. For instance, the New Maadi settlements bounded the Establ Antr slum from the eastern side, and Manshyet Nasser slum is restricted from the south by El Mokattam uniform settlements, from the east by some private construction projects, from the north and the north-east by Nasr City, and from the west by cemeteries (Fig. 122).

Furthermore, the rough topography in the east, which extends southeast of Greater Cairo, has played an effective role in blocking the growth of slums.

To the western side of GCM, the periphery is bounded by desert and the pyramid area (a protected heritage zone), where the scattered low density patches have increased along the Cairo-Alexandria road. That was attributed to the extensive new formal urban projects (including the new Egyptian

Museum), which have helped to restrict the expansion of informal settlements from the eastern side (the Nile valley). But, in my field observation, I also recorded some degradation of the Hassan Dom protected areas due to the privatization of land and the establishment of urban projects.

Moreover, the unchanged low density patches in the hinterland usually represent the villas and private compounds (gated communities), while the changed patches usually represent the middle-class settlements which are still being constructed. The new cites in GCM are composed of three contrasting urban elements: an insufficient public-private youth housing project; a decaying and inadequate resettlement housing project for victims of natural catastrophes and for other relocated urban poor who often wish to return to their informal housing in the inner city; and a private gated community for affluent and upper-middle-class residents and/or property speculators (Fahmi and Sutton 2008).

In spite of the privatization policy, which forces people to move from the center to the periphery and to the new towns, causing the depopulation of the older parts of the city (according to Bayat and Denis (2000) and Yin et al. (2005)), this study has found that the policy has actually increased informal urban activity on fertile land. This is because the infrastructure and transportation services available there are better than they are in the new cities, and because the poor and most young people cannot afford to live in the new cities, with the vast majority of residents in the core and high density informal areas falling under this social class.

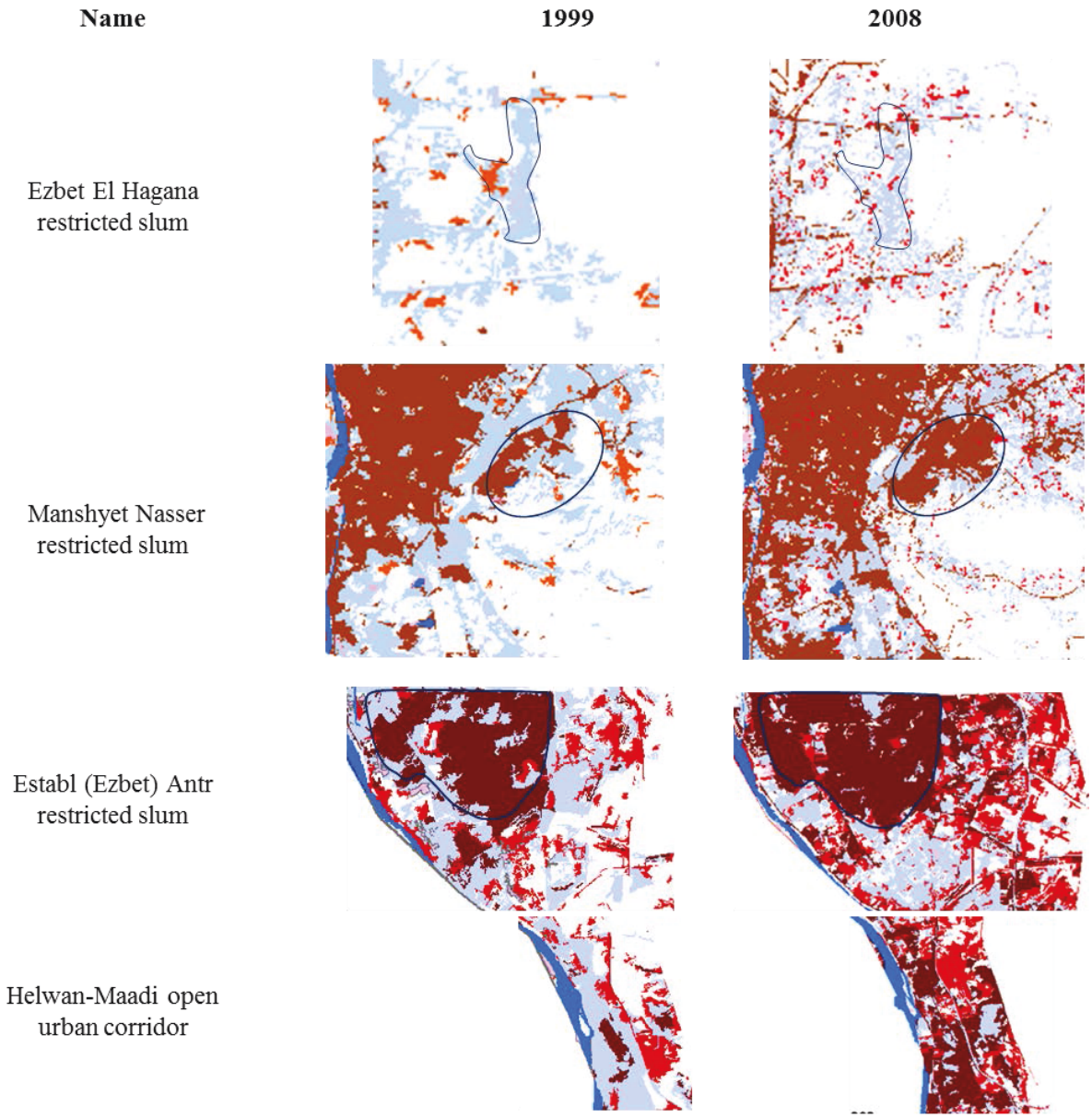


**Figure 122: Some restricted slums (informal areas) detected in GCM and one open corridor (Helwan-Maadi) (for legend, see chapter 5; e.g. Fig. 79)**

## 6.2 Fertile land loss

The first level monitoring frame work (see Chapter 4) (Figs. 51 and 52) shows that the area of cultivated land grew by 1% between 1990 and 2006 after it had fallen by 4% between 1984 and 1990, which raises the following question: what is the impact of urban growth on green cover? To answer this question and to interpret the mechanism of dynamic change of green cover, I used the maps of the three different sectors (see Chapter 5). I divided the vegetation cover into two main

sub-classes of agricultural land (uniform farmland and sparse vegetation) and a third sub-class for any rest green cover mostly unrelated to food production. I then assigned the increase in green cover in the metro-autostrad (MA) and in core-new- city (CNC) sectors mostly to the sub-class of sparse vegetation and/or other vegetation. Additionally, the vegetation cover detected in the ring-road-Giza sector showed a negative change at all levels of green cover over the time (except the increase in sparse vegetation in the hinterland). This means that the agricultural and fertile land continued to decrease while the cover of non-food-production vegetation partially increased. That confirms, as mentioned above, the restriction of informal urban growth towards the east and west of GCM, which puts pressure on the farmland towards the north and south of the core-periphery zone.

The spatial analysis of the resulting data showed different zones and corridors which characterized by the intensive loss of green cover. The process of unprecedented encroachment of urban land use on rural areas observed in Giza and El Maadi has been described as random and uncontrolled (El-Kadi 1987 and Ehlers 1989). The old satellite data from between 1984 and 1990 provided by NDVI and using change map analysis showed the old corridors of urban sprawl and fertile-land loss which were detected along the Embaba-Haram Street north to east in an arc shape and partially along north-south Cornish El Maadi-Helwan.

The results of recent data of 1999 and 2008 show new open corridors and hot zones (affected zones) of farmland loss of different sizes, dimensions and directions (Fig. 123). The most of these corridors have been affected by one or more of the development elements stated in the previous chapter. First, the Embaba-Haram corridor, which has recently been bound by the northern and southern segments of the western part of the ring road, is losing the most fertile land. This corridor ends at the perpendicular Maryotya-Sakkara corridor, which extends north-south and connects the two terminals of the western part of the ring road. Furthermore, the zone between the northern segment of the western part of the ring road and the 15$^{th}$ May Axis is the largest open hot zone influenced by urban encroachment which includes four informal agglomerations (transformed villages) elongated from west to east (from Abu Roach to Bolak). These agglomerations showed an increase in urban density, indicating that they had reached saturation state, so that the surrounding farmland is now under threat. That would lead to the formation of an elongated urban zone dominated by these four agglomerations in one mega informal urban area (Fig. 123). Furthermore it could be followed by the loss of the whole of the fertile land between the ring road and the 15$^{th}$ May Axis if the process takes a north-to-south direction after the Abu Roach to Bolak corridor has become saturated. However, the areas around the north segment of the ring road north of Cairo City represent an zone dominated obviously by what is called here fertile land loss corridors. Two of them are located to

the north of El Warak (Fig. 123) and one extends along the El-Marg metro line intersecting the ring road to the north of the Mostorod area. The El-Warak Island showed increasing fragmentation of agricultural land between 1999 and 2008, which indicates the partial loss of fertile land and the need to protect it. Similarly, some remnants of farmland are still preserved along the old corridor of Cornish El Maadi.

The resulting maps show a distinctive distribution of green cover in the new cities, which I mainly categorized as sparse vegetation, with the exception of the golf courses and some parts of the outer green belts around some new settlements, which appeared more dense and homogeneous and which I therefore categorized as uniform cultivated land. Also, in most of the formal settlement areas located on the periphery of GC, such as Nasser City, El-Maadi, and the central part of Giza City, a large proportion of public green spaces, green road ways and gardens have been preserved. Although the core of Cairo City shows a decrease in green cover and public spaces except for small parcels in some squares (e.g. Tahrir square), the slightly hilly area located between the eastern fringe of old Cairo and the cemeteries on the periphery have recently been cultivated and transformed into a public park called Azhar Park.

Generally, the spatial distribution of sparse green cover in the urban areas could be an indication of the diversity of the quality of life across the core, periphery and hinterland, and it could also be used to document the degree of densification in some of the urban areas.

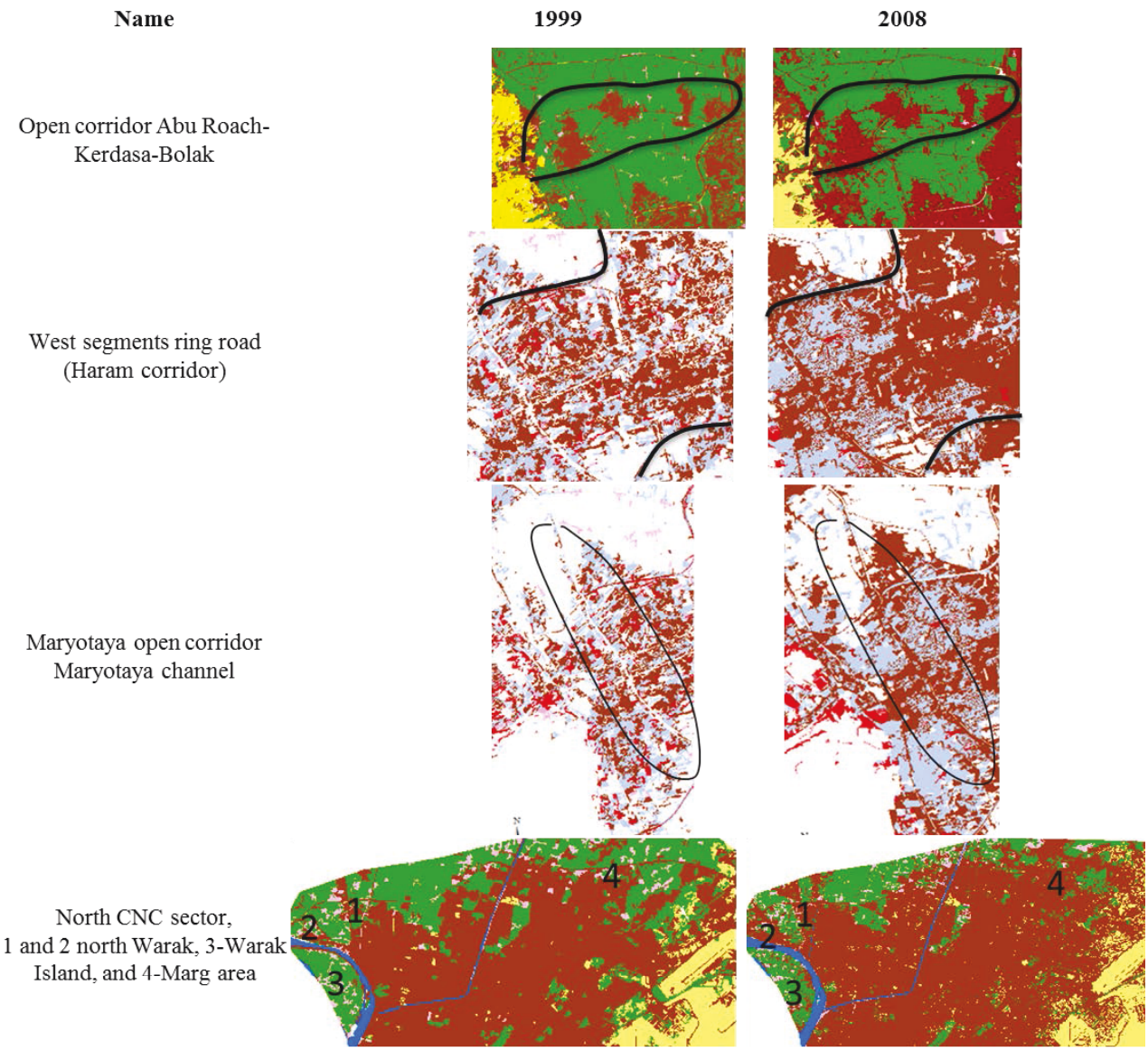


**Figure 123: Some open corridors and hot areas detected in GCM (please for legend see chapter 5; e.g. Figs. 94 and 111)**

## 6.3 Implications for response

As I have demonstrated in this study, there are different areas affected by landscape degradation and misuse of land. I have identified three types of the before mentioned areas as (1) closed urban areas (urban traps), (2) corridors of lost farmland, and (3) hot zones. All of them reflect causal relation between spatial infrastructural elements and change of land state.

The closed urban areas are mostly represented by the slum areas of Establ Antr-Basateen, Manshyet Nasser, and Ezbet El Hagana (Fig. 119 and Table 21) located on the eastern periphery of GC and near the GC core. They are characterized by small growth of the spatial area and an increase in urban density which ranges from medium-high to high (e.g. Ezbet El Hagana). They also feature a shapeless and partially discriminated spatial border with surrounding pockets of land. The main driver leading to the restriction of slum growth is the extensive use of the land between the periphery and the remote new cites under the privatization program. Most of the free land close to the slums has already been built on or is under construction (Fig. 124), or is used by the military or is in official use.

Due to the western desert fringe is far away from the core GC (Giza center), the aforementioned closed slums aren't recorded in the western periphery.

**Table 21: Spatial character of GCM for response**

| Character | Restricted and resistance | Open corridor |
|---|---|---|
| Indicator | Urbanization | Cultivated land |
| Texture | Density increase | Sparse green cover |
| Barriers | Private projects, military, and public land use | Ring road and high way axes, and hinterland projects |
| Patterns | Informal and slums | Urban sprawl, bare soil, agriculture trap |
| Directions | East old Cairo periphery | North and south core of GC |
| Example | Ezbet El Hagana | Abu Roach area |
| Resilience | Low vulnerability to change | High vulnerability to change |


**Figure 124: The limitation of slum expansion due to the formal project. Photo captured 2010**

The metro-autostrad sector is bound naturally by rough relief (Chapter 2) from the east and the Nile River from, and occupied by the Maadi and Helwan settlements along its north-south tract. This spatial structure led to intense pressure on the free land available and increased the density of urbanization between 1999 and 2008. However, the geography and nature of this sector can play a role in constraining and limiting the growth of the sector after the expected saturation.

On the other hand, the corridors of loss fertile land and the hot zones mentioned above (e.g. the zone between the north segments of the ring road and 15$^{th}$ May axes) have been influenced by spatial factors such as the construction of new roads, the availability of transportation services, increasing core density, limitation of slum growth, and the failure of the new cities to attract poor and low to middle-class people (Fig. 125). There is some farmland fragmented and isolated by random houses (e.g. parcel north Shubra) (Figs. 36 and 123), which are vulnerable to the growing and transformation process accomplished with urban sprawl.

Indeed, there are about fourteen hot spots or risky areas (under misuse) mentioned here (Figs. 122 and 123) which are in need of different responses based on the type, properties and spatial vulnerability. Accordingly, the spatial resilience of GCM can be described.

Generally, it could be mentioned that, the east and the west periphery zones, and the core of GCM are slightly-resilient while the north and the south periphery zones are resilient. That means; the

slightly-resilience represents the most restricted and saturated urbanization areas while the resilience represents the open corridors and hot zones identified in this study.

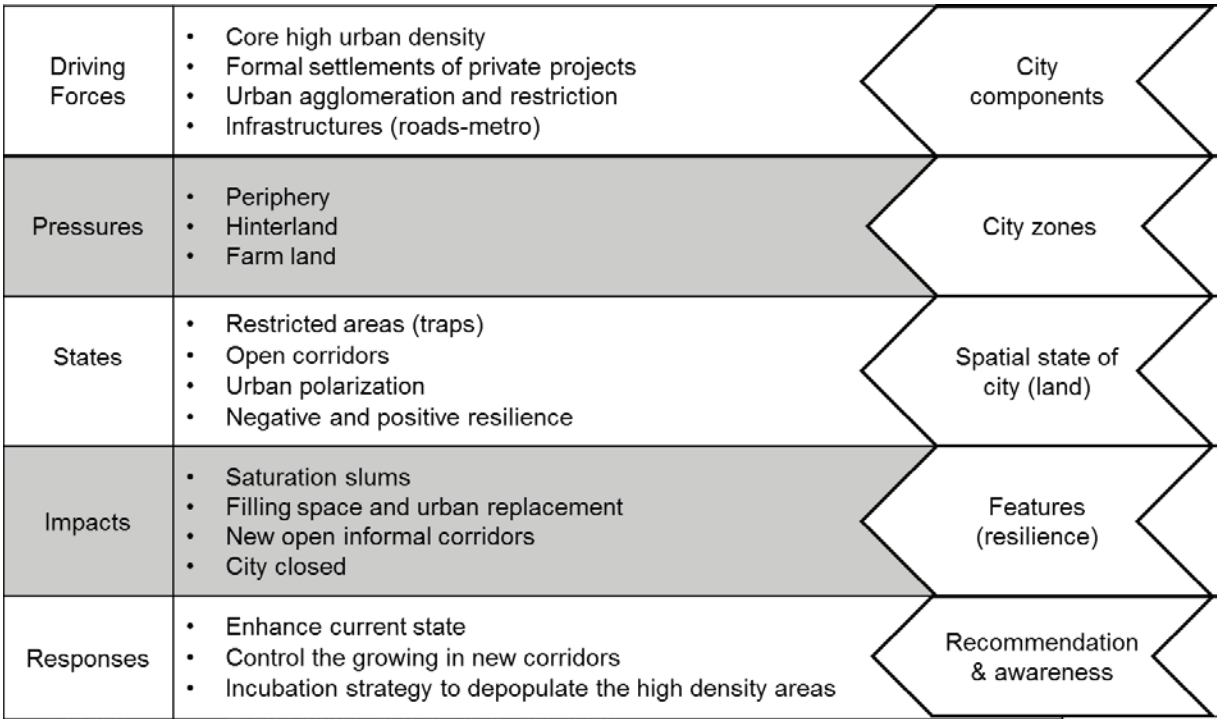


**Figure 125: DPSIR scheme to understand the spatial relations of restricted areas, open corridors, and hot zones**

## 6.4 Discussion

The relation between the urban population and the built-up surface is a matter of controversy, especially in megacities like Greater Cairo. It is understandable that the population rate decreased in the core of GCM and increased at the periphery (Mesev 1998, Portnov and Pearlmutter 1999; Bayat and Denis 2000, Yin et al. 2005, Fahmi and Suttan 2008), while urban density has increased over the last three decades due to the rapid change in spatial structure and in the form of the core and centers of GCM. Also, my field observations showed that many urban areas in the suburbs and in the south of GC are dominated by a high density of informal buildings (Fig. 126) and a high percentage of empty or nearly empty buildings. This emerged as a strong driver behind the changes in the built-up surface in those areas after 1999. Therefore, in general agreement with Ehlers (1989), Sutton and Fahmi (2001) and Yin et al. (2005) and based on the field observations, the determination of population density based on the analysis of urban density classified satellite images has a weak significance.

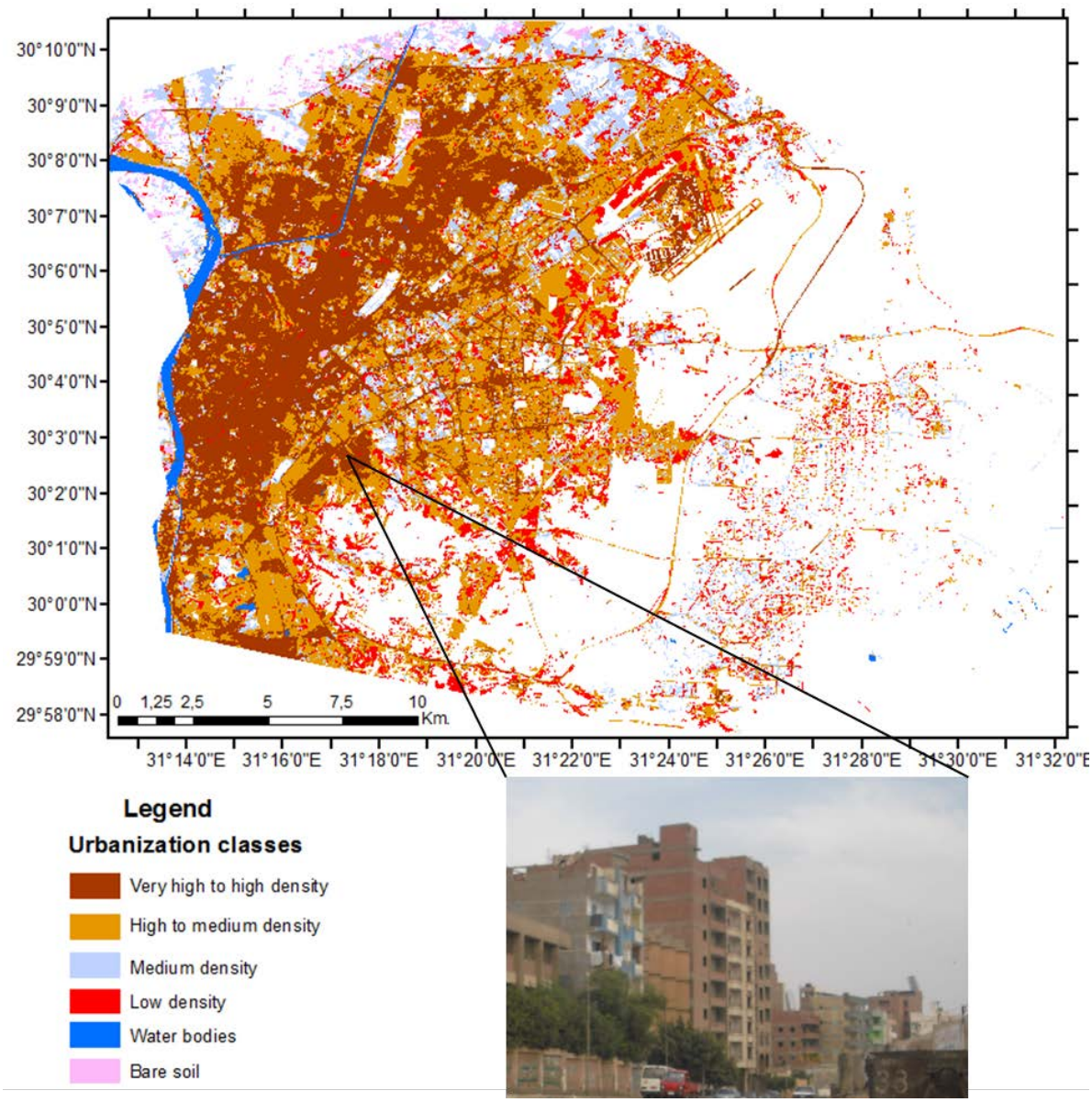


**Figure 126: High density vacant buildings (GCM east periphery). Photo captured 2010**

# 7 Conclusions and Recommendations

## 7.1 Conclusions

In this study, I have attempted to understand the spatial dynamic of a complex system such as a megacity by using advanced remote-sensing techniques and a modified conceptual model. Against this background, I simplified the sophisticated meaning of spatial resilience to grasp the city landscape changes. Land cover can therefore be considered a mirror for the different socio-economic-ecological processes interacting physically in land use and land change. Land use/land cover change (LULCC) is a process to identify the state of land over time, while spatial resilience is a broader concept concerning the interaction and interlink between the components of the complex system. All the affected and effected elements inside the LULCC process, as well as what is outside this process, should be identified and linked inside one conceptual framework. I therefore conceptualized the spatial dynamics of a megacity like Greater Cairo Metropolis (GCM) at different levels based on the information and the spatial landscape structure data available.

Generally, the understanding of the spatial resilience of urban systems consists of three phases:

- System components and spatial variants (indicators)
- Analysis of spatial growth
- Understanding the spatial vulnerability to change and transformation

Spatial monitoring and change detection of a megacity are not only to be based on classification and remote-sensing techniques, but also include societal aspects and therefore use an effective conceptual model, which is necessary to understand the social-environmental interactions and to identify the most important indicators on hot-spots or objects of change. The DPSIR (Driving Forces, Pressures, States, Impacts, and Responses) model of the OECD is useful to identify and detect the role of different components and indicators of megacities. Therefore, the monitoring framework used in this research is presented in Figures 23 and 32 (see Chapter 3).

The implementation of DPSIR model together with different satellite images and information led me to design a monitoring system which works at different levels and sub-levels. These levels are motivated by data availability, objective of research, stakeholder needs and advanced techniques. In conclusion, the application of the DPSIR-model to monitor the spatial growth and to understand the spatial resilience of megacities meets the majority of the reporting and analytical purposes in a simple way that could be oriented to serve the objective of analysis.

It can be concluded that the pixel-based classification applied to Landsat TM and ETM+ time-series images is useful for monitoring the dynamics of megacities and for obtaining initial results quickly, while the object-based classification deals more efficiently with work at different levels by using multi-algorithms and features on a group of pixels (objects). It provides the classification of specific objects such as urban environment including densities and patterns. Varying the parameter scales of object-based segmentation, which was applied to the high resolution images, is recommended with manual tools to refine the classification and increase the accuracy of classification. The time series classified images per-pixel show distinctive decreasing in overall classification accuracy, with increasing the spatial distribution of land use areas. But the classification of the same time span and study area by using per-object classification did not show such relation between overall accuracy and growing or shrinking of land use areas over time.

I also examined the integration of the object-based (OB) classification technique with the DPSIR conceptual scheme, and suggest a classification strategy in which classification at different levels and the creation of LULC subclasses play a major role. Consequently, the classification tree (rule set) will be strongly linked to the DPSIR model. The application of the proposed method can support the classification outcome of large and complex landscapes.

Conceptualizing the land use and land cover components helped not only to determine the dynamic change of GCM, but also to identify the driving forces and impacts to find out the priorities for responses. The analysis of GC change detection by using thematic mapper satellite data indicates that the most affected zones, in the last three decades were open corridors and closed “trapped quarters” around the metro area, ring road and the new cites. Stewart (1996) has stated that the Cairo ring road is designed to restrain Cairo’s urban sprawl. Upon completion, the ring road will span an extended zone of approximately 25 km. However, in this study, I found that the ring road is one of the most effective development elements, and it could be concluded that public transportation and access to the main road encourages people to raise buildings in the GCM periphery. Most of these buildings are of informal type and sprawled onto fertile land. In spite of the privatization policy that encouraged people to move from the center to the periphery and to the new towns, and which caused depopulation (Yin et al. (2005)) informal urban activity on the fertile land has increased due to the accessible infrastructure and transportation, and insufficient dwellings for poor and young people in new cities. Thus, the main driving forces are not only the increasing population, but also the way that land is used in the city.

Pressure on GCM land took two forms: on the horizontal axis, the legal and illegal use of fertile land, spaces in hinterland (desert), and in the periphery; and, on the vertical axis, the pressure of increasing urban density by replacing buildings such as in core or by using any free spaces in closed areas. This caused saturation of some areas (mostly slums).

The best way to understand the spatial state of large areas is to classify the land use/land cover at different levels. In this study, I applied two levels, the first to understand and extract the criteria of spatial change, and the second to analyze and identify the link between the classified indicators, and other spatial interaction elements. As a result, urbanization was divided into three main classes based on density (low, medium, and high), while cultivated land was identified on the basis of the form and spectral reflectance into the classes agriculture and sparse vegetation. There are fuzzy areas which comprise a mixture of buildings and vegetation. These areas could difficulty be separated at the first and second level of the monitoring framework unless I used the membership function provided by object-based classification software (eCognition).

On one hand, the informal and high density areas were restricted in their spatial extend (trapped) in the periphery zone of the east and west by the construction of new cities, land privatization, and military zones. For example; Ezebt El-Hagana, an informal area to the north of Cairo City and close to the airport, showed no effective change between 1999 and 2008, because the area is surrounded by a military sector to the north and east as well as by another piece of land sold to private companies and investors (source of information: field observations and questionnaire). On the other hand in the north and south of the periphery, the growth of informal houses and settlements is unlimited, especially in the areas close to the ring road (open corridors).

1 There are strong impacts of new Cairo cities on core and periphery. The new roads and the ring road which were established to serve the new Cairo cites caused urban sprawl at the periphery of old Cairo and the encroachment onto the area around the ring road in the north-northwest area.

2 The misuse of water to irrigate the private gardens in new cities causes water sewage into ground and leads to its accumulation mainly in the southern areas of new Cairo City.

3 The new cities have caused a diversity of urbanization which is recorded by the increasing of high density quarters and informal building activities at the city periphery.

4 The use of the hinterland to build houses mostly for the middle and upper classes, they are looking for better quality of life, led to difficulties to push the low income people out from

the old city, hazard and poverty areas to move outside to hinterland. So now they have to move to other places outside e.g. Oases (countryside).

5 The people living under high risk conditions could move to new buildings established by the government which are very close to the periphery. This is only a temporary solution, though, as people return to the old areas because they cannot afford to travel every day from the periphery to the center.

6 The area at the periphery of the east of Cairo City is overpopulated by workers who come from outside the city to work in the new Cairo City. Therefore, official statistical data on the population is not always correct because migrant and informal workers do not register in the city office (by changing the personal address in national personal identification), and do not identify themselves in the national census.

7 The growth of GCM's periphery zones to the east and west is restricted and trapped between the old city core and the new-remote sites around it.

The east and the west periphery zones of GCM are the most restricted and saturated urban areas and are slightly resilient, while the north and the south periphery zones (the open corridors and hot zones) could be considered as resilient. However, one of the negative impacts of the development process is, that it did not work for all the residents equally, which led to a sense of hopelessness and despair amongst people in this large urban agglomeration. Therefore response should differ in short term and long term and should be based on priorities. In this study, the open corridors and hot zones are in need of applicable policies and effective actions while the saturated and restricted areas are in need for management and strategy of depopulation.

Understanding the city state and the spatial features and structures before planning development projects, roads, and economic reform is necessary to sustain the system and social equality. In addition, the construction of new infrastructure such as roads should be planned to serve not investment and unsustainable development but the requirements of the people living in the whole city.

Finally, in this study I produced the geological map and rock cover scheme concerning the whole GCM that based on the application of remote sensing techniques. There are eleven rock types form the covering of the Greater Cairo metropolis outside the settlement area were analyzed, classified and displayed. They are mainly composed of carbonates and clastics with dispersed basaltic exposures. Some areas contain native structures and land forms which are categorized as protected

areas. While the field observations and false composite high resolution satellite images (SPOT) showed degradation of protected areas; e.g. the destroying of the land forms of El-Hassana Dom and the misuse of the Forest of petrified wood at Wadi Degla.

The statistical report of spectral signatures derived from PC merged TM images showed that the carbonate covers have higher digital number than clastics deposits (e.g. mean of band 1 addresses that more than 350 could be carbonate and between 350 and 320 could be clastics, while the basalt between 210 and 240 and wadi deposits reflect high values about 380). Therefore, the diverse nomenclature of the same rock units in GCM could be renamed to only systematic formations by using remote sensing techniques.

Generally, the western part of GC metropolis is dominated mainly by clastics and is characterized by low relief and less rough terrain, and the eastern part consists principally of carbonates and a rough terrain. Therefore, the western part can be more easily developed than the eastern part. The object-based classification technique would be used with customized algorithms to refine the produced map.

## 7.2 Recommendations and future research

The official governmental identification of slums and informal areas requires a strong knowledge base and a physical deprivation index (Khadr et al. 2009). Thus I recommend that the work would be continued to develop third and fourth level of monitoring framework, then I can contribute to the identification index of informal areas by using very high resolution data.

This study would give attention to the influences of spatial infrastructures on the land use and city growth for current and future projects in Egypt, such as the Suez Canal development projects or the projects in the southern Aswan-Nasser lake area.

The area between the ring road and the May axis road, west Greater Cairo (Giza), is the most affected line by land degradation and I predict that this area will be totally urbanized by 2050 unless the strategic plan to depopulate Greater Cairo takes place: One possible solution is that the government creates or encourages a large company and distributes the farmers across the fertile lands between the ring road and the 15th May axis.

There are three different recommendations will be described in next section for development strategy.

### 7.2.1 **Incubation**

Future development needs to incorporate strategies that are sensitive to changing environments. In this light, it is necessary to investigate the opportunities that exist within El Bahariya Oasis, which is a low-density area that could be a model for sustainable growth in the region. El Bahariya Oasis is located in the central part of the Western Egyptian Desert, and is linked to GCM by a highway of approximately 360 km. El Bahariya Oasis has been affected by different driving forces, such as farming, archaeological research, mining activity, handmade manufactured goods, and is recently a target region for renewable energy projects. Here, I introduce the idea of an 'incubation strategy' which could be implemented to attract parts of the population and to help to establish the nucleus of an eco-city. This would not only lead to an improved quality of life, but would also have positive effects on the global environment and climate.

**Incubation strategy (developmental catalyst)**

Incubation refers to the process by which certain oviparous animals hatch their eggs, and to the development of the embryo within the egg (http://incubator.apache.org/incubation/ Incubation_Policy.html). This term is often used in the economic term "business incubator", which is a new organizational form for promoting entrepreneurship and for stimulating new business formations (Allen 1985).

Incubation can be used by planners and sponsors of development aid to relieve the overpopulated delta cites in Egypt through encouraging skilled people and researchers to establish innovation systems and socio-environmental institutions, and to generate projects, particularly in renewable energy and ecosystem conservation, in oasis areas.

Recently, the Asian Development Bank (2011) warned that, "if migration is not carefully planned and assisted, there is a serious risk that it can turn into maladaptation, i.e. leaves people more vulnerable to environmental changes".

Thus, the environmental incubation strategy suggested here aims to provide a vision for oasis transformation that is sustainable, i.e. it promotes the equitable, ethical and efficient use of natural resources (Norberg and Cumming 2008), and to monitor and evaluate the growth and development of current and future projects for the study area. This means that an innovation unit or ecological technology research center would be set up to furnish the decision makers and stakeholders with up-to-date data and information for effective plans and policies. The skilled staff and their collaborators, such as employers, labourers, farmers, beside the Bedouins could initiate an

integrated society to attract segments of the population. As a result, opportunities for qualitative demographic change will emerge and there will be work for everyone.

### 7.2.2 **Stakeholder interaction**

After the revolution and during the period of transformation in MENA (Middle East and North Africa) countries, both people and investors are striving for reconstruction and sustainable growth in cities which suffered from corruption and conflict. Hence planners from different backgrounds want to deepen their understanding of stakeholder needs and create an environment for corporate social responsibility and sustainable growth in large urban areas like Greater Cairo. Recently, social internet networks (SINs) and non-governmental organizations (NGOs), as well as youth movements (YMs), have been referred to as an informal group and a vital force which was formed in the virtual world but is influencing real world concerns, for example human rights issues were examined during the Arab with an uprising tendency. Similarly, this study suggests that such informal groups could be reformed to establish an innovation structure and/or a new social channel, which would help modernization and secure transparency in a sustainable development. Consequently, this kind of channel (social group) could be composed of skilled young pioneers who can work alongside the professional staff, and can partially replace the traditional, corrupted networks and enable civil society to draw attention to the value of environmental conservation and of improving the quality of life. Currently, there are four opinion leaders and critical stakeholders in these urban environments: the government, investors, domestic administration, and popular society. So, we see that these new channel's characteristics allow using it to facilitate and observe the collaboration between business, civil society and government (domestic administration). Therefore, it would fill the gap between the needs of society needs and the reconstruction projects from the perspective of environmental awareness and sustainability.

### 7.2.3 **Data dissemination (Post-processing)**

Recently, development of research in geosciences and natural sciences, and their connection with humanities sciences is becoming a crucial issue for adaptation with the modern digital world. So, the importance of data management and the chance of sustainable information continuous to increase, and the innovative knowledge system and eco-service will be required to find out interconnected solutions for the environmental changes which have provided the global transformation. Furthermore, there is currently an increasing availability of large geo-spatial dataset

processed and saved in digital form. Most of these data are used to find solutions for the most common challenges which have been affected not only locally but also globally. Such challenges are climate change, rapid increase of urbanization, shortage of natural resources and their impacts on food security, water supply, quality of life,…etc. Moreover, the big cities dominate all the mentioned challenges. On the other hand, the modern technology of networking and intelligent systems is providing life to become easier since information has become highly accessible. Hence, the advanced techniques used to understand and analyze the global environmental degradation (processing stage) can be integrated with modern technologies to share, store, re-process, and find interconnection solutions based on the great availability of geo-spatial information. Therefore, knowledge data bases and data mining are taking concern in recent time (Phillips 2003). Such an approach can support data dissertation, visualization and publication (post-processing) after processing stage. Thereby, scientists are looking to store and link masses of huge digital data and make it accessible for different levels and kinds of stakeholders. The matter isn't just about putting geo-spatial data in the web. It is about making links, so that a machine can explore the web of data and a person can access, use, and react with it (Berners-Lee 2009). Such linked data can be used to solve challenges of dissemination of processed data and executable information (Kauppinen and Espindola 2011).

In this study there are some outputs of the processed data were displayed and visualized by using smart tool technology (e.g. portable screen). Such smart portable which a product of modern visualization technology is embedded into data-link base to build knowledge system that can be linked to the open digital data sources (e.g. open web map, regional government server .etc.) (Fig. 130). Therefore, the stakeholders can react with different types of spatial data and the scientists can support such knowledge system with updated information.

Concerning the post-processing phase of this study, the entire resulted map will be published for instance in one of the open source map webs and/or ArcGIS web-server (Fig. 131). Consequently, the stakeholders can react, add, and modify my results. That would be covering the gap between huge information and our digital modern world.

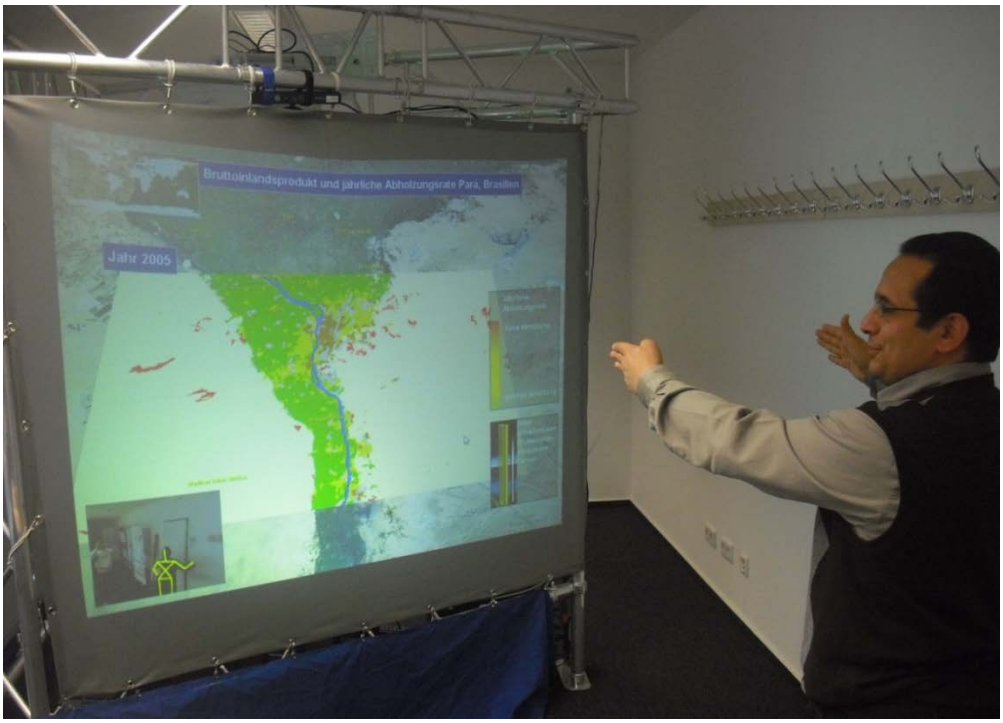


**Figure 127: Displaying processed data on the smart gesture screen (developed by Institute of Geoinformatic, Muenster University), (Video link: https://www.youtube.com/watch?v=x-iexAfE65k)**

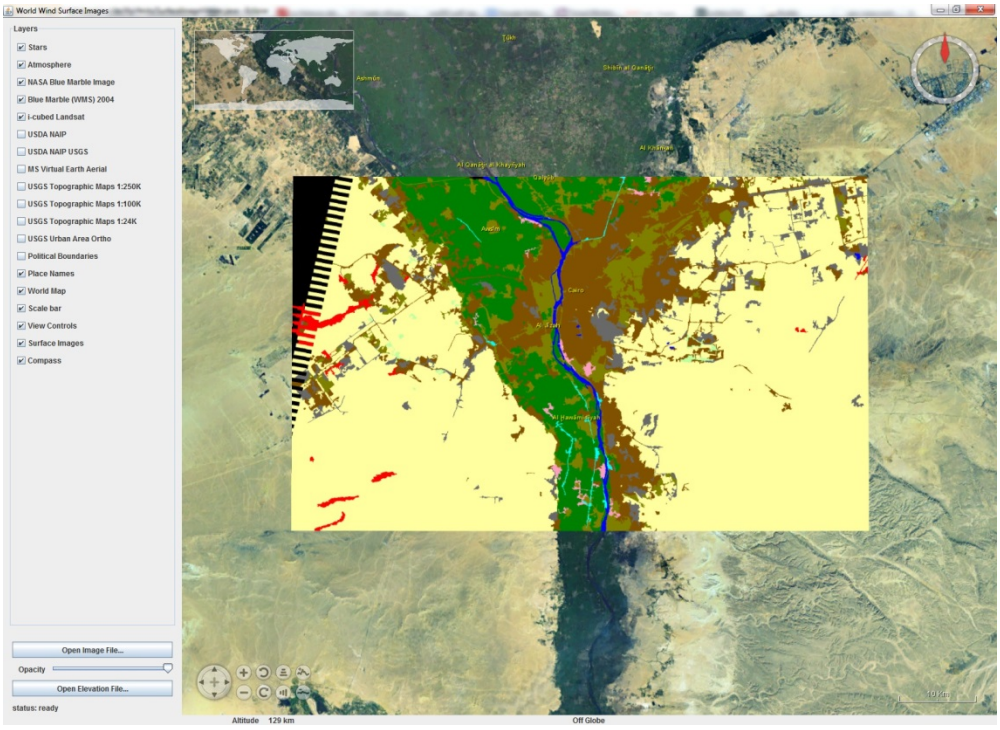


**Figure 128: Dissemination of one of resulted map of GCM on the world map, (after Institute of Geoinformatic, Muenster University)**

# 8 Summary

All over the world, megacities are growing so rapidly that it has become of paramount importance to establish an innovative response. Hence, this case study focuses on Greater Cairo Metropolis (GCM), which is the largest and one of the most densely populated cities in the world. GCM is more than just a very large city, though. Its scale creates new dynamics, a new complexity and a new simultaneity of events and processes in physical, social and economic dimensions. In this context, there is a growing demand to understand and analyze the spatial growth and resilience of GCM. This thesis therefore focuses on the main spatial developments and their mutual relationship with land use and land cover change (LULCC) in GCM. I used the spatial resilience concept, a conceptual framework, and remote sensing data (techniques). This concept could provide the GCM system with general principles (components, relations, and functions) to understand the spatial aspects of resilience at different levels of time and space.

This thesis is a monograph that consists of five chapters besides the chapters of introduction and conclusion.

**Chapter.2: Geo-cover and physiography**

Because land suitability and availability is one of the driving forces which could help to control the growth of cities, this chapter aims to present the geological and physiographic setting of the Greater Cairo Metropolis in the perspective of a digital city data and to reintroduce the Geo-map concern to the whole area. To achieve that, this study used the remote sensing technique to differentiate the rock cover types and describe the topographic relief of the area of Greater Cairo Metropolis. There are eleven rock types covering the Greater Cairo Metropolis, composed of carbonates and clastics with dispersed basaltic exposures. Although these coverings are not dominated by any valuable ores, some areas contain native structures and land forms. The western part of GCM is characterized by a low relief and less roughness topology, while the eastern part is principally built up of rough terrain. Therefore, the western part can be developed more easily than the eastern part.

**Chapter 3: Concept and Methodology**

In this chapter, a simple and flexible environmental conceptual model which distinguished driving forces, pressures, states, impacts, and responses (DPSIR) was used to conceptualize the main spatial

components affecting the growth of GCM. I identified the causal relation between the different indicators and drivers, and explored the sequence of change detection processes in the empirical framework to provide a deduction of main land influenced indicators in Greater Cairo Metropolis. Two different remote sensing classification techniques were applied to the fine to medium Landsat TM and ETM+, and medium to coarse SPOT imagery to detect the dynamic changes of GCM. There are pixel-based and more advanced object-based classifications. Use of the DPSIR with remote sensing data can provide an empirical monitoring system (spatial resilience framework) at different levels. These levels increased with increasing reflectance and spatial resolution, as well as ground information. Any level of monitoring can include sublevels which are oriented to provide a specific response for a specific indicator or component which provide the feedback (looping) mechanism inside the system. Using the data available, I examine two monitoring levels (Chapter 4 and Chapter 5).

**Chapter 4: Land use and land cover (LULC) state-impact**

To examine the first level, I am concerned with the monitoring and analysis of the LULC of the whole GCM area, which led me to define and analyze the state and impact of six main LULC classes (urbanization, cultivated land, surface water, desert (hinterland), cultivated-to-urban, and bare soil). I then investigated the fine-to-medium resolution time series of TM and ETM+ satellite images (1984, 1990 and 2006), and the utility of pixel-based versus object-based classifications. The time periods selected coincide with the driving force of economic reform from open trading to the privatization program during the last three decades. The results show that urbanization increased rapidly by taking two trajectories: the extensive construction of new cities in the hinterland (desert of GCM) and urban sprawl on the cultivated land. Also, the results pointed to some difficulties in separating some land units at this scale of spatial resolution (e.g. urban-cultivated class). However, the object-based and pixel-based classification techniques with fine data could be used to describe the state of large areas while the object-oriented classification can deal more efficiently with the dense urban environment and vegetation cover. Furthermore, the segmentation concept of the object-based technique could be integrated with the DPSIR to create a classification strategy compatible with the levels of monitoring (Chapter 5).

**Chapter 5: impact of development elements**

This chapter shows the second level in the change detection chain and the spatial impact of development (e.g. ring road, metro, and new cities) during the time of privatization. I look at three areas (metro-autostrad, core-new cities, and ring road-Giza), and use the medium to high resolution SPOT data for 1999 and 2008. The classification strategy derived from the DPSIR framework was performing stepwise extraction of the indicators into classes that are arranged in a rule set by using object based (OB) technique. There are many indices and algorithms applied to differentiate the classes and subclasses of the LUC (e.g. NDVI, LWM, GNDVI, NDMI, and RVI). As a result urban density is classified into low, medium and high to represent the urban patterns and to show the mechanism of growth. High density urbanization is mainly concentrated in the core areas and partially on the periphery; this increased and expanded in different directions. Medium and low densities dominate the newest urban areas, which could be forced through human needs, investment and development drivers. The green cover was divided into agriculture and sparse vegetation subclasses based on the uniformity and density of its spatial form. Most green cover classes in the three sectors experienced negative change with the exception of reclamation parks in the desert. Some artificial water bodies were recognized in the hinterland (new cities) in 2008 which had not been there before (1999). The water bodies and channels could be separated by using the LWM indices and fuzzy function membership. The objects of bare soil at that level of classification represented the brown land barren of vegetation with uncertainty of the nature of the soil (NDMI and GNDVI).

**Chapter 6: interpretation for response**

GCM showed three different urban densities covering five urban patterns verified by field work: core-old pattern, slums, urban sprawl over fertile land, new-cities, and villas and compounds. The slums and urban sprawl areas usually consist of informal high density buildings. On the other side, new-cities constructions were defined as formal buildings with medium and low densities, while the core buildings influenced by the increasing urbanization's activity and buildings replacement. The growth of some slums showed little change in their spatial boundary, which suggested that the growth of such slums could be restricted in the future and their spatial area restricted by their surroundings. The data on the period between 1999 and 2008 showed new open corridors and hot zones (affected zones) of loss of farmland of different sizes, dimensions and extensions. Most of these corridors have been affected by one or more of the development elements mentioned before.

Indeed, there are about fourteen hot spots or areas of risk mentioned in this study, which are in need of different responses based on their types, properties, and spatial features.

# 9 References

Abd Manap, M., Ram li, M.F., Sulaiman, W. and Surip, N. (2010): Application of Remote Sensing in the Identification of the Geological Terrain Features in Cameron Highlands, Malaysia (Aplikasi Penderiaan Jauh di dalam Pengcaman Fitur Terain Geologi di Cameron Highlands, Malaysia) Sains Malaysiana, Vol 39, No 1, pp. 1–11.

Abdelkhalek, M.L., El Sharkawi, M.A., Darwish, M., Hagras, M. and Sehim, A. (1989): Structural history of Abu Roash district, Western Desert, Egypt. Journal of African Earth science, Vol 9, No 3/4, pp. 435-443.

Abdelsalam, M.G. (1994): The Oko Shear Zone, Sudan: post-accretionary deformation in the Arabian-Nubian Shield Journal of the Geological Society, Vol 151, pp. 767-776.

Abu-Lughod, L.J. (1969): Testing the Theory of Social Area Analysis: The Ecology of Cairo, Egypt American Sociological Review, Vol 34, No 2 .pp. 198-212. Published by: American Sociological Association, Article Stable URL: Available at: http://www.jstor.org/stable/2092177 [Accessed March 2011].

Adger, W.N. (2006): Vulnerability. Global Environmental Change, Vol 16, pp. 268-281.

Aguilar A.G. (1987): Urban Planning in the 1980 in Mexico City. Habitat Intl: Vol 11, No 3, pp. 23-38.

Aguilar, A.G. and Ward, P.M. (2003): Globalization, regional development and megacity expansion in Latin America: Mexico City's peri-urban hinterland, Cities Vol 20, No 1, pp. 3-21.

Ahmed, L.A.A. and El-Khateeb, S. M. (2012): Change of Local Culture after the 25th Revolution and its Impact on Environmental Awareness. Procedia - Social and Behavioral Sciences, Vol 50, pp.997 – 1017.

Ahram English. (2011), Available at: http://english.ahram.org.eg/News/16923.aspx [Accessed May 2012].

Ali, E.M. (2003): Evaluation of the Egyptian experiment in establishment the new towns in the desert areas. Journal of engineering science, Assuit University, Vol 31, No 1, pp. 231-244.

Allen, D. (1985): Small business incubators and enterprise development. Report Prepared for the U.S. Department of Commerce, Washington, DC. (http://www.questia.com/library/journal/1G1-3835796/small-business-incubators-a-positive-environment) [Accessed Feb. 2013].

Altrock, U. and Schoon, S. (2011): The Governance of Urban Upgrading in Southern China, The Example of Urbanized Villages.In: disp: The Planning Review, Vol 187, No 4.

Amedi, J., Nagler, H. and Wessling, C. (2010): Essay (Die Bedeutung der Erneuerung der Altstadt für die Entwicklung von Großkairo). Handout (Internal Document), Cottbus University, Germany, pp. 1-22.

Anderies, J.M., Janssen, M.A. and Ostrom, E. (2004): A framework to analyse the robustness of social-ecological systems from an institutional perspective. Ecology and Society, Vol 9, No 1, Art 18, (http://www.ecologyandsociety.org/vol9/iss1/art18) [Accessed May 2010].

Anderson, J.R., Hardy, E.E., Roach, J.T. and Witmer, R.E. (1976): A Land Use and Land Cover Classification System for Use with Remote Sensor Data.Washington D. C., U.S. Geological Survey.

Anselin, L. (2001): Spatial Effects in Econometric Practice in Environmental and Resource Economics. American Journal of Agricultural Economics, Vol 83, No 3, pp. 705-710 (Published by: Oxford University Press on behalf of the Agricultural & Applied Economics Association, Article Stable URL. Available at http://www.jstor.org/stable/1245103 [Accessed March 2010].

Asian Develoment Bank (ADB) (2011): Annual Report. Online: http://www.adb.org/documents/adb-annual-report-2011[Accessed April 2012].

ASTER GDEM. (1999): http://www.ersdac.or.jp/GDEM/E/4.html. [Accessed October 2010].

Awad, A. and Zohry, A., (2005): The end of Egypt population growth in the 21th century: challenges and aspirations. The 35th annual conference on population and development issues, current situation and inspiration, pp.1-16.

Bayat, A and Denis, E. (2000): Who is afraid of Ashwaiyyat? Urban change and politics in Egypt. Environment and Urbanization, Vol 12, No 2, pp.185–199.

Belussi, A., Liguori, F., Marca, J., Migliorini, S., Negri, M., Pelagatti, G. and Visentini, P. (2011): Validation of geographical datasets against spatial constraints at conceptual level. International Archive Photogrammetry Remote Sensing. Spatial Inf. Sci., Vol 38, No 4/C21, pp. 89-94.

Berners-Lee, T. (2009): Design Issues (http://www.w3.org/DesignIssues/LinkedData.html) [Accessed February 2013].

Birth, G.S., and McVey, G.R. (1968): Measuring the colour of growing turf with a reflectance spectrophotometer. Agronomy Journal, Vol 60, pp 640-643.

Blumenfield, H. (1967): The Modern Metropolis: Its Origins, Growth, In Sprfiregen, P.D. (Ed), Characteristics and Planning, M.I.T. Press, Cambridge, Mass. 377, p.100s.

Budge, E.A.W. (1914): Short history of the Egyptian people. (London: J. M. Dent & sons limited; New York: E. P. Dutton & co.).

Budge, E.A.W. (1914): The literature of the ancient Egyptians. (London: J. M. Dent & sons limited; New York: E. P. Dutton & co.).

Burnett, C. and Blaschke, T. (2003): A multi-scale segmentation/object relationship modelling methodology for landscape analysis. Ecological Modeling, Vol 168, pp.233-249.

Cammarrota, M. and Pierantoni, I. (2007): Urban environmental indicators in the driving-presseure-state-impact-response (DPSIR) scheme, pp. 219-22. Available at http://old.sis-statistica.org/files/pdf/atti/CIMe0905p219-222.pdf [Accessed November 2010].

CAPMAS (Central Agency for Public Mobilization and Statistics), Population Census, Egypt 2006. Electronic document available at: http:www.msrintranet,capmas.gov.[Accessed May 2010].

CAPMAS: (Central Agency for Public Mobilization and Statistics), (1996) (2006) (2012): Egypt Available at: http://www.capmas.gov.eg. [Accessed January 2013].

Carr, E.R., Wingard, P.M., Yorty, S.C., Thompson, M.C., Jensen, N.K. and Roberson, J. (2007): Applying DPSIR to sustainable development. International Journal of Sustainable Development & World Ecology Vol 14, No 6, pp. 543-555.

Carroll, M., Townshend, J., DiMiceli, C., Noojipady, P., Sohlberg, R. (2009): A New Global Raster Water Mask at 250 Meter Resolution. International Journal of Digital Earth, Vol 2, No 4, pp. 291-308 (accessed online Nov. 2011: http://dx.doi.org/10.1080/17538940902951401).

Cassidy, L., Binford, M., Southworth, J. and Barnes, G. (2010): Social and ecological factors and land-use-land-cover diversity in two provinces in southeast Asia. Journal of Land Use Science, Vol 5, No 4, pp. 277-306.

Castelli V., Elvidge, C.D., Li, C.S. and Turek, J.J. (1999): Classification-based change detection Theory and applications to the NALC dataset. In Lunetta, R.S. and Elvidge, C.D. (eds). Remote Sensing change detection: Environmental monitoring methods and applications, London, UK: Taylor & Francis, pp. 53-73.

Chen, J., Wei, S., Chang, K. And Tsai, B. (2007): A comparative case study of cultivated land changes in Fujian and Taiwan. In: Land Use Policy, Vol 24, No 2, pp. 386–395. Available at: http://www.sciencedirect.com/science/article/pii/S0264837706000317 [Accessed October 2011].

Colding, J. (2007): Ecological Land-use Complementation for Building Resilience in Urban Ecosystems. Landscape and urban planning, Vol 81, pp. 46-55.

Cumming, G.S. (2011): Spatial Resilience in Social-Ecological Systems. 1st Edition. Springer Publishing, 243 p.

Cumming, G.S., Barnes, G., Perez, S., Schmink, M., Stieving, K. and Southworth, J. (2005): An exploratory framework for the empirical measurement of resilience. Ecosystems, Vol 8, pp 975-987.

Cumming, S.G. (2008): Spatial Resilience in Social-Ecological system. Springer Dordrecht Heidelberg London New York, Chapter 7 and 10.

Darbkin, D.H. (1978): Planned Land Use for Human Settlement development. Habitate Intl: Vol 3, No 1/2, pp. 89-95.

Deng, X., Liu, J., Zhuang, D.and Zhan, J. (2002): Internet based environmental monitoring information system and its application in Yili Prefecture [J]. Journal of Geographical Sciences, Vol 12, No 2, pp. 163-170.

Dick, E. and Kallert, S.E., (2011): Understanding the mega-urban from the rural: non-permanent migration and multi-locational households. The Planning Review, Vol 187, No 4, pp. 24 - 36.

DRTPC Study Experts, (2009): Urban Mobility in Greater Cairo; Trends and Prospects. Development research and Technological Planning Center (DRTPC), Cairo University; pp. 58-61.

Duh, J., Shandas, V., Chang, H. and George, L. (2008): Rates of urbanization and the resilience of air and water quality. Science of the Total Environment, Vol 400, No 1-3, pp.238-256.

EEA (2007): Available at: http://ia2dec.ew.eea.europa.eu/knowledge_base/Frameworks/doc101182/ [Accessed January 2010].

EEAA, Egyptian Environmental Affairs Agency report online; (http://www.eeaa.gov.eg/English/main/env_ozone_ecc_neg.asp) (accessed date: Nov. 2011).

Ehlers, E. (1989 ): old and new: land use conflicts in central Cairo. Bul. Soc. Geog. Egypt, Vol 74, pp. 17-35.

El Araby, M. (2002): Urban growth and environmental degradation, the case study of Cairo, Egypt. Cities (Elsevier Science press), Vol 19, No 6, pp. 389-400.

El-Arabi, N. (1999): problems of groundwater quality related to the urban environment in Greater Cairo. Impacts of Urban growth on Surface water and groundwater Quality (proceeding of IUGG 99 symposium HSS, Birmingham, July). IAHS Publ. No. 259, pp. 29-37.

El-Kadi, G. (1987): L´Urbanisation Spontaneé au Cairo. Tours, center dÉtudes et de Recherches Urbaama/Orstom: Fascicule de recherchers Nr. 18.

El-Metwally, M., Alfaro, S.C., Abdel Wahab, M.M., Zakey, A.S. and Chatenet, B. (2010): Seasonal and inter-annual variability of the aerosol content in Cairo (Egypt) as deduced from the comparison of MODIS aerosol retrievals with direct AERONET measurements. Atmospheric Research, Vol 97, No 1-2 , pp. 14-25.

Elshimy, H. (2011): Sustainable development criteria set for the transportation hubs of the national association of provinces planning. International Conference on Green Buildings and Sustainable Cities . Procedia Engineering, pp. 1024-1055.

EMA (Egyptian Metereological Authority), Available at: http://www.ema.gov.eg/productview?menu=73&lang=en [Accessed October 2010].

ERDAS. (2010): ERDAS field guide, 5th Edition, ERDAS Inc., Atlanta, Georgia, USA.

ESA (2010), Available at: http://esa.un.org/wpp/unpp/panel_population.htm [Accessed April 2012]

Evans, T., York, A. and Ostrom, E. (2008): Institutional Dynamics, Spatial Organization, and Landscape Change. In; Political Economies of Landscape Change: Places of Power, ed. Wescoat, J. and Johnston, D. (eds), pp.111–129. New York: Springer. Available at http://www.springerlink.com/content/n467528t18237383/fulltext.pdf [Accessed March 2011].

F.A.O (1976): A framework for land evaluation. Soils Bulletin, No32. F.A.O, Roma. Chapter 2: "Basic concepts" and pp. 70-80.

Fader, M., Gerten, D., Krause, M., Lucht, W. and Cramer W. (2013): Spatial decoupling of agricultural production and consumption: quantifying dependences of countries on food imports due to domestic land and water constraints. Environmental Remote Sensing, Lett. 8 014046, pp.1-15.

Fahmi, W. and Sutton, K. (2008): Greater Cairo's housing crisis: Contested spaces from inner city areas two new communities. Cities, Vol 25, pp 277-297.

Farag, I.A.M. and Ismail, M.M. (1956): Contribution to the stratigraphy of the Wadi Hof area (North-East of Helwan). Bull. Fac. Sci., Cairo, Uni., Vol 34, pp. 147-168.

Fekade, W. (2000): Deficits of formal urban land management and informal responses under rapid urban growth, an international perspective. Habitat International, Vol 24, No 2, pp 127–150.

Fernandes, K. (1998): Environmental strategies for sustainable development in urban areas: lessons from Africa and Latin America. Book review, Habitat International, Vol 24 , pp. 535-538.

Fitzpatric-lins (1987): Producing Alaska Interim Land Cover Maps from Landsat Digital and Ancillary Data, in Proceedings of the 11th Annual William T. Pecora Memorial Symposium: Satellite Land Remote Sensing: current programs and a look into the future American Society of Photogrammetry and Remote Sensing, pp. 339 – 347.

Flanders, D.M., Hall-Beyer, M. and Pereverzoff, J. (2003): Preliminary evaluation of eCognition Object-Based Software for Cut, Block, Delineation and Feature Extraction. Canadian Journal of Remote Sensing, Vol 29, pp. 441–452.

Foody, G.M. (2002): Status of land covers classification accuracy assessment. Remote Sensing of Environment, Vol 80, pp.185-201.

Forman, R.T.T. and Godron, M. (1986): Landscape ecology. New York: John Wiley & Sons.

Fouad, M. (1980): Planning for development in Egypt. Habitat Intl. Vol 7, No ¾, pp. 185-197.

Franklin, S.E. and Wulder, M.A. (2002): Remote sensing methods in medium spatial resolution satellite data land cover classification of large areas. Progress in Physical Geography, Vol 26, No 2, pp. 173–205.

Franklin, S.E., Lavigne, M.B., McCaffrey, T.M. and Wulder, M.A. (2002): Large-area forest structure change detection: An example. Canadian journal of Remote- Sensing, Vol 28, No 4, pp. 588–592.

Friedmann, J. (1986): The world city hypothesis development. (SAGE, London, Beverly Hills and New Delhi), Vol 17, No 1, pp. 69-83.

Gad, S.and Kusky, T. (2007): ASTER spectral ratioing for lithological mapping in the Arabian-Nubian shield, the Neoproterozoic Wadi Kid area, Sinai, Egypt; Gondwana research, Vol 11, No 3, pp.326-335.

GDSC. (2012): http://gdsc.nlr.nl/gdsc/en/information/earth_observation/band_combinations, [Accessed August 2013].

Gitelson, A., Kaufman, Y.J., and Merzlyak, M.N. (1996): Use of a green channel in remote sensing of global vegetation from EOS-MODIS. Remote Sensing of Environmenta, Vol 58, pp. 289-298.

GIZ (Deutsche Gesellschaft für Internationale Zusammenarbeit GmbH) (2010), Kairo Project, Available at: http://egypt-urban.net/about-pdp) [Accessed January 2012].

GOPP/IAURIF (General Organization for Physical Planning). (1990): Activity relocation policy (in Arabic). Ministry of Development, New Communities, Housing, and Public Utilities.

GOPP/IAURIF(General Organization for Physical Planning). (1991): Greater Cairo Region Master Scheme. Implementation Assessment. Updating Proposals. Ministry of Development, New Communities, Housing and Public Utilities, pp. 57-60.

Griffiths, P., Hostert, P., Gruebner, O. and Linden, S.V. (2010): Mapping megacity growth with multi-sensor data. Remote Sensing of Environment, Vol 114, No 2, pp. 426-439.

GTZ (Deutsche Gesellschaft für Technische Zusammenarbeit) Report. (2010): Improving informal areas in Greater Cairo: The cases of Ezzbet Al Nasr & DayeEl Nahia, pp. 75-80.

GTZ (Deutsche Gesellschaft für Technische Zusammenarbeit) Report. (2010): Cairo's informal areas between urban challenges and hidden potentials – facts, voices, visions, About Cairo and its Informal Areas, pp.1-45.

Gunderson, L. and Pritchard J, L. (Eds.), (2002): Resilience and the behaviour of large-scale systems. Island Press, Washington, D.C., USA. 240 p.

Gupta, R.P. (2003): Remote Sensing Geology, second edition, Springer, 655 p.

Hackenbroch, K. (2011): Urban Informality and Negotiated Space. Negotiations of Access to Public Space in Dhaka, Bangladesh.In: disp: The Planning Review, Vol 187, No 4.

Haines-Young, R.H. (2007): Tracking Change in the Character of the English Land-scape, 1999–2003. Natural England, Catalogue Number NE42. Available at: http://www.catpaisatge.net/fitxers/Tria%2014%20-%20CQC_Report.pdf [Accessed February 2011].

Haque, SK.M. and Bandyopadhyay, S. (2012): Identification of metropolitan core using geo-spatial data for Kolkata, India. Scientafic annals of "Alexanderu Ioan Cuta" University of IASI, Geography series, Vol 58, No 2-c, pp. 185-206.

Hardoy, J. and Satterthwaited, D. (1984): Third World Cities and the Environment of Poverty. Geoforum, Vol 15, No 3, pp. 307-333.

Herold, M., Gardner, M., Hadley, B. and Roberts, D. (2002): The spectral dimension in urban land cover mapping from high resolution optical remote sensing data. In, Proceedings of the 3rd symposium on remote sensing of urban areas. Istanbul, Turkey.

Herold, M., Roberts, D. A., Gardner, M. E. and Dennison, P. E. (2004): Spectrometry for urban area remote sensing, Development and analysis of a spectral library from350 to 2400 nm. Remote Sensing of Environment, Vol 91, pp.304−319.

Hofmann P., Strobl, J., Blaschke, T. and Kux, H. (2008): Detecting informal settlements from quickbird data in Rio de Janeiro using an object based approach, Springer Berlin Heidelberg, pp.531-553 Available at: http://link.springer.com/chapter/10.1007%2F978-3-540-77058-9_29#page-2 [Accessed October 2011].

Holling, J.H. (1995): How adaptation builds complexity, New York: Perseus Books p. 185.

Holling, J.H. (2001). Understanding the complexity of economic, ecological, and social systems. Ecosystems, Vol 4, pp. 390-405.

Houpin, S. (2010): Urban mobility and sustainable development in the Mediterranean Regional diagnostic outlook. United Nations Environment Programme Mediterranean Action Plan, report, pp. 16-18.

Huang, C., Davis, L. S. and Townshend, J. R. G. (2002): An assessment of support vectormachines for land cover classification. International Journal of Remote Sensing, Vol 23, pp.725−749.

Hunga, T., Uchihama, D., Ochi, S. and Yasuoka, Y. (2006): Assessment with satellite data of the urban heat island effects in Asian mega cities. International Journal of Applied Earth Observation and Geoinformation, Vol 8, pp. 34–48.

Hunt, G.R. (1977): Spectral signatures of particular minerals in the visible and near infrared, Geophysics, Vol 42, pp. 501-513.

Ibrahim, A. and El-Hefnawi, K., (2005): Protecting agricultural landform urbanization or managing the conflict between informal urban growth while meeting the demands of the communities

Lessons learnt from Egyptian policy reforms". Third Urban Research Symposium on "Land Development Urban Policy and Poverty Reduction, The World Bank Institute of Applied Economic Research -IPEABrasilia,Brazil, April 4-6.

Ibrahim, A. and Johari, M. (1997): The Correlation of the Landsat TM Images Characteristic with the Geologic Information : A Preliminary Result of a Case Study in Langkawi Islands, Malaysia, ACRS. Available at: http://www.gisdevelopment.net/aars/acrs/1997/ts10/ts10005pf.htm [Accessed August 2010].

IDRC report. (1996): Egypt economy Profile, Economic Research Forum for Arab countries, Iran and Turkey. pp. 01-07, Available at: http://www.idrc.ca/EN/AboutUs/Accountability/Pages/AnnualReport.aspx [Accessed October 2011].

Ingram, ST., Gerg, E. and Khaled, H. (2003): Application of remote sensing for mapping surface geology in heavily vegetated cover in North Mississippi, Journal of the Mississippi Academy of Sciences, Abstract.

Islam, M. and Braden, J.B. (2006): Bio-economic development of floodplains: Farming versusfishing in Bangladesh. Environment and Development Economics, Vol 11, pp. 95−126.

Islam, N. (1999): Urbanisation, migration and development in Bangladesh: Recent trends and emerging issues. CPD-UNFPA Publication Series, 26.

Islam, N. (2005): Dhaka now — Contemporary urban development. Dhaka: Bangladesh Geographical Society (BGS).

Janz, A., Linden, S.V.D., Waske, B. and Hostert, P. (2007): image SVM — A user oriented tool for advanced classification of hyperspectral data using support vector machines. In, 5th EARSeL workshop on imaging spectroscopy (p. 5). Bruges, Belgium.

JAXA. (2003): (http://www.eorc.jaxa.jp/en/hatoyama/experience/rm_kiso/mecha_howto_e.html) [Accessed August 2013].

Jenerette, G. and Potere, D. (2010): Global and simulation of land-use change associated with urbanization. Landscape Eco, Vol 25, pp.657-670.

Jensen, J.R. (1996): Introductory Digital Image Processing: a Remote Sensing Perspective, (2nd Edition), Prentice-Hall, Upper Saddle River, NJ, 318 p.

Jensen, J.R. and Cowen, D.C. (1999): Remote sensing of urban suburban infrastructure and socio-economic attributes. Photogrammetric Engineering and Remote Sensing, Vol 65, pp.611−622.

Jensen, J.R., Rutchey, K., Koch, M.S.and Narumalani, S. (1995): Inland wetland change detection in the everglades water conservation area 2A using a time series of normalized remotely sensed data. Photogrammetric Engineering and Remote Sensing 61 (2), pp. 199-209.

Johnson, L.F. (2001): Nitrogen influence on fresh-leaf NIR spectra. Remote Sensing of Environment, Vol 78, No 3, pp. 314–320.

Julien, Y., Sobrino, J.A., and Jiménez-Muñoz, J. C. (2011): Land use classification from multitemporal Landsat imagery using the Yearly Land Cover Dynamics (YLCD) method, International Journal of Applied Earth Observations and Geoinformation, Vol 13, No 5, pp. 711-720.

Kauppinen, T., and Espindola, G. M. (2011): Linked Open Science—Communicating, Sharing and Evaluating Data, Methods and Results for Executable Papers. International Conference on Computational Science, ICCS, pp. 1-6.

Kay, J. and Boyle, M. (2008): Self-organizing, holarchi, open systems (SOHOs). The ecosystem approach: complexity, uncertainty, and managing for sustainability, New York: Columbia University Press, 383 p.

Khadr, Z., Nour el Dein, M. and Hamed, R. (2010): Using GIS in constructing area-based physical deprivation indexin Cairo Governorate, Egypt. Habitat International, Vol 34, pp. 264-272.

Khalifa, M.A. (2011): Redefining slums in Egypt: Unplanned versus unsafe areas. Habitat International, Vol 35, No 1, pp.40-49.

Knorn, J., Rabe, A., Radeloff, V.C., Kuemmerle, T., Kozak, J. and Hostert, P. (2009): Land cover mapping of large areas using chain classification of neighboring Landsat satellite images. Remote Sensing of Environment, Vol 113, pp.957−964.

Kohavi, R. and John, G.H. (1997): Wrappers for feature subset selection. Artificial Intelligence, Vol 97, pp.273−324.

Kozova, M. and Finka, M. (2010): landscape development planning and management systems in selected European countries. The problems of Landscape ecology, Vol 28, pp. 101-110.

Kraas, F. (2007): Megacities and global change in East, Southeast and South Asia. Asien, Vol 103, pp.9−22.

Kraas, F. (2007): Megacities and global change: Key priorities. Geographical Journal, Vol 173, pp.79−82.

Kristensen P., (2004): The DPSIR Framework. Workshop on a comprehensive / detailed assessment of the vulnerability of water resources to environmental change in Africa using river basin approach. UNEP Headquarters, Nairobi, Kenya .

Kushwaha, S.P.S., Dwivedi, R.S. and Rao, B.R.M. (2000): Evaluation of various digital image processing techniques for detection of coastal wetlands using ERS-1 SAR data. International Journal of Remote Sensing, Vol 21, pp.565−579.

Kwarteng, A.Y. and Small, C. (2010): Remote sensing of urban environmental conditions. Rashed, T. and Juergens, C. (eds), Remote sensing of urban and suburban areas, Remote sensing and digital image processing, Vol 10. Netherlands: Springer Dordrecht, pp. 267-287.

Lang, T. (2012): How do cities and regions adapt to socio-economic crisis? Towards an institutionalist approach to urban and resilience. Raumforsch Raumordn, Vol 70, pp.285-291.

Latocha A. (2010): Saptial planning in mountain regions-present trends, threats and opportunities (Sudety Mountain case study). The problems of Landscape ecology, Vol 28, pp. 55-64.

Lee, J.S., Grunes, M.R. and Pottier, E. (2000): Quantitative comparison of classificationcapability: Fully polarimetric versus dual and single-polarization SAR. Internationalgeoscience and

remote sensing symposium (IGARSS 00), Jul 24–28, Honolulu, Hawaii (pp. 2343–2351). In English.

Li, L., Z,hang P. and Hou, W. (2005): Land use/cover change and driving forces in southern liaoning province since 1950s. chinese geographical science. Science Press, Beijing, China, Vol 15, No 2, pp. 131-136.

Li, T., shilling, F., Thorne, J., Li, F., Schott, H., Boynton, R. and Berry, A.M. (2010): Fragmentation of Chin's landscape by roads and urban areas. Lnadscape ecol, Vol 25, pp. 839-853.

Li, X. (1995): Global environment key field--land use and land cover change's international research tendency. Geographic Sinica, Vol 51, No 6, pp. 553-558.

Lillesand, T.M. and Kiefer, R.W. (1994): Remote sensing and image interpretation, John Wiley & Sons, Inc., New York, 18 p.

Lillesand, T.M., Kiefer, R.W. and Chipman, J.W. (2003): Remote sensing and image interpretation (5th ed.). Wiley publication. ISBN 0-471-15227-7, (Introduction).

Lintz, G., Wirth, P. and Harfst, J. (2012): Regional structure change and resilience. Raumforsch Raumordn, Vol 70, pp 363-375.

Liu, D. S., Song, K., Townshend, J.R.G. and Gong, P. (2008): Using local transition probability models in Markov random fields for forest change detection. Remote Sensing of Environment, Vol 112, pp.2222−2231.

Liu, D.S., Kelly, M. and Gong, P. (2006): A spatial-temporal approach to monitoring forest disease spread using multi-temporal high spatial resolution imagery. Remote Sensing of Environment, Vol 101, pp.167−180.

Lu, D. and Weng, Q. (2007): A survey of image classification methods and techniques for improving classification performance. International Journal of Remote Sensing. Vol 28, No 5, pp. 823–870.

Lunetta, R.S. and Elvidge, C.D. (1998): Remote Sensing Change Detection: Environmental Monitoring Methods and Applications, Ann Arbor Press, Chelsea, MI, 318 p.

Macleod, R.D. and Congalton, R.G. (1998): A quantitative comparison of change detection algorithms for monitoring Eelgrass from remotely sensed data. Photogrammetric Engineering and Remote Sensing, Vol 64, No 3, pp. 207-21.

Mahmoud, A.H.A. and El-Sayed, M.A. (2011): Development of Sustainable Urban Green Areas in Egyptian New Cities: the Case of El-Sadat City, Landscape Urban Plan, Vol 101, No 2, pp. 99-204.

Maktav, D., Erbek, F.S. and Jurgens, C. (2005): Remote sensing of urban areas. International journal of remote sensing, Vol 26, No 4, pp. 655−659.

Maruster, L., Faber, N.R. and Peters, K. (2008): Sustainable Information Systems: a knowledge perspective, Journal of Systems and Information Technology, Vol 10, No 3, pp.218-231, Emerald Publishing.

Matelas, L. and Prastacos, P. (2011): Sustainable urban growth for Athens. Uraban and Regional Data Management-Zlatanova, Ledoux, Fendel, and Rumor, (eds) UDMS annual, pp.193-200.

Matikainen, L., Hyyppä, J. and Engdahl, E. (2006): Mapping Built-up Areas from Multitemporal Interferometric SAR Images. A Segment-based Approach. ASPRS: (American society for photogrammetic engeineering and remote sensing), Vol 72, No 6, 701 p.

Matinfar, H.R., Sarmadian, F., Alavi Panah, S.K. and Heck, R.J. (2007): Comparisons of object-oriented and pixel-based classification of land use/land cover types based on lansadsat7, etm+ spectral bands (Case Study: Arid Region of Iran)", American-Eurasian J. Agric. & Environ. Sci., Vol 2, No 4, pp. 448-456.

Maxwell, S.K., Schmidt, G.L. and Storey, J. C. (2007): A multi-Scale segmentation approach to filling gaps in Landsat ETM+ SLC-off images. International Journal of Remote Sensing, Vol 28, pp.5339−5356.

McGranahan, G. and Satterthwaite, D. (2003): Urban centers: An assessment of sustainability. Annual Review of Environment and Resources, Vol 28, pp.243−274.

Megacities Meeting. (2010): Shaping of a sustainable future world. Future Megacities program, Essen City, Germany, pp. 3-69.

Megacity Project. (1998): Publication MCP-018D, pp. 9-27.

Meier, R.L. and Quium, A. (1991): Planning and Designing New Urban settlement on Estuaries: Bangladesh. Landscape and Urban Planning, Vol 21, pp.211−226.

Melgani, F. and Bruzzone, L. (2004): Classification of hyperspectral remote sensing images with support vector machines. IEEE Transactions on Geoscience and Remote Sensing, Vol 42, pp.1778−1790.

Mesev, V. (1998): The use of census data in urban image classification. Photogrammetric engineering and remote sensing, Vol 64, No 5, pp.431–438.

Metro information from Egypt national railway. (2005): Available at: http://www.egyptrail.gov.eg/docs/metro/metro.html [Accessed January 2011].

Metropolis. (2009): Metropolitan Regions: A network of major metropolises. Working Paper, Second Edition. pp.110-113, Available at: (www.metropolis.org) [Accessed January 2011]

Meyer, G. (1989): Bevölkerungsentwicklung und Wohnraumversorgung in der metropolitanen Agglomeration von Kairo. Mitteilungen-Österreichischen-Geographischen-Gesellschaft, Vol 131, pp. 145–170.

Michelson, D.B., Liljeberg, B.M. and Pilesjo, P. (2000): Comparison of algorithms for classifying Swedish landcover using Landsat TM and ERS-1 SAR data. RemoteS ensing of Environment, Vol 71, pp.1−15.

Mid East Web. (2007): Available at: (http://www.mideastweb.org/egypthistory.htm [Accessed October 2011].

Miller, R.B. and Small, C. (2003): Cities from space: Potential applications of remote sensing in urban environmental research and policy. Environmental Science & Policy, Vol 6, No 2, pp. 129−137.

Mourão, I., Caeiro S., Costa, M., Ramos, T. and Painho, M. (2004): Application of the DPSIR model to the Sado Estuary, In Toppen, F. and Prastacos, P. (Eds.)a GIS context – Social and Economical Pressures, Proceedings of 7th Conference on Geographic Information Science, Crete University Press. AGILE, Crete, Greece, pp. 391 – 402.

Moustafa, A.R. (1988): Wernch tectonics in the north western desert of Egypt (Abu Roash area, West of Greater Cairo). Earth Sc. Ser, Vol 2, pp 1-16.

Moustafa, A.R., El-Nahhas, F. and Abdeltawab, S. (1991): Engineering geology of Mokattam city and vicinity, eastern Greater Cairo, Egypt. Eng.Geol., Vol 31, pp. 327-344.

Moustafa, A.R., Saoudi, A., Moubasher, A., Ibrahim, I.M., Molokhia, H. and Schwartz, B. (2003): Structural setting and tectonic evolution of the Bahariya Depression, Western Desert, Egypt: Geo-Arabia, Bahrain, Vol 8, No 1, pp. 91-124.

Nalbant, S.S. and Alptekln, ö. (2010): The use of Landsat Thematic Mapper imagery for analysing lithology and structure of Korucu-Du la area in western Turkey, International Journal of Remote Sensing Publication details, including instructions for authors and subscription information: Available at: http://www.informaworld.com/smpp/title~content=t713722504).

NASA. (2008): Landsat data continuing mission, Available at: http://ldcm. nasa.gov/index.htm [Accessed January 2009].

Neill, B.C. (2000): Cairo and climate change: a win-win opportunity. Global Environmental Change, Vol 10, pp. 93-96.

Netzband, M., Stefanov, W.L. and Redman, C.L. (2007): Applied Remote Sensing for Urban Planning, Governance and Sustainability, Springer Verlag Heidelberg.

Norberg, J. and Cumming, G.S. (Eds.). (2008): Complexity Theory for Sustainable Future. New York: Columbia University Press.

Norton, P. (1967): Rock stratigraphic nomenclature of the Western Desert, Pan American U.A.R Oil Co., Internal Report, p 18.

Nystrom, M. and Folke, C. (2001): Spatial Resilience of Coral Reefs. Ecosystem, Vol 4, No 5, pp. 406-417.

OCDE. (1993): Corps central d'indicateurs de l'OCDE pour l'examen des performances environmentales, in: Rapport de synthèse du Group sur l'état de l'Environement, Paris.

Olbadwala, P. And Goldsmith, W. (1992): The sustainability of privilege: reflections on the Environment, the Third World city, and Poverty. World development, Vol 20, No 4, pp 627-640.

Osman, A. (2010): Geotechnical and Structural studies on some new cities around Cairo. Cairo University, Faculty of Science, Geology Department, pp.411-420.

Ostrom, E. (1990): A general framework for analyzing sustainability of social-ecological systems. Science, Vol 325, No 5939, pp. 419-422.

Pacifici, F., Del Frate, F., Emery, W.J., Gamba, P. and Chanussot, J. (2008): Urban mapping using coarse SAR and optical data: Outcome of the 2007 GRSS data fusion contest. IEEE Geoscience and Remote Sensing Letters, Vol 5, pp.331−335.

Pal, M. and Mather, P.M. (2005): Support vector machines for classification in remote sensing. International Journal of Remote Sensing, Vol 26, pp.1007−1011.

Park, N.W. and Chi, K.H. (2008): Integration of multitemporal/polarization C-band SAR data sets for land-cover classification. International Journal of Remote Sensing, Vol 29, pp.4667−4688.

Participatory Development Programme (PDP) of the GIZ and several Egyptian partners in Cairo from 14th to 15th October 2008.

PCSU (Privatization Coordination Support Unit) (2002): The Results and Impacts of Egypt's Privatization Program. Special Study Provided to the United States Agency for International Development by CARANA Corporation under the USAID Coordinating and Monitoring Services.

PDP (Participatory Development Programme in Urban Areas). (2010): Cairo's informal areas between urban challenges and hidden potentials - facts. voices. visions. Report, pp. 13-215. (In corporation with GIZ).

Perlman, J.E. and Blueweiss, L.R. (1990): Urban innovation for the 21st Century. A Dual Strategy for Deliberate Social Change in Cities, Cities Vol 7, No 1, pp.3-16.

Peterson, G.D. (2002): Estimating resilience across landscapes. Conservation ecology, Vol 6, pp 17-18.

Phillips, R., (2003): Application of the Technology and Innovation Concept in the Developing World: Dimensions and Considerations. In Knowledge Technology & Policy, Vol 15, No. 4, pp. 46-60.

Phinn, S., Stanford, M., Scarth, P., Murray, A.T. and Shyy, P.T. (2002): Monitoring the Composition of Urban Environments Based on The Vegetation–Impervious Surface–Soil (VIS) model by subpixel analysis techniques. International Journal of Remote Sensing, Vol 23, No 22, pp. 4131−4153.

Pickett, S.T.A., Jones, C. and Kolasa, J. (2007): Ecological understanding: the nature of theory and the theory of nature. New York: academic Press.

Piffero, E. (2009): PhD Thesis. "What Happened to Participation? Urban Development and Authoritarian Upgrading in Cairo's Informal Neighbourhoods" published by Elena Piffero, pp.178-188.

Planet Earth. (2005): Megacities -our global urban future, Earth Sciences for Society Foundation, Leiden, The Netherlands, pp. A3-A14, Available at: (www.yearofplanetearth.org) [Accessed January 2010].

Portnov, B.A. and Pearlmutter, D. (1999): Sustainable urban growth in peripheral areas. Progress in Planning, Vol 52, No 4, pp. 239-308.

Potschin, M. (2009): Land Use and The State of Natural Environment. Land Use Policy, Vol 26, No 1, pp. 170-177.

Prenzel, B. (2004): Remote Sensing Based Quantification of Land-Cover and Land-Use Change for Planning. Progress in Planning, Vol 61, pp.281-299 (283).

Procedia - Social and Behavioral Sciences. (2012): Vol 50, pp. 997–1017.

Puissant, A., Hirsch, J. and Weber, C. (2005): The utility of texture analysis to improve per-pixel classifications for high to very high spatial resolution imagery. International journal of remote sensing, Vol 26, No 4, pp. 733-745.

Quenzel, H. (1983): Principles of Remote Sensing Techniques. In: Camagni, P., Sandroni, S. (Eds.), Optical Remote Sensing of Air Pollution (Lectures of a course held at the Joint Research Center, Ispara, Italy). Elsevier Science, Amsterdam, pp. 27–43.

Rahman, T. (2011): The Emergence of Informal Governance in Neighbourhood. Upgrading in Dkaka, Bangladesh.In: disp: The Planning Review, Vol 187, No 4.

Rashed, T., Weeks, J.R., Gadalla, M.S. and Hill, A.G. (2001): Revealing the Anatomy of cities through spectral mixture analysis of multispectral satellite imagery: A case study of the Greater Cairo Region, Egypt: Geocarto Internationa,l Vol 16, No 4, pp. 5–15.

Rashid, M. (2002): Housing at Uttara Model Town in Dhaka City — An analysis and exploring ways to tackle the housing problem of middle class. Housing Development & Management: Lund Technical University.

Rashid, S.F. (2000): The urban poor in Dhaka City: Their struggles and coping strategies during the floods of 1998. Disasters, Vol 24, pp.240−253.

Reddy, M.A. (2001): Textbook of Remote Sensing and Geographical Information Systems.BSP BS Publication, Hyderabad, India.

Reimann, K.-U. (1993): Geology of Bangladesh. Berlin-Stuttgart: Gebrüder Borntraeger In German.

Resilience Alliance. (2002): http://www.resalliance.org/index.php/key_concepts [Accessed August 2010].

Richards J.A. (1999): Remote Sensing Digital Image Analysis, An introduction, Springer-Verlag, Berlin, 240 p.

Richards, J.A. (2005): Analysis of Remotely Sensed Data: The formative decades and the future. IEEE Transactions on Geoscience and Remote Sensing, Vol 43, pp.422−432.

Ridd, M.K. (1995): Exploring a V-I-S (Vegetation-Impervious Surface-Soil) Model for Urban Ecosystem Analysis through Remote Sensing: Comparative Anatomy of Cities. International Journal of Remote Sensing, Vol 16, No 12, pp.2165-2185.

Robertson, L.D. and King, J.D. (2011): Comparison of pixel- and object-based classification in land cover change mapping. International Journal of Remote Sensing Vol 32, No 6, pp. 1505–1529.

Rogan, J. and Chen D.M. (2004): Remote sensing technology for mapping and monitoring land-cover and land-use change. Progress in planning, Vol 61, No 4, pp. 301-325.

Rouse, J.W., Haas, R.H., Schell, J.A. and Deering, D.W. (1973): Monitoring vegetation systems in the Great Plains with ERTS. In3rd ERTS Symposium, NASA SP-351 I, pp. 309–317.

Rouse, J.W., Haas, R.H., Schell, J.A., Deering, D.W. and Harlan, J.C. (1974): Monitoring the Vernal Advancements and Retrogradation (Greenwave Effect) of Nature Vegetation, NASA/GSFC Final Report. NASA, Greenbelt. MD, USA.

Sabry, S. (2009): 'Egypt's Informal Areas: Inaccurate and Contradictory Data', In Kipper, R. and Fischer, M. (Eds.) Cairo's Informal Areas: Between Urban Challenges and Hidden Potentials, Facts.Voices. Visions, Cairo: GTZ Egypt, pp.29-33.

Said, R. (1962): The Geology of Egypt, Elsevier Pub. Co., Amsterdam, p.377.

Schmidt, T. (2012): Vulnerability through resilience? An example of counterproductive effect of spatially related governance in Hamburg-Wilhelmsburg. IN: Raumforsch and Raumordlung, Vol 70, No 4, pp 319-220.

Scrieciu, S.S. (2007): Can economic causes of tropical deforestation be identified at a global level? In: Ecological Economics, Vol. 62, No 3–4, pp. 603–612. Available at: http://www.sciencedirect.com/science/article/pii/S0921800906003806. [Accessed October 2011].

Sehim, A. (1993): Cretaceous tectonics in Egypt: Egypt. Jour. Geol., Vol 37, pp. 335-372.

Selman, P.H. (2000): Environmental planning: the conservation and development of biophysical resources. 2nd edition, London; Thousand Oaks: Sage Publications.

Serra, P., Pons, X. and Sauri, D. (2003): Post-classification change detection with data from different sensors: Some accuracy considerations. International Journal of Remote Sensing, Vol 24, pp.3311−3340.

Seto, K. C., Woodcock, C. E., Song, C., Huang, X., Lu, J. and Kaufmann, R. K. (2002): Monitoring land-use change in the Pearl River Delta using Landsat TM. International Journal of Remote Sensing, Vol 23, pp.1985−2004.

Seto, K.C. (2011): Exploring the dynamics of migration to mega-delta cities in Asia and Africa: Contemporary drivers and future scenarios. Global Environmental Change, Vol 21, pp. S94–S107.

Shaker, F.I., Abd-Elrahman, A., Abdel-Gawad, K. and Sherief, A. (2011): Building Extraction from High Resolution Space Images in High Density Residential Areas in the Great Cairo Region. Remote Sens., Vol 3, pp. 781-791.

Shen, L., Lee, R.K.H. and Zhang, Z. (1996): Application of BOT System for Infrastructure Projects in China, Journal of Construction Engineering and Management, Vol 122, No 4, pp. 319-323.

Shukri, N.M. (1954): Remarks on the geological structures of Egypt: Bull. Soc. Geography. Egypt, Vol 27, pp. 65-82.

Sims, D. (2003): 'The Case of Cairo, Egypt', in UN-Habitat & UCL Development Planning Unit (Eds.) Understanding IA: Case Studies for the Global Report 2003, Cairo: UNDP, pp. 1-24.

Singh, A. (1989): Review article: Digital change detection techniques using remotely-sensed data. International Jounal of Remote Sensing, Vol 10, No 6, pp. 989-1003.

Skakun, R.S., Wulder, M.A. and Franklin, .S.E. (2003): Sensitivity of the thematic mapper enhanced wetness difference index to detect mountain pine beetle red-attack damage. Remote Sensing of Environment, Vol 86, pp. 433-443.

Small, C. (2004): The landsat ETM plus spectral mixing space. Remote Sensing of Environment, Vol 93, pp.1−17.

Small, C. (2005): A global analysis of urban reflectance. International Journal of Remote Sensing, Vol 26, pp.661−681.

Smith, M.O., Ustin, S.L., Adams, J.B. and Gillespie, A.R. (1990): Vegetation in deserts: I. A regional measure of abundance from multispectral images. Remote Sensing of Environment, Vol 31, pp.1−26.

Sobrino, J.A. and Raissouni, N. (2000): Toward remote sensing methods for land cover dynamic monitoring: application to Morocco. International Journal of remote sensing, Vol 21, No 2, pp. 353-366.

Song, C.,Woodcock, C.E., Seto, K.C., Lenney, M.P. and Macomber, S.A. (2001): Classification and change detection using Landsat TM data: When and how to correct atmospheric effects? Remote Sensing of Environment, Vol 75, pp.230−244.

Stewart, D. (1996): Cities in the desert: the Egyptian New-Town Program. Annals of the Association of American Geographers, Vol 86, pp. 460–479.

Stewart, D. (1999): Changing Cairo: the political economy of urban form International Journal of Urban and Regional Research, Vol 23, No 1, pp 103–127.

Sultan, M., Arvidson, R.E. and Sturchio, N.C. (1986): Mapping of serpentinites in the Eastern Desert of Egypt by using Landsat thematic mapper data. The society of American Geology December, Vol 14, No 12, p. 995-999.

Sutton, K. and Fahmi, W. (2001): Cairo's urban growth and strategic master plan in light of Egypt's 1996 population census results.

Swedan, A.H. (1991): A note on the geology of Greater Cairo area, Annals of The Geological Survey of Egypt, Vol 17, pp. 239-251.

Taubenböck, H., Esch, T., Felbier, A., Wiesner, M., Roth, A. and Dech, S. (2012): Monitoring urbanization in mega cities from space, Remote Sensing of Environment, Vol 117, pp. 162-176.

Teraya, R. (2004): The development of the urban system and the hierarchy of the newly opened regions: Hokkaido, Japan and South Africa. Dela21, pp. 241-251.

Touzi, R. (2002): A review of speckle filtering in the context of estimation theory. Geoscience and Remote Sensing, IEE Transaction, Vol 40, No 11, pp. 2392 – 2404.

UN (1986), Demographic Yearbook 1988.

UN, (2010) United Nations Department of Economic and Social Affairs/Population Division 4 World Population Prospects, Demographic Profiles, Vol 2:

UNDP (2008), Egypt Human Development Report 2008: Egypt's Social Contract; The Role of Civil Society. Cairo: UNDP.

UN-Habitat (2009), Available at: http://www.unhabitat.org/content.asp?cid=7120&catid=192&typeid=13# [Accessed September 2010].

UN-Habitat publication. (2004/5): Cities, Globalization and Urban Culture.

UN-Habitat, united nations human settlements program. (2006): State of the world`s cities. pp.6-9.

UN-Habitat. (2006): World Urbanization Prospects: The 2005 Revision, pp.1-3

United Nations publication. (2006): Department of Economic and Social Affairs, Population Division.

United Nations publication. (2009: Department of Economic and Social Affairs, World Urbanization Prospects, pp. 4-7.

Veldkamp, A. and Verburg, P.H. (2004): Modelling land use change and environmental impact. In: Journal of Environmental Management Vol.72, No 1–2, pp. 1–3. Available at: http://www.sciencedirect.com/science/article/pii/S0301479704000684. [Accessed October 2011].

Vincent, R.K. (1997): Fundamentals of geological and environmental remote sensing, Prentice Hall series in geographic information science, University of California.

Waibel, M. And Schröder, F. (2011): The Interplay of Innovative Urban Planning Approaches and Economic Upgrading in China: The Case of Guangzhou Mega-City.In: disp: The Planning Review, Vol 187, No 4, pp.49 -58.

Walter, V. (2004): Object-based classification of remote sensing data for change detection. ISPRS Journal of photogrammetry & remote sensing, Vol 58, pp. 225– 238.

Woodcock, C.E., Macomber, S.A., Pax-Lenney, M.and Cohen, W.B. (2001): Monitoring large areas for forest change using Landsat: Generalization across space, time and Landsat sensors. Remote Sensing of Environment, Vol 78, pp.194– 203.

World Bank (2010) Available at: http://www.worldbank.org/en/country/egypt/overview [Accessed October 2011]

World Bank, (2011-13): Egypt overview. Available at: http://www.worldbank.org/en/country/egypt/overview [Accessed May 2013]

World Urbanization Prospects: The 2005 Revision. Working Paper No. ESA/P/WP/200.

Xie, Y., Mei, Y., Guangjin, T. And Xuerong, X. (2005): Socio-economic driving forces of arable land conversion: A case study of Wuxian City, China. In: Global Environmental Change, Vol 15, No 3, pp. 238–252. Available at: http://www.sciencedirect.com/science/article/pii/S0959378005000294. [Accessed October 2011].

Yin, Z., Stewart, J., Bullard, S. and MacLachlan, J. (2005): Changes in urban built-up surface and population distribution patterns during 1986–1999: A case study of Cairo, Egypt. Computers, Environment and Urban Systems, Vol 29, pp. 595–616.

Yousry, M. and Aboul Atta, T.A. (1997): The challenge of urban growth in Cairo. In The urban challenge in Africa. Growth and management of its large cities, ed. C Rakodi. UN University Press, Tokyo, pp. 111–149.

# الملخص العربى

تعتبر المدن الكبيره التي يزيد عدد سكانها عن العشرة ملايين نسمه من اكثر الأماكن التي تعاني من التدهور البيئي و عدم استدامة . ولذلك كرس العديد من العلماء في مختلف التخصصات اهتمامهم لدراسة مكونات هذه المدن الكبيرة و كشف العلاقة بين مكوناتها لايجاد حلول مبتكرة للتغلب علي المشاكل الناتجة عن النمو المتسارع ليس فقط في عدد السكان و لكن ايضا في الحيز العمراني.

و لتاثير الكثير من المشاكل البيئية , الاجتماعية , الاقتصادية و حتي السياسية علي المدن الكبيرة فقد توافق المؤلف مع ان فهم مثل هذا النظام المعقد و دراسة مكوناتة هو المنطلق الاساسي لتقديم تصور يمكن له ان يساهم في خطط التنمية المستقبلية و دعم متخذي القرار علي كافة المستويات.

و حيث ان القاهرة الكبري عاصمة مصر واحدة من اكبر المدن في العالم و اكبرها في منطقة الشرق الاوسط و افريقيا , فهي تعد نموذج واضح للنمو المتسارع و زيادة الحيز الجغرافي (العمراني) و ذلك بضغط الزيادة السكانية و المتغيران الاقتصاديه و التنمية العمرانية علي مدار الثلاثة عقود الاخيرة.

و علي ذلك فيعد دراسة التغير الحيزي و ايجاد العلاقة الصحيحة بين مكونات هذا التغير هو المنطلق الصحيح لوضع خطط التنمية المستقبلية و لايجاد حلول و استجابة للوضع الراهن.

هذه الاطروحة تقدم نموذج لمفهوم النمو الحيزي و المرونة المكانية وذلك لتوضيح العلاقة بين مكونات المكان و تاثيرها علي التركيبة المكانية مع مرور الوقت.

تتكون الدراسة من خمس فصول بجانب المقدمة و الاستنتاجات و بعض التوصيات حيث يناقش الفصل الثاني الوضع الجيولوجي و المورفولوجي للقاهرة الكبري باستخدام تقنية الاستشعار عن بعد و ذلك لانتاج خريطة رقمية لكل المنطقة بجانب اطار عام يوضح تركيبات الصخور المغطية لغرب المنطقة و شرقها و وصف لطبوغرافية المنطقة باستخدام الخرائط الرقمية للارتفاعات.

و من ثم فقد تم حصر الطبقات الصخرية المكونة للمنطقة في احدي عشر نوعا غالبيتها من الصخور الرسوبية مقسمة الي كلاستك و كالكيريس {حبيبي و جيري } بالاضافة الي بعض مكونات البازلت.

و يلي ذلك فصل كامل يتحدث عن النظرية و المبدا العام المستخدم في الدراسة و كذلك الطريقة التي تم اتباعها للوصول الي النتائج و من ثم الاستنتاجات. حيث تم التركيز علي توضيح مفهوم المرونة المكانية و حيث ان مفهوم المرونة المكانية هو ايجاد علاقة التفاعل بين مكونات النظام البيئي و الاجتماعي و حيث ان المدن و خصوصا المدن الكبري تعد نظام معقد يتدخل فيه الحيزي و الاجتماعي و الاقتصادي و حتي السياسي, فلقد تم تطبيق هذا المفهوم في هذه الدراسة علي المتغيرات المكانية مع مرور الزمن في القاهرة الكبري و تقديم اطار مبادئ و رصد يمكن من خلالة فهم العلاقة بين المؤشرات و المؤثرات داخل نظام النمو المكاني للمدينة.

و ذلك علي محورين

الاول هو استخدام نموذج تنسيقي لانشاء اطار عمل لفهم دور و الصلة بين كل مؤشر و اخر و تحديد ما يمثل قوة ضغط داخل النظام و ما هي الحالة و التاثير الناتج لذلك الضغط و من ثم ايجاد حلول او دعم متخذي القرار في الخطط المستقبلية و يسمي هذا الاطار "DPSIR".

و يمثل المحور الثاني استخدام سلسلة زمنية من صور الاقمار الصناعية الدقيقة و المتوسطة الدقة و ذلك لرصد التغير المكاني لاستخدامات الارض و غطائها.

و قد تم استخدام تقنية التقسيم اعتمادا علي مجموعة من النقاط و ليس اعتمادا علي نقطة واحدة, و هو ما يسمي

"Object based classification "

و اظهرت النتائج في الفصلين الرابع و الخامس ان التغير الحيزي للقاهرة الكبري يدفعه عوامل عدة ليس فقط النمو السكاني و لكن النمو الحيزي لعناصر البنية الاساسية مثل مترو الانفاق و الطريق الدائري و النمو المتسارع للمدن الجديده.

و هو ما ادي الي زيادة التعدي علي الارض الزراعية شمال و جنوب القاهرة الكبري وانحصار التعدي شرقا و غربا و ايضا اوضح العمل علي موستويات مختلفة من الدقة لصور الاقمار الصناعية و تقسيم ايتخدام الاراضي و خصوصا العمران و الغطاء الاخضر الي مستويات مختلفة من الكثافة و النوع, الي تحديد اماكن الضغط و الضعف في الاقليم, و تحديد مؤشرات التاثر في اكثر من اربعة عشر منطقة او نقطة حساسة لوضعها في اولاويات خطط التنمية لمتخذي القرار, و ذلك ما تم تفسيرة في الفصل السادس.

و لقد خلصت الدراسة الي ضرورة وضع مفهوم الحيز المكاني قيد الاعتبار عند دراسة المدن الكبري و قدمت الاطروحة نموذجا و اطارا يمكن تطبيقة ليس فقط في القاهرة الكبري و لكن لاي نظام معقد المكونات.

و لقد وجد ان استخدام اطار للمبادئ يمكن له ان يتكامل مع تطبيقات الاستشعار عن بعد لتحديد التغير المكاني و ذلك لانشاء نظام رصد متعدد المستويات و الاغراض يخدم العديد من متخذي القرار و الباحثين و المخططين و ايضا المستثمرين.

و لقد اوصت الدراسة بالعمل علي اعادة التوزيع الجغرافي للسكان و ذلك عن طريق تبني نظرية الحضانة لمناطق خارج القاهرة الكبري مثل سيناء و الواحات.

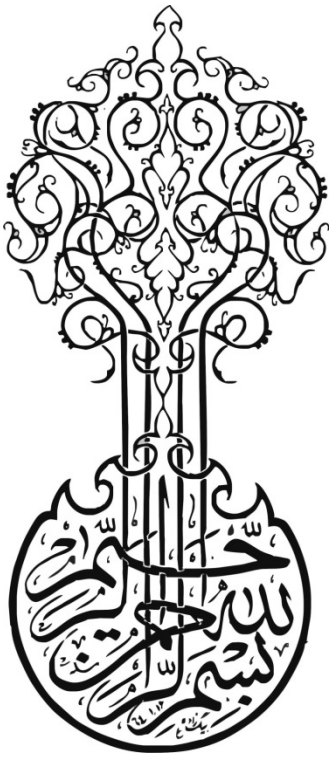


(http://my.opera.com/Carrow/albums/slideshow/?album=522825&picture=7211009)